COMPARTMENTALIZATION AND B CELL ANTIGEN RECEPTOR SIGNALING

by

TERESA LYNN JACKSON

B.Sc., The University of British Columbia, 1997

A THESIS SUBMITTED IN PARTIAL FULFILLMENT
OF THE REQUIRENENTS FOR THE DEGREE OF

DOCTOR OF PHILOSOPHY

in

THE FACULTY OF GRADUATE STUDIES

(Zoology)

THE UNIVERSITY OF BRITISH COLUMBIA

December 2005

ABSTRACT

This thesis focuses on two aspects of compartmentalization with respect to BCR signaling. In the first section, compartmentalization of the BCR to lipid rafts is considered and in the second section the subsequent compartmentalization of BLNK and PLCγ to the BCR is considered. Recent studies have suggested that the BCR translocates into lipid rafts in certain B cell stages. Yet these reports have been ambiguous and the mechanisms regulating such translocation have remained elusive. In this thesis it is demonstrated that the BCR can translocate into lipid rafts following BCR cross-linking in the immature B cell lines, WEHI 231 and CH31 (Jackson *et al.*, 2005). Additionally, it is shown that the Igα/β heterodimer, in the absence of the mIgM subunit, can translocate into lipid rafts in the immature B cell line, WEHI 303.1.5 (Jackson *et al.*, 2005). Previous studies have likewise demonstrated that the mIgM subunit, in the absence of Igα/β, can translocate into lipid rafts (Cheng *et al.*, 2001). Together, these findings may be used to help define a structural feature, common to both subunits, involved in mediating lipid raft association.

The PLCγ pathway is an integral part of the BCR signaling network. Loss-of-function studies have indicated that the BCR is coupled to PLCγ via Syk, BTK and BLNK. In this thesis, a non-lymphoid reconstitution system was used to determine if these components are sufficient to couple the BCR to PLCγ. From this it was determined that co-expression of the BCR, Syk and BLNK is sufficient to reconstitute BCR-induced PLCγ activation in the system. However, this activation is hypothesized to represent only a partial reconstitution of the pathway as neither BLNK nor PLCγ are recruited to the plasma membrane upon BCR cross-linking and as PLCγ phosphorylation appears very limited. It was hypothesized that this might be due to the absence of BTK; however, further expression of BTK within the system inhibited rather than enhanced PLCγ activation. Subsequent investigations determined that BTK is constitutively activated within this system and as such, may be inappropriately affecting the pathway. Additionally, it was hypothesized that the limited reconstitution may be a consequence of the inability to reconstitute BCR-induced BLNK and PLCγ membrane recruitment. Thus, BLNK and PLCγ were constitutively targeted to the plasma membrane within the system. From this, it was determined that membrane-targeting of PLCγ is sufficient to reconstitute BCR-induced, Syk-dependent PLCγ activation. In contrast, membrane-targeting of BLNK is not sufficient to reconstitute BCR-induced PLCγ membrane recruitment or to enhance BCR-induced PLCγ activation within this system. This suggests that there may be an additional defect in the system that is preventing the formation of a functional BCR/BLNK/PLCγ signaling complex. Moreover, these findings suggest that there may be a deficit in our current understanding of the BCR/PLCγ pathway.

In summary, these findings highlight the importance of compartmentalization in BCR signaling both with respect to compartmentalization of the BCR to lipid rafts and the subsequent compartmentalization of BLNK and PLCγ to the BCR..

TABLE of CONTENTS

LIST of TABLES

LIST of FIGURES

LIST of ABBREVIATIONS

Ac	Acylation (used to refer to fusion proteins that are targeted to the membrane via fusion with the Lyn acylation sequence)
AM	acetoxymethyl ester
ASK1	apoptosis-signaling regulating kinase
AtT20	mouse pituitary gland tumor cell line
APC	antigen presenting cell
B cell	B lymphocyte
BASH	B lymphocyte adapter protein containing a Src homology 2 domain
BCA	bicinchoninic acid
BCAP	B cell adapter for PI3K
BCR	B cell antigen receptor
Blk	B lymphocyte kinase
BLNK	B cell linker protein
BME	2-β-mercaptoethanol
BSA	bovine serum albumin
BTK	Bruton's tyrosine kinase
$CaCl_2$	calcium chloride
CD16	cluster of differentiation 16 (also known as FcγRIIIa)
CLP	common lymphoid progenitor
CO_2	carbon dioxide
CSB	cytoskeletal stabilization buffer
CsCl	cesium chloride
C-terminal	carboxyl terminal
D	aspartic acid
D	diversity segment
D_H	diversity segment of the heavy chain
DAG	diacylglycerol
DIGs	detergent-insoluble glycolipid-enriched membranes
DM lysis buffer	n-Dodecyl-β-d-maltoside lysis buffer
DMEM	Dulbecco's modified Eagle Medium
DMSO	dimethylsulfoxide
DNA	deoxyribonucleic acid
DOC	deoxycholate
D-PBS	Dulbecco's phosphate buffered saline
DRMs	detergent-resistant membranes
DTT	dithiothreitol
E	glutamic acid
E. coli	*Escherichia coli*
EC	extracellular
EDTA	(ethylenedinitrilo)tetraacetic acid
Erk	extracellular regulated kinase
g	gram
GDP	guanine diphosphate
GEMs	glycolipid-enriched membranes
GPI	glycophosphatidylinositol
GST	glutathione S-transferase

GSK-3β	glycogen synthase 3β
GTP	guanine triphosphate
hBLNK	human B cell linker protein
HBS	HEPES-buffered saline
HCl	hydrochloric acid
HM79-16	monoclonal antibody specific for the extracellular domain of murine Igβ that is purified from the HM76-19 hamster hybridoma cell line
HRP	horseradish peroxidase
HSC	haematopoietic stem cell
I	isoleucine
Ig	immunoglobulin
Igα/β	immunoglobulin alpha/beta heterodimer, signaling subunit of the BCR
IκB	inhibitor of NF-κB
IκK	Iκ kinase
IP_3	inositol tris phosphate
ITAM	immunoreceptor tyrosine-based activation motif
J	joining segment
J_H	joining segment of heavy chain
J_L	joining segment of light chain
K40B-1	pro-B like cell line
K40B-2	pre-B like cell line
KCl	potassium chloride
L	litre
L	leucine
LAB	linker of activated B cell
LAT	linker of activated T cell
LB	Luria-Bertani
LiCl	lithium chloride
LTR	long terminal repeat
MAPK	mitogen activated protein kinase
MAPKKK	MAPK kinase kinase
$MgSO_4$	magnesium sulfate
mg	milligram
MHC I	major histocompatibility complex class I
MHC II	major histocompatibility complex class II
mIgA	membrane-bound immunoglobulin A
mIgD	membrane-bound immunoglobulin D
mIgE	membrane-bound immunoglobulin E
mIgG	membrane-bound immunoglobulin G
mIgM	membrane-bound immunoglobulin M, antigen-binding subunit of the BCR
ml	millilitre
mM	millimolar
MPC	myeloid progenitor cell
mPLCγ	membrane-targeted rat Phospholipase C gamma
μg	microgram
μM	micromolar

NaCl	sodium chloride
Na_2HPO_4	sodium hydrogen phosphate
Na_3VO_4	sodium orthovanadate
NAPS Unit	Nucleic Acid Protein Service Unit at UBC
$NFAT_c$	nuclear factor of activated T cells (cytosolic component)
NP40 lysis buffer	Nonidet P40 lysis buffer
N-terminal	amino terminal
OD	optical density
PAMP	pathogen-associated molecular patterns
pBS	refers to the Bluescript plasmid
PDGRF	platelet-derived growth factor receptor
PDK1	phosphoinositide-dependent kinase 1
PDK2	phosphoinositide-dependent kinase 2
PCR	polymerase chain reaction
PH	pleckstrin homology domain
PI3K	phosphatidyly-inositol 3 kinase
PI-4-P	phosphatidyl inositol-4-phosphate
PI-3-4-P_2	phosphatidyl inositol-3-4-bisphosphate
PIP_2	phosphatidyl inositol bisphosphate
PI-3-4-5-P_3	phosphatidyl inositol-3-4-5-trisphosphate
PIP_3	phosphatidyl inositol trisphosphate
PLC	phospholipase C
PLCγ1	phospholipase C gamma 1
PLCγ2	phospholipase C gamma 2
PRR	pattern recognition receptor
PTK	protein tyrosine kinase
PTP	protein tyrosine phosphatase
RasGRP	Ras guanyl nucleotide-releasing protein
RSV	Rous sarcoma virus
Rpm	revolutions per minute
RPMI	Roswell Park Memorial Institute
RSB	running sample buffer
S. cerevisiae	*Saccharomyces cerevisiae*
SAPK	stress-activated protein kinase
SDS	sodium dodecyl sulfate
SDS-PAGE	sodium dodecylsulfate-polyacrylamide gel electrophoresis
SFK	Src family kinase
SH2	Src homology 2 domain
SH3	Src homology 3 domain
SHP-2	Src homology 2 domain-containing protein tyrosine phosphatase-2
Slp-65	Src homology 2 domain-containing leukocyte protein of 65 kD
SOS	Son of Sevenless
Syk	Spleen tyrosine kinase
T cell	T lymphocyte
TBE	Tris-buffered EDTA
TBS	tris-buffered saline
TBST	tris-buffered saline with Tween 20 detergent
TCR	T cell receptor
TE	tris/EDTA solution

TLR	Toll-like receptor
TM	transmembrane (used to refer to fusion proteins that are targeted to the plasma membrane via fusion to the T cell receptor ζ extracellular domain and the CD16 transmembrane domain)
TX-100	Triton X-100
UBC	University of British Columbia
V	variability segment
V_H	variability segment of heavy chain
V_L	variability segment of light chain
WEHI	Walter and Eliza Hall Institute
WEHI 231	immature B cell line
WEHI 303.1.5	mIgM-deficient immature B cell
Y	tyrosine
4G10	monoclonal phosphotyrosine specific antibody

ACKNOWLEDGEMENTS

Brevity has its place. But it is not here; for it is far too rare that we have or take the opportunity to thank the people in our lives that have helped us along our ways. I consider myself fortunate in knowing that I could not possibly acknowledge all those who have helped me to reach this point; I only hope that those who are not directly acknowledged here still know how much I have appreciated their support, advice and friendships.

From the Matsuuchi Lab I thank the directed study students, Gabe Woolham, Aneez Mohamed and Eric Zhou for their assistance. I thank Lorna Santos and Jared Lopes for our many conversations, scientific and otherwise. I thank May Dang-Lawson, without whom the lab would cease to function. I thank Janis Dylke, whose calm, patience and quick intelligence is always a source of inspiration. I thank Steve Macthaler and Emily McWalter for so kindly sharing their place, for their support and for their many efforts quantifying my data. I especially thank Steve for the many$^{\infty}$ favours and for making me laugh when all else fails. I thank Colm Condon for encouraging me and introducing me to Dr. Linda Matsuuchi. And I thank Linda Matsuuchi for all her assistance, patience and well-delivered lessons. Linda, I especially thank you for accepting me as me and understanding and supporting my passion for rugby and for teaching. I also thank you for teaching Biology 441 where I began to understand what a good teacher really was. I can only hope that I can translate those lessons to my students.

From other labs, I thank Mike Gold and his group for all their assistance. I thank Peter Knight and John Church for their assistance with my calcium flux assays. John, I especially thank you for being so generous with your equipment, time and expertise. I thank my committee, Dr. Vanessa Auld, Dr. Hugh Brock, Dr. Ljerka Kunst and Dr. Nelly Panté, for their many hours, for their advice and for always being available at the last minute.

From my life outside the lab, I thank my rugby team, the UBC Thunderbirds. Words fail me – and you all know how rare that is! Nonetheless, thank you for ensuring that I lived life instead of just studying it. I thank my family. I thank my grandparents Bob and Lorna Ritchie and Jean Hutchin (Jackson) who have always believed in and supported me. I thank my siblings, Dale, Dylan, Dave and Ştefania who always make sure I have both feet planted firmly on the ground while I stand on their shoulders! I thank the Corkins for taking me into their family and home. I thank my Mom who always taught me to dream big, saying "Don't just drive the tow truck, own the whole company!" I thank my Dad who taught me the work ethic, perseverance and many other skills necessary to achieve my dreams. Dad, thank you for being you and for always being there.

And finally, I thank my husband James Corkin, without whom this thesis truly would not exist. James, thank you for typing in all my references! Beyond that, I can not possible thank you for all that you do for me. With you, I am my best.

CHAPTER 1

Introduction

1.1 The Biological Problem

Every moment of every day our bodies are invaded by pathogens such as bacteria, viruses, fungi and parasites. And every day our immune system staves off such invasions. Unfortunately, at times our immune system fails, leaving us vulnerable to illness, disease and even death. Encouragingly, humanity has gained a vast knowledge of how our immune system functions and fails to function such that we can medically manipulate and reinforce our immune system to help our bodies in their continual defense against disease and death. Nonetheless, many aspects of immune function remain to be elucidated and many illnesses, immunodeficiencies and autoimmune diseases remain to be eradicated.

1.2 An Overview of the Human Immune System

Our immune system includes two cooperative branches of defense namely, the innate response and the adaptive response. The innate response is an immediate yet less-specific response that is primarily mediated by macrophages, neutrophils and dendritic cells. These cells circulate throughout our peripheral tissues where they encounter pathogens. Upon recognizing a pathogen these cells will either secrete products to degrade the pathogen or they will engulf the pathogen and degrade it intracellularly. In contrast, the adaptive response is a delayed yet more-specific response that is primarily mediated by B and T lymphocytes (B and T cells, respectively). These cells circulate throughout our blood, lymph and lymph nodes as naïve cells where they encounter antigen presenting cells (APCs; e.g. macrophages and dendritic cells of the innate response and B cells of the adaptive response). Upon specifically recognizing an APC, and upon receiving the appropriate co-stimulatory signals, B and T cells differentiate into effector cells and memory cells. Effector cells then help the innate system to specifically control the immediate infection while memory cells provide long-lasting and specific protection against re-infection. Thus, the innate and adaptive responses cooperate to provide both an immediate and a long term defense against pathogens.

A critical aspect of immune system function is the ability to recognize self from non-self (i.e., pathogen). Innate cells achieve this via germ-line encoded pattern recognition receptors (PRRs) (reviewed by Aderam and Ulevitch, 2000; Takeda and Akira, 2001; Janeway, Jr. and Medzhitov, 2002; Sieling and Modlin, 2002). PRRs bind conserved pathogen-associated molecular patterns (PAMPs) that are uniquely yet widely expressed by pathogens (reviewed by Aderam and Ulevitch, 2000; Takeda and Akira, 2001; Janeway, Jr. and Medzhitov, 2002; Sieling and Modlin, 2002). Hence, PRR-PAMP interactions enable individual innate cells to distinguish self from non-self and to respond to a broad spectrum of pathogens.

The best characterized PRRs include members of the Toll-like receptor (TLR) family. TLRs were first identified for their role in *Drosophila* development and later for their role in *Drosophila* immune defense (Lemaitre *et al.*, 1996; reviewed in Medzhitov, 2001, Takeda and Akira, 2001). Subsequently, at least ten TLRs have been identified in the mammalian immune system (reviewed in Janeway Jr. and Medzhitov, 2002). TLRs are most commonly expressed on phagocytic cells where their engagement leads the cell to engulf and degrade the pathogen and to secrete chemokines that further enhance the innate response. However, on dendritic cells, TLR engagement leads the cell to engulf the pathogen and to migrate to a lymph node where the cell then presents the pathogen to naïve T cells. If a naïve T cell specifically recognizes the presented pathogen it will differentiate into effector and memory T cells. Thus, TLRs play a pivotal role both in mediating an immediate innate response and in activating a long-term adaptive response.

Adaptive cells distinguish self from non-self via cell-surface antigen receptors that bind to immunogenic peptides (antigens) that are typically derived from pathogens. As an entire population, B and T cells express a large repertoire of antigen receptors that are capable of recognizing and responding to vast array of pathogens. However, any given cell is capable of recognizing and responding to only one specific pathogen as it expresses multiple copies of only one unique, single-specificity antigen receptor. The specificity and variability of these receptors is achieved through the process of random somatic recombination coupled with variable pairing of different polypeptide chains to form the binding site of the receptor. However, receptors capable of recognizing self-peptides are sometimes generated as the recombination event is random. Fortunately, cells expressing such receptors are typically eliminated before maturation through the process of clonal selection and deletion (refer to Chapter 1.4). Following

maturation, naïve B and T cells circulate throughout our blood and peripheral tissues where they may encounter their cognate antigen. If this encounter is accompanied by the appropriate co-stimulatory signals the cell will undergo clonal expansion where it will proliferate and differentiate into progeny effector and memory cells. These progeny express receptors of the same specificity of the parental naïve cell such that they are able to specifically respond to initiating pathogen. Thus, the adaptive response is comprised of a population of B and T cells that can distinguish self from non-self to provide a specific and tailored defense against pathogens.

Antigen receptor engagement leads to a variety of immune responses depending on the identity and developmental stage of the cell, on the identity of the antigen receptor-antigen interaction and on the context of signaling. In the case of T cells, the T cell antigen receptor (TCR) can only recognize antigens that are presented on the surface of APCs. In particular, TCRs can only recognize antigens that are associated with specialized host molecules termed major histocompatibity complexes (MHCs). Cells infected with intracellular pathogens tend to present the resulting antigens on MHC class I molecules (MHC I) whereas cells that have engulfed extracellular pathogens (e.g., macrophages and dendritic cells) tend to present the resulting antigens on MHC class II molecules (MHC II). Depending on the antigen:MHC class presented different T cell responses will be initiated. Thus, MHC molecules help to direct the T cell response to ensure that the appropriate response is mounted against the eliciting pathogen.

Many T cell responses are initiated when a naïve T cell interacts with a mature dendritic cell of the innate response. Mature dendritic cells present antigen:MHCs on their cell surface along with co-stimulatory molecules that drive naïve T cell differentiation. Dendritic cells presenting antigen:MHC I tend to drive naïve T cells to differentiate into cytotoxic T cells that are armed to recognize and destroy cells that present antigens from intracellular pathogens. In contrast, dendritic cells presenting antigen:MHC II tend to drive naïve T cells to differentiate into helper T cells that are armed to recognize cells that present antigens from extracellular pathogens. Upon such recognition, helper T cells may release cytokines that induce macrophage recruitment, differentiation and activation such that the macrophage is better able to destroy the pathogen. Alternatively, upon recognition of cognate antigen-presenting B cells, helper T cells release cytokines that induce the B cell to differentiate into an effector cell. As well, the naïve T cell proliferates and differentiates into memory T cells that provide a specific and more rapid

response upon re-infection with the same pathogen. Thus, T cell responses can provide long-term, specific adaptive immunity as well as enhance the innate response.

In the case of B cells, the BCR can recognize soluble antigens. When the BCR of a naïve B cell binds a soluble antigen it takes up the antigen via receptor-mediated endocytosis. The B cell then processes the antigen and presents that antigen on its cell surface in the context of MHC II molecules. If the antigen-presenting B cell then interacts with a helper T cell that expresses a cognate TCR both cells will become activated (reviewed in Bernard *et al.*, 2005). Initially, the B cell will activate the helper T cell to release cytokines. In turn, these cytokines will activate the B cell to proliferate and differentiate into antibody-secreting plasma cells. The resulting antibodies circulate throughout the blood where they can then specifically neutralize the initiating pathogen by either inhibiting it from interacting with host cells or by targeting it for destruction by various components of the immune response. And similar to T cells, the naïve B cell will also proliferate and differentiate into long-living memory B cells that provide a specific and more rapid response to the pathogen upon re-infection with the same pathogen.

Ultimately, the innate response and the adaptive response function coordinately to defend the body against pathogens. Initially innate cells provide a more general and immediate defense against pathogens. This defense is then reinforced when innate cells recruit and activate the adaptive response. The adaptive response then aids the innate response by specifically eliminating the initiating pathogen while also establishing a long-term defense against subsequent re-infection. Thereby, our immune system protects us from disease.

1.3 BCR Structure

The experiments of this thesis utilized the murine BCR and as such it is the murine BCR that is detailed below. Nonetheless, the overall structure of the human BCR and the murine BCR are comparable. The BCR is expressed on the cell surface in various forms throughout B cell development. The earliest form of the BCR to be expressed is the pro-BCR which is expressed on pro-B cells (refer to Chapter 1.4). The pro-BCR is multi-peptide complex that is comprised of an Igα/β disulfide-linked heterodimer that is expressed on the cell surface in association with the chaperone protein, calnexin (Koyama *et al.*, 1997; Nagata *et al.*, 1997). As well, this

complex may include a surrogate light chain (VpreB and λ5) that is expressed on the cell surface in association with the chaperone protein, gp130 (Karasuyama *et al.*, 1993; Shinjo *et al.*, 1994).

Igα and Igβ are encoded for by the *mb1* and *B29* gene, respectively (Hermanson *et al.*, 1988; Hombach *et al.*, 1988; Sakaguchi *et al., 1988*; Campbell *et al.*, 1991; Matsuo *et al.*, 1991). Igα and Igβ are both glycoproteins that possess an Ig-like extracellular domain followed by a highly charged spacer region. Within the spacer region are cysteine residues that form a disulfide bridge between Igα and Igβ to form the Igα/β heterodimer. The spacer region is followed by a hydrophobic, 22 amino acid transmembrane region that anchors Igα/β to the plasma membrane. This transmembrane region is then followed by a cytoplasmic domain, which in murine cells contains 61 amino acids and 48 amino acids for Igα and Igβ, respectively. Combined, these domains result in an approximately 34 kilodalton (kD) Igα protein and an approximately 39 kD Igβ protein.

The Igα/β heterodimer is a constant component of all functional permutations of the BCR and is required for receptor signaling. The ability of the heterodimer to transduce signals is partially-dependent upon the Immunoreceptor Tyrosine-based Activation Motif (ITAM) that is contained within the cytoplasmic domain of both Igα and Igβ (Reth, 1989). The ITAM is a conserved motif defined by the consensus sequence $D/E(X)_7D/E(X)_2Y(X)_2L/I(X)_7L/I$ (where D = aspartic acid, E = glutamic acid, Y = tyrosine, L = leucine, I = isoleucine and X = any amino acid) that is typically associated with immunoreceptor signal transduction (Reth, 1989). This motif becomes tyrosine phosphorylated and enables Igα/β to associate with a variety of signaling proteins that can specifically recognize and bind to the phosphorylated ITAM via Src homology 2 (SH2) domains.

The surrogate light chain is comprised of two non-covalently associated Ig-like light chain proteins, V_{preB} and λ5, that are encoded for by the *λ5* gene (Kudo and Melchers, 1987; Tsubata and Reth, 1990; Misener *et al.*, 1991; Minegishi *et al.*, 1999). Together, these two proteins are believed to be expressed on the cell surface in association with the chaperone protein, gp130 (Karasuyama *et al.*, 1993; Shinjo *et al.*, 1994) where they associate with the Igα/β/calnexin complex to form the pro-BCR. While the function of the surrogate light chain is unclear it may have a role both in facilitating cell surface expression of the pro-BCR and in mediating some form of ligand binding and/or receptor aggregation such that pro-BCR signaling can be initiated.

The function of the pro-BCR itself remains unclear. However, the receptor may be involved in providing signals that help drive the developmental progression from pro-B cell to pre-B cell (Nagata *et al.*, 1997).

The developmental successor to the pro-BCR is the pre-BCR which is expressed on pre-B cells (refer to Chapter 1.4). The pre-BCR (Fig. 1.1) is comprised of two non-covalently associated subunits namely, the Igα/β heterodimer and the membrane bound IgM subunit (mIgM) (reviewed in Martensson and Ceredig, 2000). The Igα/β heterodimer is essentially as described above except that it is now expressed on the cell surface in association with the mIgM subunit as opposed to calnexin (Tsubata and Reth, 1990; Minegishi *et al.*, 1999). The mIgM subunit of the pre-BCR is a 67-78 kD, disulfide linked tetramer composed of a pair of surrogate light chain/μ heavy chain heterodimers (i.e., mIgM = $[\mu]_2[V_{preB}/\lambda 5]_2$). The surrogate light chain is essentially as described above except that it is now expressed on the cell surface in association with the μ heavy chain as opposed the gp130 (Kudo and Melchers, 1987; Tsubata and Reth, 1990). Meanwhile, the murine μ heavy chain is encoded for by the heavy chain locus which undergoes random somatic recombination of the variable (V), diversity (D) and joining (J) segments during the transition from the pro-B to the pre-B cell stage. The structure of the μ heavy chain includes an extracellular region comprised of a variable domain (V_H) followed by four constant domains (C_{H1-4}), a transmembrane domain of 22 amino acids and a brief intracellular domain of 3 amino acids. Once the pre-BCR is expressed on the cell surface the cell undergoes clonal selection whereby cells expressing inappropriately reactive receptors are eliminated (reviewed in Martensson and Ceredig, 2000). Cells surviving clonal selection continue to develop, progressing from the pre-B cell stage to the immature B cell stage.

The developmental successor to the pre-BCR is the BCR which is expressed on the surface of both immature and mature B cells (refer to Chapter 1.4). The BCR (Fig. 1.1) is initially comprised of two non-covalently associated functional subunits, the signal-transducing Igα/β heterodimer and the antigen-binding membrane Ig (mIg) subunit (Schamel and Reth, 2000). The Igα/β subunit of the BCR is essentially as described above for the pre-BCR. In contrast, the mIg subunit now contains rearranged light chains (either k or λ) in place of the surrogate light chain. The murine κ and λ light chains are encoded for by the light chain locus which undergoes random somatic recombination of the V and J segments during the transition from the pre-B cell stage to the immature B cell stage. The structure of the 25-28 kD light chain includes a variable

domain (V_L) similar to the heavy chain, followed by a single constant domain (C_L). Unlike, the heavy chain, the light chain does not contain a transmembrane or an intracellular domain but rather is expressed on the cell surface by way of its disulfide linkage to the μ heavy chain. As well, the BCR mIg may contain one of five isotypes of the heavy chain including α, δ, ε, γ, and μ (mIgA, mIgD, mIgE, mIgG and mIgM, respectively). Together, the variable domains of the light and heavy chain form an antigen binding region and in turn, two disulfide linked light chain/heavy chain complexes for a mIg complex. The mIg subunit must then associate with the Igα/β heterodimer to form a functional BCR that is expressed on the cell surface.

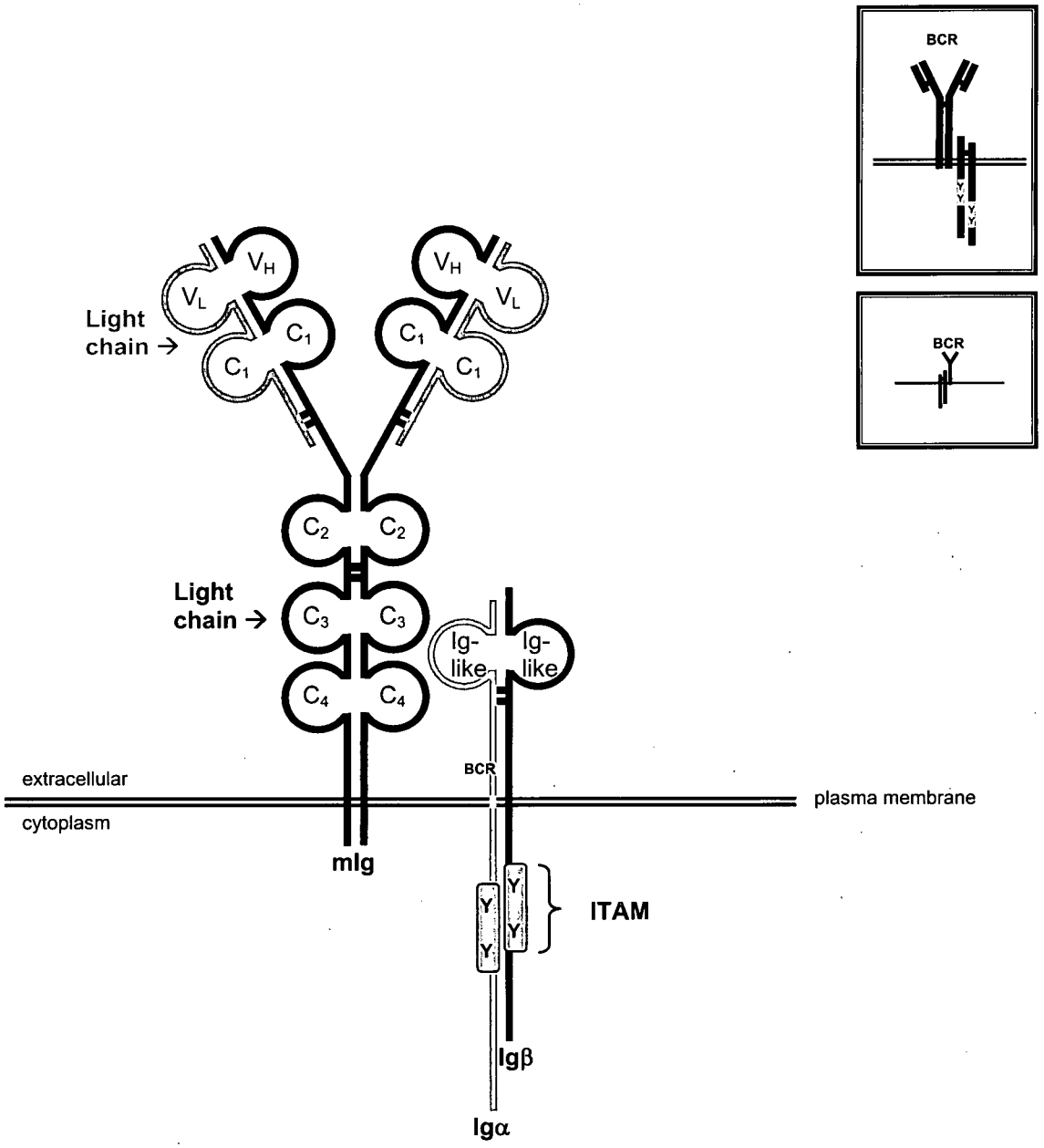

Figure 1.1. Schematic Representation of the BCR. The BCR is composed of an antigen-binding, membrane-bound subunit (mIg) that is non-covalently associated with a signaling, membrane-bound subunit (Igα/β). The mIg is composed of two disulfide linked heavy chains that are each disulfide linked to a light chain. The Igα/β subunit is composed of disulfide-linked Igα and Igβ accessory chains, each of which contains an ITAM within its cytoplasmic tail. V_H and V_L represent the variable domains of the heavy and light chain, respectively. $C_{1\text{-}4}$ represent the constant domains of the heavy and light chains. Ig-like indicates the Ig-like domains of Igα and Igβ. The insets in the top right hand corner indicate the BCR as it is represented throughout this thesis.

1.4 A Brief Overview of B Cell Development

From haematopoietic stem cell to antibody-secreting plasma cell, the B cell passes through multiple developmental checkpoints. These checkpoints help to ensure that a self-tolerant, diverse and maximally responsive B cell population is achieved. All haematopoietic cells, including the B cell, derive from the haematopoietic stem cell (HSC) within the bone marrow (Fig. 1.2). The HSC initially gives rise to a myeloid progenitor cell and a common lymphoid progenitor cell. The myeloid progenitor subsequently gives rise to polymorphonuclear leukocytes, erythrocytes and platelets while the common lymphoid progenitor gives rise to B and T cells.

The earliest defined B cell stage is that of the pro-B cell (Fig 1.3). The pro-B cell is typically characterized by cell-surface expression of the pro-BCR (described above) and is marked by the first VDJ recombination event where the D and J segments of the heavy chain locus are recombined (i.e., D_HJ_H rearrangement). Signaling studies have suggested that the pro-BCR may be involved in driving the pro-B cell to further differentiate into a pre-B cell (Nagata *et al.*, 1997). However, a pro-BCR ligand and/or a mechanism for this process has yet to be identified. Regardless, the next defined B cell stage is that of the pre-B cell.

The pre-B cell is typically characterized by the cell surface expression of the pre-BCR (detailed above) and is marked by the completion of $V_HD_HJ_H$ recombination of the μ heavy chain locus. Following $V_HD_HJ_H$ recombination the resultant μ heavy chain is expressed on the cell surface in association with the surrogate light chain and the Igα/β heterodimer as the pre-BCR. Loss-of-function studies indicate that the pre-BCR is then involved in signaling the pre-B cell to cease μ heavy chain rearrangements and to initiate V_LJ_L recombination (Miyazaki *et al.*, 1999; reviewed in Benschop and Cambier, 1999 and Martensson and Ceredig, 2000). This cessation of rearrangement is termed allelic exclusion and is necessary to ultimately ensure that each B cell expresses multiple copies of only one single-specificity antigen receptor. It is also important to note that the pre-B cell proliferates before initiating V_LJ_L recombination and progressing to the immature B cell stage. This round of proliferation is important as it ultimately results in progeny cells, each of which contains an identically rearranged heavy chain associated

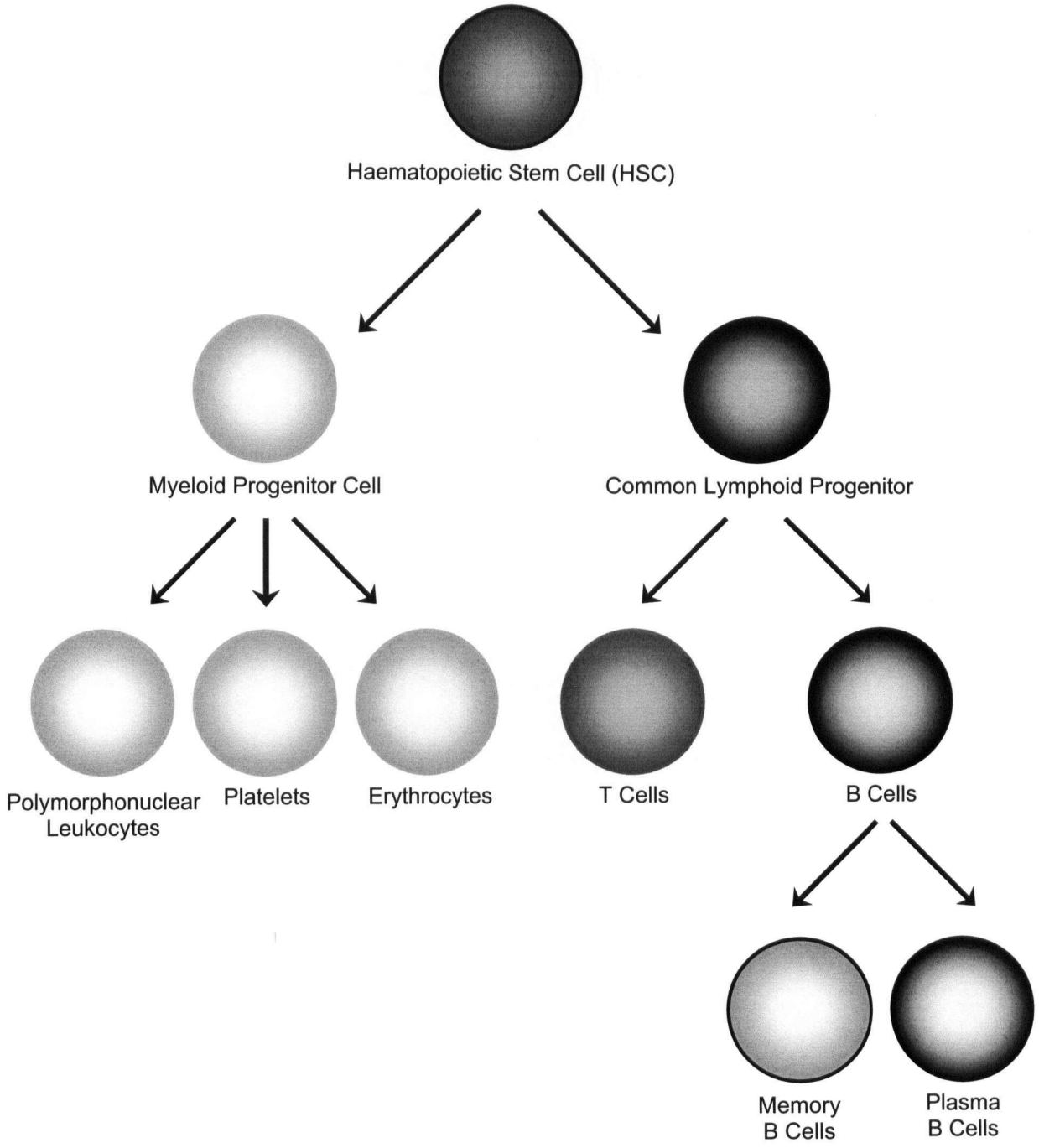

Figure 1.2. Some Cell Types Derived from the Haematopoietic Stem Cell. The Haematopoietic Stem Cell (HSC) differentiates to give rise to either a Myeloid Progenitor Cell (MPC) or a Common Lymphoid Progenitor (CLP) cell. The MPC goes on to differentiate into myeloid lineages including polymorphonuclear leukocytes, platelets and erythrocytes. The CLP goes on to differentiate into lymphoid lineages including B and T cells. B cells can further differentiate into Memory B Cells or into antibody secreting Plasma B Cells.

with a uniquely rearranged light chain; a situation which effectively increases the overall diversity of the receptor repertoire as both the heavy chain and light chain combine to form a specific antigen-binding site.

The immature B cell stage is characterized by the cell surface expression of the BCR (described above) where the rearranged light chain has replaced the surrogate light chain to produce a mature receptor. At this point the immature B cell circulates within the bone marrow where it undergoes the process of clonal selection whereby most self-reactive immature B cells are eliminated (reviewed in Rolink *et al.*, 2001). Immature B cells that survive clonal selection then migrate from the bone marrow to the blood and lymphoid organs where they progress to the mature B cell stage.

The mature B cell, like the immature BCR, is characterized by the cell surface expression of the BCR. However, the mature B cell typically undergoes isotype switching such that the BCR is comprised predominantly of mIgD as opposed to the mIgM prevalent in immature B cells (reviewed in Benschop and Cambier, 1999). The mature B cell then circulates throughout the lymphoid system where it may encounter its cognate antigen. Upon such an encounter BCR signaling is initiated. Such signaling, if accompanied by the appropriate co-stimulatory signals, culminates in the mature B cell clonally expanding and terminally differentiating into memory B cells and antibody-secreting plasma cells that ultimately provide a specific and long-term immune defense against the initiating pathogen.

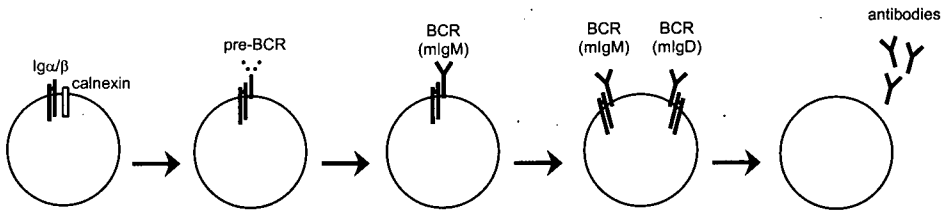

Developmental Stage	Pro-B Cell	Pre-B Cell	Immature B Cell	Mature B Cell	Plasma Cell
BCR Expression	Igα/β with calnexin	Igα/β, mIgM with surrogate light chain	Igα/β, mIgM	Igα/β mIgM & mIgD	soluble form (secreted antibodies)
Heavy Chain	germline	VDJ rearranged	VDJ rearranged	VDJ rearranged	VDJ rearranged, soluble form
Light Chain	germline	germline	VJ rearranged	VJ rearranged	VJ rearranged
Surface Markers	$B220^+$, $CD19^+$ c-Kit^+, $\lambda5^-$, $mIgM^-$, $mIgD^-$,	$B220^+$, $CD19^+$ c-Kit^-, $\lambda5^+$, $mIgM^+$, $mIgD^-$,	$B220^+$, $CD19^+$ c-Kit^-, $\lambda5^-$, $mIgM^+$, $mIgD^-$,	$B220^+$, $CD19^+$ c-Kit^-, $\lambda5^-$, $mIgM^+$, $mIgD^+$,	

Figure. 1.3. Summary of Key B Cell Developmental Stages and Indication of Some of The Cell Properties Associated With the Respective Stages.

1.5 Compartmentalization and Signal Transduction Pathways

Before a discussion of BCR signaling can be initiated compartmentalization must first be considered. Compartmentalization refers to the regulated localization of proteins to specific cellular compartments be they organelles, the cytosol, cellular membranes, membrane microdomains, or macromolecular complexes. Such compartmentalization is essential to maintain the integrity of all cellular signaling pathways. Important to this process of compartmentalization, and therefore important to any in-depth discussion of cellular signaling, are several highly conserved modular protein domains that mediate specific protein and lipid interactions. These domains include, but are not limited to, the Src homology 2 (SH2) domain, the Src homology 3 (SH3) domain, the pleckstrin homology (PH) domain, proline-rich motifs

and tyrosine-phosphorylation motifs (Fig. 1.4) (reviewed in Pawson and Nash, 2000; Castagnoli *et al.*, 2004).

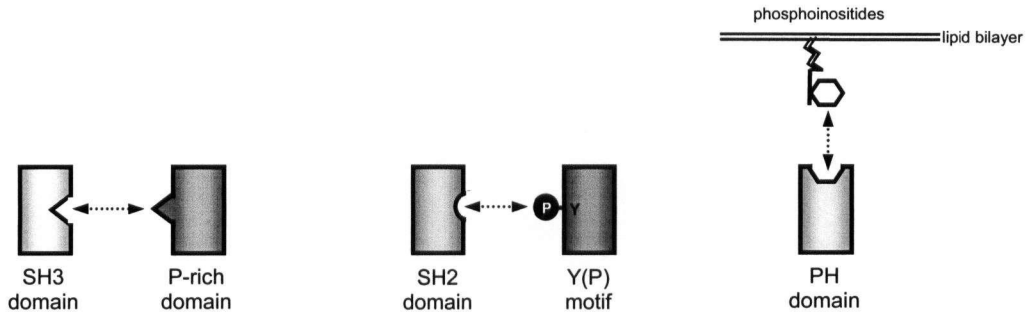

Figure 1.4. Schematic Representation of Key Protein and Lipid Interaction Domains. Proteins often contain one or more conserved protein or lipid interaction domains including; SH3 domains that associate with proline rich (P-rich) domains, SH2 domains that associate with tyrosine phosphorylation motifs [Y(P)] and PH domains that associate with membrane-bound phosphoinositides.

SH2 domains are modules of approximately 100 amino acids that specifically bind to phosphorylated tyrosine motifs (reviewed in Pawson and Nash, 2000; Castagnoli *et al.*, 2004). Different SH2 domains recognize different phosphorylated tyrosine motifs due to a secondary binding cleft within the domain that specifically recognizes the first six residues C-terminal to the phosphorylated tyrosine (reviewed in Pawson and Nash, 2000; Castagnoli *et al.*, 2004). SH2 domains not only facilitate specific protein-protein interactions, they also enable these reactions to be regulated due to the fact that their binding site (i.e., the tyrosine) can be rapidly modified. More precisely, a protein's tyrosine phosphorylation status, and therefore its ability to associate with SH2 domain-containing proteins, can be regulated and modified by the coordinate action of protein tyrosine kinases (PTKs) which phosphorylate tyrosine residues and protein tyrosine phosphatases (PTPs) which dephosphorylate tyrosine residues.

SH3 domains are conserved modules that bind to proline rich motifs with the consensus sequence proline-x-x-proline where x represents any amino acid (reviewed in Pawson and Nash, 2000; Castagnoli *et al.*, 2004). Similar to SH2 domains, different SH3 domains can specifically bind to different proline-rich motifs (reviewed in Pawson and Nash, 2000; Castagnoli *et al.*, 2004). Similar to SH2 domains, SH3 domain-mediated interactions can be regulated through phosphorylation (Broome and Hunter, 1996; MacCarthy-Morrough *et al.*, 1999). However, in

this case phosphorylation occurs on a residue within the SH3 domain to alter the domain's binding potential. Alternatively, phosphorylation of the SH3 domain-containing protein and/or its cognate proline-rich containing protein can cause the protein to undergo a conformational change such that their interaction domains' are subsequently revealed or concealed.

Dependent on their particular structure, PH domains can specifically bind to phosphatidylinositol-4,5-bisphosphate (PI-4,5-P), phosphatidylinositol-3,4-bisphosphate (PI-3,4-P), or phosphatidylinositol-3,4,5-trisphosphate (PI-3,4,5-P) (reviewed in Fruman *et al.*, 1999). Because these phosphoinositides are membrane-bound, PH domains can serve to recruit their respective proteins to the membrane, presumably to juxtapose them with their activators and/or substrates. Importantly, membrane-recruitment of various PH domain-containing proteins can be regulated by regulating the membrane concentration of their cognate phosphoinositide. This can be achieved through the coordinate action of phosphatidylinositol kinases and phosphatidylinositol phosphatases. Proline-rich motifs and tyrosine phosphorylation motifs bind to SH3 and SH2 domains, respectively, as detailed above. Thus, described are several protein and lipid interaction domains that are crucial to cellular signaling in general and to BCR signaling in particular.

1.5.1 The Role of Adapter Proteins in Signal Transduction Pathways

As mentioned previously, compartmentalization is essential to maintain the integrity of all cellular signaling pathways. Such compartmentalization is achieved, in part, by adapter proteins. Adapter proteins are non-enzymatic proteins that contain one or more of the above-mentioned conserved protein-protein or protein-lipid interaction domains (reviewed in Leo and Schraven, 2001). These domains enable adapter proteins to function as molecular scaffolds upon which macromolecular signaling complexes can be specifically assembled and regulated (reviewed in Tomlinson *et al.*, 2003; Jordon *et al.*, 2000; Pawson and Nash, 2000).

The function of adapter proteins is well-exemplified by the Ste5 adapter protein of *Saccharomyces cerevisiae* (*S. cerevisiae*) (reviewed in Schaeffer and Weber, 1999; Kelly and Chan, 2000). In *S. cerevisiae* the MAPK pathway can be activated by numerous environmental cues, and depending on these cues, can elicit numerous cellular outcomes (reviewed in Schaefer and Weber, 1999). The specificity of the MAPK pathway is determined in part by the Ste5

adapter protein which, upon pheromone stimulation, specifically assembles Ste11 (a MAPK kinase kinase) into a Ste20/Ste11/Ste7/Fus3 MAPK signaling module that regulates the mating response (reviewed in Schaefer and Weber, 1999). Alternatively, Ste11 can be assembled into a Sho1/Ste11/Pbs2/Hog1 MAPK signaling module that regulates the high osmolarity response (reviewed in Schaefer and Weber, 1999). Thus, Ste5 establishes signaling specificity by constraining promiscuous components of the MAPK pathway (i.e., Ste11) into a specific MAPK signaling module and thereby limiting inappropriate cross-talk. Furthermore, the formation of a Ste5/MAPK signaling module is thought to enhance the kinetics of the MAPK cascade by providing the reactions with an entropic advantage (reviewed in Schaefer and Weber, 1999; Reinhardt, 2004). Thus, the Ste5 adapter illustrates how adapter proteins can contribute to protein compartmentalization and in doing so regulate both signal sensitivity and specificity.

Adapter proteins are critical components of BCR signaling. In fact, several severe phenotypes have been documented in knock-out mice that lack these adapters (Torres *et al.*, 1996; Gong and Nussenzweig, 1996, Pappu *et al.*, 1999; Hayashi *et al.*, 2000; Xu *et al.*, 2000). However, these adapters are too numerous to be reviewed within this thesis and thus, the interested reader is directed to a series of excellent reviews on the topic including those by Tomlinson and colleagues (2000), by Leo and Schraven (2001), by Jordan and colleagues (2003) and by Reinhardt (2004). Rather, this thesis will focus on two key adapters that are involved in the BCR/PLCγ pathway namely the Igα/β heterodimer and the B cell linker protein (BLNK).

1.5.2 The Role of Lipid Rafts in BCR Signaling

Proteins can be sequestered in lipid rafts. Lipid rafts are detergent-insoluble, sphingolipid- and cholesterol-rich membrane microdomains. Lipid rafts are also referred to as detergent-insoluble glycolipid-enriched membranes (DIGs), detergent-resistant membranes (DRMs) or glycolipid-enriched membranes (GEMs) (reviewed in Simons and Ikonen, 1997; Brown and London, 2000; Simons and Toomre, 2000; Maxfield, 2002; Dykstra *et al.*, 2003). Rafts form when sphingolipids and cholesterol associate into a liquid-ordered phase. In the absence of cholesterol, sphingolipids associate to form a relatively tightly packed gel-like bilayer. This tight association is facilitated by the sphingolipids' saturated acyl tails which have a relatively straight three-dimensional structure yet, is limited by the sphingolipids' hydrophobic head groups which are relatively bulky and result in voids existing between the acyl chains of adjacent

sphingolipids. Cholesterol is able to fill these voids to form a liquid-ordered phase. This liquid order phase floats as lipid rafts (~70-300 nm in size) within the liquid-disordered phase of the phospholipid bilayer (Figure 1.5).

Lipid rafts are evolutionarily conserved, appearing in *Saccharomyces cerevisiae* (yeast), *Caenorhabitis elegans* (worms), *Drosophila melangaster* (fruit flies) as well as in mammals (reviewed in Langlet *et al.*, 2000). This conservation, coupled with experimental evidence, suggests that lipid rafts play a pivotal role in many cellular processes including in protein sorting and trafficking (reviewed in Brown and London, 1998; Gruenberg 2001), in cell migration (Mañes *et al.*, 1999; Mañes *et al.*, 2001), in cell adhesion (reviewed in Pande, 2000), in cell-polarity (reviewed in Gomez-Mouton *et al.*, 2001) and in signal transduction (reviewed in Pierce *et al.*, 2002, Mañes *et al.*, 2001, Simons and Toomre, 2000). Moreover, lipid rafts function in chemokine receptor signaling (reviewed in Mañes *et al.*, 2001), growth receptor signaling (reviewed in Simons and Toomre, 2000) and in immunoreceptor signaling (reviewed in Dykstra *et al.*, 2003; Pierce, 2002; Cherukuri *et al.*, 2001).

Central to their role in receptor signaling, lipid rafts segregate proteins within the lateral plane of the plasma membrane (i.e., compartmentalize proteins). Lipid rafts specifically include and/or exclude proteins from within their domain based on biochemical interactions between the lipid raft and the proteins. While the natures of these interactions have yet to be fully elucidated, some generalizations are becoming apparent (reviewed in Dykstra *et al.*, 2003; Simons and Ikonen; 1997). For example glycophosphatidylinositol (GPI)-anchored proteins preferentially associate with lipid rafts (Danielsen, 1995; Fra *et al.*, 1994; Brown and Rose, 1992) as do dually acylated proteins (e.g., Lyn and Blk of the Src family kinases) (Kosugi *et* al., 2001; McCabe and Berthiaume, 2001; McCabe and Berthiaume, 1999; van't Hof and Resh, 1997). A variety of cell surface receptors associate inducibly with lipid rafts following receptor engagement (reviewed in Pierce, 2002; Cheng *et al.*, 2001; Mañes *et al.*, 2001; Simons and Toomre, 2000). Thus, lipid rafts may aid in the spatiotemporal regulation of signaling by serving as platforms upon which macromolecular signaling complexes can be specifically assembled and regulated.

Importantly, disruption of lipid rafts impairs BCR-induced PLCγ signaling (Aman and Ravichandran, 2000; Guo *et al.*, 2000). Therefore, lipid rafts may play an important role in the BCR/PLCγ pathway. Chapter three of this thesis investigates the mechanisms regulating BCR

lipid raft translocation. At the onset of this thesis it was largely unclear how this event was mediated. Nonetheless, previous studies have demonstrated that the antigen-binding subunit (mIgM) of the BCR is capable of translocating into lipid rafts in the absence of Igα/β heterodimer (Cheng *et al.*, 2001). This suggested that the mIgM subunit may alone be responsible for directing BCR lipid raft translocation upon BCR cross-linking. Yet, the possibility remained that the Igα/β heterodimer contributes to this process. Thus, I investigated whether the Igα/β heterodimer alone is able to translocate into the lipid rafts following cross-linking. These studies helped to define the molecular mechanisms underlying BCR lipid raft translocation and further defined the roles of the mIgM and the Igα/β heterodimer in BCR signaling.

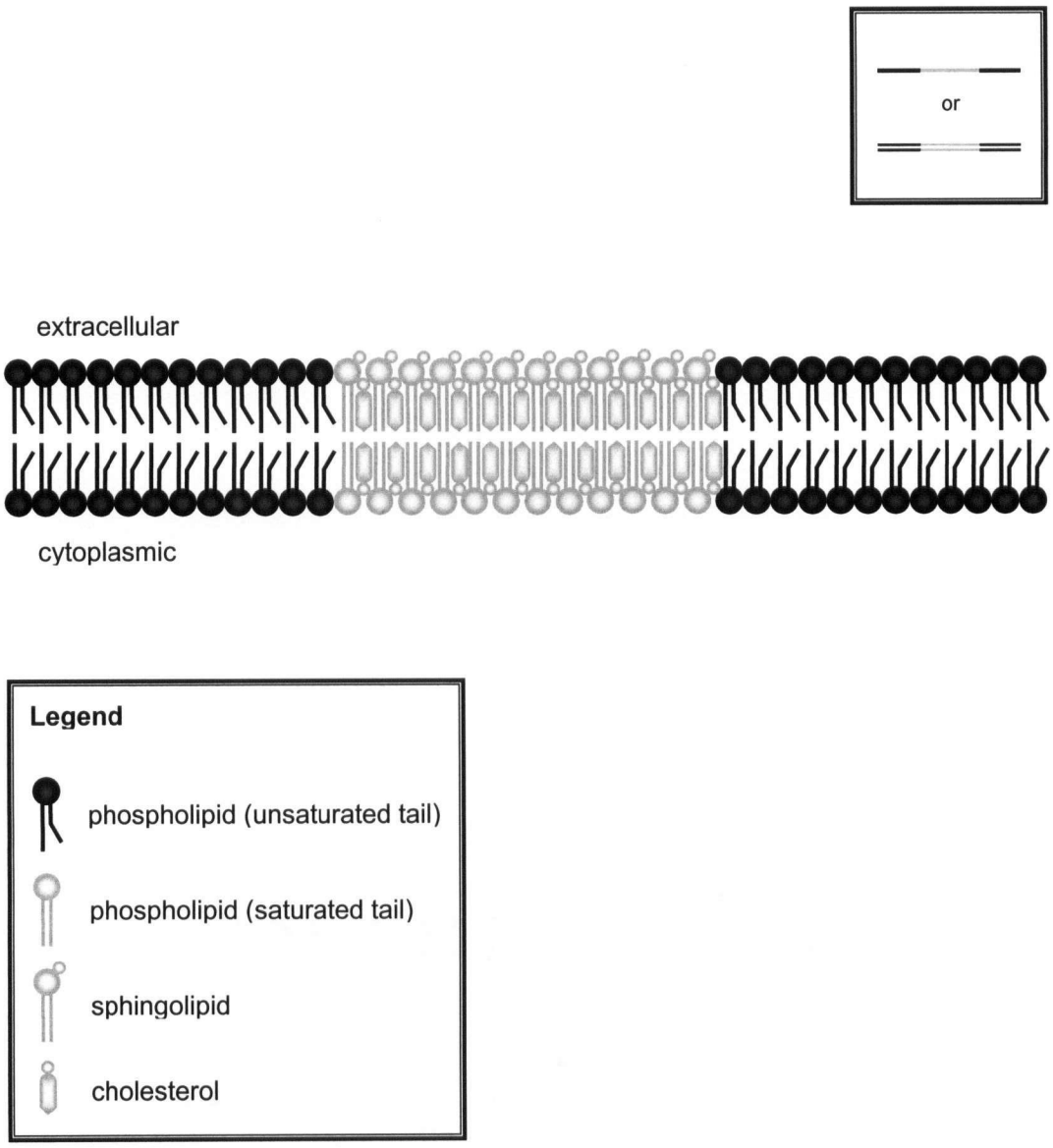

Figure 1.5 Schematic Representation of Lipid Rafts. Lipid rafts are sphingolipid- and cholesterol-rich membrane microdomains that are proposed to float within the phospholipid bilayer (reviewed in Simons and Ikonen, 1997; Brown and London, 2000; Simons and Toomre, 2000; Maxfield, 2002; Dykstra *et al.*, 2003). Based on their biochemical structure lipid rafts are proposed to preferentially include or exclude various proteins within their domains and thus, represent a specific cellular compartment. The inset in the top right hand corner indicates lipid rafts as they are represented throughout this thesis.

1.6 An Overview of BCR Signaling

B cells play an integral role in the immune system's defense against invasive microorganisms. Requisite to the B cell's protective role is its ability to signal through cell-surface BCRs. Defects in initiating or transducing BCR signals can lead to immunodeficiency diseases (in the case of abrogated signaling) or to autoimmune diseases and lymphomas (in the case of aberrant signaling). Thus, BCR signaling has been extensively researched in an effort to understand and eradicate these diseases.

While the models of BCR signaling are ever-evolving, several key pathways have been largely identified and deciphered (reviewed in Kurosaki, 1999; Kurosaki, 2000; Kurosaki *et al.*, 2000; Niiro and Clark, 2002; Gold, 2002; Pierce, 2002). BCR signaling involves three key pathways: the phosphatidyl-inositol 3 kinases (PI3K) pathway, the Ras/Mitogen Activated Protein Kinase (Ras/MAPK) pathway and the phospholipase C gamma (PLCγ) pathway. These pathways are detailed below as being linear and independent. This is done to provide the reader with some initial clarity. However, such an approach does little to illustrate the intricacies of BCR signaling that are so essential to regulating B cell fate. Thus, the reader is asked to bear in mind that these pathways are truly interconnected, forming a BCR signaling network that ultimately exists influentially and receptively within the cell's complex signaling milieu.

1.6.1 Initiation of BCR Signaling

The BCR exists as pre-formed oligomeric complexes on the surface of resting mature B cells (Schamel and Reth, 2000; reviewed in Reth *et al.*, 2000; Matsuuchi and Gold, 2001). These oligomers may weakly associate with downstream signaling components to provide a low level, antigen-dependent signal that is required for mature B cell survival (Lam *et al.*, 1997; Schamel and Reth, 2000; reviewed in Reth *et al.*, 2000; Matsuuchi and Gold, 2001). Upon antigen-binding, the oligomers coalesce into larger complexes that subsequently translocate into lipid rafts (Cheng *et al.*, 1999; Aman and Ravichandran, 2000; Petrie *et al.*, 2000; Weintraub *et al.*, 2000; Dillon *et al.*, 2000; Schamel and Reth, 2000; reviewed in Reth *et al.*, 2000; Matsuuchi and Gold, 2001; Pierce, 2002). Such translocation co-localizes the BCR oligomers with proximal signaling components while isolating them from negative regulators, thereby facilitating BCR signaling (reviewed in Matsuuchi and Gold, 2001; Pierce, 2002; Dykstra *et al.*, 2003).

Within the lipid rafts the BCR initiates a protein tyrosine phosphorylation cascade (Gold *et al.*, 1990; Gold *et al.*, 1991). This cascade involves several protein tyrosine kinases (PTKs) including the Src family kinase (SFK) members, Blk, Fyn, Lck and Lyn, the Tec family member, Bruton's tyrosine kinase (BTK), and the SH2 domain containing non-receptor protein tyrosine kinase, Syk (reviewed in Kurosaki *et al.*, 2000). Initially, the translocated BCR associates with Lyn (reviewed in Kurosaki *et al.*, 2000). Lyn is constitutively associated with and active within lipid rafts where it may be protected from its negative regulator Csk (Alland *et al.*., 1994; Koegl *et al.*, 1994; Sigal *et al.*, 1994; Cheng *et al.*, 1999; reviewed in Resh, 1999). Furthermore, Lyn associates with the non-phosphorylated Igα/β motifs via its N-terminal domain (Plieman *et al.*, 1994). Thus, Lyn is ideally positioned to associate with and phosphorylate the Igα/β ITAMs of the translocated BCR. Such phosphorylation facilitates further recruitment of Lyn, Blk, Fyn and Syk via their respective SH2 domains (Yamanashi *et al.*, 1991; Lin and Justemant, 1992; Campbell and Sefton, 1992; Law *et al.*, 1993; Burg *et al.*, 1994; Clark *et al.*, 1994; Johnson *et al.*, 1995). This recruitment brings the SFKs into close proximity such that they can undergo autophosphorylation and activation (Kurosaki *et al.*, 1994; Johnson *et al.*, 1995; Siderenko *et al.*, 1995; Takata and Kurosaki, 1995). The active SFKs then further phosphorylate the Igα/β heterodimer in a positive feedback loop. As well the SFKs phosphorylate and activate the recruited Syk and then, together with Syk, contribute to BTK phosphorylation and activation (Mahajan *et al.*, 1995; Rawling *et al.*, 1996; Afar *et al.*, 1996; Kurosaki and Kurosaki 1997; Baba *et al.*, 2001). The active SFKs, Syk and BTK then go on to perpetuate a protein tyrosine phosphorylation cascade that ultimately activates the PI3K, Ras/MAPK and PLCγ pathways (Summarized in Fig. 1.6) (Nel *et* al., 1984; Campbell and Sefton, 1990; Gold *et al.*, 1991; Law *et al.*, 1992; reviewed in Kurosaki, 1999; Kurosaki, 2000; Niiro and Clark, 2002; Gold, 2002; Pierce, 2002).

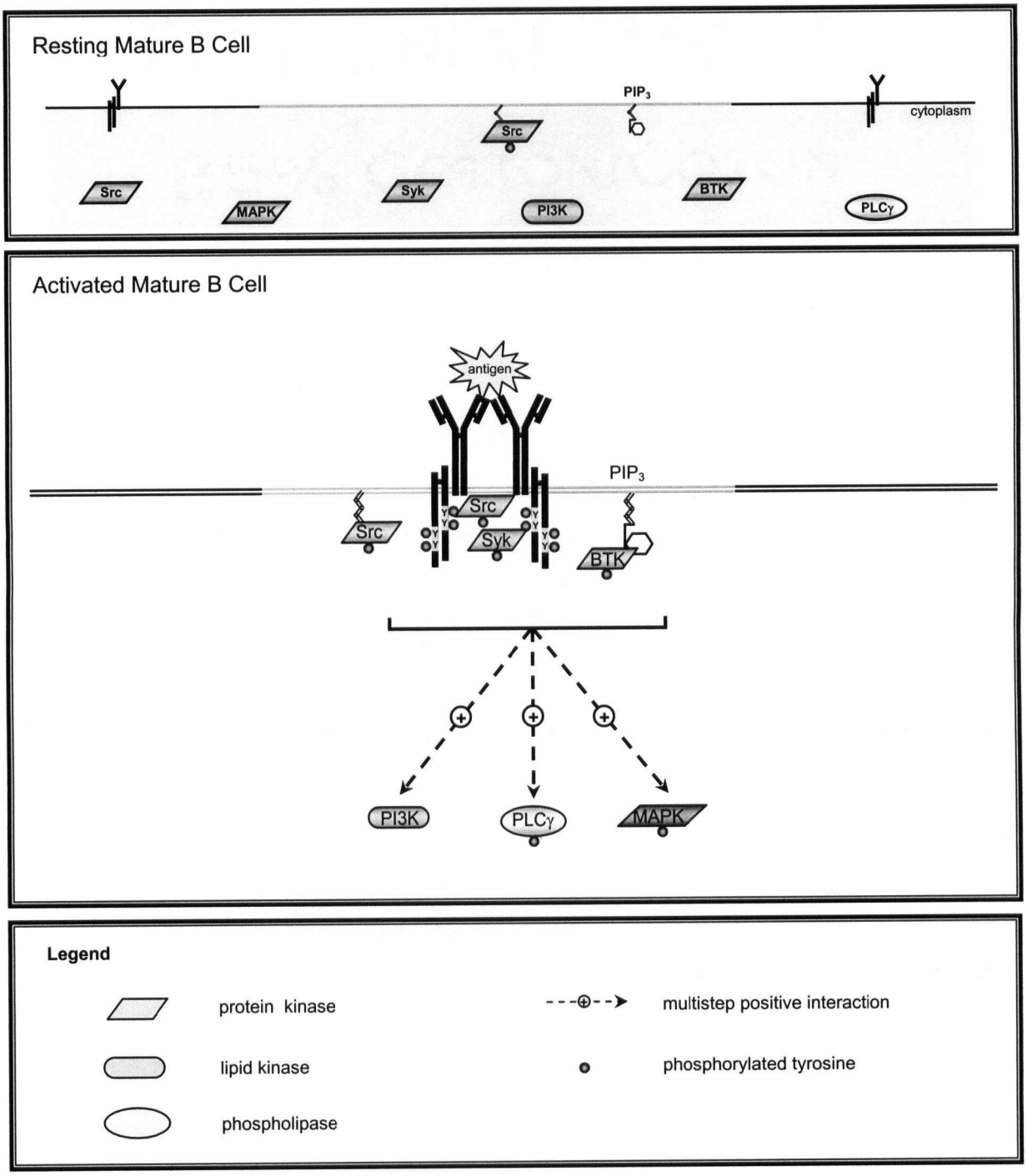

Figure 1.6. Summary of the Initial Events of BCR Signaling. In resting mature B cells the BCR is dispersed throughout the plasma membrane. While an active portion of Lyn is localized to lipid rafts the majority of the SFKs as well as Syk, BTK, PI3K, MAPK and PLCγ remain dispersed throughout the cytoplasm and inactive (top panel). Following BCR cross-linking the BCR translocates into lipid rafts where it associates with active Lyn and becomes tyrosine phosphorylated. The phosphorylated tyrosines act as docking sites for SH2 domain containing proteins including the SFKs and Syk. Once so docked the SFKs autophosphorylate and activate one another as well as phosphorylating and activating Syk. The SFKs and Syk then phosphorylate and activate BTK, which may be recruited to the plasma membrane and/or the BCR signaling complex by way of its SH2 domain binding to membrane-bound PIP_3. The active SFKs, Syk and BTK then go on to perpetuate a tyrosine phosphorylation cascade that ultimately activates the PI3K, Ras/MAPK and PLCγ pathways.

1.6.2 The PI3K Pathway

The BCR/PI3K pathway (Fig. 1.7) is required both for B cell development and for activation of mature B cells (Gold and Aebersold, 1994; Fruman *et al.*, 1999; Suzuki *et al.*, 1999; Clayton *et al.*, 2002; reviewed in Gold, 2002; Okkenhaug and Vanhaesenbrock, 2003). In mature B cells, BCR cross-linking leads to plasma membrane recruitment and activation of PI3K (reviewed in Gold, 2002; Okkenhaug and Vanhaesenbrock, 2003). PI3K subsequently phosphorylates its membrane-associated substrates, phosphatidyl inositol-4-phosphate (PI-4-P) and phosphatidyl inositol-4,5-bisphosphate (PI-4,5-P_2), to produce phosphatidyl inositol-3,4-bisphosphate (PI-3,4-P_2) and phosphatidyl inositol-3,4,5-trisphosphate (PI-3,4,5-P_3) (reviewed in Gold, 2002; Okkenhaug and Vanhaesenbrock, 2003). In turn, these products recruit various cytosolic signaling proteins to the plasma membrane and the vicinity of the BCR signaling complex by way of their pleckstrin homology (PH) domains and thereby facilitate the activation of several downstream signaling pathways.

To date it remains unclear as to how BCR-induced PI3K plasma membrane recruitment and activation is mediated. Nonetheless numerous different mechanisms have been proposed to contribute to this process (reviewed in Gold *et al.*, 1999). The predominant mechanism appears to involve PI3K being membrane-recruited via its SH2 domain. In particular, PI3K has been shown to bind to the membrane-associated, tyrosine phosphorylated proteins CD19 (Tuveson *et al.*, 1993), Gab1 (Ingham *et al.*, 2001), Gab2 (Gu *et al.*, 1998) and B cell adapter for PI3K (BCAP) (Okada *et al.*, 2000) following BCR cross-linking (reviewed in Gold, 2002). Alternatively, PI3K may be membrane-recruited via its proline-rich domains binding to the Src homology 3 (SH3) domains of plasma membrane-associated SFKs (Prasad *et al.*, 1993; Plieman *et al.*, 1994b). Still, PI3K may be membrane-recruited via an interaction with membrane-bound, active Ras (Rodriquez-Viciana *et al.*, 1994). Regardless of the mechanism, PI3K plasma membrane recruitment is necessary to bring PI3K in close proximity to its membrane-bound substrates which it then converts into PI-3,4-P_2 and PI-3,4,5-P_3.

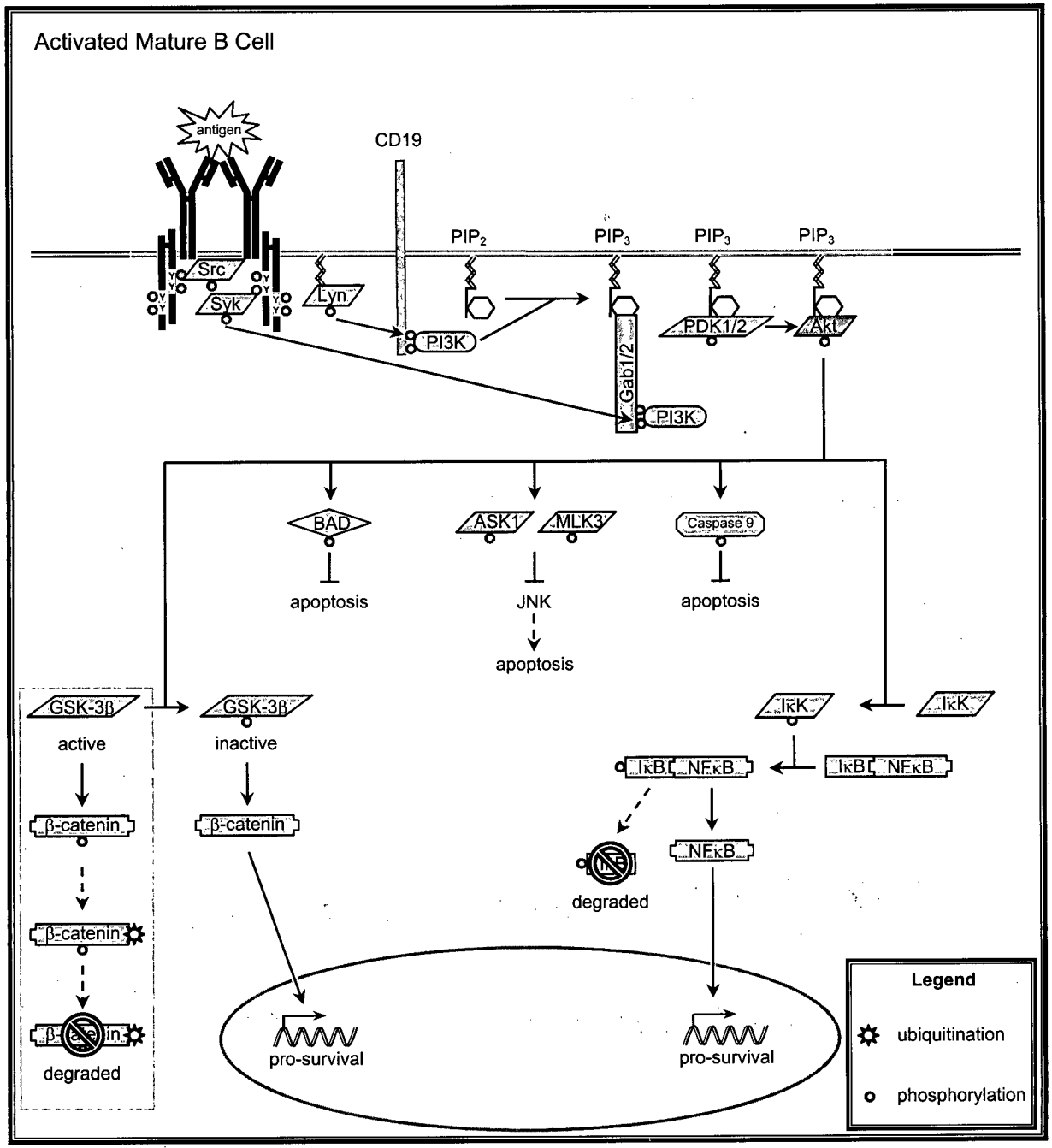

Figure 1.7. Summary of the BCR/PI3K Pathway. BCR cross-linking initiates a protein tyrosine phosphorylation cascade. Among those proteins phosphorylated is the CD19 co-receptor. PI3K is recruited to tyrosine phosphorylated CD19 by way of its SH2 domains. Once recruited and activated PI3K phosphorylated its membrane-bound substrate PIP_2 to produce PIP_3 which then serves as a membrane docking site for numerous PH domain containing proteins. In particular, the Gab1 and Gab2 (Gab1/2) adapter proteins are recruited to the plasma membrane by way of their SH2 domains. Gab1/2 subsequently become phosphorylated and serve as additional sites for PI3K membrane docking, thereby functioning as a positive feedback loop. As well, the kinases, PDK1, PDK2 and AKT are recruited to the membrane by way of their PH domains. PDK1 and PDK2 (PDK1/2) then phosphorylate and activate AKT which subsequently phosphorylates GSK-3β, BAD, ASK1, MLK3, Caspase 9 and IκK to prevent apoptosis and promote cell survival. As well, PI3K activity has been shown to contribute to activation of the PKC which subsequently activates MAPKs (Erk1/2) and SAPKs (JNK and p38) (not shown).

Plasma membrane levels of PI-3,4-P_2 and PI-3,4,5-P_3 are tightly regulated as these molecules influence numerous downstream signaling pathways. In terms of BCR signaling, the Gab1 and Gab2 adapter proteins associate with PI-3,4,5-P_3 via their respective PH domains (Gu *et al.*, 1998; Ingham *et al.*, 2001; reviewed in Gold, 2002). Once recruited to the plasma membrane, these proteins become tyrosine phosphorylated by BCR-associated and activated PTKs (Gu *et al.*, 1998; Ingham *et al.*, 2001; reviewed in Gold, 2002). These proteins then amplify the PI3K signal by further recruiting PI3K to the plasma membrane by way of its SH2 domain (Gu *et al.*, 1998; Ingham *et al.*, 2001; reviewed in Gold, 2002). As well, PI-3,4,5-P_3 facilitates the membrane recruitment of phosphoinositide-dependent kinase 1 and 2 (PDK1 and PDK2) (Alessi *et al.*, 1997a; Alessi *et al.*, 1997b) and Akt (Burgering and Coffer, 1995; Stokoe *et* al., 1997) via their respective PH domains (Alessi *et al.*, 1997a; Alessi *et al.*, 1997b). Once recruited to the plasma membrane, PDK1 and PDK2 phosphorylate Akt and contribute to its activation (Alessi *et al.*, 1997a; Alessi *et al.*, 1997b; Stokoe *et al.*, 1997; Anderson *et al.*, 1998; Filipaa *et al.*, 2000; Wick *et al.*, 2000). Activated Akt then promotes B cell survival via several pathways, only some of which are detailed here. Along one pathway, Akt phosphorylates glycogen synthase 3β (GSK-3β) (Hajduch *et al.*, 1998; van Weeren *et al.*, 1998) preventing it from associating with and phosphorylating the β-catenin transcription factor (Cross *et al.*, 1995; Pap and Cooper, 1998). This allows β-catenin to escape degradation and to translocate into the nucleus where it induces the transcription of cell-survival genes (Rubinfeld *et al.*, 1996; Monick *et al.*, 2001). Along another pathway Akt phosphorylates and inactivates the pro-apoptotic protein BAD thus further promoting B cell survival (Datta *et al.*, 1997). Additionally, Akt phosphorylates caspase 9 preventing it from initiating a pro-apoptotic proteolytic cascade (Cardone *et al.*, 1998). Moreover, Akt phosphorylates the Iκ kinase (IκK) which subsequently phosphorylates the inhibitor of NF-κB (IκB) targeting it for degradation and releasing the transcription factor, NF-κB such that it can translocate into the nucleus where it too induces the transcription of cell-survival genes (Scott *et al.*, 1998; Kane *et al.*, 1999; Ozes *et al.*, 1999; Romashkova and Makarov, 1999). As well, Akt phosphorylates the apoptosis-signaling regulating kinase (ASK1) and MLK3, inhibiting their activity which ultimately results in the inhibition of a pro-apoptotic JNK pathway (Kim *et al.*, 2001; Suhara *et al.*, 2002; Barthwal *et al.*, 2003). Thus, BCR cross-linking can be seen to promote B cell survival, in part, through the PI3K pathway.

1.6.3 The PLCγ Pathway

The BCR/PLCγ pathway (Fig.1.8) is required both for B cell development and for mature B cell proliferation (Hashimoto *et al.*, 2000; Wang *et al.*, 2000). BCR cross-linking in mature B cells leads to plasma membrane-recruitment , tyrosine phosphorylation and activation of both PLCγ1 and PLCγ2 (Bijsterbosch *et al.*, 1985; Fahey and DeFranco, 1987; Carter *et al.*, 1992; Coggeshall *et al.*, 1991; Coggeshall *et al.*, 1992; Hempel *et al.*, 1992; Roifman and Wang, 1992; Siderenko *et al.*, 1995; DeBell *et al.*, 1999). The PLCγ isoforms then hydrolyze plasma membrane-bound phosphatidyl inositol-3,4-bisphosphate (PI-3,4-P_2 or, more simply, PIP_2) to produce plasma membrane-bound diacylglycerol (DAG) and cytosolic inositol trisphosphate (IP_3). In turn, these products initiate several well-characterized signaling pathways that eventually culminate in the nucleus (reviewed in Kurosaki *et al.*, 2000; Gold; 2002) where they assist in promoting B cell survival and proliferation.

As recently as a decade ago the mechanisms coupling BCR cross-linking to PLCγ membrane recruitment, phosphorylation and activation were enigmas. PLCγ is proposed to be recruited to the BCR signaling complex via the B cell linker protein (BLNK) (Fu and Chan., 1997; Fu *et al.*, 1998; Goitsuka *et al.*, 1998; Wienands *et al.*, 1998; Ishiai *et al.*, 1999a; Ishiai *et al.*, 1999b; reviewed in Kurosaki, 2000; Gold, 2002). In the simplest model BLNK is recruited to the BCR complex by way of its SH2 domain which binds to phosphorylated Igα tyrosine residues located outside of the ITAM (Engels *et al.*, 2000, Kabak *et al.*, 2002; reviewed in Gold, 2002). This brings BLNK into close proximity with BCR-associated Syk which subsequently phosphorylates BLNK on multiple tyrosine residues (Fu *et al.*, 1998; Goitsuka *et al.*, 1998; Chui *et al.*, 2002). Tyrosine phosphorylated BLNK then associates with BTK (Hashimoto *et al.*, 1999; Su *et al.*, 1999; Chui *et al.*, 2002) and PLCγ (Fu and Chan, 1997; Fu *et al.*, 1998; Ishiai *et al.*, 1999; Chui *et al.*, 2002) by way of their respective SH2 domains. This results in the formation of a BCR/PLCγ signaling complex where the BCR, BLNK, the SFKs, Syk, BTK and PLCγ are all in close association. This in turn, enables the SFKs (Mahajan *et al.*, 1995; Rawlings *et al.*, 1996; Afar *et al.*, 1996) and Syk (Kurosaki *et al.*, 1997; Baba *et al.*, 2001) to contribute to BTK phosphorylation and activation. Then BTK, (Takata and Kurosaki, 1996; Rawlings, 1999) together with Syk (Takata *et al.*, 1994), phosphorylates PLCγ and contributes to its activation (reviewed in Kurosaki and Tsukada, 2000; Gold, 2002).

Once activated, PLCγ hydrolyses its plasma membrane-bound substrate, PIP_2 to produce the second messengers, IP_3 and DAG (Bijsterbosch *et al.*, 1985; Fahey and DeFranco, 1987; Rhee *et al.*, 1989; reviewed in Marshall *et al.*, 2000; Kurosaki *et al.*, 2000). IP_3 then binds to IP_3 receptors on the endoplasmic reticulum to induce an intracellular calcium flux that is followed by an extracellular calcium flux (Sugawara *et al.*, 1997; Miyakawa *et al.*, 1999; reviewed in Kurosaki *et al.*, 2000). The elevated intracellular calcium levels activate several calcium-dependent enzymes including the serine/threonine phosphatase, calcineurin. Active calcineurin dephosphorylates the cytosolic component of nuclear factor of activated T cells ($NFAT_c$) which then translocates into the nucleus where it forms a variety of transcriptional activation complexes that ultimately promote B cell survival and proliferation (Timmerman *et al.*, 1996; Dolmetsch *et al.*, 1997; reviewed in Marshall *et al.*, 2000; Gold, 2002).

The elevated intracellular calcium levels, along with DAG, also activate several isoforms of protein kinase C (PKC) (Sidorenko *et al.*, 1996; Barbazuk and Gold, 1999; reviewed in Marshall *et al.*, 2000). Active PKC then contributes to the phosphorylation of IκB, targeting it for degradation (DiDonato *et al.*, 1997) and affecting the release of NF-κB. NF-κB then translocates into the nucleus where it forms a variety of transcriptional activation complexes that ultimately contribute to B cell survival and proliferation (Lenardo and Baltimore, 1989; reviewed in Gold, 2002). Elevated calcium and DAG levels also influence the Ras/MAPK pathway (pathway detailed below in Chapter 1.5.4) (Casillas *et al.*, 1991; Gold *et al.*, 1992; reviewed in Gold, 2000). These effects can be mediated either by DAG binding to and activating the Ras guanyl nucleotide-releasing protein (RasGRP) that subsequently activates the pathway (Tognon *et al.*, 1998) or by PKC phosphorylating and activating downstream components of the pathway such as Raf-1, MEK1 or MEK2 (reviewed in Gold, 2000). Regardless of the mechanism, activation of Ras/MAPK pathway ultimately contributes to B cell survival and proliferation. Thus, the BCR/PLCγ pathway can be seen to promote B cell survival and proliferation both directly and indirectly.

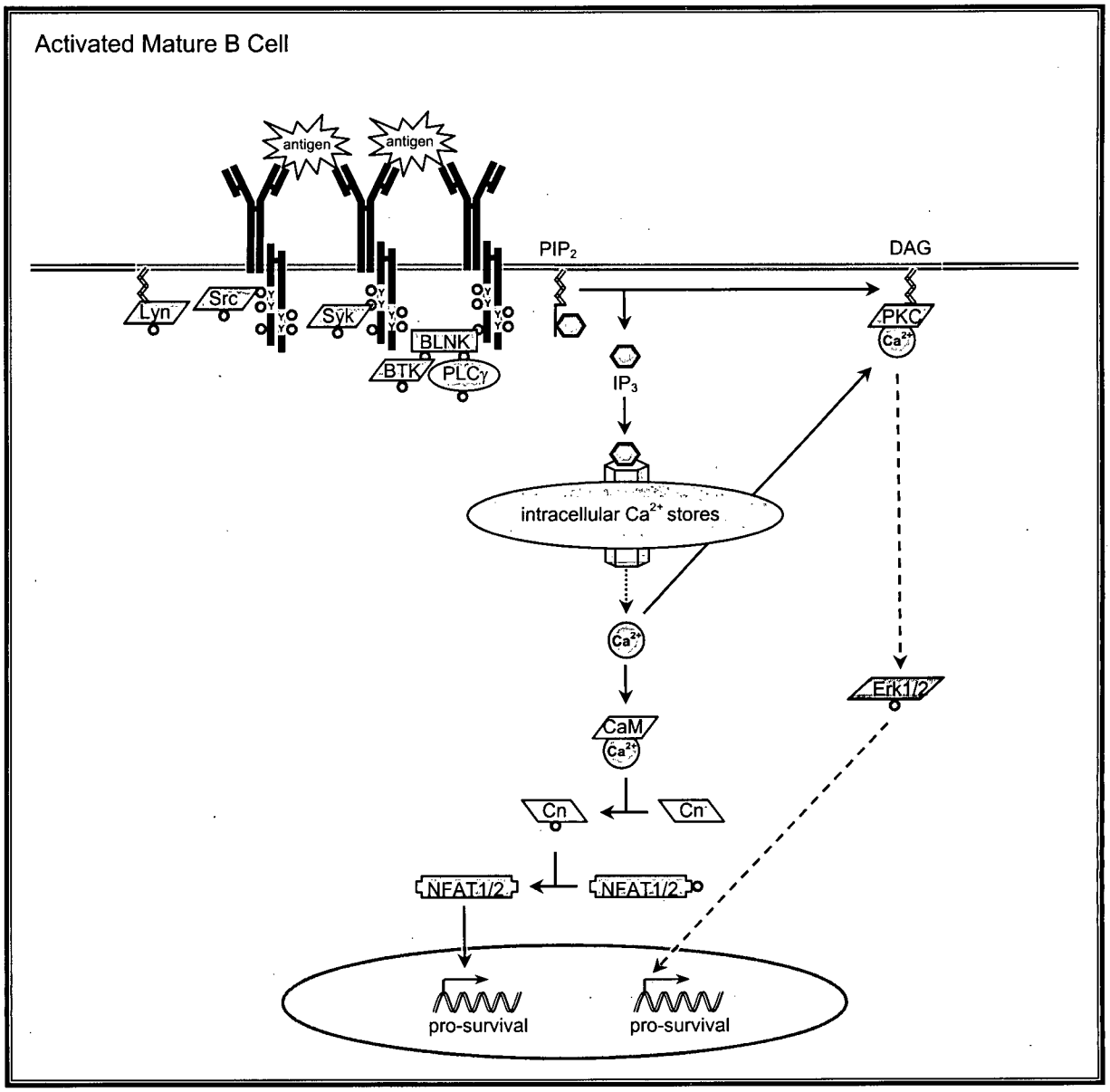

Figure 1.8. Summary of the BCR/PLCγ Pathway. BCR cross-linking initiates a protein tyrosine phosphorylation cascade. Among the first proteins phosphorylated is the Igα/β heterodimer. The cytoplasmic adapter protein, BLNK is then recruited to the BCR signaling complex by way of its SH2 domain binding to phosphorylated Igα. Such recruitment is thought to facilitate BLNK's phosphorylation by Syk. BTK and PLCγ are then recruited to the BCR complex by way of their SH2 domains binding to phosphorylated BLNK. The BCR-associated Syk and SFKs then phosphorylate the recruited BTK, contributing to its activation. In turn, BTK and Syk phosphorylate the recruited PLCγ, contributing to its activation. Active PLCγ then hydrolyzes its membrane bound substrate, PIP_2, to produce the second messengers, IP_3 and DAG. Subsequently, IP_3 binds to the IP_3 receptors, resulting in the release of intracellular calcium stores. The resultant flux in intracellular calcium leads to the activation of the protein kinase, calmodulin, which in turn phosphorylates and activates the protein phosphatase, calcineurin. Calcineurin then dephosphorylates the transcription factor, NF-AT, enabling it to translocate to the nucleus where it promotes the transcription of pro-survival genes. DAG, alone or in conjunction with the calcium flux, activates several forms of PKC which in turn contribute to the activation of the MAPK pathway (indicated by Erk1/2 in the above) which also promotes cell survival (refer to Chapter 1.5.4 for further details of the MAPK pathway).

1.6.4 The Ras/MAPK Pathway

The BCR/Ras/MAPK pathway is required for B cell development (Iritani *et al.*, 1997) and for inducing proliferation of mature B cells (Richards *et al.*, 2001). In mature B cells, BCR cross-linking leads to activation of the plasma membrane-associated GTPase, Ras, which in turn mediates the activation of a well characterized kinase cascade (Harwood and Cambier, 1993; Lazarus *et al.* 1993; Saxton *et* al., 1994; Tordai *et al.*, 1994). Ras activation itself is mediated both by a PLCγ-dependent pathway and by a PI3K-dependent pathway (reviewed in Gold, 2002) (Fig. 1.9). In the PLCγ-dependent pathway, the Ras guanyl nucleotide-releasing protein (RasGRP) is recruited to the plasma membrane and activated via its interaction with DAG, a product of active PLCγ (Tognon *et al.*, 1998; Oh-hora *et al.*, 2003). RasGRP then interacts with GDP-bound Ras where it exchanges guanine triphosphate (GTP) for the guanine diphosphate (GDP) thereby, activating Ras (reviewed in Gold, 2002). In the PI3K-dependent pathway, Ras is activated by the Son of Sevenless (SOS) guanine nucleotide exchange factor which is recruited to the plasma membrane via the formation of a PI3K-dependent multi-adapter complex (reviewed in Gold, 2002). Initially, SOS associates with the adapter protein, Grb2. The SOS/Grb2 complex is then recruited from the cytosol to the plasma membrane via Grb2's SH2 domain which associates with either the tyrosine phosphorylated adapter protein, Shc (Saxton *et al.*, 1994) or with the tyrosine phosphorylated Src homology 2 domain-containing protein tyrosine phosphatase 2 (SHP-2) (reviewed in Gold, 2002). Shc and SHP-2 are themselves localized to the plasma membrane via their SH2 domains which interact with tyrosine phosphorylated Gab1 and/or Gab2 (Gu *et al.*, 1998; Gold *et al.*, 2000). And ultimately, Gab1 and Gab2 are localized to the plasma via their PH domains which associate with the PI3K product, PI-3,4,5-P_3 (as described in Chapter 1.5.2). Thus, BCR cross-linking can activate the Ras/MAPK pathway via a PLCγ-dependent pathway or a PI3K-dependent pathway.

Once activated Ras associates with the 14-3-3/Raf complexes and dephosphorylates the 14-3-3 protein such that it can no longer inhibit Raf's activity (Cook and McCormick, 1993). Subsequently, the active Raf1 phosphorylates and activates the dual-specificity MAPK kinases MEK1 and MEK2. In turn, MEK1 and MEK2 phosphorylate the MAPKs, ERK1 and ERK2 (reviewed in Su and Karin, 1996). The phosphorylated ERKs then translocate into the nucleus where they phosphorylate multiple transcription factors that ultimately up-regulate the

expression of proliferative genes (reviewed in Su and Karin, 1996). Thereby, BCR cross-linking can be seen to promote B cell proliferation, in part, through the Ras/MAPK pathway.

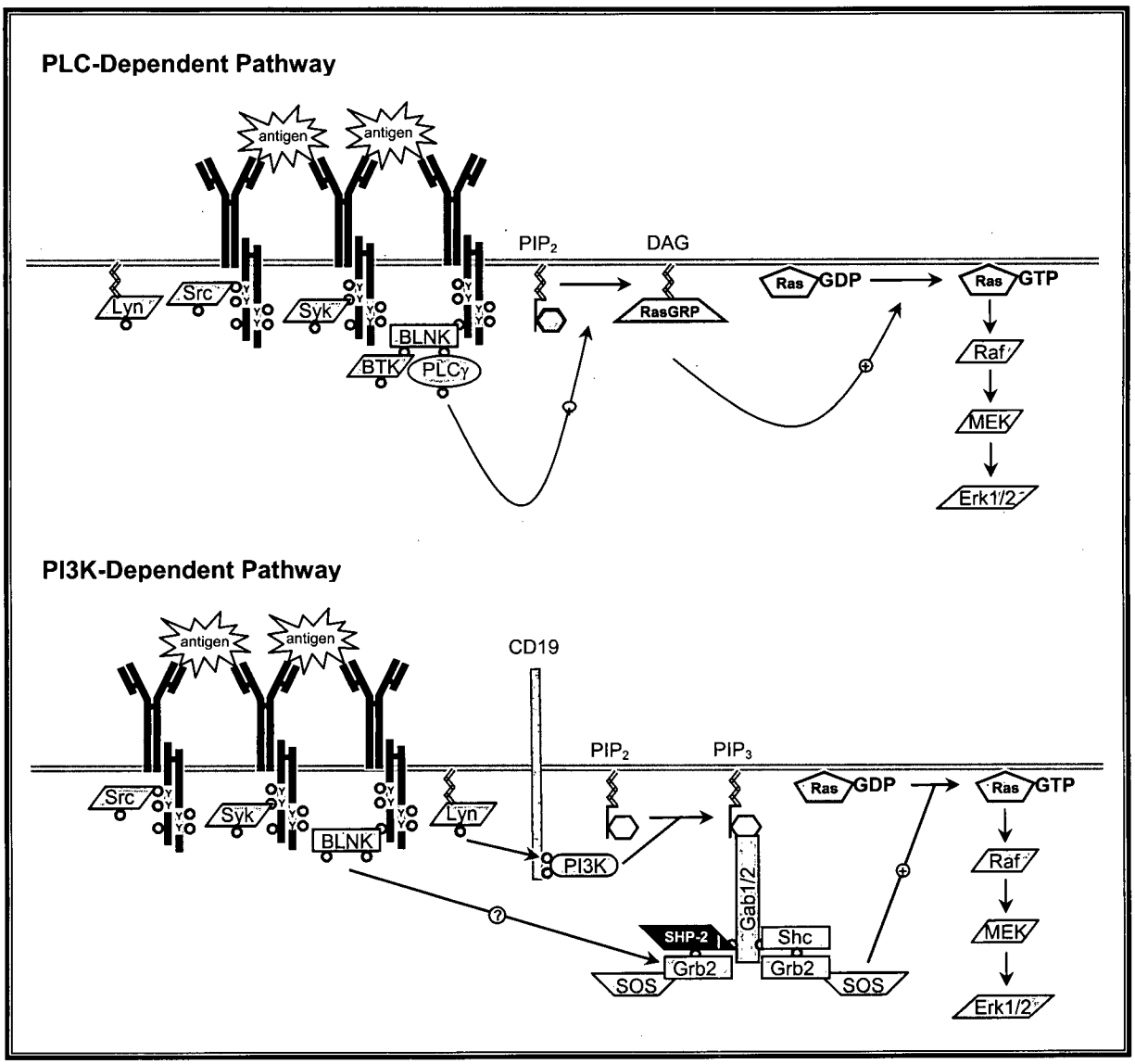

Figure 1.9. The Ras/MAPK Pathway. Ras activation is mediated both by a PLCγ-dependent pathway and by a PI3K-dependent pathway (reviewed in Gold, 2002). In the PLCγ-dependent pathway, RasGRP is recruited to the plasma membrane and activated via its interaction with DAG, a product of active PLCγ. RasGRP then interacts with GDP-bound Ras where it exchanges GTP for GDP thereby activating Ras. In the PI3K-dependent pathway, Ras is activated by the SOS guanine nucleotide exchange factor which is recruited to the plasma membrane via the formation of a PI3K-dependent multi-adapter complex (reviewed in Gold, 2002). Initially, SOS associates with the adapter protein, Grb2. The SOS/Grb2 complex is then recruited from the cytosol to the plasma membrane via Grb2's SH2 domain which associates with either tyrosine phosphorylated Shc or tyrosine phosphorylated SHP-2. Shc and SHP-2 are themselves localized to the plasma membrane via their SH2 domains which interact with tyrosine phosphorylated Gab1 and Gab2. Gab1 and Gab2 are themselves localized to the plasma via their PH domains which associate with the PI3K product, PI-3,4,5-P_3. Interestingly, BLNK has also been shown to associating with the Grb2 adapter protein forming a complex of unknown consequence. Once activated, Ras phosphorylates and activates the MAPK kinase kinase (MAPKKK), Raf1. Subsequently, Raf1 phosphorylates activates the dual-specificity MAPK kinases MEK1 and MEK2. MEK1 and MEK2 then phosphorylate the MAPKs, ERK1 and ERK2 enabling them to translocate into the nucleus where they phosphorylate multiple transcription factors that ultimately up-regulate the expression of proliferative genes. And thus, BCR cross-linking promotes B cell proliferation, in part, through a PLCγ-dependent and a PI3K-dependent Ras/MAPK pathway.

1.7 The Enigmas of BCR Signaling

As evidenced by the above discussion, our knowledge of BCR signaling has greatly advanced in the past quarter century. Loss-of-function studies have clearly established the role of PTKs and the Ras/MAPK, PI3K, and PLCγ pathways within this process. As well, the downstream components and consequences of these pathways have been well-elucidated. Nonetheless, many aspects of BCR signaling remain enigmatic and thus the investigation into BCR signaling continues. This thesis has focused primarily on elucidating the questions that remain regarding the BCR/PLCγ pathway. Therefore, to provide the reader with a better understanding of these questions and the purpose of this thesis, a more detailed account of our current understanding of the BCR/PLCγ pathway is provided below.

1.8 The BCR/PLCγ Pathway in Detail

1.8.1 PLCγ Structure and Function

The phospholipase C (PLC) family is divided into three subfamilies termed PLCβ, PLCδ, and PLCγ (reviewed in Katan, 1998; Sekiya *et al.*, 1999; Rhee, 2001). Common to all PLC family members are, from the N-terminus to the C-terminus, a PH domain, several EF-hand domains, a C2 domain, an X domain and a Y domain (Fig. 1.9). The PH domain binds to membrane-bound phosphoinositides and may assist in targeting the typically cytosolic PLC family members to the plasma membrane where they have access to their plasma membrane-bound substrate. The C2 domain binds to phosphoinositides in a calcium-dependent manner and may target PLC family members to the plasma membrane. The EF-hand domains appear to confer flexibility on the proteins such that they can undergo changes in their tertiary structure and consequently, their activity. And finally, the X and Y domains together form the catalytic site that is responsible for hydrolyzing PIP_2 to produce the second messengers, DAG and IP_3.

The PLCγ subfamily structurally differs from the PLCβ and PLCδ subfamilies by containing an approximately 400 amino acid insert between the X and Y domains (reviewed in Katan, 1998; Sekiya *et al.*, 1999). This insert contains multiple interaction domains that include two tandem SH2 domains and an SH3 domain that are flanked by a fragmented PH domain. The SH2 domains bind to tyrosine-phosphorylated proteins, the SH3 domain binds to proline-rich proteins

and the fragmented PH domain is proposed to form a functional domain in the tertiary structure that also binds to phosphoinositides. Together these domains mediate PLCγ's association with various signaling proteins and ultimately contribute to regulating its activation (reviewed in Rhee and Bae, 1997; Sekiya *et al.*, 1999; Kurosaki *et al.*, 2000; Marshall *et al.*, 2000).

The PLCγ subfamily includes PLCγ1 (~150 kD) and PLCγ2 (~145 kD). These proteins are similarly organized, share 50% amino acid sequence identity and share very similar tertiary structures (Rhee *et al.*, 1989; reviewed in Sekiya *et al.*, 1999; Rhee, 2001). Despite these similarities, the PLCγ isoforms show differences in their expression patterns and in their roles in cellular signaling (reviewed in Carpenter and Ji, 1999; Sekiya *et al.*, 1999; Kurosaki *et al.*, 2000; Marshall *et al.*, 2000; Rhee, 2001). PLCγ1 is ubiquitously expressed and is absolutely required for mammalian growth and development (Ji *et al.*, 1997; reviewed in Rhee and Bae, 1997; Carpenter and Ji, 1999; Sekiya *et al.*, 1999). In contrast, PLCγ2 expression appears to be largely restricted to B cells where it is required for BCR signaling (Takata *et al.*, 1995; reviewed in Noh *et al.*, 1995, Sekiya *et al.*, 1999; Rhee, 2001).

All told, the PLC family is responsive to over one hundred cellular receptors and as such is involved in numerous cellular processes (reviewed in Rhee, 2001). The combination and specific amino acid sequence of the various regulatory regions (i.e., the PH, SH2, SH3, EF-hand and C2 domains) determines the responsiveness of the various PLC isoforms. Based on this, PLCβ isoforms respond primarily to G protein-coupled receptors, while PLCδ isoforms respond primarily to increases in intracellular calcium levels and PLCγ isoforms (Fig. 1.10) respond primarily to receptor and non-receptor tyrosine kinases (reviewed in Rhee and Bae, 1997; Carpenter and Ji, 1999; Sekiya *et al.*, 1999; Rhee, 2001). Of particular interest to this thesis is the responsiveness of the PLCγ isoforms to the BCR.

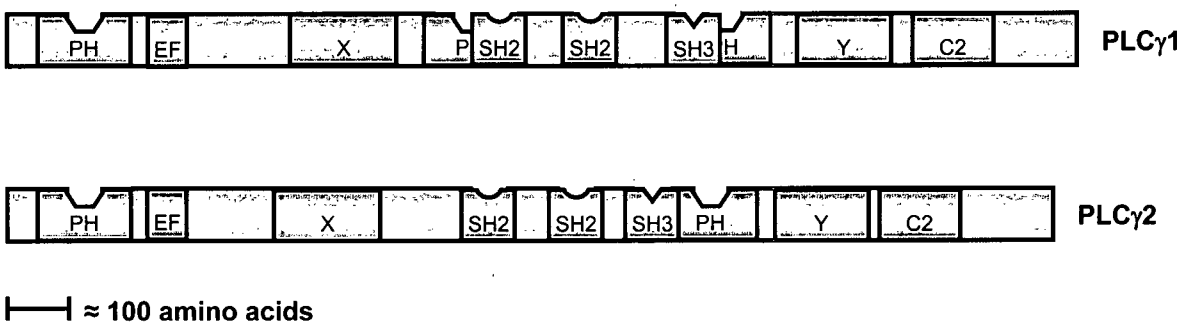

Figure 1.10. General Structure of PLCγ1 and PLCγ2. From the N-terminal to the C-terminal, PLCγ1 and PLCγ2 contain a phosphoinositide binding PH domain, followed by a calcium binding EF hand, followed by the X domain (a highly conserved domain of PLC isozymes that, together with the Y domain, forms the catalytic core of the enzyme), followed by a second PH domain that is interrupted by two phosphotyrosine-binding SH2 domains and a proline-binding SH3 domain, followed by the Y domain, followed by a C2 domain that is proposed to bind to calcium and to mediate calcium-dependent association with phosphoinositides.

PLC activity was implicated in BCR signaling when it was observed that BCR cross-linking results in DAG and IP_3 production (Coggeshall and Cambier, 1984; Bijsterbosch *et al.*, 1985; Klaus *et al.*, 1985; Fahey and DeFranco; 1987). The PLCγ isoform was further implicated as PLCγ1 and PLCγ2 were found to be tyrosine phosphorylated following BCR cross-linking (Carter *et al.*, 1991; Coggeshall *et al.*, 1992; Hempel *et al.*, 1992; Roifman and Wang, 1992). And finally, PLCγ2 was identified as the primary mediator of the BCR/PLC pathway based on loss-of-functions studies (Takata *et al.*, 1995; Hashimoto *et* al., 2000; Wang *et al.*, 2000). Having established the involvement and importance of PLCγ in BCR signaling, ensuing investigations focused on defining the proximal events in the BCR/PLCγ pathway.

1.8.2 BCR-Induced Tyrosine Phosphorylation of PLCγ

Plasma membrane recruitment and tyrosine phosphorylation are requisite steps in the pathway to PLCγ activation. Unfortunately, two steps a pathway does not make. Thus, today's BCR researchers proceed as cartographers seeking to map out the molecular pathways that connect the BCR to PLCγ membrane recruitment, tyrosine phosphorylation and activation.

BCR cross-linking initiates a protein tyrosine phosphorylation cascade that is manifested by members of the SFK, Syk and BTK (Gold *et al.*, 1990; Gold *et al.*, 1991; reviewed in Kurosaki *et al.*, 2000; Marshall *et al.*, 2000). This cascade is required to connect the BCR to PLCγ

activation (Padeh *et* al., 1991). While all of these PTKs appear to contribute to optimal BCR/PLCγ signaling, Syk and BTK both have a direct role in phosphorylating and activating PLCγ (reviewed in Kurosaki *et al.*, 2000; Marshall *et al.*, 2000). Genetic ablation of Syk results in an almost complete loss of PLCγ phosphorylation and activation (as indicated by abrogated IP_3 generation and calcium flux) following BCR cross-linking in the chicken DT40 cell line suggesting that it is absolutely required for PLCγ activation (Takata *et al.*, 1994). Additionally, *in vitro* studies demonstrate that Syk can directly phosphorylate PLCγ1 on the key regulatory residue, tyrosine 783 (Y783) (Law *et al.*, 1996). Syk ablation does not completely inhibit PLCγ phosphorylation, suggesting that another PTK may contribute to this process. This PTK could be Lyn as *in vitro* studies indicate that Lyn can directly phosphorylate PLCγ1 on tyrosine 771. However, genetic ablation of Lyn has a minimal impact on PLCγ phosphorylation and activation following BCR cross-linking in the chicken DT40 cell line (Takata *et al.*, 1994). Interestingly, genetic ablation of BTK only slightly diminishes PLCγ phosphorylation while significantly inhibiting PLCγ activation (as evidenced by abrogated IP_3 production) (Takata and Kurosaki, 1996). Concordantly, human B cell lines from X-linked agammaglobulinemia patients lacking a functional BTK gene show impaired BCR-induced IP_3 production and calcium mobilization (Fluckiger *et al.*, 1998). Moreover, reconstitution studies demonstrate that ectopic expression of BTK is sufficient to rescue these pathways in these cells (Fluckiger *et al.*, 1998) Finally, *in vitro* studies demonstrate that human BTK can directly phosphorylate rat PLCγ2 on several tyrosine residues including tyrosines 753, 759, 1197 and 1217. Thus, it is concluded that PLCγ becomes directly phosphorylated and activated by the co-operative activities of Syk and BTK following BCR cross-linking.

Having established the role Syk and BTK in BCR-induced PLCγ phosphorylation, the questions naturally arise as to how these PTKs themselves are activated and as to how they come to associate with PLCγ following BCR cross-linking. The former question will be addressed here while the latter question is addressed in detail in Chapter 1.9.3.

Syk is a member of the ZAP-70/Syk family of non-receptor PTKs and is primarily expressed in B cells (Hutchcroft *et al.*, 1991; Hutchroft *et al.*, 1992; Kong *et al.*, 1995). Structurally Syk is a 72 kD, cytosolic protein that possesses two N-terminal SH2 domains and a C-terminal kinase domain (also known as a Src Homology 1 Domain or SH1 domain) (Fig. 1.11) (Zioncheck *et al.*, 1986; Zioncheck *et al.*, 1988; Taniguchi *et al.*, 1991). The SH2 domains are proposed to bind to the phosphorylated Igα/β heterodimer and thus recruit Syk to the BCR signaling complex

following BCR-cross linking (Law *et al.*, 1994; Rowley *et al.*, 1995). This recruitment juxtaposes Syk with the BCR-associated SFKs. The SFKs then phosphorylate and activate Syk. In particular, Lyn is implicated in this process as genetic ablation of Lyn dramatically inhibits Syk activation following BCR cross-linking in the chicken DT40 B cells (Kurosaki *et al.*, 1994). However, it is unclear whether Lyn directly phosphorylates Syk or whether Lyn is simply required upstream of this process to phosphorylate the Igα/β heterodimer and thus facilitate Syk's membrane recruitment. Notably, some Syk activity persists in the Lyn knockout system suggesting that a Lyn-independent mechanism also exists for coupling the BCR to Syk activation (Kurosaki *et al.*, 1994). While this Lyn-independent mechanism remains unclear it is important as it helps us to reconcile the findings that Syk, but not Lyn, is required for PLCγ activation (reviewed in Kurosaki *et al.*, 2000; Takata *et al.*, 1994). Regardless of mechanism, BCR cross-linking clearly leads to plasma membrane recruitment, phosphorylation and activation of Syk (Kurosaki *et al.*, 1994; Law *et al.*, 1994; Rowley *et al.*, 1995) and Syk activity is clearly required to maintain a functional BCR/PLCγ pathway (Takata *et al*, 1994; reviewed in Kurosaki *et al.*, 2000).

BTK is a member of the Tec family of PTKs involved in BTK signaling (Saouaf *et al.*, 1994; Aoki *et al.*, 1994; De Weers *et al.*, 1994). Structurally BTK is a 76 kD, cytosolic protein that possesses an N-terminal PH domain followed by an SH3 domain, followed by an SH2 domain, followed by a C-terminal kinase domain (Fig. 1.11) (reviewed in Lewis *et al.*, 2001). Mutational studies show that the PH domain and the SH2 domain are required to maintain BTK's role in the BCR/PLCγ pathway (Takata and Kurosaki, 1996). The PH domain is proposed to bind to membrane-bound PI-3,4,5-P_3 and thereby recruit BTK to the plasma membrane where it will be in close proximity to the BCR signaling complex (Salim *et al.*, 1996; Kojima *et al.*, 1997; Varnai *et al.*, 1999; reviewed in Kurosaki *et al* ., 2000). This recruitment is thought to facilitate BTK's phosphorylation by the BCR-associated SFKs and/or Syk (Mahajan *et al.*, 1995; Afar *et al.*, 1996; Rawlings *et al.*, 1996; Kurosaki and Kurosaki, 1997; Baba *et al.*, 2001). However, the precise mechanism of BTK phosphorylation remains controversial. Loss-of-function studies clearly indicate that Syk and Lyn are required for this process yet it is unknown if this requirement reflects indirect or direct interactions. For example Lyn may simply be required to activate Syk as discussed above. Alternatively, Lyn could directly phosphorylate BTK itself as is suggested by reconstitution studies in various non-lymphoid cells (Afar *et* al., 1996; Rawlings *et al.*, 1996). Similarly, Syk could directly phosphorylate BTK or it may

phosphorylate some other unidentified PTK that then goes on to phosphorylate BTK. Whatever the case, ablation of either Syk or Lyn only partially inhibits BTK phosphorylation while ablation of both Syk and Lyn completely inhibits BTK phosphorylation (Kurosaki and Kurosaki, 1997). Thus, both proteins are proposed to function cooperatively to activate BTK (reviewed in Kurosaki, 2000).

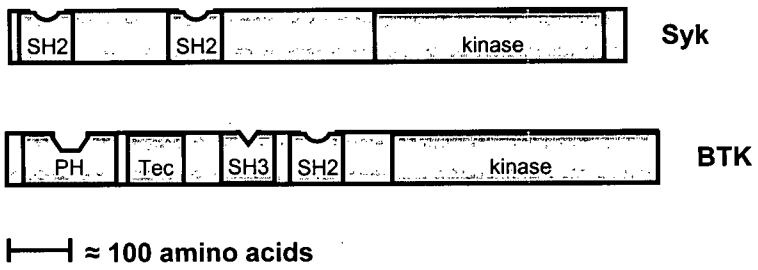

Figure 1.11. General Structure of Syk and BTK. Syk is a 72 kD, cytosolic protein that possesses two N-terminal SH2 domains and a C-terminal kinase domain (also known as an Src Homology 1 Domain or SH1 domain). BTK is a 76 kD, cytosolic protein that possesses an N-terminal PH domain followed by an conserved Tec domain (common to all Tec family members), followed by an SH3 domain, followed by an SH2 domain, followed by a C-terminal kinase domain. Recall that SH2 domains specifically associate with phosphorylated tyrosine residues, PH domains specifically associate with membrane bound phosphoinositides and SH3 domains specifically associate with proline-rich sequences. Note that the N-terminal is to the left and the C-terminal is to the right in the diagram.

1.8.3 BCR-Induced Membrane Recruitment of PLCγ

Thus sketched, is our current understanding of the pathways that connect the BCR to Syk and BTK activation. Yet the question remains, "How do the membrane-localized, active Syk and BTK come to associate with and activate cytosolic PLCγ?" Recent loss-of-function studies have made significant contributions to an emerging model of this process. Initial models suggested that PLCγ may be recruited to the plasma membrane by way of its PH domains binding to membrane-bound PIP_3. These models were based on analogy to the platelet-derived growth factor receptor (PDGFR)/PLCγ pathway where loss-of-function studies demonstrated that PLCγ1's N-terminal PH domain is required for its membrane recruitment and activation (Falasca *et al.*, 1998; reviewed in Marshall *et al.*, 2000; Rhee, 2001). According to these models, PLCγ recruitment and activation would lie downstream of PI3K as PIP_3 is a PI3K product. Indeed, inhibitors of PI3K have been shown to have a negative effect of PLCγ activation in B cells

(reviewed in Rhee, 2001). However, it remains unclear whether this represents a direct or indirect effect. The possibility of an indirect effect exists as PI3K and its product, PIP_3, may recruit and activate BTK, which itself is proposed to contribute to PLCγ phosphorylation and activation (refer to Chapter 1.9.2). Thus, it remains unclear whether or not PLCγ's PH domain plays a significant role in mediating PLCγ's membrane recruitment and activation in the BCR/PLCγ pathway.

Alternate models propose that PLCγ may be recruited to the plasma membrane by way of its SH2 domain, similar to what is observed in several receptor PTK/PLCγ pathways (Anderson *et al.*, 1990; Kashishian and Cooper, 1993; Margolis *et al.*, 1990; Valius *et al.*, 1993; Zhu *et al.*, 1992). At the outset, BCR-associated Syk was proposed to facilitate PLCγ membrane recruitment because PLCγ1's SH2 domain binds to tyrosine phosphorylated Syk in an association that is required for PLCγ1's membrane recruitment, phosphorylation and activation (Sillman and Monroe, 1995; Law *et al.*, 1996). Unfortunately, this model does not seem applicable to PLCγ2, the predominate isoform of the BCR/PLCγ pathway (reviewed in Kurosaki *et al.*, 2000). This necessitated further studies that eventually identified BLNK as a key component in the BCR/PLCγ pathway.

BLNK was first isolated from a human B cell line based on its ability to associate with the C-terminal SH2 domain of PLCγ1 (Fu and Chan, 1997). Interestingly, human BLNK exists in two alternatively spliced forms termed hBLNK (~ 70 kD when phosphorylated) and hBLNK-s (~ 68 kD when phosphorylated) that do not overtly differ in expression pattern or function (Fu and Chan; 1997; Fu *et al.*, 1998). Concurrently, the mouse homolog of BLNK, termed the SH2 domain containing leukocyte protein of 65 kD (Slp-65) or murine BLNK (mBLNK) was isolated from a murine B cell line and shares 82 % amino acid identity with hBLNK (Wienands *et al.*, 1998; Fu *et al.*, 1998). As well, the chicken homologue of BLNK, termed the B lymphocyte adapter protein containing a SH2 domain (BASH) or the chicken phosphorylated protein of 80 kD (pp80) has been isolated (Goitsuka *et al.*, 1998; Ishiai *et al.*,1999).

The structure of hBLNK is detailed herein because hBLNK is used throughout this thesis (Fig. 1.11). Nonetheless, the general structure of BLNK is conserved across all its homologues (Fu and Chan, 1997; Fu *et al.*, 1998; Goitsuka *et al.*, 1998; Wienands *et al.*, 1998; Ishiai *et al.*, 1999a; Ishiai *et al.*, 1999b). From the N-terminus to the C-terminus, hBLNK is comprised of a

basic domain (approximately 50 amino acids), followed by an acidic domain (approximately 70 amino acids), followed by a proline-rich domain (approximately 250 amino acids), followed by an N-terminal SH2 domain (approximately 110 amino acids) (Fig. 1.12). As well, these domains are interspersed with thirteen tyrosine phosphorylation motifs (Chiu *et al.*, 2002). Thus, structurally hBLNK appears to be an ideal candidate for an adapter protein as it contains multiple protein interaction domains while lacking a catalytic domain. This supposition is further supported by numerous functional studies (discussed below).

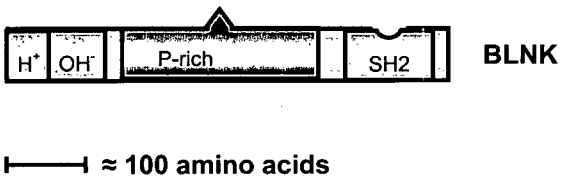

Figure 1.12. General Structure of hBLNK. From the N-terminus to the C-terminus (left to right in the above diagram) hBLNK is comprised of a basic domain (approximately 50 amino acids in length), followed by an acidic domain (approximately 70 amino acids length), followed by a proline-rich domain (approximately 250 amino acids in length), followed by an N-terminal SH2 domain (approximately 110 amino acids in length). Recall that proline-rich domains specifically associate with PH domains and SH2 domains specifically associate with phosphorylated tyrosine residues.

BLNK was first identified as a component of BCR signaling pathways when it was observed to become membrane-recruited and tyrosine phosphorylated following BCR cross-linking (Fu and Chan, 1997; Fu *et* al., 1998; Goitsuka *et al.*, 1998; Wienands *et al.*, 1998). Loss-of-function studies demonstrate that BLNK is required for B cell development and activation (Minegishi *et al.*, 1999; Pappu *et al.*, 1999; Hayashi *et al.*, 2000; Xu *et al.*, 2000; Jumaa *et al.*, 2001; Tan *et al.*, 2001; Schebesta *et al.*, 2002 Xu and Lam, 2002; Hayashi *et al.*, 2004; Taguchi *et al.*, 2004). These studies, combined with mutational and protein association studies, have led to a model of BCR signaling wherein BLNK lies at the junction of several key signaling cross-roads including the PLCγ pathway and the MAPK pathway.

Of particular interest to this thesis is BLNK's role in the BCR/PLCγ pathway. BLNK was first implicated in the PLCγ pathway when it was found to associate with both PLCγ1 and PLCγ2

following BCR cross-linking (Fu and Chan, 1997; Fu *et al.*, 1998; Ishiai *et al.*, 1999a; Ishiai *et al.*, 1999b; Chui *et al.*, 2002). Since then studies have established a model whereby BLNK is required to facilitate PLCγ's membrane recruitment, tyrosine phosphorylation and activation following BCR cross-linking (Fig. 1.12) (Ishiai *et al.*, 1999; reviewed in Kurosaki and Tsukada, 2000; Kurosaki *et al.*, 2000; Marshall *et al.*, 2000). As described in Chapter 1.5.3, this model envisions cytoplasmic BLNK being recruited to the BCR signaling complex by way of its SH2 domain binding to the non-ITAM, phosphorylated tyrosine residue 204 of Igα following BCR cross-linking (Engels *et al.*, 2001; Kabak *et al.*, 2002). This brings BLNK into close proximity with BCR-associated Syk which subsequently phosphorylates BLNK on multiple tyrosine residues (Fu *et al.*, 1998; Goitsuka *et al.*, 1998; Chui *et al.*, 2002). Tyrosine phosphorylated BLNK then associates with BTK (Hashimoto *et al.*, 1999; Su *et al.*, 1999; Chui *et al.*, 2002) and PLCγ (Fu and Chan, 1997; Fu *et al.*, 1998; Ishiai *et al.*, 1999; Chui *et al.*, 2002) by way of their respective SH2 domains. This results in a BCR/PLCγ signaling complex with the BCR, BLNK, the SFKs, Syk, BTK and PLCγ all in close association. This in turn, enables the SFKs (Mahajan *et al.*, 1995; Rawlings *et al.*, 1996; Afar *et al.*, 1996) and Syk (Kurosaki *et al.*, 1997; Baba *et al.*, 2001) to contribute to BTK phosphorylation and activation. Then, BTK (Takata and Kurosaki, 1996; Rawlings, 1999) together with Syk (Takata *et al.*, 1994), phosphorylates PLCγ and contributes to its activation (reviewed in Kurosaki and Tsukada, 2000; Gold, 2002). PLCγ then hydrolyzes PIP_2 to IP_3 and DAG. These secondary messengers subsequently activate several downstream signaling pathways that ultimately influence transcription and contribute to directing B cell activation, proliferation and differentiation (as described in Chapter 1.5.3).

As mentioned above, BLNK has also been implicated in several other BCR signaling pathways including the MAPK and stress-activated protein kinase (SAPK; i.e., p38 and Jnk) pathways. At first, BLNK's involvement in this pathway may seem intuitive as the PLCγ pathway has been shown to intersect with the MAPK pathway at the location of DAG-mediated recruitment of the Ras-GRP protein (refer to chapter 1.5.3 and Fig. 1.13). However, BLNK may also directly affect the MAPK pathway through its association with the Grb2 adapter protein (Fu *et al.*, 1998). While the physiological significance of this association remains unclear, BLNK may recruit Grb2 and its associated Ras guanine nucleotide exchange factor, Son of Sevenless (SoS), to the proximity of Ras, thereby facilitating Ras' activation and subsequently, the phosphorylation and activation of Erk (Fig. 1.13) (Fu *et al.*, 1998; reviewed in Gold, 2002). Thus, it appears that BLNK may facilitate Erk phosphorylation via a PLC-dependent and a PLC-independent

pathway. This is of particular consequence to this thesis as Erk phosphorylation is used as a downstream indicator of PLCγ activation in a reconstitution system involving BLNK. To distinguish between PLC-dependent and PLC-independent contributions to Erk phosphorylation I used the PLC inhibitor, U73122. In particular, PLC-dependent reconstitution of Erk phosphorylation should be inhibited by U73122 treatment whereas PLC-independent reconstitution of Erk phosphorylation should not be inhibited by U73122.

Tyrosine phosphorylated BLNK also associates with the adapter protein Cbl (Yasuda *et al.*, 2000). This protein is a negative regulator of the BCR/PLCγ pathway as it binds to phosphorylated BLNK and competitively inhibits BLNK from associating with PLCγ (Yasuda *et al.*, 2000). Consequently, PLCγ is neither recruited to the BCR complex, phosphorylated nor activated (Yasuda *et* al., 2000). Given this, BLNK may serve as a site of both negative and positive regulation in the BCR/PLCγ pathway.

When all the above is considered a map of the pathways connecting the BCR to PLCγ begins to emerge. Yet at times our map reads more as a list of signposts, proposing steps along the way rather than as a clearly defined pathway. Thus, the endeavor to fill in the details of the pathways continues in an effort to better understand these pathways and how they may go astray.

The first portion of the pathway requiring further definition is that connecting the BCR to BLNK membrane recruitment. At the onset of this thesis this pathway was completely obscure. But, by way of analogy with Slp-76, BLNK's homologue in the TCR/PLCγ signaling pathway, BLNK might be recruited to the plasma membrane by way of its SH2 domain binding to a tyrosine phosphorylated, transmembrane adapter protein (akin to the Linker of Activated T cells [LAT] in TCR signaling). Several possible candidates for this protein were identified including the Linker for Activated B cells (LAB) (Janssen *et al.*, 2003). LAB is a transmembrane protein that contains multiple tyrosines within its cytoplasmic domain that become phosphorylated upon BCR cross-linking suggesting that it may function as a membrane docking site for SH2 domain-containing proteins (Janssen *et al.*, 2003). Furthermore, genetic ablation of LAB reduces BCR-mediated calcium flux and Erk activation suggesting a role for it in the BCR/PLCγ pathway. Thus, LAB may mediate BLNK membrane recruitment. However, co-association studies failed to detect an association between endogenous LAB and endogenous BLNK (Janssen *et al.*, 2003). In contrast, *in vitro* studies did indicate that LAB can bind the SH2 domains of PLCγ suggesting

the possibility that LAB directly recruits PLCγ to the membrane (Janssen *et al.*, 2003). Yet, this observation could not be repeated *in vivo*, calling into question the validity of this model. Interestingly, LAB does associate with Grb2 *in vivo* (Jansenn *et al.*, 2003). This suggests a mechanism for LAB-mediated membrane recruitment of BLNK as proline-rich BLNK associates with Grb2's SH3 domain (Wienands *et al.*, 1998). Still, further studies are required to validate this model. In particular, mutational analysis can be performed to determine if mutations of Grb2's SH3 domain and/or BLNK's proline rich domain have a significant impact on BCR-mediated BLNK membrane recruitment and phosphorylation and on PLCγ membrane recruitment, phosphorylation and activation.

An alternative model for BLNK membrane recruitment was suggested based on its association with BTK. In particular, BTK could itself be recruited to the plasma membrane by way of its PH domain binding to membrane-bound phosphoinositides (Salim *et al.*, 1996; Kojima *et al.*, 1997; Varnai *et al.*, 1999; reviewed in Kurosaki *et al* ., 2000). In turn, BTK could serve as a docking site for BLNK. However, this seems unlikely given that BTK's association with BLNK is mediated by BTK's SH2 domain binding to tyrosine phosphorylated BLNK (Hashimoto *et al.*, 1999; Su *et al.*, 1999). Such a model would require BLNK to become tyrosine phosphorylated prior to being membrane recruited, which is unlikely given that BLNK is presumably phosphorylated by BCR-associated, membrane localized Syk.

A third model for BLNK membrane recruitment is suggested based on its association with phosphorylated Syk (Engels and Wienands, unpublished results; reported in Engels *et al.*, 2001). This association suggests BLNK could be recruited to the plasma membrane by way of its SH2 domain binding to BCR-associated, phosphorylated Syk. However, further studies supporting this model have not been reported.

Finally, Igα may be another candidate membrane docking protein for BLNK. Mutational analysis of Igα tyrosines indicated that the non-ITAM tyrosines, Y176 and Y204, are required for BLNK membrane recruitment and phosphorylation as well as for PLCγ phosphorylation and calcium mobilization (Kabak *et al.*, 2002). Moreover, Y204 is required for Igα association with BLNK (Engels *et al.*, 2001; Kabak *et al.*, 2002). However, it remains debatable whether or not this association is direct. Kabak and colleagues (2002) claim that this association is direct based on *in vitro* based studies. First, Kabak and colleagues (2002) demonstrated that a Sepharose-

coupled Igα phospho-Y204 peptide precipitates BLNK from lysates of stimulated B cells (Kabak *et al.*, 2002). Second, a GST-BLNK-SH2 domain fusion protein precipitates the PDGFRβ/Igα chimera containing the Igα cytoplasmic domain with an intact ITAM and Y204. Finally, the GST-BLNK-SH2 domain fusion protein directly binds to the PDGFRβ/Igα chimera in a far western blot (Kabak *et* al., 2002). However, while the first two studies do indicate that BLNK can associate with the cytoplasmic domain of Igα, they do not rule out the possibility that this association is mediated by another cellular component contained within the lysates. Furthermore, the PDGFRβ/Igα chimera and truncated GST-BLNK-SH2 domain association may not necessarily represent the Igα-BLNK interaction as it would occur within the cellular context. Given this, it still remains to be determined if BLNK's association with Igα is direct or indirect.

The second aspect of the BCR/PLCγ pathway that needs to be better defined involves the determination as to whether all of the components thus far identified are sufficient to reconstitute the pathway. In particular, loss-of-function studies have clearly shown that Syk, BTK and BLNK are all required to link the BCR to PLCγ. Yet, the possibility remains that other, yet to be identified, lymphoid specific components are required to complete this pathway. Thus, a reconstitution approach has been employed in this thesis to determine if these components are indeed sufficient to reconstitute the BCR/PLCγ pathway and to further define the underlying mechanisms of this pathway (detailed below).

1.9 Thesis Goals

Initial Hypothesis:

Co-expression of the BCR, Syk, BLNK and BTK will be sufficient to reconstitute BCR-mediated activation of endogenous PLCγ1 in the non-lymphoid AtT20 reconstitution system.

Subsequent Objectives:

I. To investigate the mechanisms that regulate BCR lipid raft translocation and the role of such translocation in BCR signaling (Chapter 3).

II. To determine if co-expression of the BCR, Syk, BLNK and BTK is sufficient to reconstitute BCR-induced activation of endogenous PLCγ1 in the non-lymphoid

AtT20 reconstitution system as determined by monitoring PLC-dependent, BCR-mediated Erk phosphorylation (Chapter 4).

III. To determine why co-expression of the BCR, Syk, BLNK and BTK appears to have a limited ability to reconstitute BCR-induced activation of endogenous PLCγ1 in the AtT20 system. This includes the ancillary objectives:

i. To determine if co-expression of these various components is sufficient to reconstitute BCR-induced tyrosine phosphorylation of BLNK, BTK and PLCγ in the AtT20 system (Chapter 5).

ii. To determine if co-expression of these various components is sufficient to reconstitute BCR-induced co-association of BLNK, BTK and/or PLCγ in the AtT20 system (Chapter 5 and Appendix 3).

iii. To determine if co-expression of these various components is sufficient to reconstitute BCR-induced membrane recruitment of BLNK, BTK and/or PLCγ in the AtT20 system (Chapter 5).

iv. To determine if co-expression of the BCR, Syk and constitutively membrane-targeted BLNK and/or PLCγ is sufficient to reconstitute BCR-induced activation of PLCγ in the non-lymphoid AtT20 reconstitution system as determined by monitoring PLC-dependent, BCR-mediated Erk phosphorylation (Chapter 6).

Experimental System:

To date, the BCR/PLCγ pathway has been mapped out primarily based on data from loss-of-function studies. Loss-of-function studies are invaluable for identifying key landmarks in a pathway as they can determine whether or not a protein is necessary to a pathway's function. However, such studies often miss the more subtle, intervening topography of a pathway as they are often confounded by the existence of functionally redundant proteins and/or pathways that compensate for and ultimately mask the contributions of the genetically ablated protein being studied. As well, loss-of-function studies may fail to identify all of the components involved in a pathway. Thus, any concerted mapping effort typically couples the techniques of loss-of-

function studies with those of reconstitution studies. Reconstitution studies are invaluable as they can determine whether or not a particular set of proteins are sufficient to reconstitute a given pathway. As well, such studies allow components to be investigated in isolation, alleviating the concerns of functional redundancy and enabling a more directed and detailed investigation of the pathway. Thus, this thesis employs the non-lymphoid AtT20 reconstitution system to further investigate the BCR/PLCγ pathway.

The AtT20 reconstitution system is derived from the murine pituitary cell line, AtT20 (described in Moore *et al.*, 1983). Being non-lymphoid, the AtT20 system does not endogenously express the BCR nor the lymphoid specific components required to couple the BCR to the PI3K, Ras/MAPK or PLCγ pathways. Nonetheless, the AtT20 system does express endogenous PI3K, Ras, PLCγ, and Fyn (Matsuuchi *et al.*, 1992 and Richards *et al.*, 1996). Moreover, the AtT20 system has proven amenable to transfection (Moore *et al.*, 1983; Matsuuchi *et al.*, 1992; Richards *et al.*, 1996). Thus, the AtT20 system lends itself well to BCR reconstitution studies. In particular, various lymphoid specific components can be transfected into this system in an effort to determine their sufficiency to reconstitute BCR-induced activation of the PI3K, Ras/MAPK and/or PLCγ pathways.

Two AtT20-derived cell lines have previously been established (Matsuuchi *et al.*, 1992; Richards *et al.*, 1996). The 100.33 cell line (termed "BCR" herein) expresses intact exogenous BCRs on its cell surface (Matsuuchi *et al.*, 1992). In contrast, the Syk13 cell line (termed "BCR/Syk" herein) expresses the BCR along with exogenous Syk (Richards *et al.*, 1996). Studies with these cell lines clearly indicate that expression of the BCR alone is sufficient to reconstitute BCR-induced Igα/β heterodimer phosphorylation and PI3K activation in this system (Matsuuchi *et al.*, 1992). Furthermore, co-expression of the BCR and Syk is sufficient to reconstitute a robust BCR-induced tyrosine phosphorylation cascade as well as Ras/MAPK activity in this system (Richards *et al.*, 1996). However, expression of the BCR, alone or in conjunction with Syk, is not sufficient to reconstitute BCR-induced PLCγ activation. Thus, it appears that additional lymphoid specific components may be required to link the BCR to PLCγ in this system (Richards *et al.*, 1996). As such, this thesis concentrates on attempting to reconstitute the BCR/PLCγ within this system in an effort to better understand how this pathway may function or fail to function to contribute to the immune response.

1.10 Thesis Summary

This thesis contains two sections, each of which considers a distinct aspect of compartmentalization with respect to BCR signaling. In the first section the mechanisms involved in regulating the translocation of the BCR into lipid rafts were investigated. Herein it was demonstrated that the BCR can translocate into lipid rafts following BCR cross-linking in the immature B cell lines, WEHI 231 and CH31 (Jackson *et al.*, 2005). Additionally, it was demonstrated that the Igα/β heterodimer, in the absence of the mIgM subunit, can translocate into lipid rafts following cross-linking in the m-IgM deficient immature B cell line, WEHI 303.1.5 (Jackson *et al.*, 2005). This finding is significant as it suggests that Igα/β, in the absence of the mIgM subunit, contains sufficient structural information to facilitate its association with lipid rafts. Similarly, previous studies have demonstrated that the mIgM subunit, in the absence of Igα/β, contains sufficient structural information to facilitate its association with lipid rafts (Cheng *et al.*, 2001). Considered together, these findings may be used to help define any structural regions involved in mediating lipid raft association. In particular, it may be hypothesized that these subunits use a similar mechanism to associate with lipid rafts and then it may be further hypothesized that the subunits share common structural feature to mediate this association. Given the structures of mIgM and the Igα/β, such a common feature would most likely lie within their transmembrane or membrane proximal domains. And thus, the Matsuuchi Lab is performing mutational analyses within these regions to further define any structural features that may help govern BCR lipid raft association and translocation.

In the second section, the molecular requirements for the BCR/PLCγ pathway were investigated. In particular, the AtT20 reconstitution system was used to determine if co-expression of the BCR, Syk, BLNK and BTK is sufficient to reconstitute the BCR/PLCγ pathway. Herein, it was determined that co-expression of the BCR, Syk and BLNK is sufficient to reconstitute BCR-induced PLCγ activation in the AtT20 system. However, this activation is hypothesized to represent only a partial reconstitution of the pathway as neither BLNK nor PLCγ are recruited to the plasma membrane upon BCR cross-linking and as PLCγ phosphorylation appears very limited compared to what is typically observed in B cell lines. This limited reconstitution was hypothesized to be due to the absence of BTK; however, further expression of BTK within the system did not enhance PLCγ activation, but rather inhibited it. Further investigations determined that BTK is constitutively activated within this system and as such, may be

inappropriately influencing the components of the BCR/PLCγ pathway. Thus, further studies are in order to address this issue.

Alternatively, it was hypothesized that the limited reconstitution of BCR-induced PLCγ activation may be a result of the apparent inability to reconstitute BCR-induced BLNK and PLCγ membrane recruitment. Thus, BLNK and PLCγ were constitutively targeted to the plasma membrane within the AtT20 system. From this, it was determined that membrane-targeting of PLCγ is sufficient to reconstitute BCR-induced Syk-dependent PLCγ activation, despite the absence of BLNK. This finding highlights the importance of PLCγ membrane compartmentalization to its activation. In contrast, membrane-targeting of BLNK is not sufficient to reconstitute BCR-induced PLCγ membrane recruitment or to enhance BCR-induced PLCγ activation within this system. This suggests that there may be an additional defect in the system that is preventing the formation of a functional BCR/BLNK/PLCγ signaling complex. In particular, it is hypothesized that Igα and BLNK phosphorylation may not be fully reconstituted within this system. Furthermore, it is hypothesized that the SFKs may be required to reconstitute such phosphorylation. Thus, future studies will focus on addressing these possibilities.

Through the course of this thesis it was also determined that PLCγ phosphorylation does not predicate PLCγ activation. This finding is taken to further emphasize the requirement for appropriate membrane compartmentalization in the process of PLCγ activation. Additionally, BLNK that is targeted to the plasma membrane in general (TmBLNK) was found to have a different effect on BCR-induced PLCγ phosphorylation than BLNK that is targeted to lipid rafts within the plasma membrane. This suggests that all membrane compartmentalization is not equivalent and alludes to the precision required to regulate appropriate compartmentalization. And thus, the work in this thesis demonstrates the importance of compartmentalization in BCR signaling both with respect to compartmentalization of the BCR to lipid rafts and the subsequent compartmentalization of BLNK and PLCγ to the BCR.

This page is meant to be blank.

CHAPTER 2

Materials and Methods

2.1 Reagents

2.1.1 Antibodies

The rabbit polyclonal antibodies; anti-BLNK (H-80), anti-PLCγ1 (1249), anti-PLCγ2 (Q-20) and anti-ERK 1 (K-23); the mouse monoclonal antibodies, anti-CD16 (GRM1) and anti-BLNK (2B11); and the goat polyclonal antibodies, anti-BLNK (C-19) and anti-BTK (C-20) were all purchased from Santa Cruz Biotechnology (Santa Cruz, California). The anti-Syk rabbit antiserum (described in Richards *et al.*, 1996) and the anti-mouse Igα rabbit antiserum (described in Gold *et al.*, 1991) were produced by the Matsuuchi Laboratory (University of British Columbia; Vancouver, British Columbia). The anti-Akt, anti-phospho-AKT (S473), anti-phospho-BLNK (Y96), anti-phospho-BTK (Y223), and anti-phospho-Erk1/2 (T202/Y204) were purchased from Cell Signaling Technology (Beverly, Massachusetts). The anti-phospho-tyrosine mouse monoclonal antibody (4G10) was purchased from Upstate Biotechnology (Charlottesville, Virginia). The anti-Igβ cytoplasmic tail rabbit antiserum was kindly provided by Dr. Marcus Clark (University of Chicago; Chicago, Illinois). The anti-κ light chain rabbit polyclonal antibody and the anti-actin mouse monoclonal antibody were purchased from ICN Biomedicals (Irvine, California). The anti-mouse μ heavy chain rabbit polyclonal antibody was purchased from Jackson ImmunoResearch Laboratories Incorporated (West Grove, Pennsylvania; distributed by Bio/Can Scientific, Mississauga, Ontario).

The stimulating antibodies (antibodies used to cross-link the BCR on B cells and/or AtT20-derived cell lines) included the anti-mouse IgM (μ chain specific) and anti-human IgM (μ chain specific) goat polyclonal antibodies purchased from Jackson ImmunoResearch Laboratories Incorporated. The HM79-16 monoclonal antibody that recognizes the extracellular domain of murine Igβ was purified from HM79-16 hamster hybridoma cells that were a kind gift from Dr. T. Nakamura (University of Tokyo; Tokyo, Japan). The antibody was purified from the hybridoma culture media using a Protein-G-agarose affinity column and biotinylated using N-hydroxysuccinimido biotin (NHS-biotin; Pierce Biotechnology; Rockford, Illinois). Further cross-linking of the biotinylated HM79-16 monoclonal antibody was achieved using streptavidin (Molecular Probes; Eugene, Oregon).

The horseradish peroxidase (HRP)-conjugated secondary reagents, Protein A-HRP and Protein G-HRP, were purchased from Amersham Biosciences Canada (Baie d'Urfe, Quebec). The goat-anti-rabbit IgG-HRP was purchased from Jackson ImmunoResearch Laboratories Incorporated, the goat anti-mouse IgG-HRP was purchased from Invitrogen Life Technologies (Burlington, Ontario) and the donkey anti-goat IgG-HRP, was purchased from Santa Cruz Biotechnology.

2.1.2 Plasmids

The *pWZL Blast 1* and *pWZL Blast 2* vectors that encode for blasticidin resistance were kindly provided by Dr. Stephen Robbins (University of Calgary; Calgary, Alberta). The *LPCsrf* vector that encodes for puromycin resistance was kindly provided by Dr. Anthony DeFranco (University of California, San Francisco; San Francisco, California). The *pMSCV-puro* vector and the *pSVneo* vector were purchased from BD Biosciences Clonetech (Palo Alto, California).

The *pBSmyc-human-BLNK (pp70)* vector (described in Fu *et al.*, 1998) that encodes for the myc-tagged human BLNK (pp70) fusion protein and the pApuro-mPLCγ2 vector that encodes for the membrane-targeted human FcγRIIIA/CD16 extracellular domain/human T cell receptor ζ transmembrane domain/rat PLCγ2 fusion protein (described in Ishiai *et al.*, 1999) were kindly provided by Dr. Andrew Chan (while at Washington University School of Medicine; St. Louis, Missouri; currently at Genetech, California). The *pBS-human-PLCγ2* vector that encodes for human PLCγ2 and the *LPCX-BTK-2* vector that encodes for puromycin resistance and murine BTK were kindly provided by Dr. David Rawlings (University of Washington; Seattle, Washington).

The *RSVpLpA* vector (kindly provided by Dr. Marika Walter and Dr. David Standring of the University of California, San Francisco; San Francisco, California) was used as a parental plasmid to create several of the vectors described below. The *RSVpLpA* vector contains a multiple cloning site flanked by the Rous Sarcoma Virus (RSV) long terminal repeat (LTR) promoter and enhancer elements on the 5' side and the SV40 polyadenylation site and splice site on the 3' side. This particular combination of regulatory elements has proven successful in producing high levels of exogenous protein expression within transfected AtT20-derived cell lines (Matsuuchi and Kelly, 1991; Matsuuchi *et al.*, 1992).

2.1.3 Plasmids Created for This Thesis

RSVpLpA-myc-human-BLNK (pp70)

The sequence encoding the myc-tagged human BLNK was excised from the *pBSmyc-human-BLNK (pp70)* vector with *Xba I* and ligated into the *Xba I* digested *RSVpLpA* vector (Fig.2.1). Correct orientation of the myc-tagged human BLNK sequence within the *RSVpLpA* vector was confirmed by restriction enzyme digests and nucleotide sequencing. Nucleotide sequencing was conducted by the Nucleic Acid Protein Service Unit (NAPS Unit) at the University of British Columbia (UBC).

RSVpLpA-human-PLCγ2

The sequence encoding human PLCγ2 was amplified from the *pBS-human-PLCγ2* vector using the polymerase chain reaction (PCR). Two primers, TJ1 and TJ2 (Table 2.1), were created to amplify the human PLCγ2 sequence from the *pBS-human-PLCγ2* vector such that the resultant

PCR product encoded for human PLCγ2 flanked by *Xba I* sites. The PCR product was then digested with *Xba I* and ligated into *Xba I* digested *RSVpLpA* vector (Fig.2.2). Correct orientation of the human PLCγ2 sequence within the resultant *RSVpLpA-human-PLCγ2* vector was confirmed by restriction enzyme digests and by nucleotide sequencing by the NAPS Unit at UBC.

Table 2.1. Summary of Primers Used To Create the Various Plasmids.

Primer Name	Primer Sequence	Description
TJ1	5' *ATC AAC TAG TT**C TAG A**GC CAA ACC CGG GGC* 3'	sense sequence, **bold** = Xba I site, *italics* are complimentary to the 5' end of human PLCγ2 as found in the *pBS-human-PLCγ2* vector
TJ2	5' *GG GGC GGC CGC **T CT AGA** GTT TTT TTT TTT* 3'	anti-sense sequence, **bold** = Xba I site, *italics* are complimentary to the 3' end of human PLCγ2 as found in the *pBS-human-PLCγ2* vector
TJ3	5' CGA **CGC GT***T CCA CCA CGG TCA ATG TAG ATT* 3'	sense sequence, **bold** = Mlu I site, *italics* = 5' end of human PLCγ2 beginning with the second codon (i.e., ATG removed)
TJ4	5' CGA **CGC GT***C TTC TCT CTT **A**AC CTC TTG TTG* 3'	anti-sense sequence, **bold** = Mlu I site, **bold** = stop codon, *italics* = 3' end of human PLCγ2
TJTM5	5' TGC **T CT AGA** GCA *ATG TGG CAG CTG CTC CTC CCA ACT* 3'	sense sequence, **bold** = Xba I site, *italics* = 5' end of TM construct (human FcR IIIa/CD16)
TJTM3	5' TGC **T CT AGA** TCA **A CG CGT** *GCT CCT GCT GAA CTT CAC* 3'	anti-sense sequence, **bold** = Xba I site, **bold** = Mlu I site, *italics* = 3' end of TM construct (human TCR ζ)
TJ7	5' CGA **CGC GT***G ACA AGC TTA ATA AAA TAA CCG* 3'	sense sequence, **bold** = Mlu I site, *italics* = 5' end of human BLNK beginning with the second codon (i.e., myc tag and ATG removed)
TJ8	5' CGA **CGC GT***C CCC CTT **TA**T GAA ACT TTA ACT* 3'	anti-sense sequence, **bold** = Mlu I site, ***bold*** = stop codon, *italics* = 3' end of human BLNK
5' Ac	5' TGC **T CT AGA** GCA *ATG GGA TGT ATT AAA TCA* 3'	sense sequence, **bold** = Xba I site, *italics* = 5' end murine Lyn encoding amino acids 1- 6)
3' Ac	5' TGC **T CT AGA** TCA **A CG CGT** *GAG ATT GTC TTT* 3'	anti-sense sequence, **bold** = Xba I site, **bold** = Mlu I site, *italics* = 5' end of murine Lyn, encoding amino acids 9-12

RSVpLpA-TM

For subsequent cloning procedures an *RSVpLpA-TM* vector was created. This vector allows sequences to be cloned in-frame to a transmembrane-targeting (TM) construct. Specifically, *RSVpLpA-TM* encodes for the extracellular domain of human FcRIIIa/CD16 (amino acids 1-208)

fused in-frame to transmembrane domain of the human T cell receptor (TCR) ζ chain (amino acids 31-58). In *RSVpLpA-TM* the TM construct can be further fused to any sequence of interest via an in-frame *Mlu I* site. The resulting sequence should then encode for a TM-fusion protein that should be constitutively targeted to the plasma membrane.

The *RSVpLpA-TM* vector was created by first digesting the *RSV-pLpA* vector with *Mlu I*, blunt-ending the digested product and then re-ligating the vector to create *RSV-pLpA-Mlu I(-)* (Fig.2.3). This procedure effectively eliminated an extraneous *Mlu I* site that would have interfered with the cloning strategy. The sequence encoding the TM construct was then amplified from the *pApuro-mPLCγ2* vector (Chapter 2.1.2) using PCR.[1] Two primers, TJTM5 and TJTM3 (Table 2.1), were created to amplify the TM construct from the *pApuro-mPLCγ2* vector such that the resultant PCR product encoded for the TM construct with flanking *Xba I* sites and an in-frame 3' *Mlu I* cloning site. The PCR product was then digested with *Xba I* and ligated into the *Xba I* digested *RSV-pLpA-Mlu I(-)* vector (Fig.2.3). Correct orientation of the TM construct within the resultant *RSV-pLpA-TM* vector was confirmed by restriction enzyme digests and by nucleotide sequencing by the NAPS Unit at UBC.

RSVpLpA-TM-human-BLNK

The sequence encoding human BLNK was amplified from the *pBSmyc-human-BLNK (pp70)* vector using PCR. Two primers, TJ7 and TJ8 (Table 2.1), were created to amplify the human BLNK sequence from the *pBSmyc-human-BLNK (pp70)* vector such that the resultant PCR product encoded for human BLNK (myc-tag and first codon removed) flanked by *Mlu I* sites (with the 5' site being in-frame). The PCR product was then digested with *Mlu I* and ligated into the *Mlu I* digested *RSV-pLpA-TM* vector (Fig.2.4). Correct orientation of human BLNK within the resultant *RSV-pLpA-TM-human-BLNK* vector was confirmed by restriction enzyme digests and by nucleotide sequencing by the NAPS Unit at UBC.

RSVpLpA-Ac

For subsequent cloning procedures an *RSVpLpA-Ac* vector was created. This vector allows sequences to be cloned in-frame to the acylation-targeting (Ac) sequence of murine Lyn. The sequence encoding the Ac sequence (amino acids 1-12) was amplified from the *RSVpLpA-murine-Lyn* vector (described in Santos, 2003) using PCR. Two primers, 5'Ac and 3'Ac (Table 2.1), were created to amplify the Ac sequence from the *RSVpLpA-Lyn* vector such that the resultant PCR product encodes for the Ac sequence with flanking *Xba I* sites and an in-frame 3' *Mlu I* cloning site. The PCR product was then digested with *Xba I* and ligated into the *Xba I* digested *RSVpLpA-Mlu I(-)* vector (Fig.2.5). Correct orientation of the Ac sequence within the

[1] It should be noted that the Ishiai *et al.* (1999) reports the TM construct encodes for human FcRIIIa/CD16 amino acids 1-212 fused in-frame to human TCR zeta amino acids 30-58. However, our sequencing results indicate that the TM construct actually encodes for human FcRIIIa/CD16 amino acids 1-208 fused in-frame to human TCR zeta amino acids 31-58.

resultant *RSVpLpA-Ac* vector was confirmed by restriction enzyme digests and by nucleotide sequencing by the NAPS Unit at UBC.

RSVpLpA-Ac-human-BLNK

The sequence encoding human BLNK was amplified from the *pBSmyc-human-BLNK (pp70)* vector using PCR. Two primers, TJ7 and TJ8 (Table 2.1), were created to amplify the human BLNK sequence from the *pBSmyc-human-BLNK (pp70)* vector such that the resultant PCR product encoded for human BLNK (myc-tag and first codon removed) flanked by *Mlu I* sites (with the 5' site being in-frame). The PCR product was then digested with *Mlu I* and ligated into the *Mlu I* digested *RSVpLpA-Ac* vector (Fig.2.6). Correct orientation of human BLNK within the resultant *RSVpLpA-Ac-human-BLNK* vector was confirmed by restriction enzyme digests and by nucleotide sequencing by the NAPS Unit at UBC.

RSVpLpA-Ac-human-PLCγ2

The sequence encoding human PLCγ2 was amplified from the *RSVpLpA-human-PLCγ2* vector (described above) using PCR. Two primers, TJ3 and TJ4 (Table 2.1), were created to amplify the human PLCγ2 sequence from the *RSVpLpA-human-PLCγ2* vector such that the resultant PCR product encoded for human PLCγ2 flanked by *Mlu I* sites (with the 5' site being in-frame). The PCR product was then digested with *Mlu I* and ligated into the *Mlu I* digested *RSVpLpA-Ac* vector (Fig.2.6). Correct orientation of human PLCγ2 within the resultant *RSVpLpA-Ac-human-PLCγ2* vector was confirmed by restriction enzyme digests and by nucleotide sequencing by the NAPS Unit at UBC.

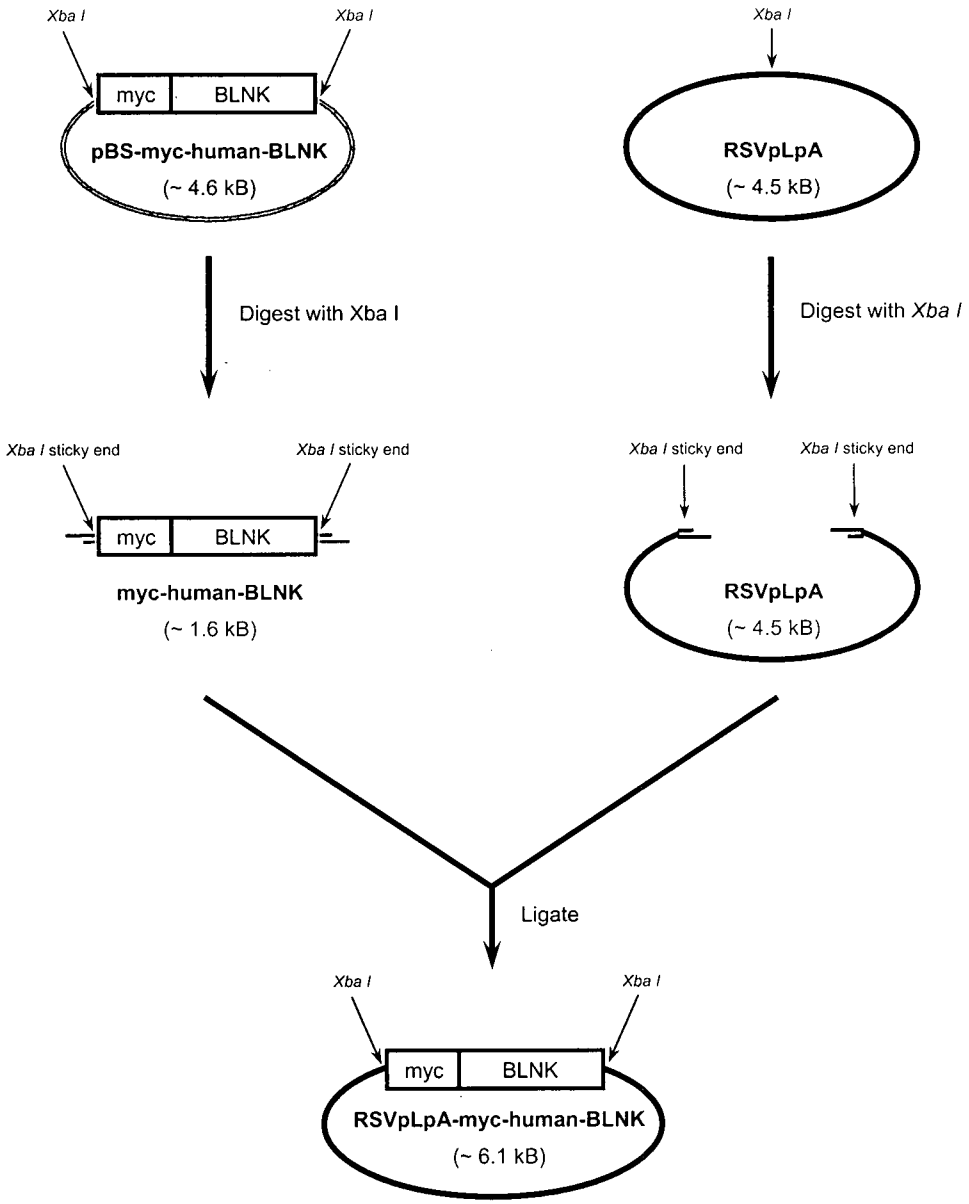

Figure 2.1. Schematic representation of how the *RSVpLpA-myc-human-BLNK* (pp70) expression vector was developed. The *pBS-myc-human-BLNK* vector (~ 4.6 kB) was digested with *Xba I* to drop out the sequence encoding myc-tagged human BLNK (~ 1.6 kB). This sequence was then purified and ligated into the mammalian expression vector, *RSVpLpA* (~ 4.5 kB), that had similarly been digested with *Xba I*. Correct orientation of the myc-tagged human BLNK insert within the resultant *RSVpLpA-myc-human-BLNK* vector (~ 6.1 kB) was then confirmed by restriction enzyme digests and nucleotide sequencing.

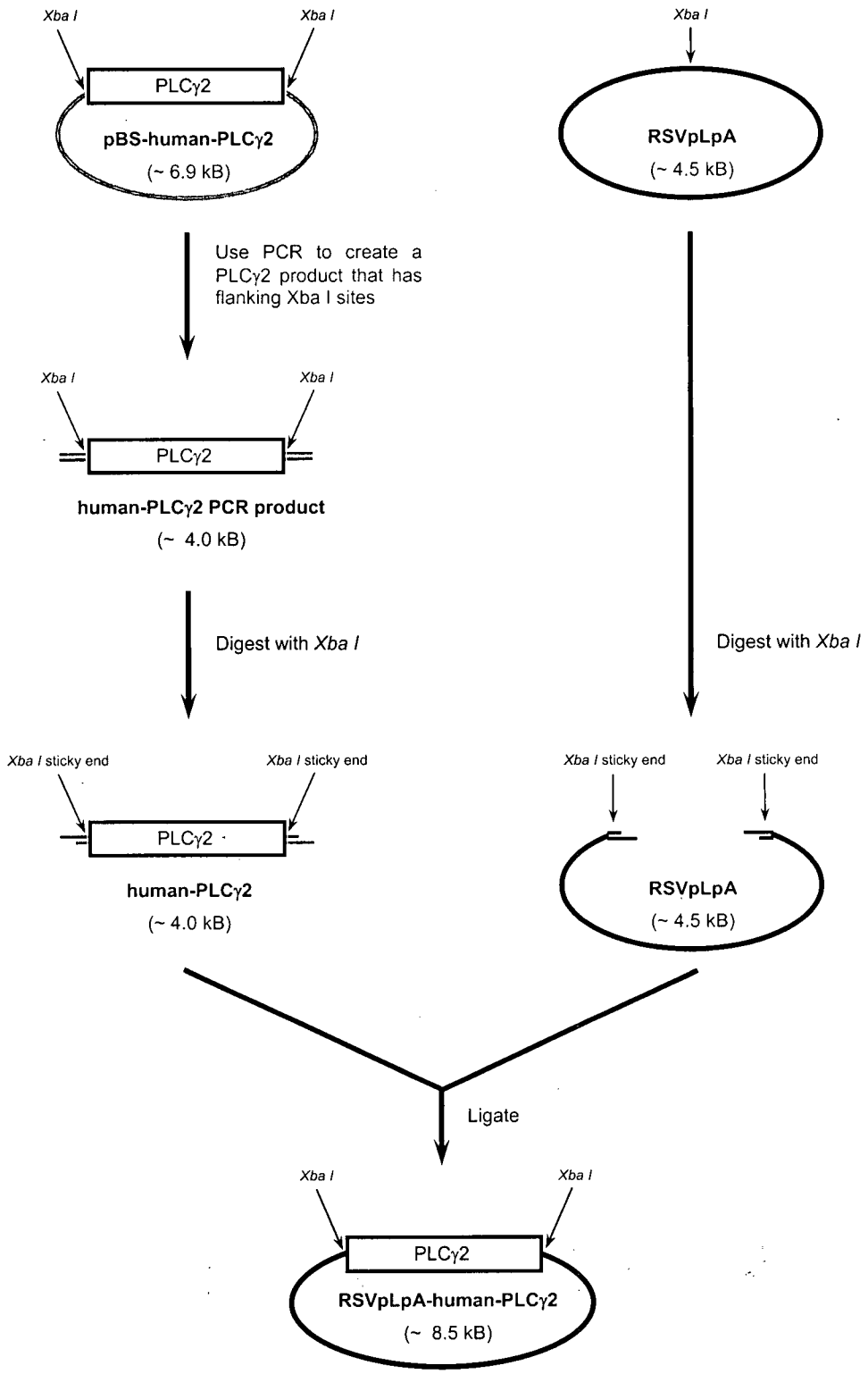

Figure 2.2. Schematic representation of how the *RSVpLpA-human-PLCγ2* expression vector (~ 8.5 kB) was developed. The sequence for human PLCγ2 (~ 4.0 kB) was amplified from the *pBS-human-PLCγ2* vector (~ 6.9 kB) using PCR. The resultant PCR product (~ 4.0 kB) was digested with *Xba I*, purified and ligated into the mammalian expression vector, *RSVpLpA* (~ 4.5 kB) that had similarly been digested with *Xba I*. Correct orientation of the human PLCγ2 insert within the resultant *RSVpLpA-human-PLCγ2* vector was then confirmed by restriction enzyme digests and nucleotide sequencing.

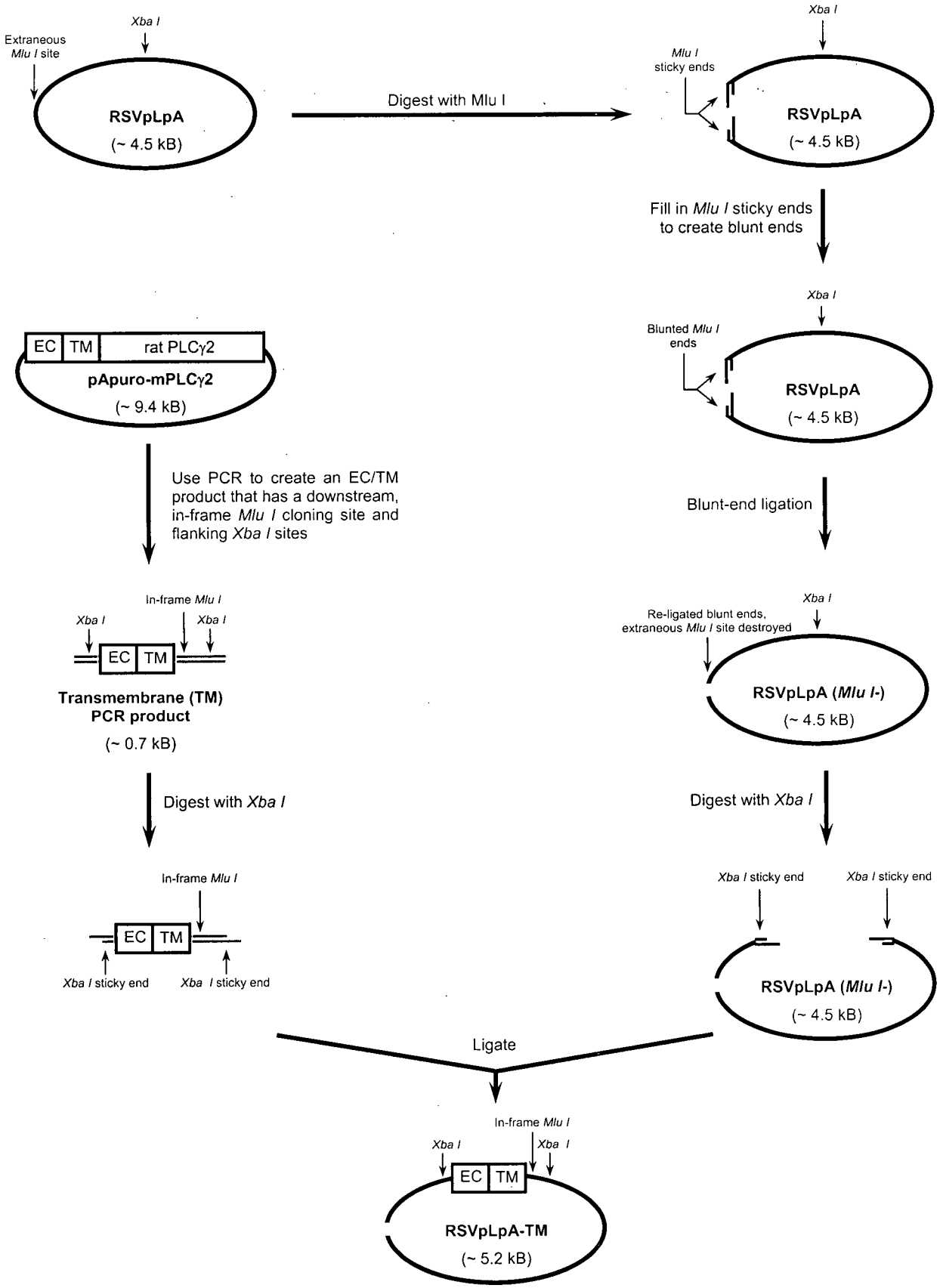

Figure 2.3. Schematic representation of how the *RSVpLpA-TM* expression vector (~ 5.2 kB) was developed. Refer to Chapter 2.3.1 for a detailed explanation of how the vector was created.

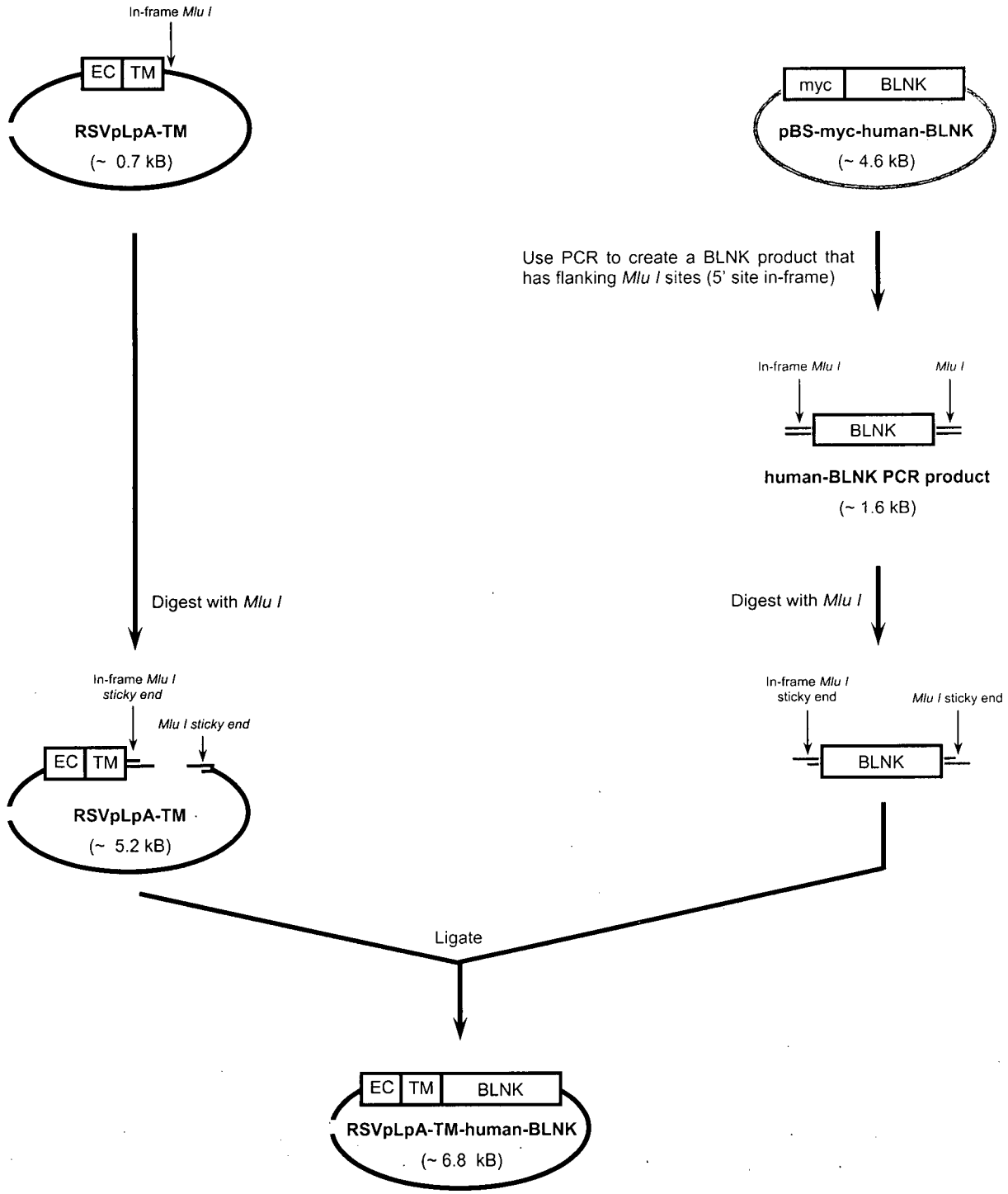

Figure 2.4. Schematic representation of how the *RSVpLpA-TM-human-BLNK* expression vector (~ 6.8 kB) was created. The sequence for human BLNK was amplified from the *pBS-myc-human-BLNK* vector using PCR. The primers, TJ7 and TJ8, were used such that the resultant PCR product (~ 1.6 kB) would encode for human BLNK (with the myc-tag and first codon removed) flanked by *Mlu I* sites (with the 5' site being in-frame with the BLNK sequence). The PCR product was then digested with *Mlu I*, purified and ligated into the *RSVpLpA-TM* vector (~ 5.2 kB) that had similarly been digested with *Mlu I*. Correct orientation of the human BLNK insert within the resulting *RSVpLpA-TM-human-BLNK* vector was then confirmed by restriction enzyme digests and nucleotide sequencing.

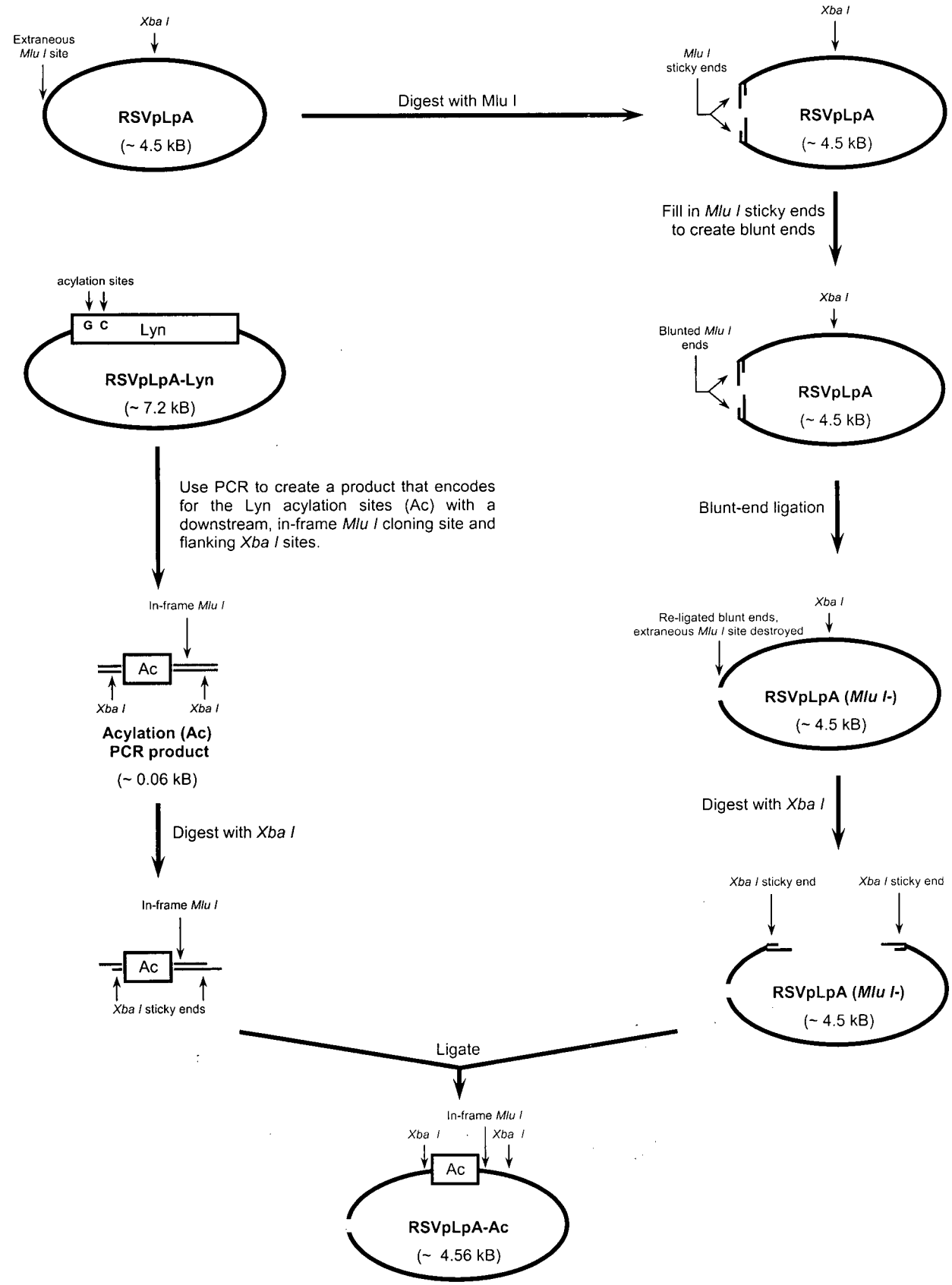

Figure 2.5. Schematic representation of how the *RSVpLpA-Ac* expression vector (~ 4.56 kB) was developed. Refer to Chapter 2.3.1 for a detailed explanation of how the vector was created

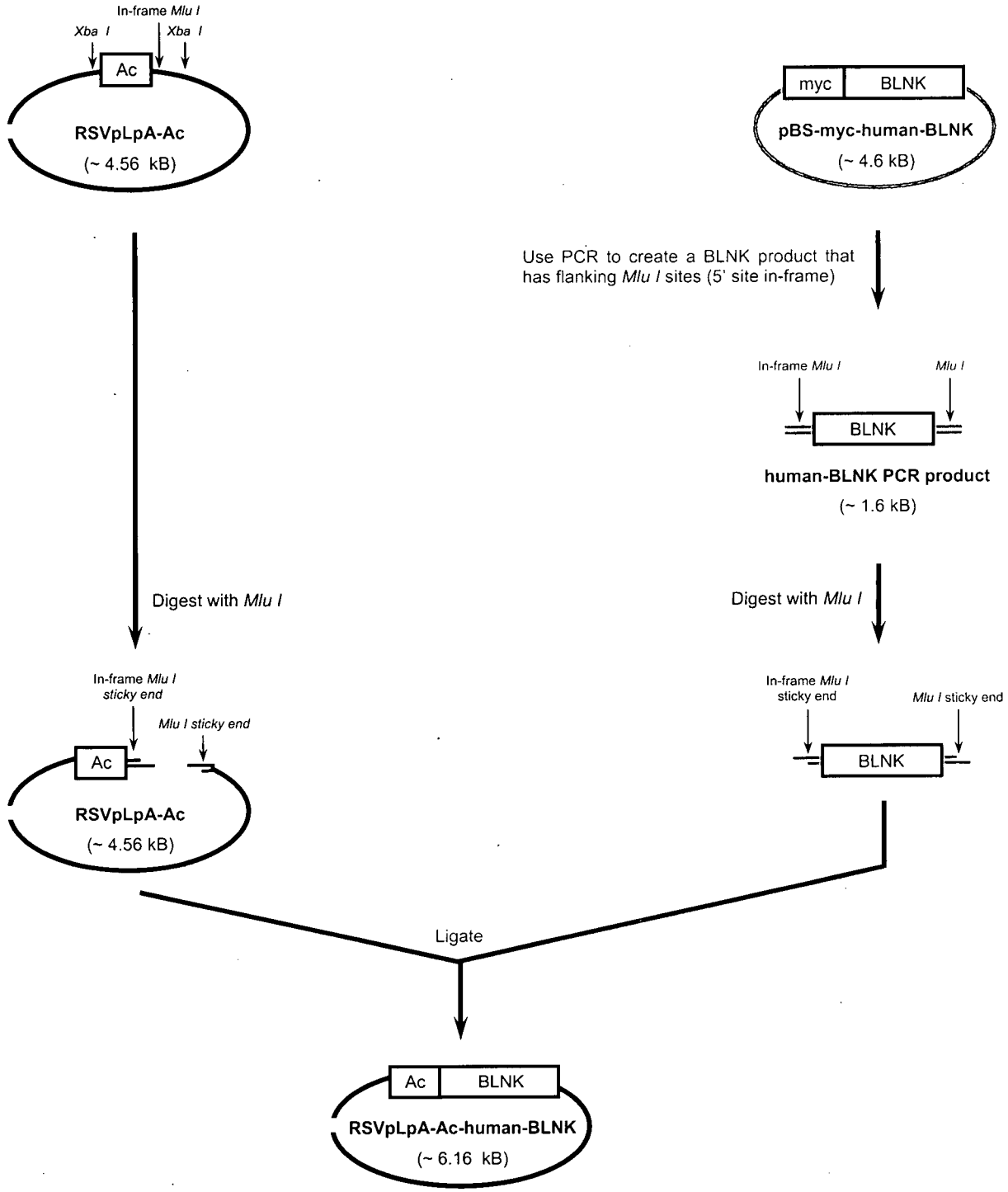

Figure 2.6. Schematic representation of how the *RSVpLpA-Ac-human-BLNK* expression vector (~ 6.16 kB) was developed. The sequence for human BLNK was amplified from the *pBS-myc-human-BLNK* vector using PCR. The primers, TJ7 and TJ8, were used such that the resultant PCR product (~ 1.6 kB) would encode for human BLNK (with the myc-tag and first codon removed) flanked by *Mlu I* sites (with the 5' site being in-frame with the BLNK sequence). The PCR product was then digested with *Mlu I*, purified and ligated into the *RSVpLpA,-Ac* vector (~ 4.56 kB) that had similarly been digested with *Mlu I*. Correct orientation of the human BLNK insert within the resultant *RSVpLpA-Ac-human-BLNK* vector was then confirmed by restriction enzyme digests and nucleotide sequencing.

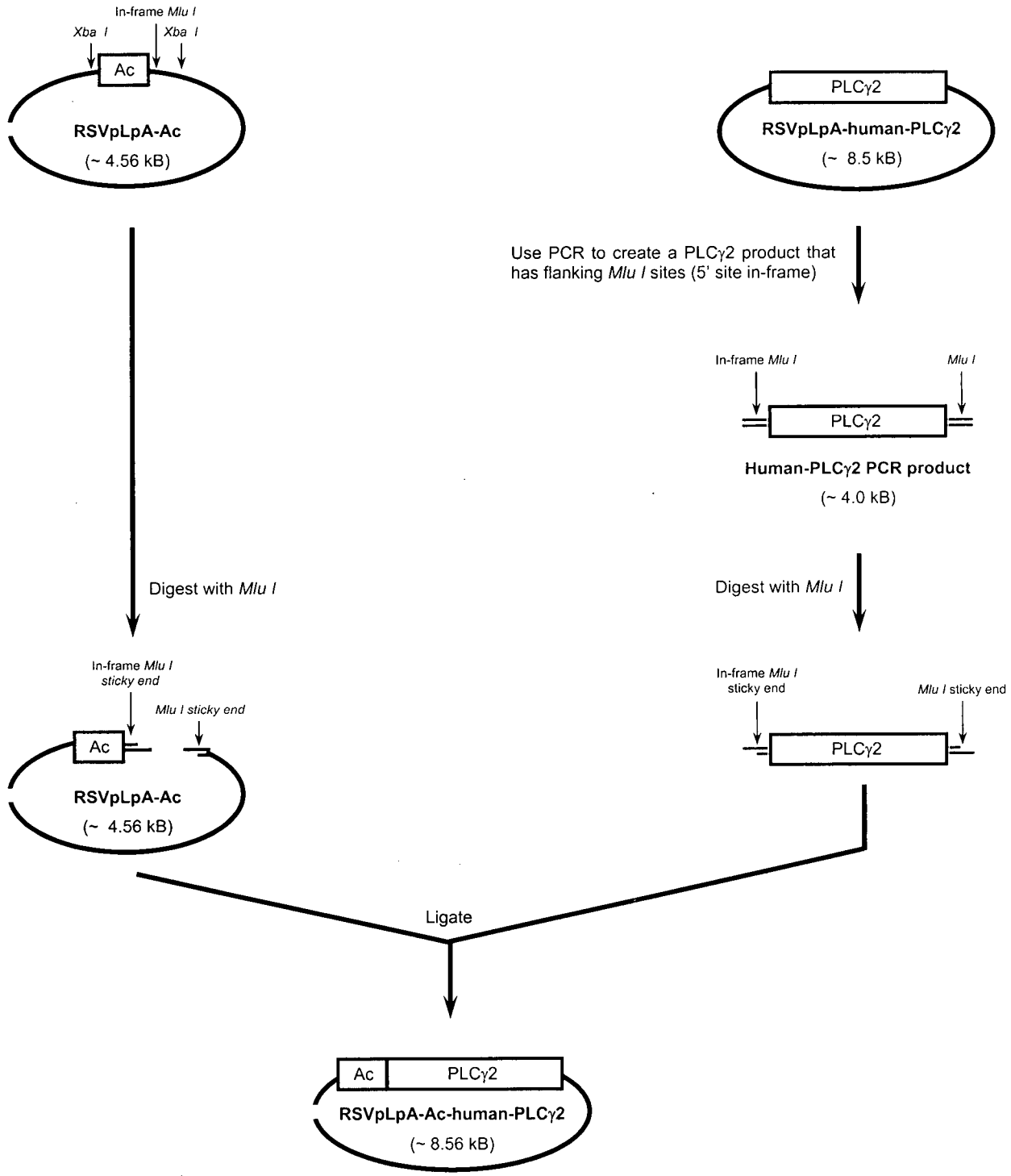

Figure 2.7. Schematic representation of how the *RSVpLpA-Ac-human-PLCγ2* expression vector (~ 8.56 kB) was developed. The sequence for human PLCγ2 was amplified from the *RSVpLpA-human-PLCγ2* vector (~ 8.5 kB) using PCR. The primers, TJ3 and TJ4, were used such that the resultant PCR product (~ 4.0 kB) would encode for human PLCγ2 (with the first codon removed) flanked by *Mlu I* sites (with the 5' site being in-frame with the PLCγ2 sequence). The PCR product was then digested with *Mlu I*, purified and ligated into the *RSVpLpA,-Ac* vector (~ 4.56 kB) that had similarly been digested with *Mlu I*. Correct orientation of the human PLCγ2 insert within the resultant *RSVpLpA-Ac-human-PLCγ2* vector was then confirmed by restriction enzyme digests and nucleotide sequencing

2.2 Molecular biology methods

2.2.1 Restriction endonuclease digests

Restriction enzymes were purchased from Roche Diagnostics (Laval, Quebec), Invitrogen Life Technologies, New England Biolabs (Pickering, Ontario) and Promega (Madison, Wisconsin) and were used according to the manufacturers' instructions. In general, the total amount of restriction enzyme(s) added to any given reaction was equal to or less than 10 % of the total volume of the digest. Digests were performed for 2-10 hours at 37 °C. Where necessary, the digested products were isolated by agarose gel purification.

2.2.2 Alkaline phosphatase reactions

Linearized vectors where treated with alkaline phosphatase (Roche Diagnostics) to prevent self-ligation. Where required, alkaline phosphatase was added to the restriction endonuclease digest for the final hour of the digest (using 20 units of alkaline phosphatase/1 μg of digested vector). Reactions were terminated by adding EDTA to a final concentration of 1 mM and heating samples in a heating block at 65 °C for 5 minutes. The digested DNA was then purified either by agarose gel purification or by phenol/chloroform extraction.

2.2.3 Phenol/Chloroform extraction

Phenol/chloroform extraction was performed essentially as described in the second edition of Molecular Cloning: A Laboratory Manual (Sambrook *et al.*, 1989). An equal volume of phenol was added to the DNA sample. The DNA/phenol solution was vortexed for 30 seconds and then centrifuged at room temperature at 14 000 rpm for 30 seconds. The aqueous phase containing the DNA (top layer) was then carefully removed, transferred to a fresh tube and again mixed with an equal volume of phenol, vortexed and centrifuged as before. The aqueous phase was then carefully removed and transferred to a fresh tube where it was mixed with an equal volume of Sevag (24:1 chloroform:isoamyl alcohol), vortexed for 30 seconds and then centrifuged as before. The aqueous phase containing the DNA was then carefully removed, transferred to a fresh tube and again mixed with an equal volume of Sevag, vortexed and centrifuged as before. The aqueous phase containing the DNA was then carefully removed, and transferred to a fresh tube. The phenol fractions and Sevag fractions were then sequentially back extracted with an equal volume of distilled water to recover any remaining DNA. The distilled water/DNA extract was then pooled with the aqueous phase containing the DNA. The DNA was then ethanol-precipitated.

Sodium acetate was added to the DNA sample to a final concentration of 0.3 M to facilitate precipitation of the DNA. Two and one-half volumes of ice-cold 95 % ethanol were then added to the solution. Following a 1 hour incubation at –20 °C the solution was then centrifuged at 4 °C at 14 000 rpm for 10 minutes. The supernatant was carefully removed and the remaining DNA pellet was washed with 750 μl of ice-cold 95 % ethanol. The ethanol was then carefully

removed and the DNA pellet was left to air dry for 10 minutes before being re-suspended in an appropriate volume of the appropriate buffer (generally 25-200 µl of distilled water). Purified DNA samples were stored at -20 °C.

2.2.4 Agarose gel electrophoresis

DNA samples were resolved on agarose gels. Agarose gels contained 0.5-2.0g agarose (GibcoBRL; Grand Island, New York) and 25 µg/ml ethidium bromide (GibcoBRL) in 100 ml of Tris/Boric Acid/EDTA (TBE; Chapter 2.14.1). DNA samples were mixed with 6x DNA sample buffer (5 parts sample to 1 part 6x sample buffer; Chapter 2.14.2) prior to loading on gels. Gels were then electrophoresed at a constant voltage of 100 volts in TBE for varying lengths of time dependant of the size and agarose percentage of the gel. Resolved DNA was then examined using ultraviolet light.

2.2.5 Gel purification of DNA

DNA was purified from agarose gels using either the Qiaquick Gel Extraction Kit (Qiagen; Mississauga, Ontario) or the Elutip-D Gel Extraction Kit (Schleicher and Schuell Bioscience GmbH; Keene, New Hampshire) as per the manufacturers' recommended instructions.

2.2.6 DNA ligation reactions

DNA ligations were performed with the Rapid DNA Ligation kit (Roche Diagnostics) as per the manufacturer's instructions. Generally, 0.5 µg of digested, purified vector DNA was mixed with 1-10 µg of digested, purified insert DNA (a molecular ratio of 2:1 of insert:plasmid DNA was used) along with 2 µl of the 5x DNA dilution buffer (kit component) and distilled water to a total volume of 10 µl. 10 µl of 2x Ligation Buffer and 1 µl of T4 DNA Ligase (kit components) were then added to the DNA solution. The reaction was then incubated at room temperature for 1 hour prior to being used to transform competent bacteria.

2.2.7 Transformation of competent *Escherichia coli* bacteria

Competent *Escherichia coli* (*E. coli*) bacteria were prepared by May Dang-Lawson (Matsuuchi Laboratory Technician; University of British Columbia; Vancouver, British Columbia). Competent bacteria were removed from –80 °C and allowed to thaw on ice. One hundred microlitres of thawed competent bacteria were then mixed with 100-300 ng of plasmid DNA and returned to ice for 20 minutes. The bacteria/DNA mixture was then incubated in a 42 °C water bath for 2 minutes before being returned to ice for 5 minutes. Finally, the bacteria/DNA mixture was plated on Luria-Bertani (LB) agar plates (Chapter 2.14.4) containing 100 µg/ml ampicillin (Sigma-Aldrich Canada; Oakville, Ontario). Plated bacteria were then incubated upside down at 37 °C overnight or until bacteria colonies were visible to the naked-eye.

2.2.8 Polymerase chain reactions (PCR)

Oligonucleotide primers for PCR were purchased through the NAPS Unit at UBC. Primers were re-suspended at a concentration of 10 pmol/μl in distilled, autoclaved water. Template DNA was similarly diluted to a concentration of 0.002 μg/μl. 2.5 μl of each primer (forward and reverse), 2.5 μl of template DNA and 17.5 μl of distilled autoclaved water were then added per tube of puReTaq Ready-To-Go-Beads (Amersham Biosciences Canada). The PCR mix was then overlaid with 25 μl of autoclaved mineral oil. Tubes were then placed in a DNA Thermocycler 480 (Perkin Elmer CETUS) and subjected to 30 cycles of 95 °C for 45 seconds, 55 °C for 120 seconds and 72 °C for 120 seconds. Finally, PCR products were collected from below the mineral oil layer and gel purified (described in Chapter 2.2.4 and 2.2.5).

2.2.9 Qiagen-mediated preparation of DNA (Small Quantity preparations)

Individual bacteria colonies were used to inoculate 4 ml of LB broth (Chapter 2.14.3) containing 100 μg/ml ampicillin. Inoculated LB broth was then incubated overnight at 37 °C with gentle shaking. Plasmid DNA was then isolated from transformed bacterial cultures using the Qiaprep Spin Miniprep Kit (Qiagen) as per the manufacturer's instructions.

2.2.10 Cesium chloride-mediated preparation of DNA (Large Quantity Preparations)

Individual bacteria colonies were used to inoculate 40 ml of LB broth (Chapter 2.14.3) containing 100 μg/ml ampicillin (adapted from Clewell and Helinski, 1972). Inoculated LB broth was then incubated overnight at 37 °C with gentle shaking. This culture was then transferred to 1 L of M9 growth media (Chapter 2.14.5) and incubated overnight at 37 °C with gentle shaking. Bacteria were pelleted by centrifugation at room temperature at 7500 rpm for 10 minutes in a JLA-16.250 rotor and Avanti centrifuge J-25I (Beckman Coulter; Fullerton, California). The supernatant was then removed and the bacterial pellet frozen at –20 °C for at least 1 hour. The pellet was subsequently thawed on ice and re-suspended in 15 ml of sucrose solution (Chapter 2.14.6). The bacteria were lysed by the addition of 3 ml of bacteria lysis buffer I (Chapter 2.14.7) for 5 minutes on ice followed by the addition of 1.5 ml of 250 mM EDTA (pH 8.0) for 15 minute on ice followed by the addition of 15 ml triton lytic mix (Chapter 2.14.8) for 30 minutes on ice. The resulting lysate was then cleared by centrifugation at room temperature at 18 000 rpm for 90 minutes in a JA 25.50 rotor and Avanti centrifuge J-25I. The resulting supernatant was collected and adjusted to a final concentration of 1.6 g/ml of cesium chloride. The supernatant was then transferred to Beckman Quick-Seal centrifuge tubes (16 x 76 mm) (Beckman Coulter) containing 1 mg of ethidium bromide/tube. Once full, the tubes were sealed and centrifuged at room temperature at 48 000 rpm for 48 hours in a 70.1 Ti rotor and L8-70M Ultracentrifuge (Beckman Coulter). Following centrifugation, plasmid DNA (indicated as the bottom of two ethidium bromide containing bands) was carefully removed from the gradient, extracted with cesium chloride-saturated isopropanol and dialysed extensively against 6 L of Tris/EDTA (TE; Chapter 2.14.11) over 2-3 days at 4 °C. Plasmid DNA was then precipitated

with ethanol (described in Chapter 2.2.14), centrifuged and re-suspended in 1 ml of distilled, autoclaved water. The optical density was measured at 260 nm and 280 nm to determine the OD_{260nm}/OD_{280nm}. This was then used to determine the concentration of DNA based on the equation:

$$\text{Concentration of double-stranded DNA} = 50\ \mu g/ml\ (OD_{260nm}/OD_{280nm})$$

2.3 Tissue culture

2.3.1 Tissue culture cell lines

The AtT20 murine endocrine cell line (described in Matsuuchi and Kelly, 1991) was kindly provided by Dr. Regis Kelly (University of California, San Francisco; San Francisco, California). The CH31 murine B lymphoma, K40B-1 pro-B cell and K40B-2 pre-B cell lines were kindly provided by Dr. Anthony DeFranco (University of California, San Francisco; San Francisco, California). The WEHI 231 murine B lymphoma, Ramos human B lymphoma and Daudi human B lymphoma were purchased from the American Type Tissue Culture Collection (Manassas, Virginia). The WEHI 231 murine B lymphoma variant, WEHI 303.1.5 (described as WEHI 303.1.5LM in Condon *et al.*, 2000) was characterized by the Matsuuchi Laboratory.

2.3.2 Maintenance of tissue culture of cell lines

AtT20-derived murine endocrine cell lines were maintained in complete Dulbecco's Modified Eagle Medium (complete DMEM; Invitrogen Life Technologies; Chapter 2.14.12). Cells were plated on 10 cm polystyrene tissue culture plates (Falcon; Franklin Lakes, New Jersey) and maintained at 37 °C in a 10 % CO_2 atmosphere water-jacketed incubator. Cells were generally grown to 90 % confluence before being passaged. To passage cells, the media was removed from the plate, cells were washed with 8 ml of Dulbecco's Phosphate-Buffered Saline (D-PBS) (Invitrogen Life Technologies) and then incubated at room temperature with 1 ml of trypsin solution (Invitrogen Life Technologies; Chapter 2.14.16) for 1-2 minutes. Cells were then re-suspended in 8 ml of fresh complete DMEM and transferred to a fresh culture dish. Cells were passaged at various dilutions ranging from 1:20-1:2 dependent on experimental requirements.

Human and murine B lymphoma cell lines were maintained in complete Roswell Park Memorial Institute (RPMI)-1640 media (Invitrogen Life Technologies; Chapter 2.14.14). Cells were grown either in 10 cm polystyrene tissue culture plates or in tissue culture flasks of various sizes (Falcon) and maintained at 37 °C in a 5% CO_2 atmosphere water-jacketed incubator. Cells were passaged every 3-4 days at various dilutions ranging from 1:20-1:2 dependent on experimental requirements.

Tissue culture cell lines were generally not passaged for longer than three months as extended passages may encourage the accumulation of mutations within the cell populations. Thus, multiple copies of the various cell lines were stored in 2 ml cryovials (Simport Plastics; Beloell,

Quebec) in liquid nitrogen. AtT20-derived cell lines were frozen down in complete DMEM further supplemented with 10 % dimethyl sulfoxide (DMSO; Sigma-Aldrich Canada). Human and murine B lymphoma cell lines were frozen down in fetal calf serum supplemented with 10 % DMSO.

2.3.3 Calcium phosphate-mediated transfections of AtT20-derived cell lines

AtT20-derived cell lines were transfected essentially as described by Matsuuchi and Kelly (1991). The desired AtT20-derived cell line was grown to approximately 70 % confluency on 10 cm polystyrene tissue culture plates. DNA was prepared for transfection by first mixing 50 μg of the desired plasmid(s), 20 μg of a selectable drug resistance plasmid, 94 μl of 2 M $CaCl_2$ and distilled water (such that the final volume of reagents totaled 750 μl) together. The entire 750μl solution was then added drop-wise to 750 μl of 2x HEPES-buffered saline (Chapter 2.14.17) while vortexing the solution at maximum speed. The DNA/HEPES solution was then incubated at room temperature for 40 minutes to allow a calcium phosphate/DNA precipitate to form. Cells to be transfected were washed twice with 1x HEPES-buffered saline (Chapter 2.14.18). The precipitated DNA/HEPES solution (should appear slightly cloudy) was then added drop-wise to the washed cells (1.5 ml/plate). Cells were then returned to the 37 °C, 10 % CO_2 incubator for 20 minutes. Following 20 minutes, complete DMEM media was added to the cells (8 ml/plate). Cells were then returned to the 37 °C, 10 % CO_2 incubator. Six to eight hours later the DNA/HEPES/media solution was aspirated from the cells. The cells were then glycerol-shocked for 1 minute with a room temperature 25 % glycerol/75 % complete DMEM media solution (1ml/plate). After 1 minute the solution was diluted with room temperature D-PBS (8 ml/plate) and removed by aspiration. Cells were then washed twice with room temperature D-PBS (8ml/plate). Complete DMEM media was then added to the cells (8 ml/plate) and the cells were returned to the 37 °C, 10 % CO_2 incubator for 2-3 days.

2.3.4 Drug selection of transfected cells and isolation of individual clones

Two to three days following transfection the cells were split 1:3 into selection media (i.e., one 10 cm polystyrene tissue culture plate of cells was passaged to 3 fresh 10 cm polystyrene tissue culture plates (described in Section 2.14.2). Selection media comprised of complete DMEM supplemented with either 2 μg/ml blasticidin (Invitrogen Life Technologies), 0.4 mg/ml G418 neomycin (Invitrogen Life Technologies) or 0.4 μg/ml puromycin (Calbiochem; La Jolla, California), as appropriate to the transfection. Once passaged, cells were maintained within the same plates for approximately 3-6 weeks. The transfected cells were washed every 3-4 days with D-PBS (8 ml/plate) to remove any cells that had perished. Individual drug-resistant clones were isolated when they became visible to the eye (approximately at the 64-128 cell stage). To isolate clones the cells were gently washed with room temperature D-PBS (8 ml/plate). The D-PBS was then aspirated from the plate and sterile 9 mm Teflon cloning rings (Fisher Scientific; Ottawa, Canada) were placed over well-isolated, individual clones (note: the bottom of the

cloning rings were coated with a thin layer of high vacuum grease [Dow Corning; Midland, Michigan] so that a seal could be established between the cloning ring and the polystyrene tissue culture plate). One drop of trypsin solution was then added into the cloning ring to facilitate removal of the individual clone from the plate. Two minutes later 4 drops of the appropriate selection media were added to the cloning ring and the cells were re-suspended by gently pipetting the solution up and down. The re-suspended cells were then transferred to a well in a 24-well polystyrene tissue culture plate (Falcon) and topped up with the appropriate selection media (1 ml/well). As clones grew confluent they were successively passaged to larger wells (from a 24-well plate to a 12-well plate to duplicate 6 well plates). Once in six well plates, the clones of one duplicate plate were lysed while the clones in the other duplicate plate were maintained for further passage and experiments. Lysis was achieved essentially as described below (Chapter 2.4) with the exception that 150-300 µl of Triton X-100 lysis buffer (Chapter 2.14.21) was used per well of a six well plate. Successful expression of the desired plasmids' given products were confirmed by immunoblot analysis of the lysates.

2.4 Stimulation and lysis of cell lines

AtT20-derived cell lines were grown to approximately 90 % confluency on 10 cm polystyrene tissue culture plates. Prior to stimulation the cells were washed twice with 8 ml/plate of D-PBS containing 1g/L dextrose (Fisher Scientific). Cells were then incubated in 8 ml/plate of modified HEPES-buffered saline (modified HBS; Chapter 2.1.19) for 15 minutes at 37 °C and 10 % CO_2. BCR-mediated cell stimulation was achieved by cross-linking the BCR with 200 µg/plate of affinity purified goat anti-mouse IgM (µ chain specific) antibody. Cells were then incubated at 37 °C and 10 % CO_2 for the desired length of stimulation. To terminate stimulation cells were washed twice with ice-cold D-PBS containing 1 mM Na_3VO_4 (also known as sodium pervanadate; from Sigma-Aldrich Canada). Cells were then immediately lysed on ice for 20 minutes with 0.5-1.0 ml/plate of ice-cold Triton X-100 lysis buffer. The lysate was then transferred from the 10 cm plate to a 1.5 ml eppendorf tube (Eppendorf/Brinkmann Instruments; Mississauga, Ontario) and centrifuged at 14 000 rpm at 4 °C for 15 minutes to pellet out nuclei and other detergent insoluble material. The cleared lysate (supernatant) was then transferred to a fresh 1.5 ml eppendorf tube where sodium dodecyl sulfate (SDS; Bio-Rad Laboratories; Hercules, California) and deoxycholate (DOC; Fisher Scientific) were added to a final concentration of 0.3% and 0.4 %, respectively. The protein concentration of each sample was determined using the bicinchoninic acid (BCA) protein assay kit (Pierce Biotechnology). Lysates were stored at –20 °C.

B cell lymphoma cell lines were grown to confluency either in 10 cm polystyrene tissue culture plates or in tissue culture flasks of various sizes (Falcon). Prior to stimulation cells were washed twice with modified HBS and then re-suspended in this buffer at a concentration of 25 x 10^6 cells/ml. Re-suspended cells were warmed to and maintained at 37 °C in a water bath for the

duration of the stimulation. BCR-mediated stimulation was achieved by cross-linking the BCR with either 100 μg/ml of affinity purified goat anti-mouse IgM (μ chain specific) antibodies or with 100 μg/ml affinity purified goat anti-human IgM (μ chain specific) antibodies, as appropriate. To terminate the stimulation cells were washed twice with ice-cold D-PBS containing 1 mM Na_3VO_4. Cells were then lysed on ice for 20 minutes in 0.5-1.0 ml of ice-cold Triton X-100 lysis buffer. The lysate was then centrifuge at 14 000 rpm at 4 °C for 15 minutes to pellet out nuclei and other detergent insoluble material. The cleared lysate (supernatant) was then transferred to a fresh 1.5 ml eppendorf tube where SDS and DOC were added to a final concentration of 0.3% and 0.4%, respectively. The protein concentration of each sample was determined using the BCA protein assay kit. Lysates were stored at –20 °C.

Non-stimulated cell lysates were prepared by washing the cells twice with room temperature D-PBS. Cells were then lysed as described above.

2.5 SDS-PAGE and immunoblot analysis

Samples (whole cell lysates, immunoprecipitates and fractions) were mixed with 5x running sample buffer (5x RSB; mixed as 4 parts sample to 1 part 5x RSB; Chapter 2.14.28). Samples were then heated in a boiling water bath for 5 minutes prior to sodium dodecyl sulfate-polyacrylamide gel electrophoresis (SDS-PAGE). Once boiled, samples were loaded into individual wells of a polyacrylamide (Bio-Rad Laboratories) mini-gel (1.0 mm or 1.5 mm thick; 9%, 10 %, 12% or 15%). A 5 μl sample of Benchmark pre-stained protein molecular weight standard (Invitrogen Life Technologies) was also added to one well of the gel. Samples were then resolved at a constant current of 20 milliamps/gel for 2-3 hours in a dual vertical mini-gel apparatus (CSB Scientific; Del Mar, California) in running buffer (Chapter 2.14.29). The resolved proteins were then transferred from the gel to a Protran nitrocellulose filter (VWR International; Delta, British Columbia) in a Transblotter Transfer Apparatus (Bio-Rad Laboratories) at a constant voltage of 125 volts for 2 hours in transfer buffer (Chapter 2.14.30).

Nitrocellulose filters were generally blocked for 1-2 hours at room temperature with Tris-buffered saline (TBS; Chapter 2.14.31) containing 5% skim milk powder. However, filters that were immunoblotted with the phospho-Erk antibody were blocked for only 15 minutes at room temperature with TBS containing 5% skim milk powder and filters that were immunoblotted with the 4G10 antibody were blocked for a minimum of 2 hours at room temperature with TBS containing 5% bovine serum albumin (BSA). Blocked filters were rinsed once with TBS containing 0.1% Tween 20 (TBST; Chapter 2.14.33) before being rocked overnight at 4°C in the desired primary antibody (10 ml solution/filter). Primary antibodies were diluted 1:500-1:2000 in TBST containing either 0-5% BSA or 0-5% skim milk powder (the ideal conditions for each antibody were determined empirically). The next day, filters were washed at room temperature for 4 x 15 minutes with TBST (50 ml/filter/wash). Filters were then rocked at room temperature

for 1 hour with the appropriate HRP-conjugated secondary reagent (10 ml solution/filter). Secondary reagents were diluted 1:5000 - 1:10 000 in TBST containing either 0-5% BSA or 0-5% skim milk powder (again, ideal conditions were determined empirically). Filters were then washed at room temperature for 4 x 15 minutes with TBST (50 ml/filter/wash). The immunoreactive bands on the filters were then visualized by enhanced chemiluminescence (ECL; Amersham Biosciences Canada) coupled with exposure of the filters to Kodak autoradiography film (Mandel Scientific; Guelph, Ontario).

To re-immunoblot, filters were briefly re-hydrated in distilled water (50 ml/filter). Previously bound antibodies were removed from the re-hydrated filter by incubating the filter at room temperature for 15 minutes with Stripping TBS (Chapter 2.14.32) (50 ml/filter). Filters were then washed at room temperature for 2 x 15 minutes with TBS (50 ml/filter). Finally, filters were blocked and re-immunoblotted as described above.

2.6 Immunoprecipitation studies

Cell lysates were prepared essentially as described above (in Chapter 2.4) with cells being lysed with either Triton X-100 lysis buffer or n-Dodecyl-β-d-maltoside lysis buffer (DM Lysis Buffer; Chapter 2.14.22) or Nonidet P40 lysis buffer (NP40 Lysis Buffer; Chapter 2.14.23). 500-3000 μg of lysate were pre-cleared for 30 minutes at 4 °C with either 20-50 μl of 50 % (v:v in D-PBS) Protein A- or Protein G-Sepharose 4B beads (Sigma-Aldrich Canada). Pre-cleared lysates were then immunoprecipitated for 1 hour at 4 °C with 1-3 μg of immunoprecipitating antibody and 40-100 μl of 50 % Protein A- or Protein G-Sepharose 4B beads. The beads were then collected by centrifugation and washed twice with 500 μl of the lysis buffer that corresponded with the original lysate preparation. The immunoprecipitated proteins were eluted from the beads with 35 μl of 1x running sample buffer (Chapter 2.14.27). The immunoprecipitated samples were then resolved by SDS-PAGE mini-gels (as described in Chapter 2.5) with co-immunoprecipitation (i.e., co-association) of various proteins being investigated by immunoblotting (as described in Chapter 2.5).

2.7 Membrane enrichment of cell lines

AtT20-derived cell lines were grown to confluency on 10 cm polystyrene tissue culture plates (as described in Chapter 2.3.2). One plate of cells was used per treatment. Cells were removed from tissue culture plates using 5 ml of D-PBS containing 10 mM EDTA. Cells were incubated with the D-PBS/EDTA solution on a shaker at room temperature for 5-10 minutes. Cells were then collected in a 15 ml polypropylene conical centrifuge tubes (Falcon), centrifuged at low speed (1500 rpm at room temperature for 3 minutes in a tabletop centrifuge) and washed twice with 5 ml of room temperature D-PBS containing 1 g/l glucose and once with 10 ml of modified HBS. Cells were then re-suspended in 1 ml of 37 °C modified HBS and warmed for 15 minutes in a 37 °C water bath. Cells were stimulated by cross-linking the BCR with affinity purified goat

anti-mouse IgM (μ chain specific) antibodies (200 μg/ml). After 5 minutes the stimulation was terminated by adding ice-cold D-PBS containing 1 mM of Na_3VO_4 to the reaction (500 μl/tube), centrifuging at low speed (1500 rpm at 4 °C for 3 minutes) and removing the supernatant from the pelleted cells. Cells were washed once more with ice-cold D-PBS containing 1 mM of Na_3VO_4 (1 ml/tube). Cells were then re-pelleted, the supernatant was removed and the pelleted cells were frozen in liquid nitrogen for 15 seconds. The cells were then incubated on ice for 5 minutes with non-detergent lysis buffer (200 μl/tube) (Chapter 2.14.24). Following incubation, cells were re-suspended and then centrifuged at 4 °C for 5 minutes at 14 000 rpm. The supernatant (cytosolic fraction) was then transferred to a new 1.5 ml eppendorf tube containing 20 μl of 10 % Triton X-100 (v:v in distilled water). The remaining pellet was washed twice with 300 μl of non-detergent lysis buffer before being re-suspended in 220 μl of Triton X-100 lysis buffer and then centrifuged at 4 °C for 5 minutes at 14 000 rpm. The supernatant (membrane-enriched fraction) was then transferred to a new 1.5 ml eppendorf tube and the remaining pellet was discarded. The protein concentration of each sample was determined using the BCA protein assay kit. Samples were stored at –20 °C.

2.8 Cytoskeletal-based lipid raft preparation

Cells were cultured for 16-20 hours in low serum RPMI-1640 media (Chapter 2.14.25). Cells were then washed twice with modified HBS and then re-suspended in this buffer at a concentration of 1.25 x 10^7 cells/ml. For each condition, 2 ml of re-suspended cells were warmed to and maintained at 37 °C in a water bath for the duration of the stimulation. Stimulation was achieved by cross-linking the components of the BCR with either 50 μg/ml of affinity purified goat anti-mouse IgM (μ chain specific) antibodies or with 300 μg/ml of biotinylated anti-Igβ antibody (monoclonal HM79-16 antibody) plus 40μg/ml streptavidin, as appropriate. The cells were then washed twice with ice-cold D-PBS containing 1 mM Na_3VO_4 to stop the stimulation. Cells were then subjected to cytoskeletal-based lipid raft preparation.

Cytoskeletal-based lipid rafts were prepared essentially as described by Weintraub *et al.* (2000). Cells were re-suspended at a concentration of 1.25 x 10^7 cells/375 μl of ice cold Low Salt Cytoskeleton Stabilization Buffer (Low Salt CSB; Chapter 2.14.25). After 10 minutes on ice, cells were centrifuged for 10 minutes at 2000 rpm in a 4 °C microfuge. The supernatant was collected and retained as the "detergent-soluble" supernatant fraction. The pellet was re-suspended in 375 μl of ice cold Low Salt CSB buffer and then centrifuged for 15 minutes at 2000 rpm in a 4 °C microfuge. The supernatant was then discarded as a wash and the pellet was re-suspended in 110 μl of ice-cold High Salt CSB (Chapter 2.14.26). The re-suspended pellet was centrifuged for 15 minutes at 2000 rpm in a 4 °C microfuge. The supernatant was collected and retained as the "detergent-insoluble, salt extractable" lipid raft fraction. The protein

concentration of each fraction was determined using the BCA protein assay kit. Samples were stored at –20 °C until undergoing SDS-PAGE and immunoblot analysis.

2.9 Inositol phosphate assay

Inositol phosphate production was measured essentially as described by Matsuuchi *et al.*, (1992). Please refer to Appendix 4 for further information regarding attempts to optimize this assay. Cells were plated out in six well plates (Falcon) by adding 2 x 10^5 cells in complete DMEM to each well. Cells were then returned to a 10 % CO_2, 37 °C incubator. After 48 hours the media was aspirated from the cells and replaced with 2 ml/well of low serum DMEM (Chapter 2.14.13). Cells were then returned to a 10 % CO_2, 37 °C incubator overnight. The next day cells were washed twice with 2 ml/well of PBS containing 1g/L glucose. Modified HBS containing 10 mM LiCl was then added back to the cells (1.5 ml/well). After 15 min at 10 % CO_2 and 37 °C the cells were again washed twice with 2 ml/well of PBS containing 1g/L glucose. Modified HBS containing 10 mM LiCl was then added back to the cells (1.5 ml/well) along with the appropriate stimulus (either 200 µl/well of 10 % fetal calf serum, 15 µl of 100 µM serotonin/well or 60 µg of affinity purified goat anti-mouse IgM [µ chain specific] antibodies). After 15 minutes at 10 % CO_2 and 37 °C, the reactions were terminated by washing the cells twice with PBS and then adding 1 ml/well of ice cold 10 % trichloroacetic acid. Cells were then removed from the plate using a rubber policeman and the contents of each well were transferred to a 1.5 ml eppendorf tube. Insoluble material was removed by centrifuging for 5 minutes at 14 000 rpm in a 4 °C microfuge. The supernatant was then transferred to a glass tube and extracted six times with ice cold water-saturated ethyl ether. The inositol phosphates were then collected from the extracted solution by running the solution over an AG 1-X8 Resin formate column (Bio-Rad Laboratories). The inositol phosphates were then eluted from the column with 20 ml of a 1 M ammonium formate/0.1 M formic acid solution. Five millilitres of the resulting eluate were then transferred to a scintillation vial and mixed with 5 ml of Ready Gel liquid scintillation cocktail (Beckman Coulter). As well, the insoluble material (pellet) was re-suspended in 1 ml of methanol, transferred to a scintillation vial and mixed with 5 ml of Ready Gel liquid scintillation cocktail. Samples were then counted for ^{3}H-inositol using a Beckman LS 5000TA scintillation counter (Beckman Coulter).

2.10 Population-based calcium flux assay

Population-based calcium flux assays were performed essentially as described below. Please refer to Appendix 5 for further information regarding attempts to optimize this assay.

Initially, 20 x 10^6 AtT20-derived cells were plated on adherent 10 cm tissue culture plates (Falcon) and returned to a 10 % CO_2, 37 °C incubator overnight. The next day the media was aspirated from the cells and replaced with 1.0 ml of serum-free DMEM containing 10.0 µM Fura-2 acetoxymethyl ester (Fura-2 AM; Molecular Probes). Cells were returned to a 10 % CO_2,

37 °C incubator for 40 minutes. Following this, cells were gently washed from the plate with the existing media and pelleted by centrifugation for 5 minutes at 1500 rpm at 4 °C in an IEC Centra-8R Tabletop Centrifuge (International Equipment Company; Needham Heights, Massachusetts) and re-suspended in 3 ml of modified HBS. The re-suspended cell sample was then placed in a 3 ml cuvette that was then placed in a Perkin Elmer LS50B Luminescence Spectrometer and allowed to warm to 37 °C for 5 minutes. The appropriate stimulus (6.0 μM serotonin or 50-100 μg of affinity purified goat anti-mouse IgM [μ chain specific] antibody) was then added to the sample. Two minutes later 2.0 μM of ionomycin (an ionophore) were added to the sample as a positive control. Following another two minutes the cells were lysed by the addition of 0.1 mM digitonin as a further positive control. Finally, two minutes later, 70 μM of Tris and 10 μM of EDTA were added to the sample to chelate the calcium as yet another control. Throughout the experiment calcium flux was monitored by determining the ratio of the fluorescence intensities at 510 nm (emission wavelength) that was produced by excitation of Fura-2 AM at 340 nm and 380 nm (excitation wavelengths) as an increase in the ratio of fluorescence intensities (340 nm/380 nm) is indicative of increased calcium-binding by Fura-2 AM.

2.11 Single cell-based calcium assay

Single cell-based calcium assays were performed essentially as described in Church *et al.* (1998). Cells were initially plated on 15 mm poly-D-lysine coated coverslips. Poly-D-lysine coated coverslips were prepared by submerging the coverslips in a poly-D-lysine solution (1 mg/ml poly-D-lysine [Sigma-Aldrich Canada], 50 mM sodium borate pH 8.5) for two hours at room temperature. Coverslips were then rinsed three times with PBS followed by three times with distilled water. Once confluent, cells were loaded with Fura-2 AM by placing the coverslip (cell side up) in 2 ml of modified HBS containing 7.5 μM Fura-2 AM for 1 hour at 10 % CO_2 and 37 °C. Cells were then rinsed for 10 minutes at room temperature in 2 ml of modified HBS. The coverslip was then mounted in a temperature controlled perfusion chamber such that the coverslip (cell side up) formed the base of the chamber. The cells were then superfused with the modified HBS at a rate of 2 ml/minute. After 2 minutes the cells were superfused with calcium-free modified HBS (Chapter 2.14.20) at a rate of 2 ml/minute. After 5 minutes the flow was stopped and serotonin (or the agonist of choice) was added to the solution to a final concentration of 6 μM. After 2 minutes the flow of calcium free modified HBS was resumed to rinse the serotonin from the chamber. Two minutes later the flow was switched to modified HBS. Cells were superfused with the calcium containing solution for 10 minutes to enable reloading of the cells' calcium stores. Cells were then once again superfused with calcium-free modified HBS at a rate of 2 ml/minute. After 5 minutes the flow was stopped and the PLC activator, m-3M3FBS, (or agonist of choice) was added to the solution to a final concentration of 50 μM. After 2 minutes the flow of calcium free modified HBS was resumed to rinse the PLC activator from the

chamber. Finally, after 2 minutes, flow was stopped and ionomycin was added to the solution to a final concentration of 10 μM.

Throughout the experiment calcium flux was monitored utilizing a digital fluorescence microscopy system (Atto Instruments, Incorporated; Rockville, Maryland; and Carl Zeiss Canada Limited; Don Mills, Ontario). This system allows for the simultaneous real-time monitoring of fluorescence emissions from single cells. In particular, the intensity of fluorescence emissions at 510 nm were monitored following excitation of Fura-2 AM at 334 nm and 380 nm where an increase in the ratio of emission intensities (334 nm/380 nm) indicates of increased calcium-binding by Fura-2 AM.

2.12 Production of anti-BLNK polyclonal antibodies

Rabbit polyclonal antibodies were produced against peptides corresponding to specific regions of BLNK. Vectors encoding the peptides fused in-frame with Glutathione S-Transferase (GST) were kindly provided by Rob Ingham (from Anthony Pawson's Lab at the Lunenfeld Institute at the University of Toronto; Ontario, Canada) (refer to Table 2.2). The GST-fusion peptides were prepared and purified by Gabe Woollam, a former undergraduate student of the Matsuuchi Laboratory. Briefly, a single bacteria colony was used to inoculate 20 ml of LB Broth containing 100 μg/ml ampicillin. The culture was then incubated overnight at 37 °C before being used to further inoculate 1 L of LB broth containing 100 g/ml ampicillin. This culture was then incubated at 37 °C until the optical density (OD_{600nm}) of the culture was between 0.8-1.0 (approximately 4-6 hours) at which point isopropylthio-β-galactopyranoside (Invitrogen Life Technologies) was added to a final concentration of 100 μM. The culture was then incubated overnight at 37 °C with shaking. The next day, bacteria were pelleted by centrifugation and re-suspended in 10 ml of bacteria lysis buffer II (Chapter 2.14.9) and incubated on ice for 30 minutes. The lysate was then sonicated for 2 minutes on ice before being centrifuged for 45 minutes at 30,000 rpm at 4 °C in a SW70 Ti rotor and a Beckman L8-70 Ultracentrifuge. The GST-fusion peptide was then purified from the cleared lysate using glutathione-Sepharose 4B beads (Sigma-Aldrich Canada). Lysate and beads were incubated together for 1 hour at 4 °C to allow the GST-fusion peptide to bind to the beads. The beads were then collected by centrifugation and washed three times with bead wash buffer (Chapter 2.14.10). Bound GST-fusion peptide was then eluted from the beads using a mild non-denaturing elution buffer (50 mM Tris base, 20 mM glutathione [Amersham Biosciences Canada], pH 8.0). Subsequently, the eluate was dialyzed against 10 mM Tris-HCl (pH 8.0) at 4 °C to remove any free glutathione. The concentration of the GST-fusion peptide was determined by measuring the OD_{280} ($OD_{280}/1.46 \cong$ mg/ml of protein) and its purity confirmed by SDS-PAGE and Coomassie Blue staining.

Once purified, the GST-fusion protein was emulsified in complete Freund's Adjuvant (Difco Laboratories; Detroit, Michigan) for the initial injection and then in Incomplete Freund's Adjuvant (Difco Laboratories) for subsequent injections. Rabbits, TJ1 and TJ2, were injected with the GST-BLNK SH2 fusion peptide (Table 2) while TJ3 was injected with the GST-BLNK Proline Rich fusion peptide (Table 2). All injections were intramuscular and were carried out approximately every 18 days. 7-10 days following injection, approximately 10 ml of blood was collected from the ear vein of each rabbit. The blood sample was then stirred and left overnight at 4 °C to promote clotting. The next day the clot was carefully removed and the remaining serum was stored at -80 °C. Working aliquots were stored in 50 % glycerol at -20 °C.

Table 2.2. Summary of Fusion Peptides Used to Immunize Rabbits to Produce Anti-BLNK Antibodies. Note that PB refers to prebleed, B to Bleed and TB to termination Bleed. TJ*x*B*y* refers to the rabbit number (x) and bleed number (y).

Fusion Peptide	Description	Corresponding Rabbit	Resulting Antibodies
GST-BLNK SH2	GST (aa 1-242) fused in-frame to BLNK's SH2 domain (aa 386-507)	TJ1 and TJ2	TJ1PB, TJB1-10, TJTB 1-7 TJ2PB, TJ2B1-11, TJ2TB1-6
GST-BLNK Proline Rich (P-Rich)	GST (aa 1-242) fused in-frame to BLNK's Proline rich domain (aa 152-388)	TJ3	TJ3PB, TJ3B1-9, TJ3TB1-7

2.13 Surface biotinylation of cells

AtT20-derived cell lines were grown to confluency on 10 cm polystyrene tissue culture plates (as described in Chapter 2.3.2). Cells to be labeled were rinsed five times with 1x ice-cold PBS. After rinsing, 2.5 ml of ice-cold Sulfo-NHS-biotin/1x PBS solution was added per 10 cm plate (Sulfo-NHS-biotin from Pierce Biotechnology; Sulfo-NHS-biotin/1x PBS solution made by initially dissolving 25 mg of Sulfo-NHS-biotin in 125µl of DMSO and then further diluting 25 µl of the Sulfo-NHS-biotin/DMSO solution per 10 ml of 1x PBS). The plate was then placed on ice on a rocker for 20 minutes. After 20 minutes the reaction was quenched by adding 5 ml of ice-cold DMEM containing 2mg/ml lysine was per plate. The DMEM solution was then immediately aspirated off, the plate rinsed with 10 ml of 1x PBS containing 2 mg/ml lysine, and 10 ml of fresh DMEM containing 2 mg/ml lysine added back to the plate. The plate was then left to rock for an additional 5 minutes. Subsequently, the plate was rinsed 8x with ice-cold 1x PBS containing 2mg/ml lysine prior to be lysed as described above in Chapter 2.4.

2.14 Summary of solutions

2.14.1 Tris/Boric Acid/EDTA (TBE)

90 mM Tris-HCl (pH 8.2)

90 mM boric acid (Fisher Scientific)

2 mM	ethylenedinitrilotetraacetic acid (EDTA)

2.14.2 6x DNA Sample Buffer

0.24 %	bromophenol blue (Sigma-Aldrich Canada)
0.24 %	xylene cyanol FF (Sigma-Aldrich Canada)
60 % (w/v)	sucrose

2.14.3 Lauria-Bertani Broth (LB Broth)

5 g	NaCl
5 g	yeast extract (Difco Laboratories)

Total volume made up to 1 L with distilled water

2.14.4 Lauria-Bertani Agar (LB Agar)

5 g	NaCl
5 g	yeast extract (Difco Laboratories)
15 g	agar (Difco, Laboratories)

Total volume made up to 1 L with distilled water

2.14.5 M9 Growth Media

100 µg/ml	ampicillin (Sigma-Aldrich Canada)
1 L	M9 salts (refer to Molecular Cloning Laboratory Manual, Second Edition by Sambrook, Fritsch and Maniatis)
1 µM	$CaCl_2$
1 mM	$MgSO_4$
0.4 %	glucose
0.4 %	cosamino acids
0.004 %	proline
0.004 %	leucine
0.004 %	threonine

2.14.6 Sucrose Solution

25 %	sucrose
50 mM	Tris (pH 8.0) (ICN Biomedicals)
1 mM	EDTA (pH 8.0)

2.14.7 Bacteria Lysis Buffer I

5 mg/ml	lysozyme (Sigma-Aldrich Canada)
25 mM	Tris (pH 8.0)

2.14.8 Triton Lytic Mix

0.1 %	Triton X- 100
62.5 mM	EDTA (pH 8.0)
50 mM	Tris (pH 8.0)

2.14.9 Bacteria Lysis Buffer II

50 mM	Tris-HCl (pH 8.0)
150 mM	NaCl
1 %	Triton-X 100 (Sigma-Aldrich Canada)
1 mg/ml	Lysozyme (Sigma-Aldrich Canada)
0.1 mg/ml	DNAse I
10 mg/ml	soybean trypsin inhibitor (Roche Diagnostics)
10 µg/ml	leupeptin (Roche Diagnostics)
1 µg/ml	aprotinin (Roche Diagnostics)
1 mM	phenymethylsulfonyl fluoride (Roche Diagnostics)

2.14.10 Bead Wash Buffer

25 mM	Tris-HCl (pH 8.0)
150 mM	NaCl
0.1 %	Triton-X 100 (Sigma-Aldrich Canada)
10 mg/ml	soybean trypsin inhibitor
10 µg/ml	leupeptin (Roche Diagnostics)
1 µg/ml	aprotinin (Roche Diagnostics)
1 mM	phenymethylsulfonyl fluoride (Roche Diagnostics)

2.14.11 Tris/EDTA (TE)

10 mM	Tris (pH 8.0) (ICN Biomedicals)
1 mM	EDTA (pH 8.0)

2.14.12 Complete DMEM

500 ml	DMEM (containing 4.5g/L glucose, 2 mM L-glutamine, 110 mg/L sodium pyruvate; Invitrogen Life Technologies)
50 ml	heat-inactivated fetal calf serum (Invitrogen Life Technologies)
50 units/ml	penicillin (Invitrogen Life Technologies)
50 µg/ml	streptomycin sulfate (Invitrogen Life Technologies)

2.14.13 Low Serum DMEM

500 ml	DMEM (containing 4.5g/L glucose, 2 mM L-glutamine, 110 mg/L sodium pyruvate; Invitrogen Life Technologies)
1 ml	heat-inactivated fetal calf serum (Invitrogen Life Technologies)
50 units/ml	penicillin (Invitrogen Life Technologies)

50 μg/ml	streptomycin sulfate (Invitrogen Life Technologies)

2.14.14 Complete RPMI-1640

500 ml	RPMI-1640 (Invitrogen Life Technologies)
50 ml	heat-inactivated fetal calf serum (Invitrogen Life Technologies)
2 mM	L-glutamine (Invitrogen Life Technologies)
1 mM	sodium pyruvate (Invitrogen Life Technologies)
50 μM	2-β-mercaptoethanol (Sigma-Aldrich Canada)
50 units/ml	penicillin (Invitrogen Life Technologies)
50 μg/ml	streptomycin sulfate (Invitrogen Life Technologies)

2.14.15 Low Serum RPMI-1640

500 ml	RPMI-1640 (Invitrogen Life Technologies)
1 ml	heat-inactivated fetal calf serum (Invitrogen Life Technologies)
2 mM	L-glutamine (Invitrogen Life Technologies)
1 mM	sodium pyruvate (Invitrogen Life Technologies)
50 μM	2-β-mercaptoethanol (Sigma-Aldrich Canada)
50 units/ml	penicillin (Invitrogen Life Technologies)
50 μg/ml	streptomycin sulfate (Invitrogen Life Technologies)

2.14.16 Trypsin Solution (Invitrogen Life Technologies)

0.25 %	trypsin in DMEM
1 mM	EDTA

2.14.17 2x HEPES-Buffered Saline (2x HBS)

50 mM	HEPES (pH 7.2) (Sigma-Aldrich Canada)
10 mM	KCl
12 mM	glucose
280 mM	NaCl
1.5 mM	Na_2HPO_4

2.14.18 1x HEPES-Buffered Saline (1x HBS)

25 mM	HEPES (pH 7.2) (Sigma-Aldrich Canada)
5 mM	KCl
6 mM	glucose
140 mM	NaCl
750 μM	Na_2HPO_4

2.14.19 Modified HBS

25 mM	HEPES (pH 7.2) (Sigma-Aldrich Canada)
125 mM	NaCl
5 mM	KCl
1 mM	$CaCl_2$
1 mM	Na_2HPO_4
500 μM	$MgSO_4$
1 mg/ml	glucose
2 mM	L-glutamine
1 mM	sodium pyruvate
2 %	BSA (ICN Biomedicals).

2.14.20 Calcium Free Modified HBS

25 mM	HEPES (pH 7.2) (Sigma-Aldrich Canada)
125 mM	NaCl
5 mM	KCl
1 mM	Na_2HPO_4
1.5 mM	$MgSO_4$
1 mg/ml	glucose
2 mM	L-glutamine
1 mM	sodium pyruvate
2 %	BSA (ICN Biomedicals)

2.14.21 Triton X-100 Lysis Buffer

20 mM	Tris-HCl (pH 8.0)
137 mM	NaCl
1 %	Triton X-100 (Sigma-Alrdich Canada)
2 mM	EDTA
10 %	glycerol
10 μg/ml	leupeptin (Roche Diagnostics)
1 μg/ml	aprotinin (Roche Diagnostics)
1 mM	pepstanin A (Sigma-Aldrich Canada)
1 mM	Na_3VO_4 (Sigma-Aldrich Canada)
1 mM	phenylmethylsulfonyl fluoride (Roche Diagnostics)

2.14.22 DM Lysis Buffer

20 mM	Tris-HCl (pH 8.0)
137 mM	NaCl
1 %	n-dodecyl-β-d-maltoside (Sigma-Alrdich Canada)

2 mM	EDTA
10 %	glycerol
10 μg/ml	leupeptin (Roche Diagnostics)
1 μg/ml	aprotinin (Roche Diagnostics)
1 mM	pepstanin A (Sigma-Aldrich Canada)
1 mM	Na_3VO_4 (Sigma-Aldrich Canada)
1 mM	phenylmethylsulfonyl fluoride (Roche Diagnostics)

2.14.23 NP40 Lysis Buffer

10 mM	Tris-HCl (pH 8.0)
150 mM	NaCl
1 %	Nonidet P40 (NP40) (BDH Laboratory Supplies; distributed by VWR Canlab; Mississauga, Ontario)
10 μg/ml	leupeptin (Roche Diagnostics)
1 μg/ml	aprotinin (Roche Diagnostics)
1 mM	pepstanin A (Sigma-Aldrich Canada)
1 mM	Na_3VO_4 (Sigma-Aldrich Canada)
1 mM	phenylmethylsulfonyl fluoride (Roche Diagnostics)

2.14.24 Non-Detergent Lysis Buffer

10 mM	Tris-HCl (pH 8.0)
137 mM	NaCl
10 %	glycerol
2 mM	EDTA
10 μg/ml	leupeptin (Roche Diagnostics)
1 μg/ml	aprotinin (Roche Diagnostics)
1 mM	pepstanin A (Sigma-Aldrich Canada)
1 mM	Na_3VO_4 (Sigma-Aldrich Canada)
1 mM	phenylmethylsulfonyl fluoride (Roche Diagnostics)

2.14.25 Low Salt Cytoskeletal Stabilization Buffer

20 mM	HEPES (pH 7.6)
0.5 %	Triton X-100 (Sigma-Alrdich Canada)
10.3 %	sucrose
20 mM	NaCl
5 mM	$MgCl_2$
0.1 mg/ml	BSA (ICN Biomedicals)
500 μg/ml	leupeptin (Roche Diagnostics)
500 μg./ml	aprotinin (Roche Diagnostics)

0.8 µg/ml	pepstanin A (Sigma-Aldrich Canada)
2 mM	sodium orthovanadate
2.5 mM	phenylmethylsulfonyl fluoride (Roche Diagnostics)

2.14.26 High Salt Cytoskeletal Stabilization Buffer

20 mM	HEPES (pH 7.6)
0.5 %	Triton X- 100 (Sigma-Alrdich Canada)
10.3 %	sucrose
150 mM	NaCl
5 mM	$MgCl_2$
0.1 mg/ml	BSA (ICN Biomedicals)
500 µg/ml	leupeptin (Roche Diagnostics)
500 µg./ml	aprotinin (Roche Diagnostics)
0.8 µg/ml	pepstanin A (Sigma-Aldrich Canada)
2 mM	sodium orthovanadate
2.5 mM	phenylmethylsulfonyl fluoride (Roche Diagnostics)

2.14.27 1x Running Sample Buffer (RSB)

62.5 mM	Tris-HCl (pH 6.8)
4 %	glycerol
2.5 %	SDS
0.02 %	bromophenol blue (Sigma-Aldrich Canada)
100 mM	dithiothreitol (DTT) (Sigma-Aldrich Canada)

2.14.28 5x Running Sample Buffer (RSB)

312.5 mM	Tris-HCl (pH 6.8)
20 %	glycerol
12.5 %	SDS
0.1 %	bromophenol blue (Sigma-Aldrich Canada)
500 mM	dithiothreitol (DTT) (Sigma-Aldrich Canada)

2.14.29 Running Buffer

50 mM	Tris (ICN Biomedicals)
0.4 M	glycine (Fisher Scientific)
0.1 %	SDS

2.14.30 Transfer Buffer

20 mM	Tris-HCl (pH 8.0)

150 mM	glycine
20 %	Methanol

2.14.31 Tris Buffered Saline (TBS)

10 mM	Tris-HCl (pH 8.0)
150 mM	NaCl

2.14.32 Stripping Tris Buffered Saline (TBS)

10 mM	Tris-HCl (pH 2.0)
150 mM	NaCl

2.14.33 Tris Buffered Saline with Tween 20 (TBST)

10 mM	Tris-HCl (pH 8.0)
150 mM	NaCL
0.1 %	Tween 20 (Sigma-Aldrich Canada)

2.15. Mean Pixel Intensity Analysis of BCR-Induced Erk Phosphorylation Immunoblots

To calculate the mean pixel intensity of the phosphorylated Erk "band" it was first necessary to define the "band". This was done by visually identifying the largest band in the immunoblot and then manually selecting a square area around that band that captured all the pixels of the band yet minimized the capture of background pixels. An equivalent square area was then selected around the remaining bands again ensuring that all the pixels of the band were captured. The mean pixel intensity of the "bands" was then calculated using Matlab (The Mathworks; Natick, Massachusetts). By this method the mean pixel intensity should correlate to the band size and intensity, and this in turn should correlate with the amount of protein actually present in the immunoblot. Thus, a larger mean pixel intensity should represent a larger and more intense band, and this in turn should represent a larger amount of protein present in the immunoblot. With this method "bands" within the same immunoblot can be compared. However, this method can not be used to compare "bands" across different immunoblots as pixel intensity can vary across immunoblots due to differences in exposure quality as well as differences in the actual amount of protein present in the immunoblot. Nonetheless, this method allows one to determine whether a trend in band intensity is apparent within an immunoblot and to determine if this trend is consistent across various immunoblots.

CHAPTER 3

The Solo Igα/β Heterodimer Can Localize to Lipid Rafts

3.1 Introduction

Spatiotemporal regulation of protein interactions is an essential aspect of cellular signaling. Such regulation is often achieved via compartmentalization whereby specific proteins are sequestered within defined cellular locations. These defined cellular locations include specialized membrane microdomains within the plasma membrane termed lipid rafts (detailed in Chapter 1.5.2). In the past decade, lipid rafts have gained prominence in the B cell field where they appear to play a role in regulating certain aspects of BCR signaling (reviewed in Dykstra *et al.*; 2003, Pierce, 2002; Dykstra *et al.*, 2001; Cherukuri *et al.*, 2001; Matsuuchi and Gold, 2001).

Numerous groups have reported that the BCR translocates into lipid rafts following BCR cross-linking and that such translocation is necessary for BCR uptake, for antigen targeting and for BCR signaling (Su *et al.*, 2002; Stoddart *et al.*, 2002; Cheng *et al.*, 2001; Aman and Ravichandran, 2000; Guo *et al.*, 2000; Petrie *et al.*, 2000; Wientraub *et al.*, 2000; Cheng *et al.*, 1999). Nonetheless, some reports suggest that the BCR does not always translocate into lipid rafts upon cross-linking (Sproul *et al.*, 2000; Wientraub *et al.*, 2000). In particular, Wientraub and his colleagues (2000) demonstrated that the BCR translocates into lipid rafts following cross-linking in naïve B cells but not in tolerant B cells. Furthermore, they confirmed that BCR signaling was robust in naïve B cells where the BCR translocates but limited in tolerant cells where the BCR did not translocate. Thus, it was suggested that lipid raft inclusion/exclusion of the BCR may serve as a mechanism for regulating BCR signaling in different B cell types. Additionally, Sproul and his colleagues (2000) reported that BCR signaling can occur outside of lipid rafts in immature B cell and lead to apoptosis. Similarly, Trujillo and his colleagues (2003) demonstrated that lipid raft disruption did not inhibit BCR-induced apoptosis in a variety of B cell lines. Thus, lipid raft inclusion/exclusion may not serve merely as an on/off switch for BCR signaling but rather as a mechanism that couples the BCR to different signaling pathways. Indeed, it may be that inclusion within lipid rafts would compartmentalize the BCR with signaling components that lead to B cell proliferation and differentiation whereas exclusion from

lipid rafts may compartmentalize the BCR with signaling components that lead to B cell anergy and apoptosis.

If lipid raft inclusion/exclusion does truly represent a mechanism for regulating BCR signaling the question arises as to how lipid raft inclusion/exclusion is itself regulated. In one scenario, it is hypothesized that BCR lipid raft translocation is regulated as a consequence of BCR signaling itself. In this case, cross-linking of the BCR may induce signal-dependent protein associations that facilitate BCR lipid raft translocation. However, this scenario seems unlikely as the BCR has been found to translocate into lipid rafts prior to any detectable BCR signaling events (Weintraub *et al.*, 2000) and even in the complete absence of BCR signaling (Cheng *et al.*, 2001). In an alternate scenario it is hypothesized that BCR lipid raft translocation is regulated as a consequence of BCR cross-linking itself. In this case, BCR cross-linking is envisioned to cause a structural change within the BCR that facilitates its association with lipid rafts. Such structural changes may involve exposing previously hidden "lipid raft affinity domains" (LRADs) within the BCR or involve the assembling of LRADs via oligomerization of the BCR. Interestingly, previous studies have demonstrated that the mIgM subunit alone is able to translocate into lipid rafts upon cross-linking (Cheng *et al.*, 2001) That is to say, that the mIgM subunit does not have to be associated with the Igα/β signaling subunit in order to translocate into lipid rafts (Cheng *et al.*, 2001). This suggests first, that mIgM lipid raft translocation occurs independent of signaling and second, that the mIgM itself may contain structural features that facilitate lipid raft translocation upon cross-linking. However, the precise nature of these structural features remains to be determined as does whether or not these structural features are sufficient and/or necessary to direct the intact BCR to the lipid rafts. In this chapter, I further investigate the mechanisms involved in regulating BCR lipid raft translocation.

Central to these investigations was the possession of the WEHI 303.1.5 B cell line, a unique B cell line that expresses the Igα/β signaling subunit on its cell surface despite the absence of mIgM (Condon *et al.*, 2000). Using this cell line, the ability of the Igα/β subunit to independently translocate into lipid rafts was assessed and compared to that of the mIgM subunit (as reported by Cheng *et al.*, 2001) and of the intact BCR itself. Essentially, by comparing the independent translocation abilities of the mIgM subunit and the Igα/β subunit we are performing a gross deletion analysis of the BCR. With this approach it is possible to compare the translocation abilities and the structures of the two subunits in an attempt to narrow down the

possible regions of the proposed LRADs. For example, if it is found that each subunit can translocate into lipid rafts independently it may be suggested that the subunits share a common structural feature that facilitates this translocation. Thus, it would be advisable to perform further mutational analyses within any common structural regions (e.g., the transmembrane domains or the membrane proximal regions) in an effort to identify a possible LRAD. Alternatively, if only one subunit is found to translocate it may be suggested that that subunit contains a unique structural feature (as compared to the other subunit) that facilitates its translocation. Thus, it would be advisable to perform further mutational analyses within the unique structural regions of the translocatable subunit.

Using this approach it was determined that both the antigen-binding subunit (mIgM) (previously reported by Cheng *et al.*, 2001) and the signaling subunit (Igα/Igβ) (reported here) are capable of localizing to lipid rafts, independent of each other. This finding is important in several aspects. First, as described above, it suggests that the common structural domains (e.g., the transmembrane domains and membrane proximal regions) of these subunits should be further investigated in an attempt to identify a possible LRAD. And second, the finding that solo Igα/β[1] can localize to lipid rafts is biologically relevant as the solo Igα/β of Pro-B cells has been proposed to function as a pro-BCR. Given this, the finding that Igα/β can localize to lipid rafts in the absence of mIgM may suggest that lipid rafts play a role in pro-BCR signaling

3.2 Results

3.2.1 The BCR Translocates into Lipid Rafts in the Immature B Cell Lines, WEHI 231 and CH31

The mIgM-deficient variant of the WEHI 231 immature B cell line, WEHI 303.1.5, was used to assess the ability of Igα/β to translocate into lipid rafts. WEHI 303.1.5 has previously been shown to express Igα/β on its surface despite the absence of mIgM expression (Fig. 3.1) (Condon *et al.*, 2000). Surface expression of solo Igα/β is abnormal in immature and mature B cells as quality control mechanisms typically ensure that incompletely assembled forms of the BCR are retained in the endoplasmic reticulum (ER). However, the Igα/β of the WEHI 303.1.5 cell line

[1] Solo Igα/β is used throughout this thesis to denote Igα/β heterodimers that are expressed on the cell surface despite the absence of mIgM expression.

contains a point mutation that encodes for a proline to leucine change at amino acid 126 within the extracellular domain of Igα. This change is proposed to inhibit Igα's interaction with ER chaperone proteins such that the solo Igα/β subunit is able to escape ER retention. While this mutation may make the WEHI 303.1.5 cell line amenable for the studies discussed herein it also presents a caveat to any findings. In particular, this mutation may alter the structure of the Igα/β subunit such that the mutant form may associate with lipid rafts in a manner different from that of the wild-type. To control for this possibility, investigations were also performed with the K40B-1 pro-B cell line that naturally expresses solo Igα/β on its cell surface in association with the chaperone protein, calnexin (Shapiro *et al.*, 1993; Matsuuchi, unpublished observations). Finally, the WEHI 231 immature B cell line, the CH31 immature B cell line and the K40B-2 pre-B cell line, all of which express fully intact BCRs on their cell surfaces, were used as positive controls to ensure that the BCR cross-linking and lipid raft isolation protocols were functional (these cell lines have been previously described in Condon *et al.*, 2000; Shapiro *et al.*, 1993, respectively) (please note that the BCR expression patterns of the above-mentioned cell lines are confirmed in Fig. 3.1).

Before solo Igα/β lipid raft association could be considered it was necessary to first confirm lipid raft association of the intact BCR in immature B cell lines. While many studies have indicated that the BCR translocates into lipid rafts following BCR cross-linking (Cheng *et al.*, 2001; Petrie *et al.*, 2000; Weintraub *et al.*, 2000; Cheng *et al.*, 1999) two recent studies have suggested that this may not be the case for immature B cell lines (Sproul *et al.*, 2000; Cheng *et al.*, 2001). Thus the WEHI 231 and CH31 immature B cell lines were used to investigate BCR/lipid raft translocation in the immature B cells. These cell lines were initially stimulated by cross-linking the BCR with a μ heavy chain specific antibody for the indicated length of time (time "0" indicates non-stimulated cells). Lipid rafts were then collected from the cell lines using a salt-extractable lipid raft isolation method. This same method was previously used to demonstrate that the BCR translocates into lipid rafts in naïve splenic B cells following BCR cross-linking (described in Weintraub *et al.*, 2000). The fractions were subsequently resolved by SDS-PAGE, transferred to nitrocellulose filters and immunoblotted with Igα, Igβ, μ heavy chain and κ light chain specific antibodies (note that the μ heavy chain and κ light chain together form the mIgM subunit in these cell lines). Filters were also immunoblotted with a CD45 specific antibody (data not shown) as a control to ensure that the lipid raft fraction was not contaminated with a non-raft

fraction. The protein tyrosine phosphatase, CD45, is well-known to be excluded from lipid rafts (Rogers and Rose, 1996) and thus, should not be found in pure lipid raft fractions.

Using the above approach, the levels of Igα/β, μ heavy chain and κ light chain decrease over time in the supernatant fraction of the WEHI 231 immature B cell line following receptor cross-linking (Fig. 3.2; left portion of the image). Concomitantly, the levels of these proteins increase over time in the lipid raft fraction (Figs. 3.2; right portion of the image). Similarly, Igα, Igβ, μ heavy chain and κ light chain also appear to translocate into the lipid raft fraction following μ-based BCR cross-linking in the CH31 immature B cell line (Fig. 3.3). Thus, these findings suggest that the BCR translocates into lipid rafts following anti-μ-based BCR cross-linking in these immature B cell lines. As these findings are controversial (refer to Sproul *et al.*, 2000; Cheng *et al.*, 2001), a second method, namely the discontinuous sucrose gradient method (described in Deans *et al.*, 1998), was used to isolate lipid rafts in an attempt to support these findings. The results obtained with this second methodology are in agreement with those of the salt-extractable lipid raft method discussed above (experiments were performed by Lorna Santos, formerly of the Matsuuchi lab; published in Jackson *et al.*, 2005). Additionally, the WEHI 231 and CH31 cell lines were confirmed to undergo apoptosis in response to BCR cross-linking as is expected of healthy immature B cell lines (data not shown). Thus, given the findings from the two different immature B cell lines and the two different lipid raft isolation methods, it appears that a portion of the intact BCR is indeed localized within lipid rafts. Moreover, the BCR appears able to translocate into lipid rafts following receptor cross-linking in immature B cell lines.

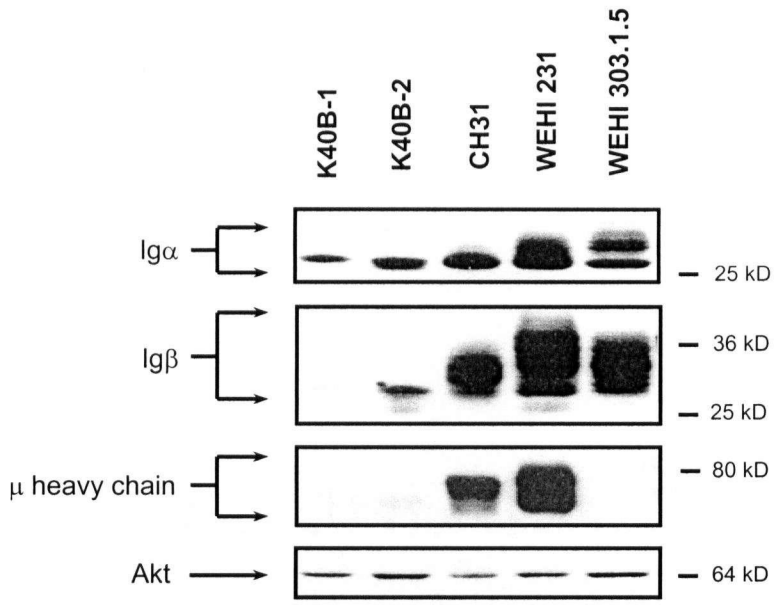

Figure 3.1. Characterization of Igα, Igβ and mIgM (as determined by μ chain) expression in the experimental B cell lines. 40 μg of whole cell lysate was resolved by SDS-PAGE for the K40B cell lines. In contrast, only 2.0 μg of whole cell lysate was resolved by SDS-PAGE for the WEHI 231, WEHI 303.1.5 and CH31 cell lines. Following electrophoresis, the gels were transferred to nitrocellulose filters that were subsequently immunoblotted with Igα, Igβ or μ chain specific antibodies (as indicated on the left-hand side of the panels). Similarly Akt expression was characterized in these cell lines using 15 μg of whole cell lysate. Akt expression was characterized as increases in Akt phosphorylation are indicative of successful BCR cross-linking (Ingham *et al.*, 2001).

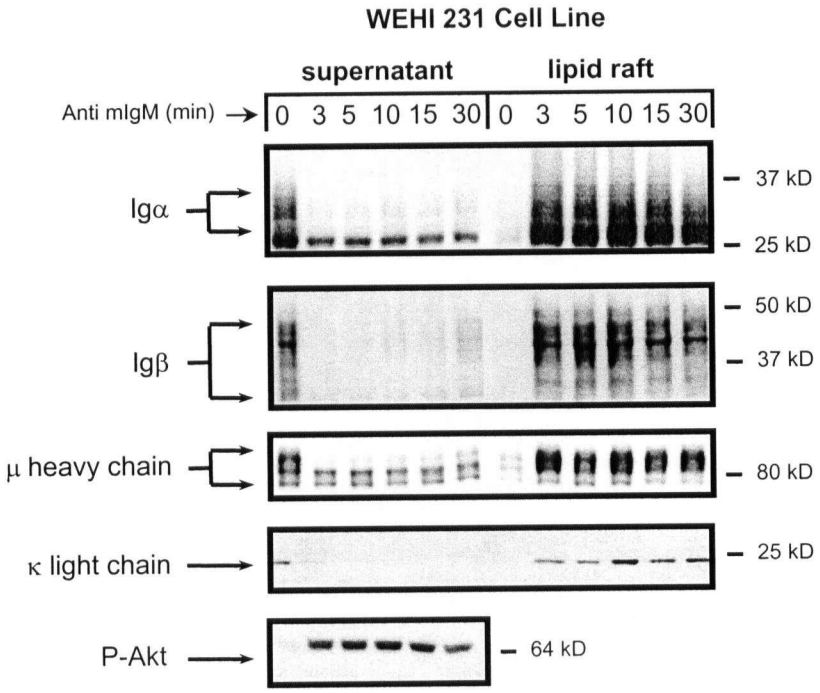

Figure 3.2. The BCR translocates into a detergent-insoluble, salt-extractable lipid raft fraction in the WEHI 231 immature B cell line following BCR cross-linking. 25 x 10^6 cells were stimulated with 100 μg of anti mIgM antibody for the indicated time points. The detergent soluble fraction (supernatant) and the detergent-insoluble, salt-extractable fraction (lipid raft) were then collected. Equivalent amounts of protein for each fraction were resolved by SDS-PAGE. Following electrophoresis the gels were transferred to nitrocellulose filters that were subsequently immunoblotted with Igα, Igβ, κ light chain or μ chain specific antibodies (the latter two being components of mIgM). Successful receptor cross-linking was confirmed by monitoring for increased Akt phosphorylation (bottom panel). Data are representative of three independent experiments.

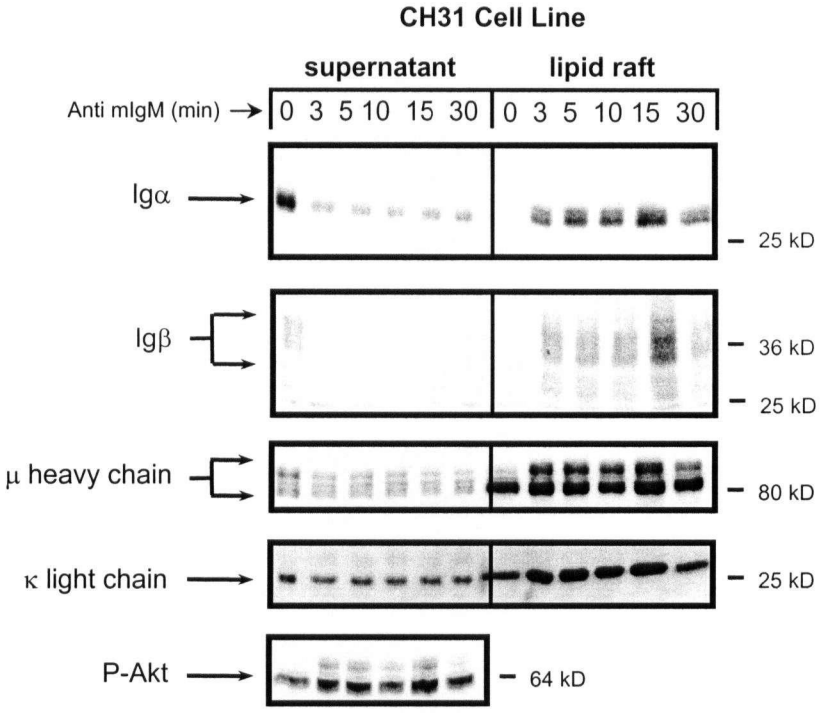

Figure 3.3. The BCR translocates into a detergent-insoluble, salt-extractable lipid raft fraction in the CH31 immature B cell line Following BCR cross-linking. 25 x 10^6 cells were stimulated with 100 μg of anti mIgM antibody for the indicated time points. The detergent soluble fraction (supernatant) and the detergent-insoluble, salt-extractable fraction (lipid raft) were then collected. Equivalent amounts of protein for each fraction were resolved by SDS-PAGE. Following electrophoresis the gels were transferred to nitrocellulose filters that were subsequently immunoblotted with Igα, Igβ, κ light chain or μ chain specific antibodies (the latter two being components of mIgM). Successful receptor cross-linking was confirmed by monitoring for increased Akt phosphorylation (bottom panel). Data are representative of three independent experiments.

3.2.2 A Portion of Solo Igα/β Localizes to Lipid Rafts in the Mutant Immature B Cell Line, WEHI 303.1.5.

As cross-linking appears necessary to initiate BCR translocation (Cheng *et al.*, 2001; Petrie *et al.*, 2000; Weintraub *et al.*, 2000; Cheng *et al.*, 1999) it was hypothesized that cross-linking would similarly be required to induce solo Igα/β translocation. Thus, it was necessary to develop a method to successfully cross-link Igα/β. To this end, the WEHI 231 cell line was stimulated by cross-linking the Igβ with a biotinylated anti-Igβ mAb and streptavidin. Lipid rafts were then collected from the cell lines using the salt-extractable lipid raft method. The fractions were subsequently resolved by SDS-PAGE, transferred to nitrocellulose filters and immunoblotted with Igα, Igβ, μ heavy chain, κ light chain and phospho-Akt specific antibodies. Samples were analyzed for phosphorylated Akt as increased Akt phosphorylation is a well-characterized downstream consequence of BCR cross-linking (Astoul *et al.*, 1999; Craxton *et al.*, 1999; Gold *et al.*, 1999) and thus, is indicates successful receptor cross-linking and signaling.

Treatment of the control cell line, WEHI 231, with biotinylated anti-Igβ mAb and streptavidin leads to increased Akt phosphorylation (Fig. 3.4, bottom panel). Therefore, this treatment is sufficient to induce BCR-like signaling and likely reflects successful cross-linking of the BCR through Igβ. Following Igβ-based receptor cross-linking, the levels of Igα, Igβ and the μ heavy chain appear to slightly decrease in the supernatant fraction while they coincidentally increase in the lipid raft fraction (Fig. 3.4; comparing the left side of image to the right side). While this trend is comparable to that seen following μ heavy chain-based receptor cross-linking it should be noted that the relative decreases and increases of protein levels in the respective fractions do not appear to be as significant with the former method as compared to the latter (Igβ versus μ heavy chain-based receptor cross-linking) (compare Figs. 3.4 and 3.2, respectively). These differences may reflect differences in the Igβ and μ heavy chain specific antibodies' abilities to efficiently bind to and cross-link the receptor (refer to discussion). Regardless, Igβ-based receptor cross-linking appears sufficient to cross-link the receptor and to induce both BCR-like signaling and BCR translocation into lipid rafts in the control cell line, WEHI 231. Therefore, Igβ-based cross-linking was then used to investigate whether or not solo Igα/β is able to associate with and translocate into lipid rafts in mIgM deficient cell lines.

The mIgM deficient experimental cell line, WEHI 303.1.5, was stimulated by cross-linking the Igβ with a biotinylated anti-Igβ mAb plus streptavidin for the indicated length of time. Lipid rafts were then collected from the cell lines using the aforementioned salt-extractable lipid raft method (Weintraub *et al.*, 2000). The fractions were subsequently resolved by SDS-PAGE, transferred to nitrocellulose filters and immunoblotted with phospho-Akt, CD45, Igα and Igβ specific antibodies. Samples were analyzed for phosphorylated Akt as increased Akt phosphorylation indicates successful BCR cross-linking (Astoul *et al.*, 1999; Craxton *et al.*, 1999; Gold *et al.*, 1999). However, it should be noted that increased Akt phosphorylation would be indicative of successful solo Igα/β cross-linking only if solo Igα/β can in fact induce BCR-like signaling in the absence of mIgM. Fortunately, Igβ-based cross-linking leads to an increase in Akt phosphorylation in the WEHI 303.1.5 cell line (Fig. 3.5). This suggests that the anti-Igβ based method is sufficient to cross-link the solo Igα/β and furthermore, that cross-linking of solo Igα/β is sufficient to induce BCR-like signaling. Interestingly, a small proportion of Igα and Igβ is clearly evident within the lipid raft fraction prior to Igβ cross-linking (Fig. 3.5, the right side of the image, time zero). Additionally, the levels of Igα and Igβ appear to slightly decrease in the supernatant fraction while they coincidentally increase in the lipid raft fraction following Igβ cross-linking (Fig. 3.5, comparing the left side of the image to the right side of the image). Thus, it appears that a portion of solo Igα/β is able to constitutively associate with lipid rafts and that a further portion of solo Igα/β is able to translocate into lipid rafts following Igβ cross-linking in the WEHI 303.1.5 cell line.

Finally, solo Igα/β lipid raft association was investigated in the K40B-1 cell line to ensure that the ability of Igα/β to associate with lipid rafts in the absence of mIgM is not unique to the WEHI 303.1.5. The K40B-1 cell line is a pro-B-like cell line that expresses low levels of solo Igα/β on its cell surface in association with calnexin (Fig. 3.1). The solo Igα/β of the K40B-1 cell line may function as a pro-B cell receptor and its ability to associate with lipid rafts may reflect its ability to function as a receptor. As a control, Igα/β lipid raft association was also investigated in the K40B-2 cell line which is the developmental successor of the K40B-1 cell that expresses low levels of the intact pre-BCR on its cell surface. Unfortunately, the relatively low expression levels of Igα and Igβ within the KB40 cell lines (refer to Fig. 3.1) made it unfeasible to assess Igα/β lipid raft association with the sucrose density gradient method. Rather, Igα/β lipid raft association within the K40B cell lines was assessed using only the salt-extraction method (Weintraub *et al.*, 2000) as this method allows for greater recovery of the various

fractions. Thus, the K40B cell lines were stimulated by cross-linking the Igβ with a biotinylated anti-Igβ mAb plus streptavidin for the indicated length of time. Lipid rafts were then collected from the cell lines using the salt-extractable lipid raft method (Weintraub *et al.*, 2000) and analyzed as before. As with the WEHI cell lines, Ig/β cross-linking was successful as evidenced by an increase in Akt phosphorylation following treatment with biotinylated anti-Igβ mAb plus streptavidin (Fig. 3.6 and 3.7 bottom panel). Additionally, it can be seen that, despite their relatively low expression levels, a portion of both Igα and Igβ is constitutively associated with lipid raft fraction in the K40B cell lines (Fig. 3.6 and 3.7). However, this portion does not appear to significantly increase following Igβ cross-linking in the K40B-1 cell line (Fig. 6a). In contrast, this portion appears to increase ever-so-slightly in the K40B2 cell line following Igα/β cross-linking (Fig. 3.7). These findings may suggest that solo Igα/β does not efficiently translocate into lipid rafts in the K40B cell lines. Alternatively, it may simply be difficult to elicit or detect lipid raft translocation of the solo Igα/β in the K40B cell lines due to the low expression levels of Igα/β. Nonetheless, it is clearly evident that solo Igα/β is able to associate with lipid rafts in the K40B cell lines and therefore, such associations are not unique to the WEHI 303.1.5 cell line.

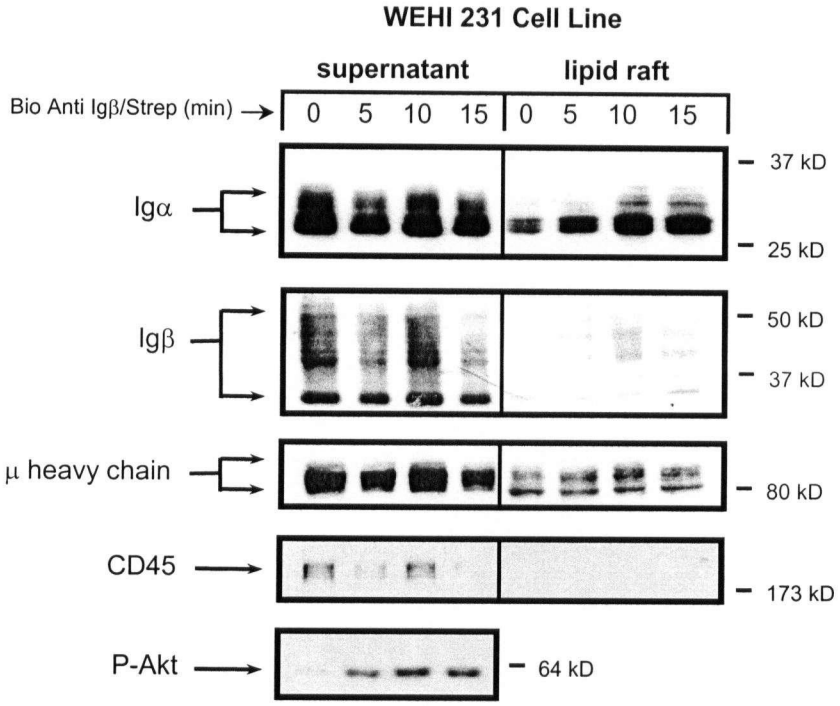

Figure 3.4. The BCR translocates into a detergent-insoluble, salt-extractable lipid raft fraction in the WEHI 231 immature B cell line following Igβ cross-linking. 25 x 10^6 cells were stimulated with 60 μg of biotinylated anti-Igβ antibody along with 80 μg of streptavidin for the indicated time points. The detergent soluble fraction (supernatant) and the detergent-insoluble, salt-extractable fraction (lipid raft) were then collected. Equivalent amounts of protein for each fraction were resolved by SDS-PAGE. Following electrophoresis the gels were transferred to nitrocellulose filters that were subsequently immunoblotted with Igα, Igβ, μ chain (component of mIgM) or CD45 specific antibodies (as indicated to the left of each panel). Fractions were analyzed for CD45 content as a control as CD45 has been shown to be excluded from B Cell lipid raft fractions. Successful receptor cross-linking was confirmed by monitoring for increased Akt phosphorylation (bottom panel). Data are representative of three independent experiments.

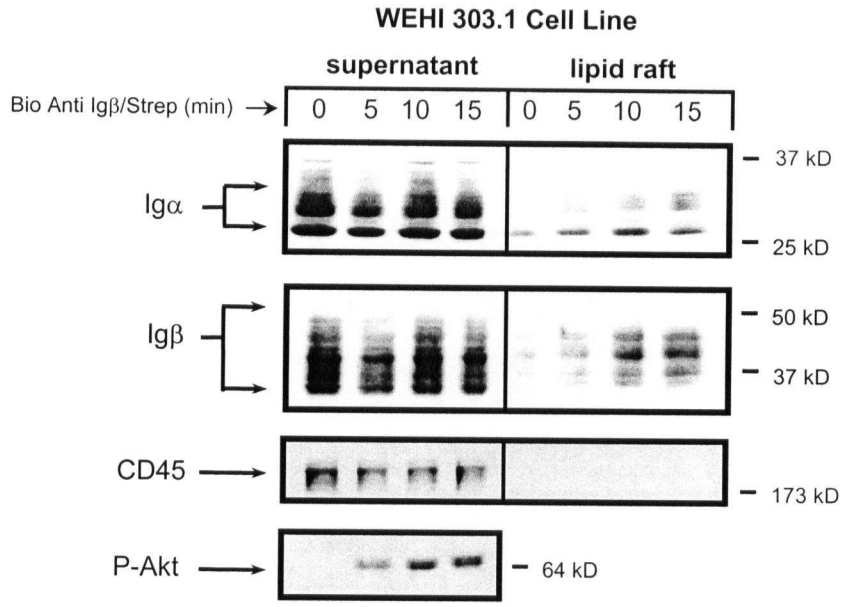

Figure 3.5. A portion of the solo Igα/Igβ heterodimer localizes to detergent-insoluble, salt-extractable lipid raft fraction in the mutant WEHI 303.1.5 cell line (mIgM negative). A further portion of the solo Igα/β heterodimer appears to translocate into the detergent-insoluble, salt-extractable lipid raft fraction in the mutant WEHI 303.1.5 cell line (mIgM negative) upon Igβ cross-linking. 25 x 10^6 cells were stimulated with 60 μg of biotinylated anti-Igβ antibody along with 80 μg of streptavidin for the indicated time points. The detergent soluble fraction (supernatant) and the detergent-insoluble, salt-extractable fraction (lipid raft) were then collected. Equivalent amounts of protein for each fraction were resolved by SDS-PAGE. Following electrophoresis the gels were transferred to nitrocellulose filters that were subsequently immunoblotted with Igα, Igβ, or CD45 specific antibodies (as indicated to the left of each panel). Fractions were analyzed for CD45 content as a control as CD45 has been shown to be excluded from B Cell lipid raft fractions. Successful receptor cross-linking was confirmed by monitoring for increased Akt phosphorylation (bottom panel). Data are representative of three independent experiments.

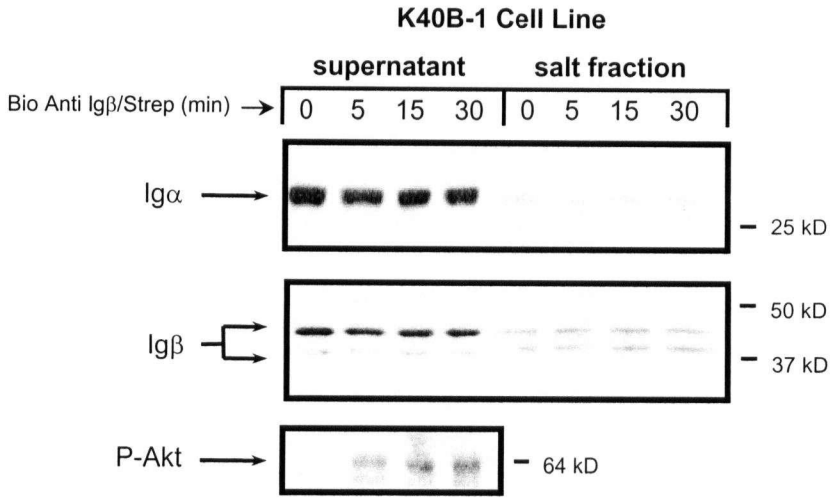

Figure 3.6. A portion of the solo Igα/Igβ heterodimer localizes to the detergent-insoluble, salt-extractable lipid raft fraction in the K40B-1 pro-B-like cell line (mIgM negative). 25 x 10^6 cells were stimulated with 60 μg of biotinylated anti-Igβ antibody along with 80 μg of streptavidin for the indicated time points. The detergent soluble fraction (supernatant) and the detergent-insoluble, salt-extractable fraction (lipid raft) were then collected. Equivalent amounts of protein for each fraction were resolved by SDS-PAGE. Following electrophoresis the gels were transferred to nitrocellulose filters that were subsequently immunoblotted with Igα or Igβ (as indicated to the left of each panel). Successful receptor cross-linking was confirmed by monitoring for increased Akt phosphorylation (bottom panel). Data are representative of three independent experiments using similar time courses.

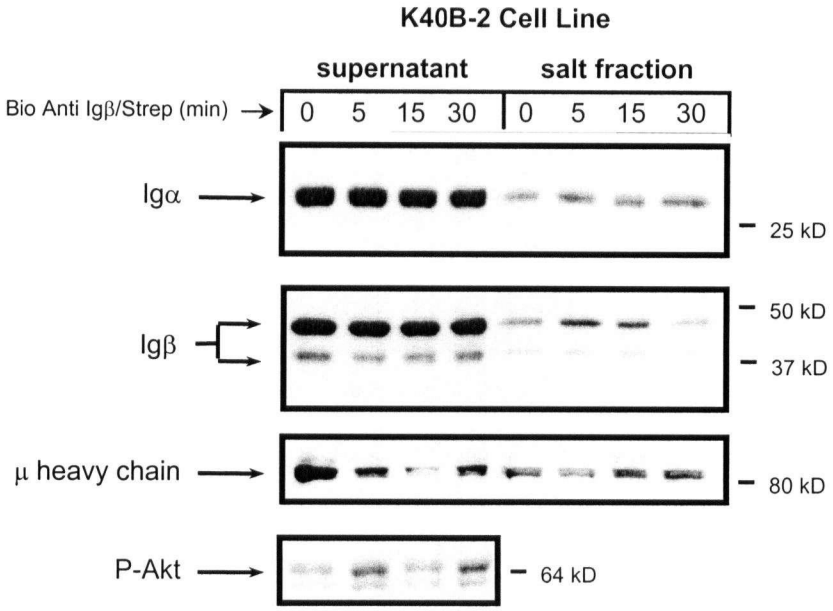

Figure 3.7. A portion of the Igα/Igβ heterodimer localizes to the detergent-insoluble, salt-extractable lipid raft fraction in the K40B-2 pre-B-like cell line (mIgM positive). 25 x 10^6 cells were stimulated with 60 μg of biotinylated anti-Igβ antibody along with 80 μg of streptavidin for the indicated time points. The detergent soluble fraction (supernatant) and the detergent-insoluble, salt-extractable fraction (lipid raft) were then collected. Equivalent amounts of protein for each fraction were resolved by SDS-PAGE. Following electrophoresis the gels were transferred to nitrocellulose filters that were subsequently immunoblotted with Igα, Igβ, or μ heavy chain specific antibodies (as indicated to the left of each panel). Successful receptor cross-linking was confirmed by monitoring for increased Akt phosphorylation (bottom panel). Data are representative of three independent experiments using similar time courses.

3.3 Discussion

As mentioned in the introduction, previous studies have shown that the BCR translocates to lipid rafts following BCR engagement (Cheng *et al.*, 2001; Petrie *et al.*, 2000; Weintraub *et al.*, 2000; Cheng *et al.*, 1999). Furthermore, these studies suggest that such translocation is necessary for appropriate BCR signaling (Su *et al.*, 2002; Cheng *et al.*, 2001; Aman and Ravichandran, 2000; Guo *et al.*, 2000; Petrie *et al.*, 2000). Thus, it appears that a comprehensive understanding of BCR signaling will require a further understanding of BCR lipid raft translocation. Accordingly, this chapter of my thesis focused on investigating the molecular mechanisms that govern BCR translocation into lipid rafts.

It is clear that BCR lipid raft association is enhanced following BCR engagement (Cheng *et al.*, 2001; Petrie *et al.*, 2000; Weintraub *et al.*, 2000; Cheng *et al.*, 1999). However, it is unclear whether this enhanced association is a consequence of BCR signaling itself (e.g., induced association with raft associated proteins), a consequence of a structural change within the engaged BCR or a consequence of some combination of structural and signaling events initiated by BCR engagement. It seems unlikely that enhanced lipid raft association is mediated strictly by BCR signaling as the BCR has been found to translocate into lipid rafts in the absence of BCR signaling (Cheng *et al.*, 2001). Thus, we are left to consider the alternative, that enhanced lipid raft association is mediated by a structural change within the engaged BCR. As mentioned above, such structural changes may involve exposing previously hidden "lipid raft affinity domains" (LRADs) within the BCR or likewise may involve the assembling of LRADs via oligomerization of the BCR. Thus, the initial hypothesis was that the BCR itself contains structural information of some form (termed here as LRADs) that, upon receptor engagement, directly promotes its translocation to lipid rafts.

As previous studies have demonstrated that the solo antigen-binding subunit of the BCR (mIgM) translocates into lipid rafts (Cheng *et al.*, 2001) it was of interest to determine if the solo Igα/β subunit could likewise translocate into lipid rafts. This investigation would help to further define structural regions within the subunits (Igα/β and mIgM) that may contain the proposed LRADs. Furthermore, this investigation could help to shed light on BCR-like signaling processes in pro-B cells which express solo Igα/β on its surface in association with calnexin (Nagata *et al.*, 1997).

Lipid raft association and translocation of solo Igα/β was investigated in the mutant, mIgM-deficient immature B cell line, WEHI 303.1.5. However, before proceeding with these investigations, a control investigation was performed to confirm that the intact BCR does indeed associate with and translocate into lipid rafts in wild-type immature B cell lines. This was necessary as Susan Pierce's group has reported that such translocation may not occur (Sproul *et al.*, 2000; Chung *et al.*, 2001). If this were to be the case our experimental system would be inappropriate for investigating BCR lipid raft translocation. Fortunately, using the Weintraub salt-based lipid raft isolation method, the intact BCR was found to associate with and translocate into lipid rafts in the wild-type immature B cell line, WEHI 231 (Fig. 3.2; published in Jackson *et al.*, 2005). Due to the controversial nature of this finding, BCR lipid raft association and translocation was further investigated using a second immature B cell line (CH31) and a second lipid raft extraction method (sucrose density gradient method performed by Lorna Santos). The findings from these secondary approaches confirmed that the BCR does in fact translocate into lipid rafts in at least two immature B cell lines following BCR cross-linking (Fig. 3.3 and data not shown; published in Jackson *et al.*, 2005). The reported differences between the Pierce Lab's findings (Sproul *et al.*, 2000; Cheng *et al.*, 2001) and the Matsuuchi Lab's findings may reflect differences in lipid raft preparations, subtle differences in the cell lines used and/or differences in the sensitivity of the methods used to detect the BCR within the lipid raft fractions. Interestingly, while the Pierce lab reports that "B cell antigen receptor signaling occurs outside lipid rafts in immature B cells" based on their inability to detect BCR lipid raft association, they did not report performing the loss-of-function study whereby they disrupt the lipid rafts with chemical agents to demonstrate that lipid rafts are not required for BCR signaling in immature B cell lines (Sproul *et al.*, 2000; Cheng *et al.*, 2001). Indeed, BCR association and/or lipid raft translocation, while being difficult to detect, may yet contribute to BCR signaling in immature B cells. Regardless, the ability to detect BCR lipid raft association and translocation within wild-type immature B cell lines within the Matsuuchi Lab enabled us to further investigate solo Igα/β lipid raft association and translocation within the mutant, immature B cell line, WEHI 303.1.5.

To investigate solo Igα/β lipid raft translocation it was first necessary to establish a protocol for cross-linking the solo Igα/β. To this end, the WEHI 231 cell line was treated with a biotinylated Igβ specific antibody plus streptavidin. Igβ-based cross-linking appears to induce BCR lipid raft translocation in the WEHI 231 immature B cell line (Fig. 3.4). However, this translocation does

not appear as efficient as that induced by mIgM-based cross-linking (compare Fig. 3.4 to 3.2). The apparent differences in translocation efficiency may reflect differences in the antibodies' abilities to cross-link the receptor. In particular, the mIgM specific antibody is a polyclonal antibody that can bind to multiple sites within the mIgM to induce BCR cross-linking/oligomerization whereas the Igβ antibody is a monoclonal antibody that can only bind one specific site within the Igβ to induce BCR cross-linking/oligomerization. Regardless of the apparent differences in efficiency, treatment with a biotinylated Igβ specific antibody plus streptavidin appears sufficient to cross-link the BCR and as such this treatment was used to cross-link the solo Igα/β in subsequent investigations.

Solo Igα/β lipid raft association was investigated in the mIgM-deficient, mutant immature B cell line, WEHI 303.1.5. These investigations found that solo Igα/β can associate with and translocate into lipid rafts. This suggests that, similar to solo mIgM, solo Igα/β contains structural information that is sufficient to mediate its association with lipid rafts. Hypothesizing that the two subunits employ similar mechanisms to associate with lipid rafts, it may be predicted that they share common structural features that mediate this association. Given the structures of mIgM and the Igα/β such a common feature would most likely lie within their transmembrane or membrane proximal domains. Thus, the Matsuuchi Lab is performing numerous mutational analyses within these particular regions to further define any structural features that may help govern BCR lipid raft association and translocation.

Second, the finding that solo Igα/β can translocate into lipid rafts and induce BCR-like signaling may be physiologically relevant. In particular, the putative pro-B cell receptor is expressed on the surface of pro-B cells as a solo Igα/β in association with calnexin (Nagata *et al.*, 1997). While this receptor has been proposed to be involved in development-dependent signaling it has been unclear whether such signaling could occur in the absence of an antigen-binding subunit. The findings here suggest that such signaling could indeed occur, and may occur from within lipid rafts, providing that there is a physiological ligand capable of cross-linking the solo Igα/β. While such a ligand has yet to be identified, it has been speculated that the ligand may have lectin-like properties such that it is able to bind and cross-link the putative pro-B cell receptor via the carbohydrate chains of the Igα/β heterodimer.

To ensure that these findings are not a unique phenomenon of the mutant WEHI 303.1 cell line, similar investigations were performed with the naturally mIgM-deficient K40B-1 pro-B cell line and the mIgM positive K40B-2 control cell line. Similar to the WEHI 303.1.5 cell line, a significant portion of solo Igα/β was found to be constitutively associated with lipid rafts in the K40B-1 cell line (Fig. 3.6; published in Jackson *et al.*, 2005). However, unlike in the WEHI 303.1.5 cell line, the Igα and Igβ do not appear to translocate into the lipid rafts following Igβ-based cross-linking (Fig. 3.5; published in Jackson *et al.*, 2005). This finding may indicate that solo Igα/β does not translocate into lipid rafts upon cross-linking in the K40B-1 cell line. Alternatively, it may also reflect an inability to induce or detect such translocation with the approaches used. As noted above, cross-linking of Igβ may not be ideally efficient. Additionally, the K40B-1 cell line expresses very low levels of Igα/β (Fig. 3.1). Together, these two factors may make it difficult to detect inducible lipid raft translocation of the solo Igα/β in the K40B-1 cell line. This would be especially true if the translocating Igα/β represented a very small fraction of the total Igα/β (as was seen with the WEHI 303.1.5 cell line). Nonetheless, the fact that a portion of solo Igα/β is constitutively associated with the lipid rafts in the K40B-1 cell line indicates that this association may occur in wild-type cell lines and is not a phenomenon unique to the mutant WEHI 303.1.5 immature B cell line. Moreover, cross-linking of solo Igα/β was found to induce BCR-like signaling in the K40B-1 cell line (Fig. 3.6; published in Jackson *et al.*, 2005), further supporting the notion that solo Igα/β may indeed be able to act as a signaling receptor to mediate pro-B cell development.

Given these findings several future investigations are suggested. First, mutational analysis should be performed on the transmembrane and membrane proximal domains of the mIgM subunit and the Igα/β. Such analysis may help to identify structures within the subunits that enable them to associate with lipid raft (i.e., identify the proposed LRAD). These studies are currently being pursued within the Matsuuchi Lab by Steven Machtaler. Second, further investigations should be performed to determine whether or not lipid raft translocation is necessary for solo Igα/β signaling. In particular, loss of function studies could be performed using cholesterol sequestering agents to disrupt lipid rafts. Such studies would help to further determine if solo Igα/β lipid raft translocation is physiologically relevant and to further define the role of lipid raft translocation in BCR and BCR-like signaling.

CHAPTER 4

Co-Expression of the BCR, Syk, and BLNK Is Sufficient to Reconstitute BCR-Induced PLCγ Activation in AtT20-Derived Cell Lines

4.1 Introduction

The ability to recruit and/or sequester proteins within defined cellular locations is essential to intracellular signaling. Such compartmentalization enables the efficient assembly of macromolecular signaling complexes and aids in the regulation of cross-talk between various signaling pathways. Adapter proteins represent one mechanism by which compartmentalization can be achieved. These proteins are typically non-enzymatic proteins that contain multiple protein interaction domains that enable specific and multiple protein associations (detailed in Chapter 1.5 and 1.5.1). Depending on the nature of the protein interaction domains, the resulting protein associations may be constitutive or inducible. Thus, similar to lipid rafts, adapter proteins are postulated to serve as platforms upon which macromolecular signaling complexes can be specifically assembled and regulated.

Within the past decade the B cell linker protein (BLNK) has been identified as a key adapter protein in B cell signaling (Fu *et* al., 1997; Fu *et al.*, 1998; Goitsuka *et al.*, 1998; Wienands *et al.*, 1998; Ishiai *et al.*, 1999a; Ishiai *et al.*, 1999b; reviewed in Kurosaki, 2000; Gold, 2002). In particular, BLNK has been suggested to play a pivotal role in coupling the engaged BCR to PLCγ activation (Fu *et* al., 1997; Fu *et al.*, 1998; Goitsuka *et al.*, 1998; Wienands *et al.*, 1998; Ishiai *et al.*, 1999a; Ishiai *et al.*, 1999b; reviewed in Kurosaki, 2000; Gold, 2002). Understanding how the BCR is coupled to PLCγ activation is important as defects in this pathway have been shown to contribute to several immune system disorders including autosomal recessive agammaglobulinemia (BLNK defects) and X-linked agammaglobulinemia (BTK defects) which render sufferers unable to mount an effective humoral response against pathogens (reviewed in Fischer, 2004 and the online Immunodeficiency Resource at http://bioinf.uta.fi/idr/).

Our current understanding of how the BCR is coupled to PLCγ activation is predominantly based on loss-of-function studies (detailed in Chapter 1.5.3). These studies have clearly indicated that Syk is necessary to couple the BCR to PLCγ activation and that BTK and BLNK are necessary

for this process to occur efficiently. Given the current loss-of-function data, prevailing models of the BCR/PLCγ signaling pathway envision that BLNK is recruited to the cross-linked BCR at the plasma membrane where it is phosphorylated by BCR-associated Syk. Once phosphorylated, BLNK is proposed to bind to both BTK and PLCγ via their respective SH2 domains. This process is thought to facilitate the co-localization of Syk, BTK and PLCγ such that Syk and BTK can phosphorylate and activate PLCγ. While these models (summarized in Fig. 4.1) are suggestive, many details of the pathway remain to be elucidated and/or confirmed. Most significantly, it remains to be determined whether Syk, BTK and BLNK are sufficient to couple the engaged BCR to PLCγ activation or whether additional lymphoid specific components are required to mediate this signaling pathway. Thus, I have used a reconstitution approach to investigate the molecular requirements and mechanisms underlying BCR-induced PLCγ activation.

As discussed in Chapter 1.10, the AtT20 reconstitution system is derived from a non-lymphoid, endocrine cell line that endogenously expresses the PI3K, Ras, PLCγ, and Fyn signaling enzymes (Matsuuchi *et al.*, 1992 and Richards *et al.*, 1996). While these enzymes obviously function in non-lymphoid signaling pathways within the AtT20 system they have also been identified as key downstream signaling components in BCR signaling pathways. This, along with the fact that the AtT20 cell line is amenable to transfection, enables it to be used as a reconstitution system into which lymphoid specific components can be transfected in an effort to determine the sufficiency of these components to reconstitute BCR-induced activation of the various downstream signaling enzymes.

AtT20 cells have previously been transfected with and shown to express the intact BCR on their cell surface (Matsuuchi *et al.*, 1992). Cross-linking the transfected BCRs has proven sufficient to induce some aspects of BCR signaling within these cells including phosphorylation of the Igα/β heterodimer and phosphorylation and activation of PI3K (Matsuuchi *et al.*, 1992). However, expression of the transfected BCRs alone has proved insufficient to reconstitute a robust tyrosine phosphorylation cascade or PLCγ activation in these cells (Matsuuchi *et al.*, 1992). This situation was partially rectified by further transfecting the cells with the lymphoid specific protein tyrosine kinase, Syk (Richards *et al.*, 1996). Co-expression of the BCR and Syk proved sufficient to reconstitute a robust BCR-induced protein tyrosine phosphorylation cascade as well as to reconstitute BCR-induced Erk activation (Richards *et al.*, 1996). Still, co-

expression of the BCR and Syk proved insufficient to reconstitute BCR-induced PLCγ activation in the transfected cells suggesting that additional lymphoid specific components may be required to couple the BCR to PLCγ (Richards *et al.*, 1996). These findings are in agreement with loss-of-function studies which, as mentioned above, suggest that BLNK and BTK may be necessary to effectively couple the BCR to PLCγ activation. Thus, I further transfected the BCR and BCR/Syk AtT20-derived cell lines with BTK and/or BLNK to determine if these components are sufficient to reconstitute BCR-induced PLCγ activation within this system.

4.2 Results

4.2.1 Expression of the BCR, Syk, BTK and BLNK within AtT20-Derived Cell Lines.

A reconstitution system expressing transfected lymphoid specific components was established to investigate the molecular mechanism underlying BCR-induced PLCγ activation. Initial transfections were performed into two previously established AtT20-derived cell lines that will be termed the "BCR" and "BCR/Syk" cell lines throughout this thesis. The BCR cell line expresses transfected BCRs on its cell surface (Matsuuchi *et al.*, 1992; previously referred to as 100.33) while the BCR/Syk cell line expresses transfected BCRs on its cell surface and transfected Syk within its cytoplasm (Richards *et al.*, 1996; previously referred to as Syk13). For the purpose of this thesis, the BCR and BCR/Syk cell lines were further transfected with a plasmid encoding for a drug resistance marker along with a plasmid encoding for myc-tagged human BLNK and/or a plasmid encoding for human BTK (refer to Chapter 2.1.2 and 2.1.3 for details). Following the transfections, drug-resistant clones were isolated and screened for their ability to express the desired proteins (detailed in Chapter 2..3.3 and 2.3.4). From this process multiple AtT20-derived cell lines were established including BCR/BLNK, BCR/BTK, BCR/BLNK/BTK, BCR/Syk/BLNK, BCR/Syk/BTK and BCR/Syk/BLNK/BTK, respectively. As may be anticipated, the names of the various cell lines reflect the transfected proteins that they have been demonstrated to successfully express (Figure 4.2). It should be noted that several clones were obtained for each described cell line and that initial experiments were performed with multiple clones (data not shown). As the results from the various clones were consistent, and for the sake of clarity, only one clone has been shown for each described cell line (Figure 4.2).

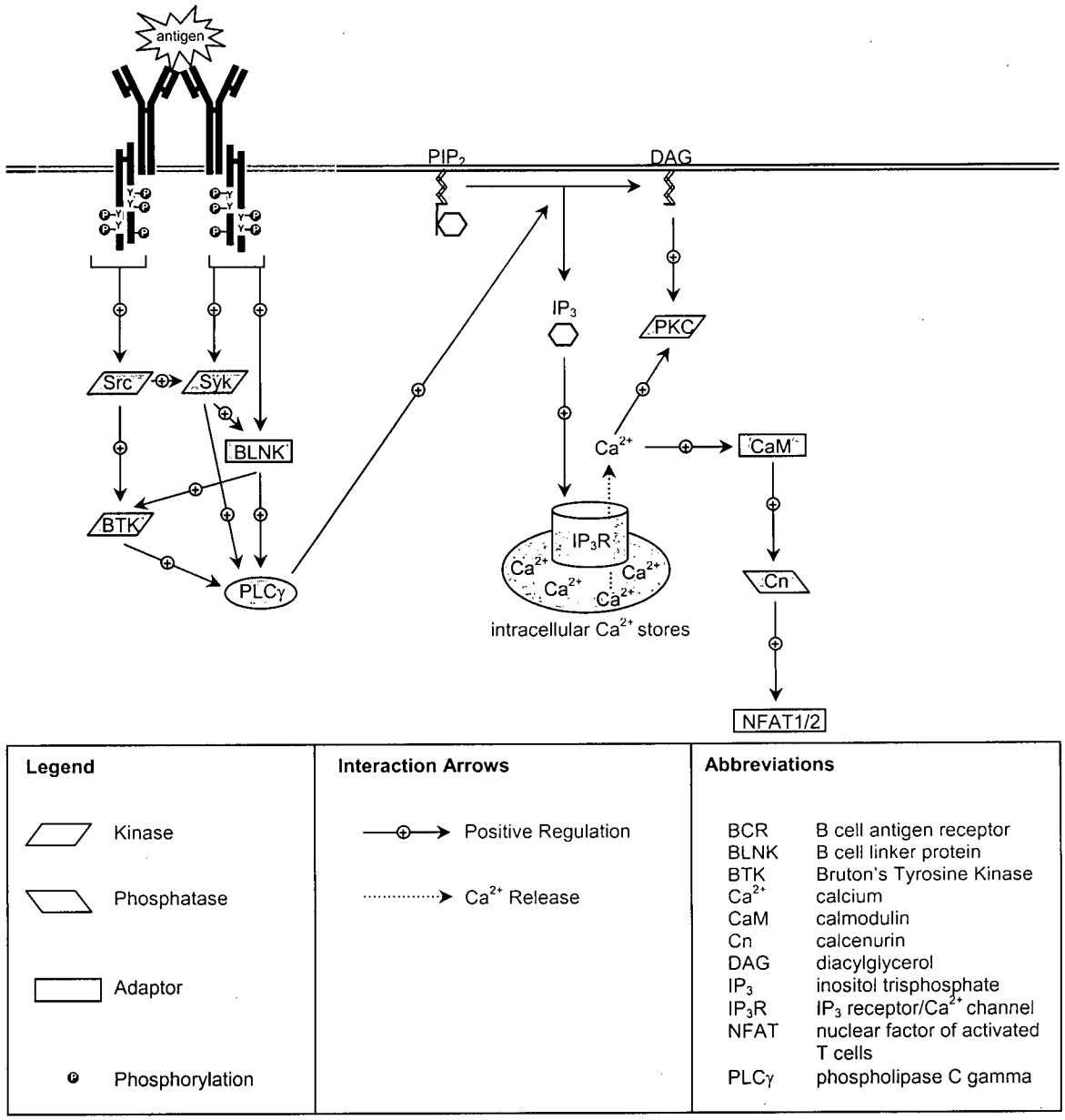

Figure 4.1. Basic Overview of the BCR/PLCγ Signaling Pathway. Cross-linking of the BCR initiates the activation of several PTKs (e.g., Src family members, Syk and BTK) that coordinate the activation of the Ras/MAPK, PI3K and PLCγ signaling pathways. Following BCR cross-linking Igα/β becomes phosphorylated. BLNK is then proposed to be recruited to phosphorylated Igα via its SH2 domain. BLNK is then phosphorylated by Syk such that it can then associate with BTK and PLCγ via their respective SH2 domains. Thus, BLNK acts as an adapter protein facilitating the co-localization of BTK, Syk and PLCγ such that the PTKs can efficiently phosphorylate PLCγ. Once activated, PLCγ hydrolyzes PIP_2 to DAG and IP_3. IP_3 then binds to IP_3R causing the release of intracellular calcium stores. Calcium and DAG then contribute to the activation of several enzymes (including PKC and calcineurin) which in turn influence the status of numerous transcription factors which ultimately assist in the regulation of the differentiation and proliferation of the B cell. Additionally, PLCγ has been shown to activate the MAPKs, Erk1/2 via the Ras pathway (refer to Fig. 4.3). Adapted from "AFCS Nature, The Signaling Gateway" (online at http://www.signaling_gateway.org/molecule/maps/bcr.html).

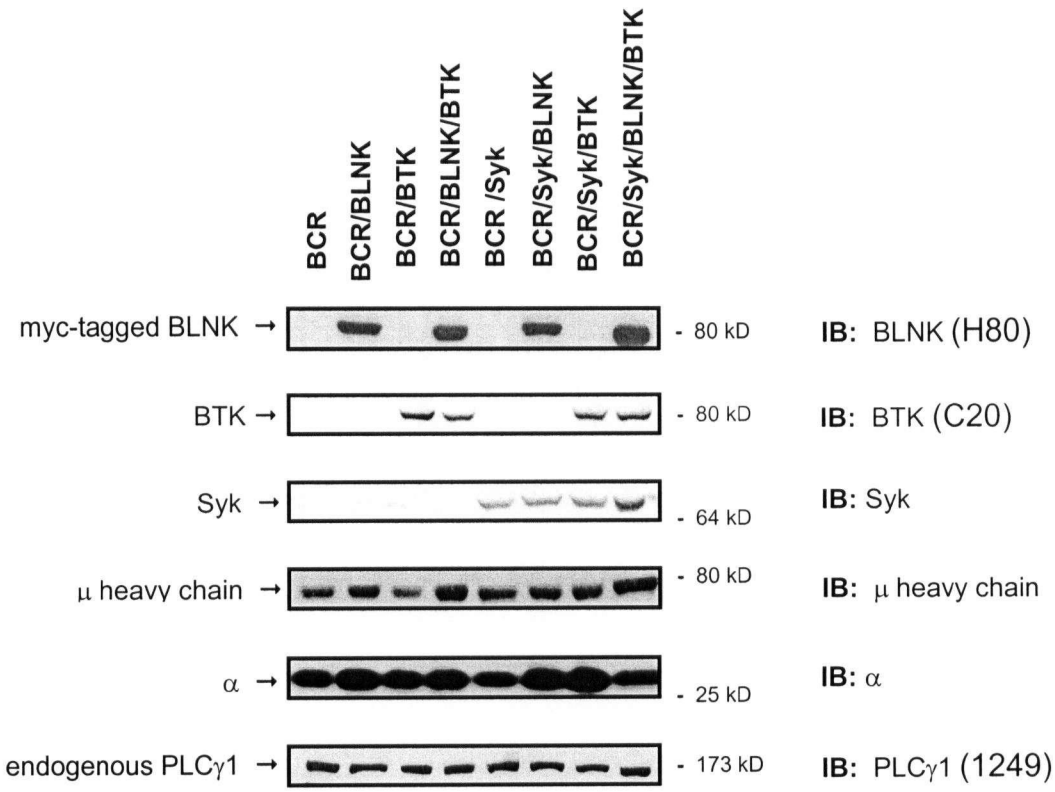

Figure 4.2. Characterization of α, μ, Syk, BLNK, BTK and PLCγ1 Expression in Transfected AtT20 Cell Lines. 35 μg of whole cell lysate were resolved by SDS-PAGE. Following electrophoresis, gels were transferred to nitrocellulose filters that were subsequently immunoblotted with antibodies specific for α, μ, BLNK, BTK, Syk and PLCγ1. Note that α is a component of the Igα/β signaling subunit of the BCR whereas μ is a component of the mIgM antigen-binding subunit of the BCR. IB indicates the immunoblotting antibody.

4.2.2 Co-Expression of the BCR, BLNK and/or BTK Is Not Sufficient to Reconstitute BCR-Induced Erk Phosphorylation in AtT20-Derived Cell Lines.

Having established a reconstitution system that expresses various combinations of the desired proteins, it was next necessary to establish a method to assay for BCR-induced PLCγ activation. While membrane-recruitment and tyrosine phosphorylation of PLCγ are suggestive of its activation these events have yet to be established as hallmarks of PLCγ activation. Thus, PLCγ activation is best assessed by monitoring downstream targets and/or consequences of PLCγ activation. Initially, it was proposed that PLCγ activation could be assayed by monitoring for increased IP_3 production and induced calcium fluxes as these are well-known downstream consequences of PLCγ activation (refer to Chapter 1.5.3 and Figure 4.1). Unfortunately, these assays proved inconclusive in the AtT20 system (summarized in Appendix II and Appendix III, respectively). Alternatively, BCR-induced PLCγ activation was assessed by monitoring for BCR-induced Erk phosphorylation as increased Erk phosphorylation has been demonstrated to be a downstream consequence of BCR-induced PLCγ activation (refer to Chapter 1.5.3 and 1.5.4). However, the BCR can induce Erk phosphorylation both via PLC-dependent and PLC-independent pathways (reviewed in Gold, 2002; refer to Fig. 4.3). Thus, a PLC inhibitor (U73122) was used to distinguish between PLC-dependent and PLC-independent changes in BCR-induced Erk phosphorylation.

According to previous studies and models, co-expression of the BCR along with BLNK and/or BTK should not be sufficient to reconstitute BCR-induced Erk phosphorylation within the AtT20 system. Rather, Syk is proposed to be necessary to initiate most BCR signaling pathways including both the PLC-independent and the PLC-dependent pathways that contribute to Erk phosphorylation. Nonetheless, it is possible that Syk and BTK may perform partially redundant functions or that some unidentified AtT20-specific PTK may exist that, along with BLNK, could initiate BCR-induced PLCγ activation within this system. Thus, to address these possibilities, the sufficiency of BLNK and/or BTK, to reconstitute BCR-induced Erk phosphorylation was investigated first.

As can be seen in Figure 4.4, no apparent increase in ERK phosphorylation is found following BCR cross-linking in AtT20-derived cell lines that co-express the BCR along with BLNK and/or BTK (Figure 4.4). This suggests that co-expression of the BCR along with BLNK and/or BTK

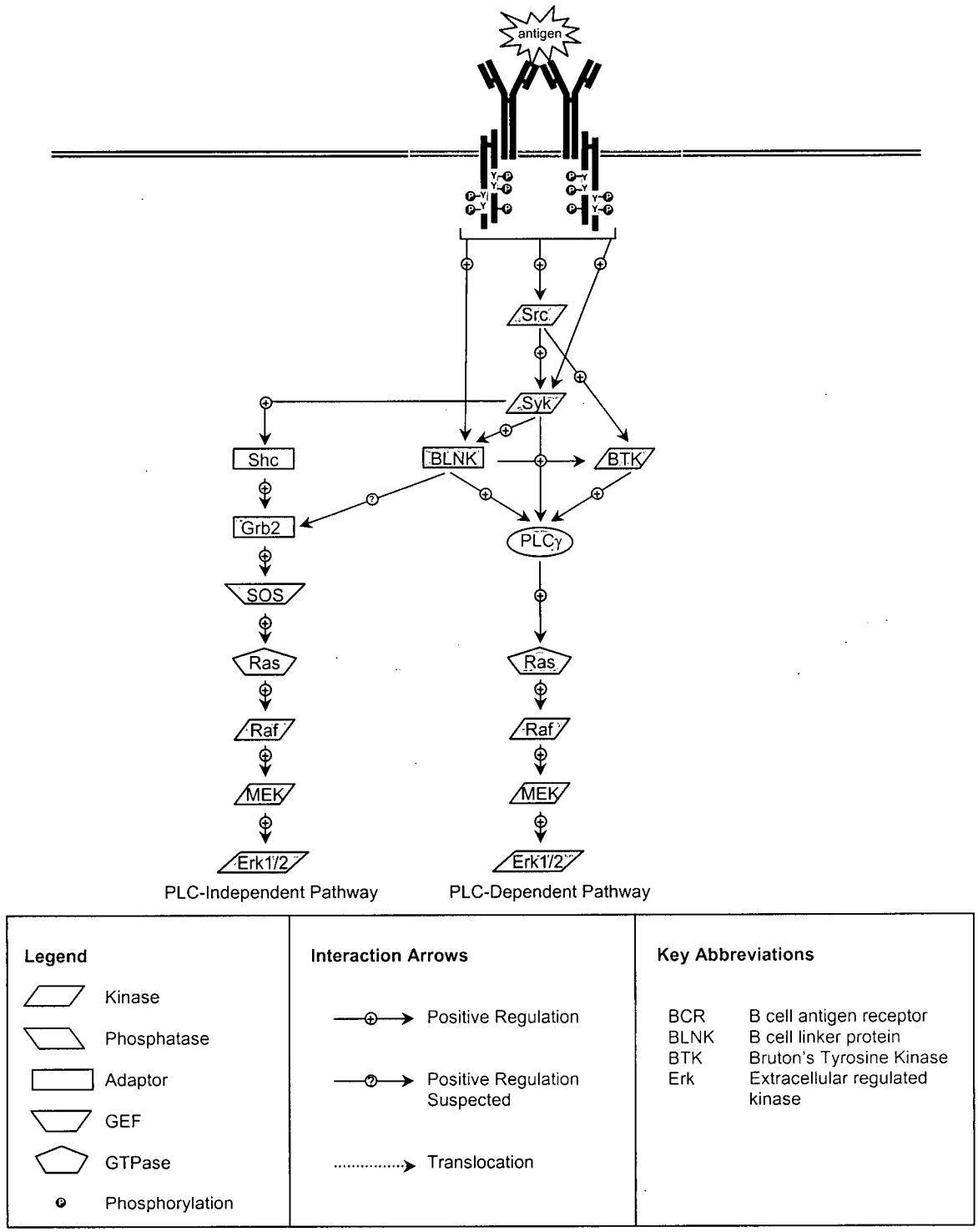

Figure 4.3. Basic Overview of BCR-Induced Erk Phosphorylation via the PLCγ-Independent and PLCγ-Dependent Signaling Pathways. Note that BLNK can associate with Grb2 of the PLC-independent pathway (Fu *et al.*, 1998). While this is believed to be a positive association the physiological significance remains to be determined. Furthermore, BLNK-associated Grb2 does not appear to associate with Shc (Fu *et al.*, 1998) as would be expected for the PLC-independent pathway. Reviewed in Gold (2002). Adapted from "AFCS Nature, The Signaling Gateway" (online at http://www.signaling_gateway.org/molecule/maps/bcr.html).

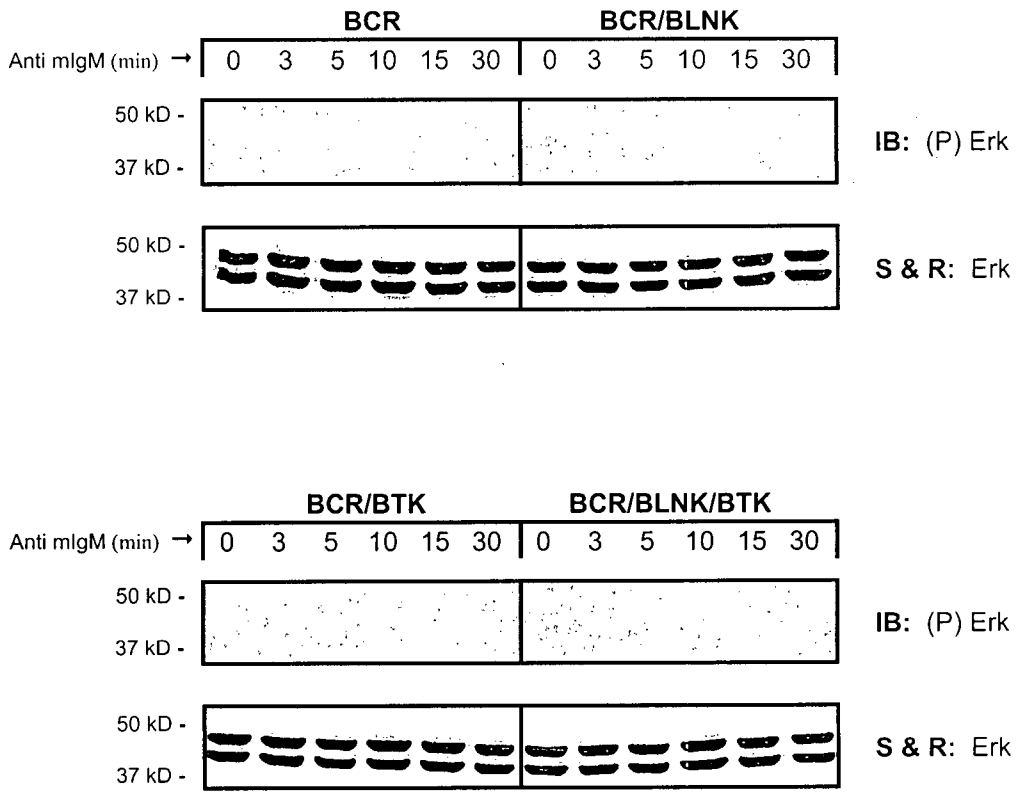

Figure 4.4 Co-Expression of the BCR, BLNK and/or BTK Is Not Sufficient to Reconstitute BCR-Induced Erk Phosphorylation in AtT20-Derived Cell Lines. The BCR was cross-linked with anti mIgM antibodies at 37 °C for the indicated length of time. Cells were then lysed and 50 μg of whole cell lysate were resolved by SDS-PAGE. Following electrophoresis, gels were transferred to nitrocellulose filters that were subsequently immunoblotted with a phospho-Erk (Thr202/Tyr204) specific antibody. Finally, filters were stripped and reprobed with an Erk specific antibody. IB indicates the immunoblotting antibody while S&R indicates the antibody used to reprobe the filter. Data are representative of three independent experiments. Note that these experiments were performed concurrently with those shown in Figures 4.5 and 4.6. Thus, the experiments shown in Figure 4.5 and 4.6 serve as positive controls that demonstrate that Erk phosphorylation is indeed detectable in the reconstitution system

is not sufficient to reconstitute BCR-induced Erk phosphorylation in the AtT20-derived system. This in turn suggests that co-expression of these components is not sufficient to reconstitute BCR-induced PLCγ activation. As mentioned above, this result is as expected as Syk, the putatively essential protein tyrosine kinase, is absent in these cell lines (refer to discussion).

4.2.3 Co-Expression of the BCR and Syk Is Sufficient to Reconstitute BCR-Induced, PLC-Independent Erk Phosphorylation in AtT20-Derived Cell Lines.

As previous studies and models suggest that Syk is essential to initiate most BCR signaling pathways, the sufficiency of Syk to reconstitute BCR-induced Erk phosphorylation was investigated next. As can be seen in Figure 4.5, an increase in ERK phosphorylation is evident following BCR cross-linking in AtT20-derived cell lines that co-express the BCR and Syk. The increase in ERK phosphorylation is evident within 3 minutes of BCR engagement and appears to be sustained for at least 15 minutes before beginning to decrease by 30 minutes (Fig. 4.5 a and b). This increase in Erk phosphorylation suggests that co-expression of the BCR and Syk is sufficient to reconstitute BCR-induced Erk phosphorylation in the AtT20-derived system. The PLC inhibitor, U73122, was then used to determine whether or not the Erk phosphorylation was being mediated by a PLC-dependent and/or a PLC-independent pathway. If the Erk phosphorylation is being mediated by a PLC-independent pathway one would predict that addition of the inhibitor should not affect BCR-induced Erk phosphorylation. In contrast, if the Erk phosphorylation is being mediated by a PLC-dependent pathway one would predict that addition of the inhibitor will repress Erk phosphorylation. In this case, it was found that addition of the inhibitor does not appear to significantly repress BCR-induced Erk phosphorylation in the BCR/Syk cell line (Figure 4.5 a and b). This suggests that co-expression of the BCR and Syk is sufficient to reconstitute BCR-induced, PLC-independent Erk phosphorylation in the AtT20-derived system. Furthermore, these findings suggest that co-expression of the BCR and Syk is not sufficient to reconstitute BCR-induced PLCγ1 activation within this system as assayed by Erk phosphorylation. Again, these finding are not unexpected as the prevailing models suggest that BLNK and/or BTK are required, along with Syk, to couple the BCR to PLCγ. Thus, the sufficiency of Syk, BLNK and/or BTK to reconstitute BCR-induced Erk phosphorylation in AtT20-derived cell lines was investigated next.

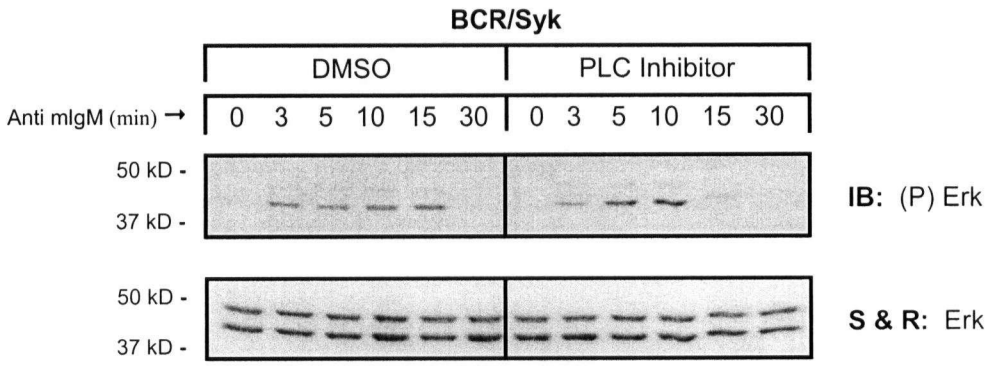

Figure 4.5. (a) Co-Expression of the BCR and Syk Is Sufficient to Reconstitute PLC-Independent, BCR-Induced Erk Phosphorylation in AtT20-Derived Cell Lines. Cells were treated either with DMSO (negative control) or the PLC inhibitor, U73122 (in DMSO, at a final concentration of 10 μM) for 1 hour. The BCR was then cross-linked with anti mIgM antibodies at 37 °C for the indicated length of time. Cells were then lysed and 50 μg of whole cell lysate were resolved by SDS-PAGE. Following electrophoresis, gels were transferred to nitrocellulose filters that were subsequently immunoblotted with a phospho-Erk (Thr202/Tyr204) specific antibody. Finally, filters were stripped and reprobed with an Erk specific antibody. IB indicates the immunoblotting antibody while S&R indicates the antibody used to reprobe the filter. Data are representative of at least four independent experiments.

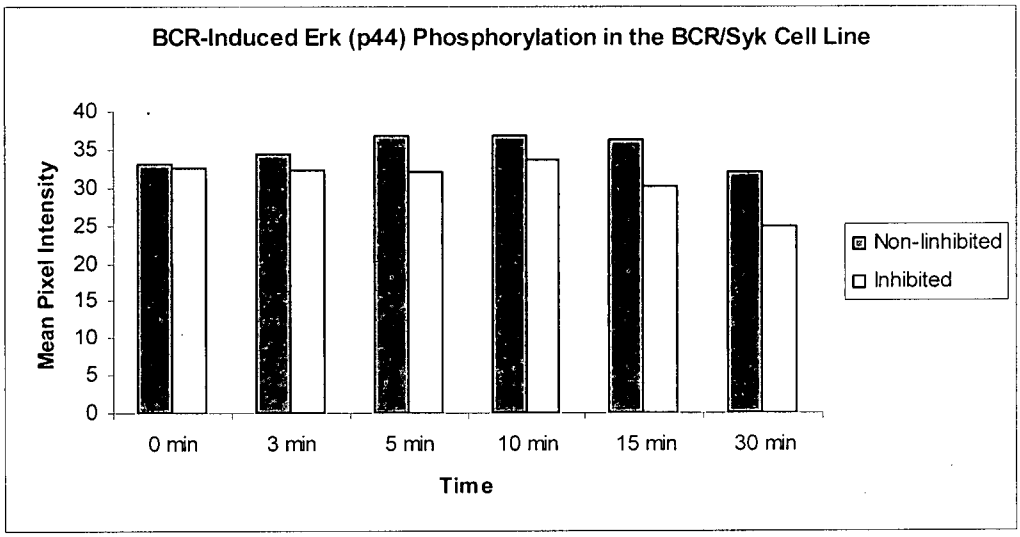

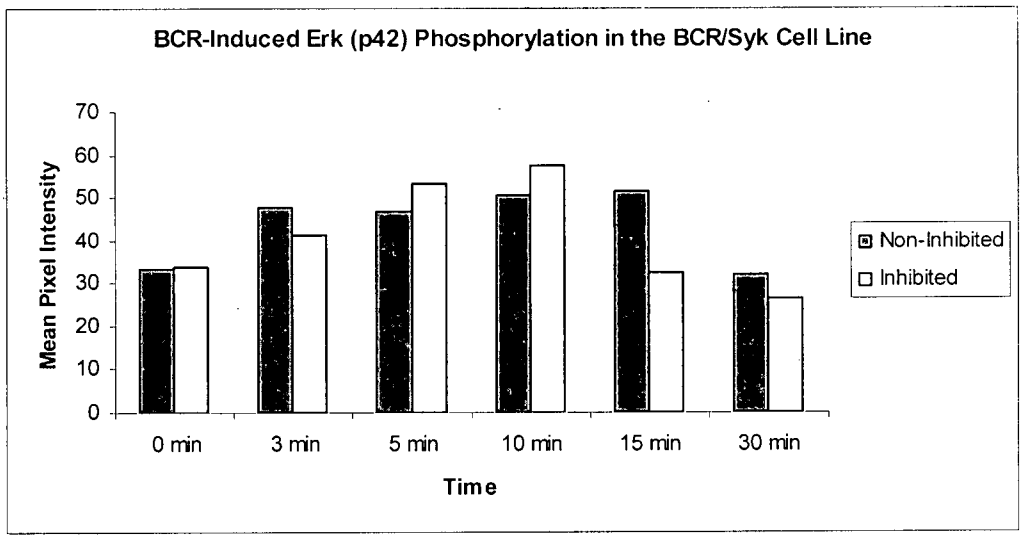

Figure 4.5. (b) Comparison of Mean Pixel Intensity of the Phosphorylated Erk "Bands" in the BCR/Syk Cell Line in Non-Inhibited and PLC-Inhibited Co-Expression Samples. To calculate the mean pixel intensity of the phosphorylated Erk "band" it was first necessary to define the "band". This was done by visually identifying the largest band in the immunoblot and then manually selecting a square area around that band that captured all the pixels of the band yet minimized the capture of background pixels. An equivalent square area was then selected around the remaining bands again ensuring that all the pixels of the band were captured. The mean pixel intensity of the "bands" was then calculated using Matlab (refer to Chapter 2.15 for further details). By this method the mean pixel intensity should correlate to the band size and intensity such that the larger the mean pixel intensity the larger and more intense the band. The top graph considers the band intensities of the top phosphorylated Erk band (p44) and the bottom graph considers the band intensities of the bottom phosphorylated Erk band (p42).

4.2.4 Co-Expression of the BCR, Syk and BLNK Is Sufficient to Reconstitute BCR-Induced, PLC-Dependent Erk Phosphorylation in AtT20-Derived Cell Lines.

Existing models suggest that BLNK is required to couple the BCR to PLCγ activation. Thus, co-expression of the BCR, Syk and BLNK may be predicted to reconstitute BCR-induced PLCγ activation and therefore, enhance BCR-induced Erk phosphorylation in this system. However, as can be seen in figure 4.6a, BCR-induced ERK phosphorylation does not appear to be enhanced in the BCR/Syk/BLNK cell line as compared to the BCR/Syk cell line. If anything, BCR-induced ERK phosphorylation appears to be slightly, yet reproducibly, inhibited in the BCR/Syk/BLNK cell line (Fig. 4.6a). Thus, it appears that co-expression of BLNK may inhibit BCR-induced Erk phosphorylation in the AtT20-derived system.

Given the complexity of the system and the pathways contributing to BCR-induced Erk phosphorylation these results must be interpreted with caution. In fact, it is possible that BLNK may be enhancing BCR-induced Erk phosphorylation by activating the PLC-dependent pathway while at the same time inhibiting BCR-induced Erk phosphorylation by repressing the PLC-independent pathway (refer to discussion). If this is the case, BCR-induced increases in Erk phosphorylation may or may not be evident, depending on the relative contributions of the two pathways. Thus, the PLC inhibitor, U73122 was used to clarify whether or not PLC-dependent changes in BCR-induced Erk phosphorylation were occurring in the BCR/Syk/BLNK cell line. As can be seen in Figure 4.6b and 4.6c, U73122, does appear to inhibit BCR-induced Erk phosphorylation. This suggests that co-expression of the BCR, Syk and BLNK may be sufficient to reconstitute BCR-induced, PLC-dependent Erk phosphorylation in the AtT20-derived system. Although these components appear sufficient to reconstitute BCR-induced PLCγ activation in the AtT20-system it is unclear whether or not maximal PLCγ activity has been achieved. Indeed, as mentioned above, BTK expression may be required to achieve maximal PLCγ phosphorylation and activation. Thus, the effect of BTK expression within this system was investigated next.

It is important to note that BLNK appears to be concomitantly inhibiting PLC-independent Erk phosphorylation while enhancing PLC-dependent Erk phosphorylation. This is based on the observations that while co-expression of the BCR, Syk and BLNK appears to enhance PLC-

a.

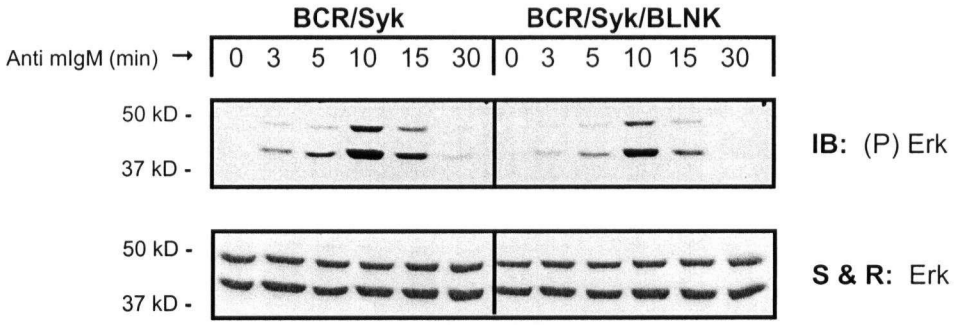

b.

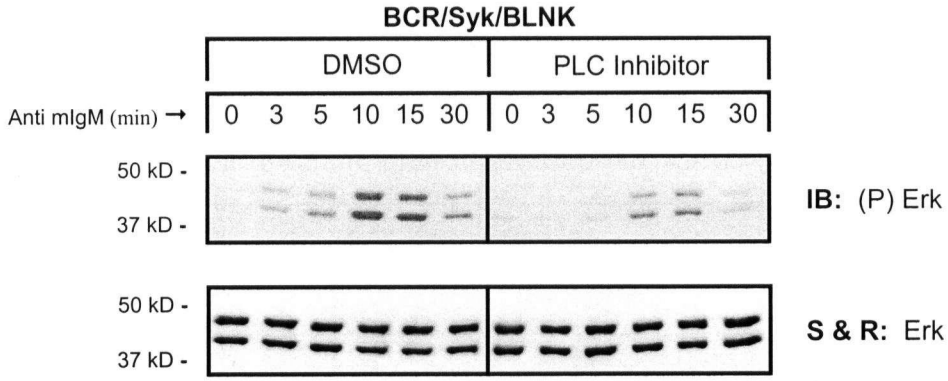

Figure 4.6. (a) Co-Expression of BLNK, Along with Syk and the BCR, Appears to Slightly Inhibit BCR-Induced Erk Phosphorylation in AtT20-Derived Cell Lines. The BCR was cross-linked with anti mIgM antibodies at 37 °C for the indicated length of time. Cells were then lysed and 50 μg of whole cell lysate were resolved by SDS-PAGE. Following electrophoresis, gels were transferred to nitrocellulose filters that were subsequently immunoblotted with a phospho-Erk (Thr202/Tyr204) specific antibody. Finally, filters were stripped and reprobed with an Erk specific antibody. IB indicates the immunoblotting antibody while S&R indicates the antibody used to reprobe the filter. Data are representative of three independent experiments. **(b) Co-Expression of BLNK, Along with Syk and the BCR, Is Sufficient to Reconstitute BCR-Induced, PLC-Dependent Erk Phosphorylation in AtT20-Derived Cell Lines.** Cells were treated either with DMSO (negative control) or the PLC inhibitor, U73122 (in DMSO, at a final concentration of 10 μM) for 1 hour. The BCR was then cross-linked with anti mIgM antibodies at 37 °C for the indicated length of time. Cells were then lysed and 50 μg of whole cell lysate were resolved by SDS-PAGE. Following electrophoresis, gels were transferred to nitrocellulose filters that were subsequently immunoblotted with a phospho-Erk (Thr202/Tyr204) specific antibody. Finally, filters were stripped and reprobed with an Erk specific antibody. IB indicates the immunoblotting antibody while S&R indicates the antibody used to reprobe the filter. Data are representative of three independent experiments.

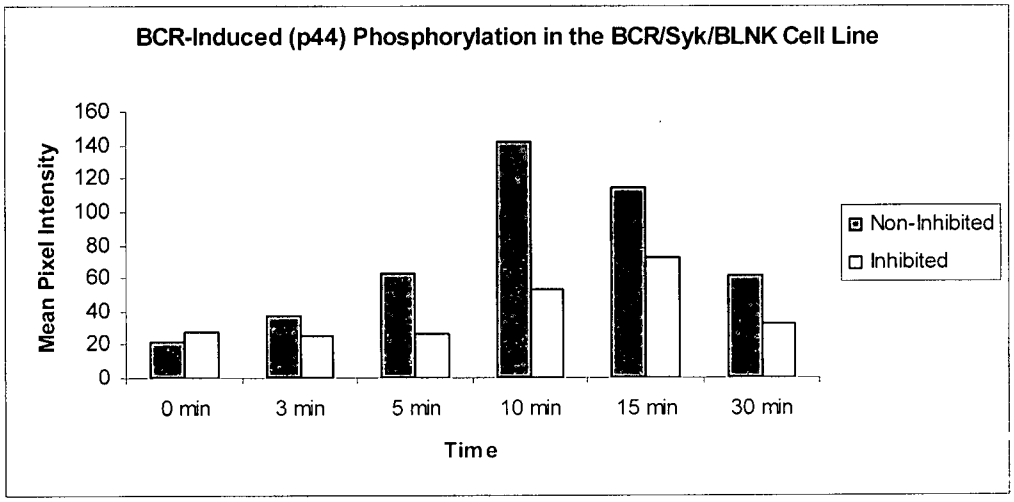

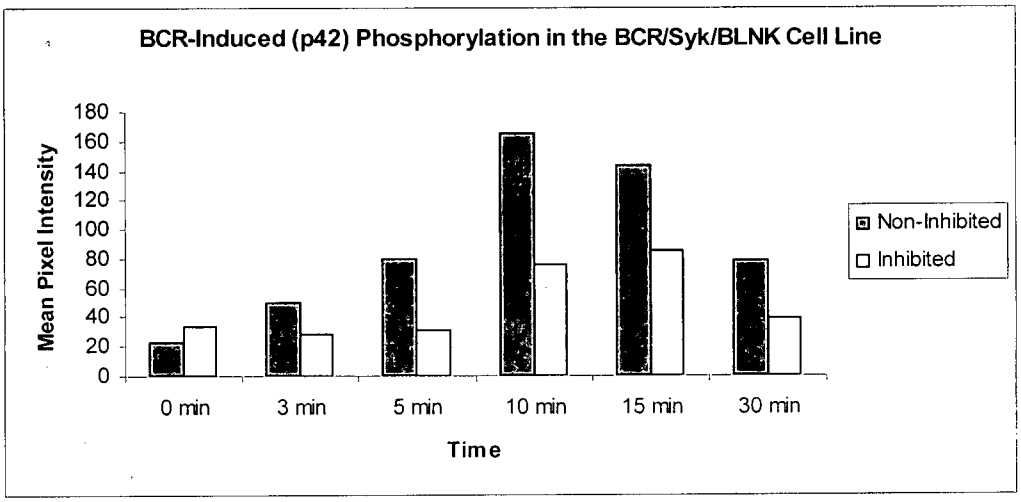

Figure 4.6. (c) Comparison of Mean Pixel Intensity of the Phosphorylated Erk "Bands" in the BCR/Syk/BLNK Cell Line in Non-Inhibited and PLC-Inhibited Co-Expression Samples. To calculate the mean pixel intensity of the phosphorylated Erk "band" it was first necessary to define the "band". This was done by visually identifying the largest band in the immunoblot and then manually selecting a square area around that band that captured all the pixels of the band yet minimized the capture of background pixels. An equivalent square area was then selected around the remaining bands again ensuring that all the pixels of the band were captured. The mean pixel intensity of the "bands" was then calculated using Matlab (refer to Chapter 2.15 for further details). By this method the mean pixel intensity should correlate to the band size and intensity such that the larger the mean pixel intensity the larger and more intense the band. The top graph considers the band intensities of the top phosphorylated Erk band (p44) and the bottom graph considers the band intensities of the bottom phosphorylated Erk band (p42).

dependent Erk phosphorylation (Fig. 4.6b) it also appears to slightly inhibit overall Erk phosphorylation as compared to the BCR/Syk expressing cell line (Fig. 4.6a). This finding was quite unexpected and is discussed further in Chapter 4.3.

4.2.5 Co-Expression of the BCR, Syk and BTK Is Not Sufficient to Reconstitute BCR-Induced PLC-Dependent Erk Phosphorylation in AtT20-Derived Cell Lines.

As existing models suggest that BTK is required for efficient BCR-induced PLCγ activation it may be predicted that co-expression of BTK will enhance BCR-induced, Syk-dependent PLCγ activation and therefore BCR-induced Erk phosphorylation within this system. However, as can be seen in figure 4.7a, BCR-induced ERK phosphorylation does not appear to be enhanced in the BCR/Syk/BTK cell line as compared to the BCR/Syk cell line. Rather, BCR-induced ERK phosphorylation appears to be reproducibly inhibited in the BCR/Syk/BTK cell line (Fig. 4.7a). Thus, it appears that co-expression of BTK may inhibit BCR-induced Erk phosphorylation in the AtT20-derived system.

Again, given the complexity of the system and the pathways contributing to BCR-induced Erk phosphorylation these results must be interpreted with caution. It is possible that BTK may be enhancing BCR-induced Erk phosphorylation by activating the PLC-dependent pathway while at the same time inhibiting BCR-induced Erk phosphorylation by repressing the PLC-independent pathway (refer to discussion). Thus, the PLC inhibitor, U73122 was used to clarify whether or not PLC-dependent changes in BCR-induced Erk phosphorylation were occurring in the BCR/Syk/BTK cell line. As can be seen in Figure 4.7b and 4.7c, inhibitor treatment does not appear to affect BCR-induced Erk phosphorylation in the BCR/Syk/BTK cell line. This suggests that co-expression of the BCR, Syk and BTK is not sufficient to reconstitute BCR-induced PLCγ1 activation in the AtT20 system. This finding is not surprising given that numerous studies have suggested that BLNK is required to efficiently couple Syk and BTK to PLCγ. In contrast, the finding that BTK expression inhibits PLC-independent Erk phosphorylation within this system was unanticipated and thus, is discussed further in Chapter 4.3.

a.

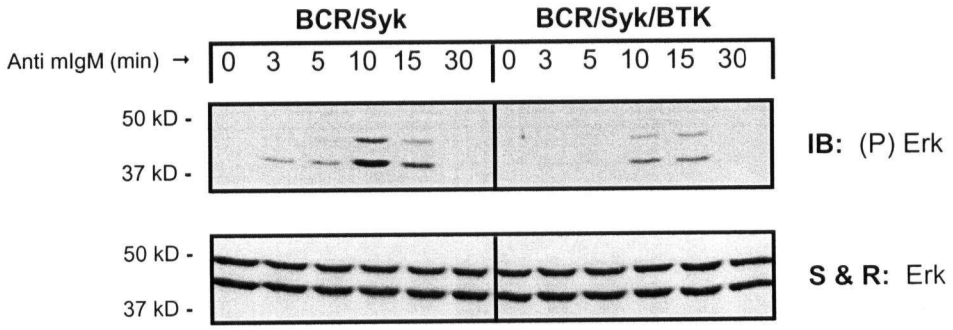

b.

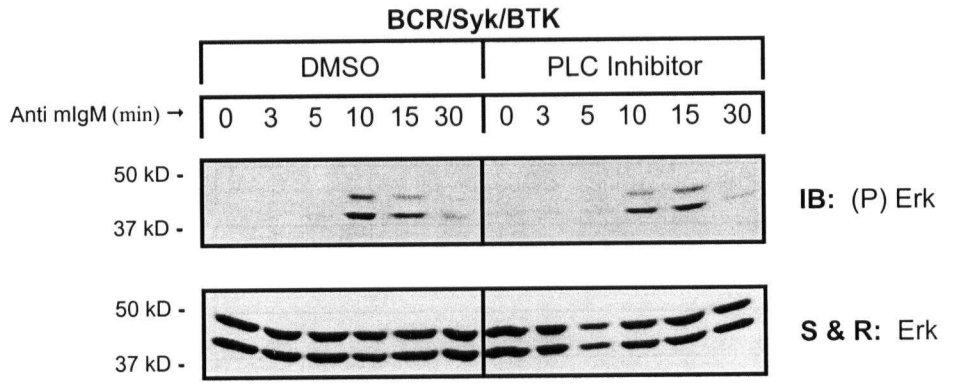

Figure 4.7. (a) Co-Expression of BTK, Along with Syk and the BCR, Appears to Slightly Inhibit BCR-Induced Erk Phosphorylation in AtT20-Derived Cell Lines. The BCR was cross-linked with anti mIgM antibodies at 37 °C for the indicated length of time. Cells were then lysed and 50 μg of whole cell lysate were resolved by SDS-PAGE. Following electrophoresis, gels were transferred to nitrocellulose filters that were subsequently immunoblotted with a phospho-Erk (Thr202/Tyr204) specific antibody. Finally, filters were stripped and reprobed with an Erk specific antibody. IB indicates the immunoblotting antibody while S&R indicates the antibody used to reprobe the filter. Data are representative of three independent experiments. **(b) Co-Expression of BTK, Along with Syk and the BCR, Is Not Sufficient to Reconstitute BCR-Induced, PLC-Dependent Erk Phosphorylation in AtT20-Derived Cell Lines.** Cells were treated either with DMSO (negative control) or the PLC inhibitor, U73122 (in DMSO, at a final concentration of 10 μM) for 1 hour. The BCR was then cross-linked with anti mIgM antibodies at 37 °C for the indicated length of time. Cells were then lysed and 50 μg of whole cell lysate were resolved by SDS-PAGE. Following electrophoresis, gels were transferred to nitrocellulose filters that were subsequently immunoblotted with a phospho-Erk (Thr202/Tyr204) specific antibody. Finally, filters were stripped and reprobed with an Erk specific antibody. IB indicates the immunoblotting antibody while S&R indicates the antibody used to reprobe the filter. Data are representative of three independent experiments.

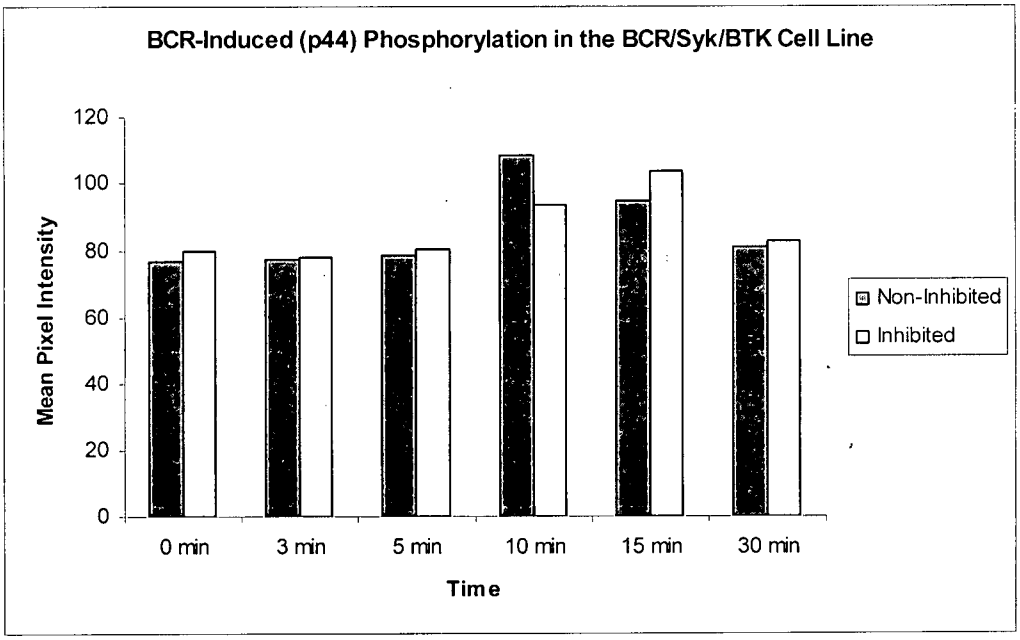

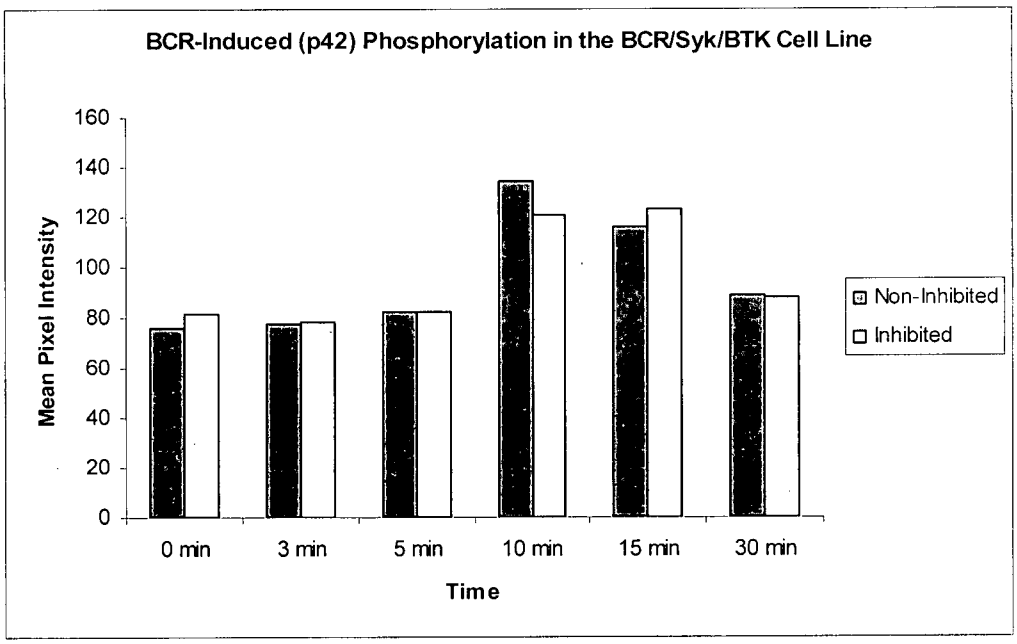

Figure 4.7. (c) Comparison of Mean Pixel Intensity of the Phosphorylated Erk "Bands" in the BCR/Syk/BTK Cell Line in Non-Inhibited and PLC-Inhibited Co-Expression Samples. To calculate the mean pixel intensity of the phosphorylated Erk "band" it was first necessary to define the "band". This was done by visually identifying the largest band in the immunoblot and then manually selecting a square area around that band that captured all the pixels of the band yet minimized the capture of background pixels. An equivalent square area was then selected around the remaining bands again ensuring that all the pixels of the band were captured. The mean pixel intensity of the "bands" was then calculated using Matlab (refer to Chapter 2.15 for further details). By this method the mean pixel intensity should correlate to the band size and intensity such that the larger the mean pixel intensity the larger and more intense the band. The top graph considers the band intensities of the top phosphorylated Erk band (p44) and the bottom graph considers the band intensities of the bottom phosphorylated Erk band (p42).

4.2.6 Co-Expression of the BCR, Syk, BTK *and* BLNK Is Not Sufficient to Reconstitute BCR-Induced, PLC-Dependent Erk Phosphorylation in AtT20-Derived Cell Lines.

Current models suggest that BLNK, Syk and BTK are all required to couple the BCR to PLCγ activation. Thus it is hypothesized that maximal PLCγ activation would be achieved in a cell line reconstituted with all these components as compared to a cell line reconstituted with only some of these components. To test this hypothesis the BCR/Syk/BLNK/BTK cell was created and assessed for its ability to reconstitute BCR-induced PLCγ activation. As can be seen in Figure 4.8a the PLC inhibitor does not appear to inhibit BCR-induced Erk phosphorylation in the BCR/Syk/BLNK/BTK cell line. This suggests that co-expression of the BCR, Syk, BLNK *and* BTK *is not* sufficient to reconstitute BCR-induced PLCγ activation. This is very surprising both given the proposed models of BCR/PLCγ signaling and the previous finding that co-expression of the BCR, Syk and BLNK alone *is* sufficient to reconstitute BCR-induced PLCγ activation (Fig. 4.6b). Considered together, these findings suggest that expression of BTK inhibits, rather than enhances, BCR-induced PLCγ activity within this system. As these findings are quite unexpected they are discussed at greater length in Chapter 4.3.

Interestingly, while BTK expression appears to inhibit BCR-induced PLC-dependent Erk phosphorylation it also appears to enhance the overall Erk phosphorylation in the BCR/Syk/BLNK/BTK cell line as compared to either the BCR/Syk/BLNK cell line or the BCR/Syk/BTK cell line (compare Fig. 4.8b to Fig. 4.6a and 4.7a, respectively). In fact, co-expression of the BCR, Syk, BLNK and BTK appears sufficient to restore overall BCR-induced Erk phosphorylation to levels comparable to those observed for the BCR/Syk cell line (Fig. 4.8b). This apparent restoration likely reflects a release of the inhibition of the PLC-independent pathway that is apparent in the BCR/Syk/BLNK and BCR/Syk/BTK cell lines. While, the reasons for this initial inhibition and its subsequent release are unclear some possible explanations are presented in Chapter 4.3.

a.

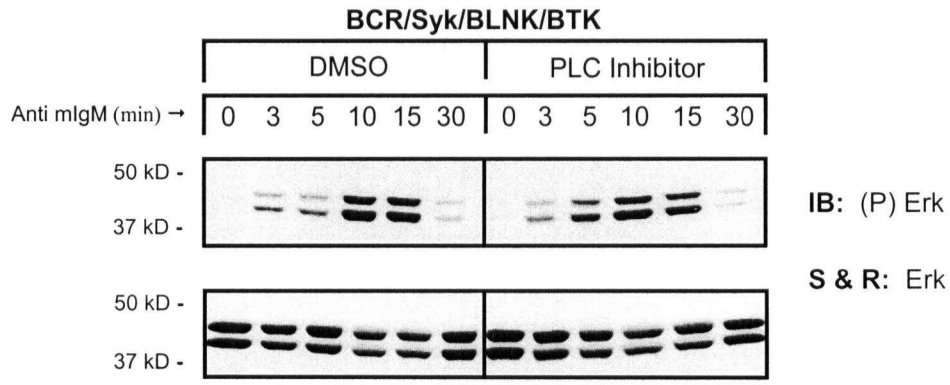

b.

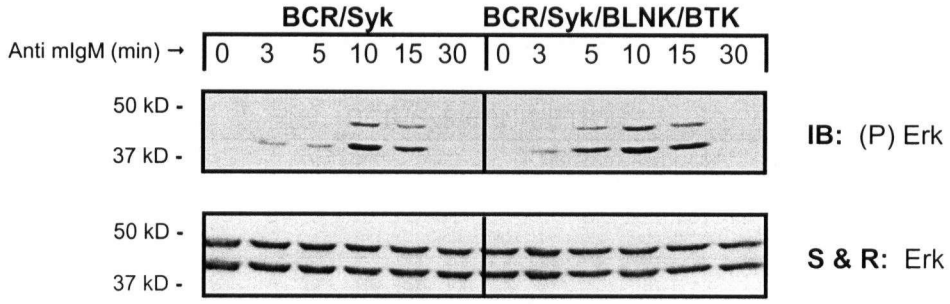

Figure 4.8. (a) Co-Expression of the BCR, Syk, BLNK and BTK Is Not Sufficient to Reconstitute BCR-Induced, PLC-Dependent Erk Phosphorylation in AtT20-Derived Cell Lines. Cells were treated either with DMSO (negative control) or the PLC inhibitor, U73122 (in DMSO, at a final concentration of 10 μM) for 1 hour. The BCR was then cross-linked with anti mIgM antibodies at 37 °C for the indicated length of time. Cells were then lysed and 50 μg of whole cell lysate were resolved by SDS-PAGE. Following electrophoresis, gels were transferred to nitrocellulose filters that were subsequently immunoblotted with a phospho-Erk (Thr202/Tyr204) specific antibody. Finally, filters were stripped and reprobed with an Erk specific antibody. IB indicates the immunoblotting antibody while S&R indicates the antibody used to reprobe the filter. Data are representative of three independent experiments. **(b) Overall BCR-Induced Erk Phosphorylation is Comparable in the BCR/Syk and BCR/Syk/BLNK/BTK Cell Lines.** The BCR was cross-linked with anti mIgM antibodies at 37 °C for the indicated length of time. Cells were then lysed and 50 μg of whole cell lysate were resolved by SDS-PAGE. Following electrophoresis, gels were transferred to nitrocellulose filters that were subsequently immunoblotted with a phospho-Erk (Thr202/Tyr204) specific antibody. Finally, filters were stripped and reprobed with an Erk specific antibody. IB indicates the immunoblotting antibody while S&R indicates the antibody used to reprobe the filter. Data are representative of three independent experiments.

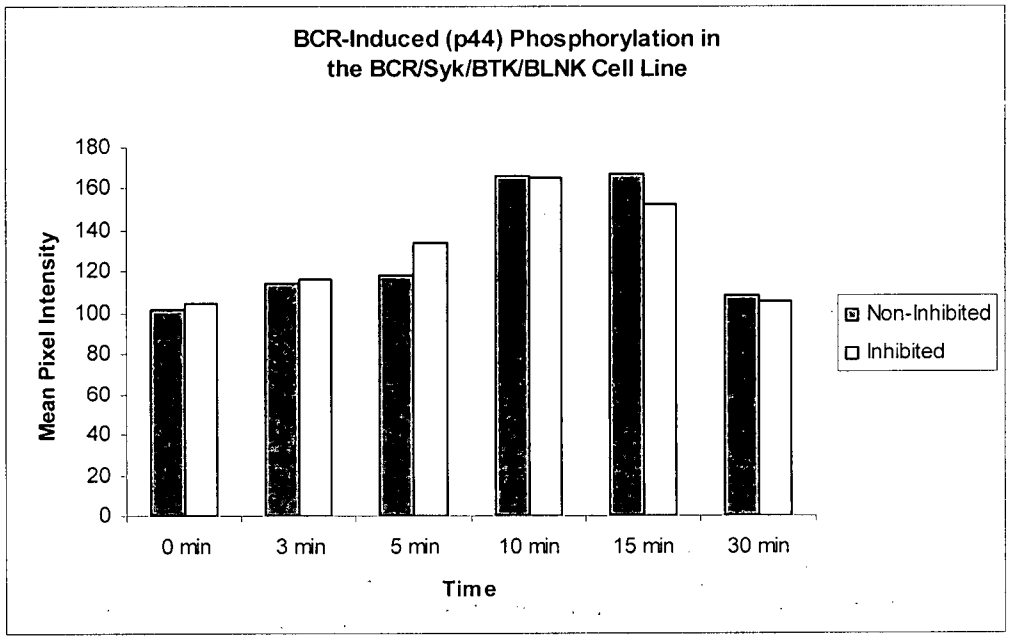

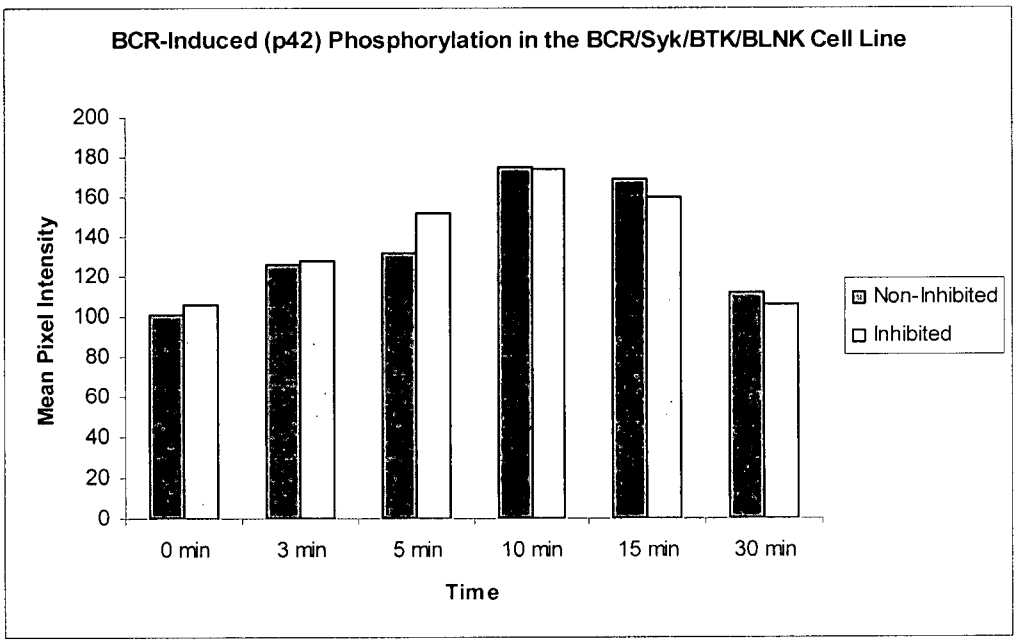

Figure 4.8. (c) Comparison of Mean Pixel Intensity of the Phosphorylated Erk "Bands" in the BCR/Syk/BTK/BLNK Cell Line in Non-Inhibited and PLC-Inhibited Co-Expression Samples. To calculate the mean pixel intensity of the phosphorylated Erk "band" it was first necessary to define the "band". This was done by visually identifying the largest band in the immunoblot and then manually selecting a square area around that band that captured all the pixels of the band yet minimized the capture of background pixels. An equivalent square area was then selected around the remaining bands again ensuring that all the pixels of the band were captured. The mean pixel intensity of the "bands" was then calculated using Matlab (refer to Chapter 2.15 for further details). By this method the mean pixel intensity should correlate to the band size and intensity such that the larger the mean pixel intensity the larger and more intense the band. The top graph considers the band intensities of the top phosphorylated Erk band (p44) and the bottom graph considers the band intensities of the bottom phosphorylated Erk band (p42).

4.3 Discussion

4.3.1 Syk is Necessary and Sufficient to Reconstitute BCR-Induced, PLC-Independent Erk Phosphorylation in the AtT20 System.

Previous loss-of-function studies clearly suggest that Syk, BTK and BLNK are required to efficiently couple the BCR to PLCγ activation (Fig. 4.8). However, loss-of-function studies can not determine whether these proteins are sufficient to achieve a functional pathway or whether additional components are required. Thus, I employed a reconstitution approach to investigate the molecular requirements and mechanisms underlying BCR-induced PLCγ activation.

Reconstitution experiments were performed in AtT20-derived cell lines where BCR-induced activation of PLCγ was assayed by monitoring BCR-induced increases in Erk phosphorylation. Increases in Erk phosphorylation can be indicative of PLCγ activation as Erk phosphorylation is a downstream consequence of PLCγ activation. However, it should be noted that Erk phosphorylation can also be achieved as a downstream consequence of the BCR-induced PLC-independent pathway (Figure 4.3). Therefore, a PLC inhibitor was employed to distinguish between PLC-dependent and PLC-independent increases in BCR-induced Erk phosphorylation.

Initial reconstitution studies were performed in AtT20-derived cell lines that co-expressed the BCR along with BLNK and/or BTK. As mentioned above, previous studies clearly suggest that Syk is required to couple the BCR to downstream signaling pathways including the PLC-dependent and PLC-independent pathways that regulate BCR-induced Erk phosphorylation (Fig. 4.8; reviewed in Weiss and Littman, 1994, Gold and Matsuuchi, 1995; Reth and Weinands, 1997, Gold *et al.*, 2000). Thus, one may predict that co-expression of the BCR along with BLNK and/or BTK would be insufficient to reconstitute BCR-induced Erk phosphorylation. Nonetheless, it is prudent to confirm these predictions within the AtT20 system and to ensure that BTK or some unidentified AtT20-specific PTK is not able to compensate for the absence of Syk.

As predicted, co-expression of the BCR along with BLNK and/or BTK is not sufficient to reconstitute BCR-induced Erk phosphorylation within the AtT20 system (Fig. 4.2). These findings are in agreement with previous loss-of-function studies that clearly demonstrated that

Syk is required for activation of the PI3K, Ras and PLCγ pathways in B cells (reviewed in Weiss and Littman, 1994, Gold and Matsuuchi, 1995; Reth and Weinands, 1997, Gold *et al.*, 2000). In contrast, co-expression of the BCR and Syk is sufficient to reconstitute BCR-induced Erk phosphorylation (Fig. 4.4a). However, as the PLC inhibitor does not appear to inhibit this process (Fig. 4.4b), it appears that Syk is reconstituting BCR-induced Erk phosphorylation via a PLC-independent pathway within this system. Again, these findings are in agreement with previous studies that have shown that co-expression of the BCR and Syk is sufficient to reconstitute BCR-induced Ras phosphorylation and Erk activation, yet insufficient to reconstitute PLCγ activation (as assayed via IP_3 production) within the AtT20 system (Matsuuchi *et al.*, 1992; Richards *et al.*, 1996). Thus, it appears that Syk is necessary and sufficient to reconstitute BCR-induced, PLC-independent Erk phosphorylation in the AtT20 system.

4.3.2 The Effects of Syk, BTK and/or BLNK Expression on BCR-Induced Erk Phosphorylation in the AtT20 System.

The effects of Syk, BTK and/or BLNK expression on BCR-induced Erk phosphorylation are quite varied and complex within the AtT20 System. Thus, these effects are summarized in Table 4.3.1 below in an effort to provide the reader with some clarity. Several unexpected findings were made during the course of the abovementioned investigations. These include:

(1) When comparing the BCR/Syk cell line to the BCR/Syk/BLNK cell line, BLNK addition appears to enhance the PLC-dependent Erk pathway while concomitantly inhibiting the PLC-independent Erk pathway. Upon initial inspection it may appear contradictory that BLNK should enhance Erk phosphorylation via the PLC-dependent pathway while at the same time inhibiting it via the PLC-independent pathway. Indeed, a parsimonious model would propose that BLNK, if anything, should enhance the PLC-independent pathway as well as the PLC-dependent pathway. However, natural selection (being blissfully unaware of scientists' penchant for parsimony) may have rendered a situation where BLNK may differentially influence the pathways as ultimately each pathway influences a multitude of outcomes beyond mere Erk phosphorylation. Unfortunately, the AtT20 reconstitution system is not ideal for investigating whether this hypothesis is physiologically accurate. Rather, the DT40 knockout system may be better suited to such an investigation. In particular, BCR-induced Erk phosphorylation should be compared in the PLCγ knockout versus the BLNK/PLCγ double knockout. If one were to

Table 4.1. The Effects of Syk, BTK and/or BLNK Expression on BCR-Induced Erk Phosphorylation in the AtT20 System. Note that arrow indicates that BCR-induced phosphorylation was detected. The colour of the arrow is intended to roughly indicate the intensity of the observed phosphorylation relative to the other cell lines. BCR-induced PLC-dependent Erk phosphorylation is distinguished from BCR-induced PLC-independent with the aid of the PLC inhibitor, U73122. The intensity of the PLC-independent phosphorylation is inferred by comparing the overall Erk phosphorylation to the PLC-dependent Erk phosphorylation. BCR-induced PLCγ activation is inferred to occur if BCR-induced PLC-dependent Erk phosphorylation is observed.

AtT20-Derived Cell Line	Overall Erk (P) (observed)	PLC-dependent Erk (P) (observed)	PLC-independent Erk (P) (inferred)	PLCγ Activation (inferred)
BCR	none	none	none	none
BCR/Syk	↑	none	↑	none
BCR/BTK	none	none	none	none
BCR/BLNK	none	none	none	none
BCR/Syk/BTK (Fig. 4.7)		none		none
BCR/Syk/BLNK (Fig. 4.6)		↑		yes
BCR/BTK/BLNK	none	none	none	none
BCR/Syk/BLNK/BTK (Fig. 4.8)	↑	none	↑	none

hypothesize that BLNK positively influences BCR-induced Erk-phosphorylation solely via the PLCγ-dependent pathway then one would predict that BCR-induced Erk phosphorylation would be equally impaired in the PLCγ as compared to the BLNK/PLCγ double knockout. In contrast, if one were to hypothesize that BLNK positively influences BCR-induced Erk-phosphorylation via both the PLCγ-dependent and PLC-independent pathways one would then predict that BCR-induced Erk phosphorylation would more significantly impaired in the BLNK/PLCγ double knock-out as compared to the PLCγ knockout. Finally, if one were to hypothesize that BLNK positively influences BCR-induced Erk-phosphorylation via the PLCγ-dependent pathway while negatively influencing it via the PLC-independent pathway one would predict that BCR-induced Erk phosphorylation would be less impaired in the BLNK/PLCγ double knockout as compared to the PLCγ knockout.

Alternatively, parsimony may have been victorious and BLNK may well only enhance BCR-induced Erk phosphorylation, either via the PLC-dependent pathway alone or via both the PLC-dependent and PLC-independent pathways. If this is the physiological reality, then the observed results may merely be a reflection of some inadequacy or anomaly within the AtT20 system. In particular, BLNK could be associating with a component of the PLC-independent pathway in a way that is inhibiting that component's normal function. Indeed, BLNK has been shown to associate with Grb2, a putative component of the PLCγ-independent pathway (Fu *et al.*, 1998). And while this association has been proposed to have a positive influence on the pathway (Fu *et al.*, 1998), the true physiological significance of the association has yet to be confirmed.

(2) When comparing the BCR/Syk cell line to the BCR/Syk/BTK cell line, BTK addition appears to inhibit the PLC-independent Erk pathway while not affecting the PLC-dependent pathway. Similar to BLNK, BTK may be associating with a component of the PLC-independent pathway in a way that is inhibiting that component's normal function. Interestingly, there is little in the literature to connect BTK to the BCR-induced PLC-independent Erk pathway. Nonetheless, given these results, it may be prudent to revisit the literature regarding BTK in an effort to determine if any physiological connection is hinted at and furthermore, such a connection should be further investigated within this system.

(3) When BLNK and BTK are added together in the BCR/Syk/BLNK/BTK cell line, they appear to release the inhibition of the PLC-independent pathway that is observed when they are

expressed independently in the BCR/Syk/BLNK and BCR/Syk/BTK cell lines. At first glance this observation may appear contradictory to the above two observations however, it is possible to explain. Primarily, BTK and BLNK, may preferentially interact with each other when co-expressed within the AtT20 system. Now, based on the aforementioned hypothesis, this interaction may prevent BLNK and/or BTK from forming inhibitory/non-productive associations with components of the PLC-independent pathway and may thereby release the inhibition of the PLC-independent Erk pathway.

Due to time constraints the hypotheses regarding possible inhibitory interactions between BLNK and/or BTK and components of the PLC-independent pathways were not investigated. However, these hypotheses could be investigated, in part, via co-immunoprecipitation studies. In particular, co-immunoprecipitation studies can be performed to determine whether or not BLNK associates with Grb2 and/or any other components of the PLC-independent pathway within this system. While such studies cannot indicate whether or not such an association is inhibitory they would be suggestive; especially if further co-immunoprecipitation studies were to find that that association of a particular component with BLNK correlated with decreased association between that component and others of the PLC-independent pathway. Such an observation would suggest that BLNK may be disrupting the formation of functional PLC-independent signaling complexes which in turn could inhibit BCR-induced PLC-dependent Erk phosphorylation.

(4) When the BCR, Syk and BLNK are co-expressed, BCR-induced PLC-dependent Erk phosphorylation appears to be reconstituted in the AtT20 system. However, when the BCR, Syk, BLNK *and* BTK are co-expressed, BCR-induced PLC-dependent Erk phosphorylation no longer appears to be reconstituted. This finding is quite surprising as loss-of-function studies clearly indicate that BTK has a positive influence on the BCR/PLCγ pathway in a physiological setting (Takata and Kurosaki, 1996; Fluckinger *et al.*, 1998; detailed in Chapter 1.9). This finding may be explained if BTK and BLNK are preferentially associating with each other (as suggested above) to form a non-functional signaling complex. As single proteins, BLNK and BTK may be able to exercise a positive influence on the PLC-dependent Erk pathway. However, as a non-functional complex they may lose this ability. Given this, the question arises as to why BTK and BLNK may be forming a non-functional as opposed to a functional signaling complex within the AtT20 system

Ultimately, co-expression of the BCR, Syk, and BLNK is sufficient to reconstitute BCR-induced PLCγ activity (as assayed by increased PLC-dependent Erk phosphorylation) within the AtT20 system. However, it remains unclear whether or not these components alone are sufficient to achieve maximal reconstitution of the pathway. Indeed, loss-of-function studies clearly suggest that BTK should also be required to achieve such maximal reconstitution. However, as discussed above, BTK expression appears to have a negative rather than a positive affect on the BCR/PLCγ pathway within the AtT20 system. Thus, the BCR/PLCγ pathway is further dissected within the AtT20 system in an effort to determine where the pathway may be aligning with or diverging from the proposed B cell model.

CHAPTER 5

Phosphorylation, Protein Association and Compartmentalization Status of BLNK, BTK and PLCγ in the AtT20 System

5.1 Introduction

Based on loss-of-function studies Syk, BTK and BLNK are all proposed to be necessary to couple the BCR to PLCγ activation. Furthermore, in recent models (detailed in Chapter 1.9 and reviewed in Fig. 5.1) it has been hypothesize that these components should be sufficient to couple the BCR to PLCγ activation. Thus, the initial focus of this thesis was to employ a reconstitution approach to determine if these components are indeed sufficient to couple the BCR to PLCγ activation. Having confirmed sufficiency, subsequent investigations would then be performed to further dissect the molecular mechanisms that govern this process. However, as determined and discussed in Chapter Four, while co-expression of the BCR, Syk, and BLNK is sufficient to reconstitute BCR-induced PLCγ activation within the AtT20 reconstitution system it is unclear whether or not maximal activation is achieved. Moreover, co-expression of the BCR, Syk, BLNK *and* BTK is not sufficient to reconstitute the BCR-induced PLCγ pathway. Hence, subsequent investigations focused on determining why these components may not be sufficient to effectively couple the BCR to PLCγ activation within this system.

Recalling the proposed model (reviewed in Fig. 5.1), numerous events are required to couple the BCR to PLCγ activation. Included in these steps are the phosphorylation of BLNK, Syk, BTK and PLCγ. As well, BTK and PLCγ must associate with BLNK to form a functional BCR/PLCγ signaling complex. And ultimately, these components must be recruited from the cytosol to the plasma membrane. Should one of these steps fail to occur, it is likely that PLCγ activation itself would fail to occur. Thus, the phosphorylation, association and compartmentalization status of these various components were assayed within the AtT20 system.

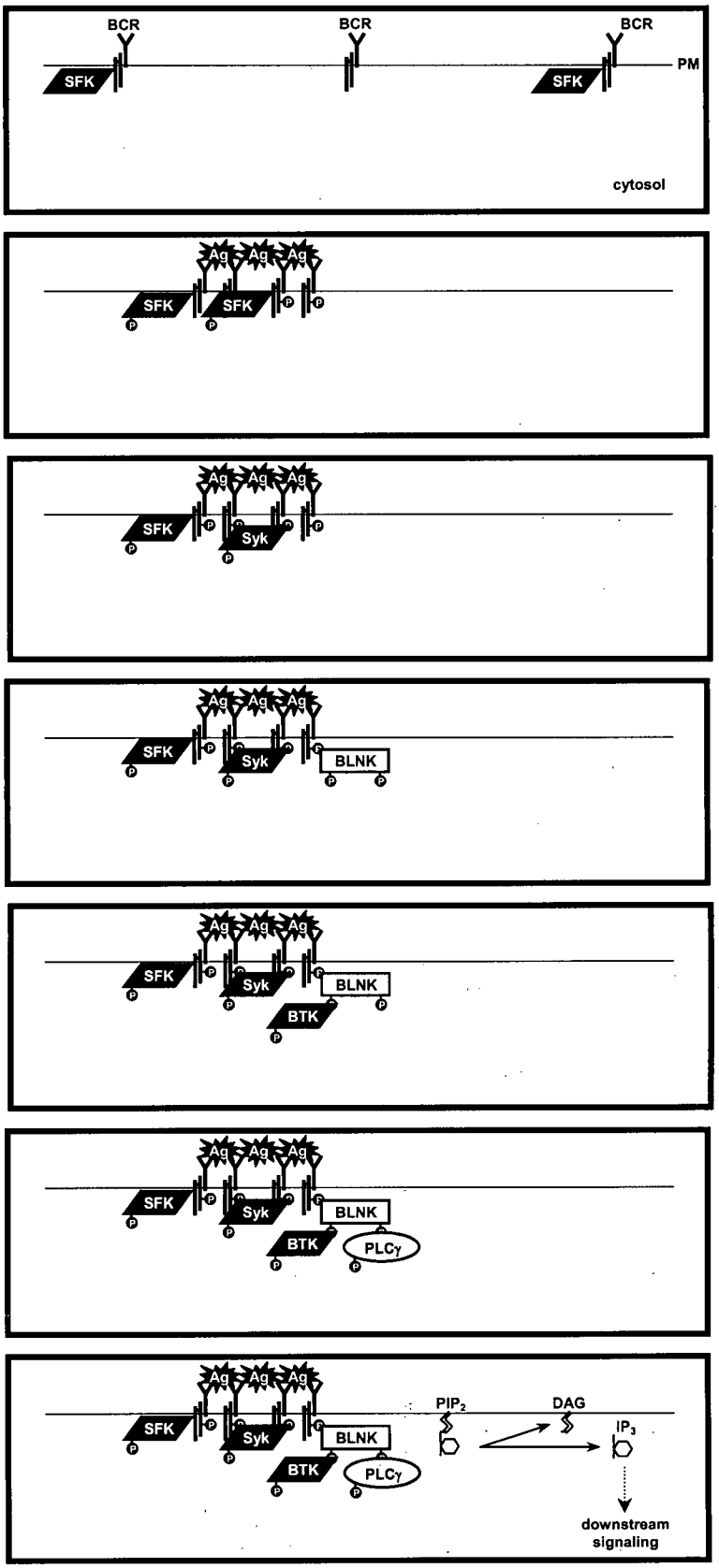

a. In resting B lymphocytes the BCR is distributed throughout the plasma membrane (PM). As well, there are some Src family kinases constitutively associate with the Igα/β heterodimer of the BCR.

b. Following antigen (Ag) engagement the BCRs become cross-linked and aggregated. This enables the SFKs to autophosphorylate and activate each other as well as to phosphorylate the Igα/β heterodimer.

c. Syk is then recruited from the cytosol to the phosphorylated Igα/β heterodimer via its SH2 domain. Subsequently, Syk is phosphorylated and activated by the BCR-associated SFKs.

d. Similarly, BLNK is proposed to be recruited from the cytosol to the phosphorylated Igα/β heterodimer via its SH2 domain. BLNK is then phosphorylated by the BCR-associated Syk. Phosphorylated BLNK is then able to recruit a variety of SH2-containing proteins to itself thereby acting as a scaffolding or adapter protein.

e. BTK is proposed to be recruited from the cytosol to phosphorylated BLNK via its SH2 domain. BTK is then phosphorylated and activated by the BCR-associated and/or the BCR-associated Syk.

f. Additionally, PLCγ is proposed to be recruited from the cytosol to phosphorylated BLNK via its SH2 domain. Such recruitment facilitates PLCγ's association with Syk and BTK such that these kinases can then phosphorylate it.

e. Recruitment of PLCγ to BLNK not only facilitates its phosphorylation, it also facilitates PLCγ's association with its membrane-associated substrate, PIP_3 which it hydrolyzes to the second messengers DAG and IP_3.

Figure 5.1. Review of Proposed Model of BCR-Induced PLCγ Activation.

5.2 Results

5.2.1 Co-Expression of the BCR and BLNK Is Not Sufficient to Reconstitute BCR-Induced PLCγ Phosphorylation in AtT20-Derived Cell Lines

PLCγ activation is dependent, in part, on its phosphorylation (Carter *et al.*, 1991; Coggeshall *et al.*, 1992; Hempel *et al.*, 1992; reviewed in Rhee, 2001). Given this, any inability to reconstitute BCR-induced PLCγ activation may reflect an inability to appropriately phosphorylate PLCγ. Thus, investigations were performed to assay PLCγ's phosphorylation status within this system. Prior studies have indicated that Syk is necessary to mediate PLCγ phosphorylation (Takata *et al., 1994*). Nonetheless, endogenous PTKs, such as Fyn, may be able to compensate for Syk in the AtT20 system. To investigate this possibility PLCγ phosphorylation was initially assayed in the BCR and BCR/BLNK, cell lines. To do this, the cell lines were first stimulated by cross-linking the BCR with anti mIgM antibodies for a set length of time (as indicated in the figures). Cells were then lysed and PLCγ1 was immunoprecipitated from 1000 μg of whole cell lysate using a PLCγ1-specific antibody. The immunoprecipitates were then resolved by SDS-PAGE and the resultant gels were transferred to nitrocellulose filters that were subsequently immunoblotted with a pan-phospho-tyrosine specific antibody (4G10) (Figure 5.2).

As can be seen in Figure 5.2, PLCγ1 does not appear to become phosphorylated following BCR cross-linking in either the BCR or the BCR/BLNK cell lines. This suggests that co-expression of the BCR and BLNK is not sufficient to reconstitute BCR-induced PLCγ phosphorylation in the AtT20 system. Moreover, it suggests that there are not any endogenous PTKs within the system that are able to compensate for Syk and phosphorylate PLCγ1. (Fig. 5.2). These findings are not unexpected as Syk has repeatedly been demonstrated to be necessary to BCR-induced PLCγ phosphorylation and activation (Takata *et al.*, 1994). Thus, studies progressed to investigate whether or not co-expression of the BCR and Syk is sufficient to reconstitute BCR-induced PLCγ phosphorylation.

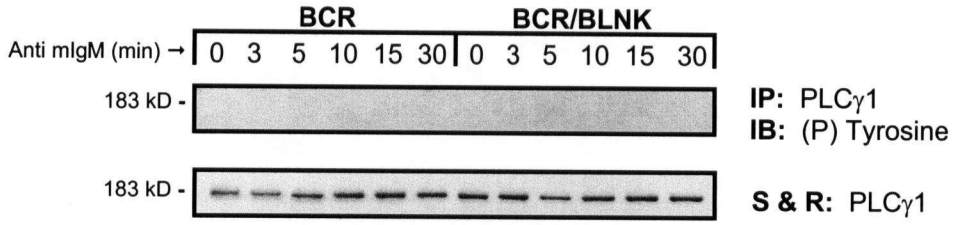

Figure 5.2. Co-Expression of the BCR and BLNK Is Not Sufficient to Reconstitute BCR-Induced PLCγ1 Phosphorylation in AtT20-Derived Cell Lines. The BCR was cross-linked with anti mIgM antibodies at 37 °C for the indicated length of time. Cells were then lysed and PLCγ1 was immunoprecipitated from 1000 μg of whole cell lysate using Protein A-sepharose and a PLCγ1 specific antibody. Immunoprecipitates were resolved by SDS-PAGE. Following electrophoresis, gels were transferred to nitrocellulose filters that were subsequently immunoblotted with a pan-phospho-tyrosine specific antibody (4G10 monoclonal antibody). Finally, filters were stripped and reprobed with a PLCγ1 specific antibody. IP indicates the immunoprecipitating antibody, IB indicates the immunoblotting antibody and S&R indicates the antibody that was used to reprobe the filter. Data are representative of three independent experiments. Note that these experiments were performed concurrently with those shown in Figures 5.3 and 5.4. Thus, the experiments shown in Figure 5.3 and 5.4 serve as positive controls that demonstrate that PLCγ phosphorylation is indeed detectable in the reconstitution system

5.2.2 Co-expression of the BCR with Syk and/or BTK is Sufficient to At Least Partially Reconstitute BCR-Induced PLCγ Phosphorylation in AtT20-Derived Cell Lines

As stated above, previous studies have indicated that Syk is necessary to mediate PLCγ phosphorylation (Takata *et al.*, 1994). Additional studies have also suggested that BTK is required to achieve maximal BCR-induced PLCγ phosphorylàtion and activation (Takata and Kurosaki, 1996). Thus, the ability of Syk and/or BTK to reconstitute BCR-induced PLCγ phosphorylation was investigated within this system. To do this, the BCR, BCR/Syk, BCR/BTK and BCR/Syk/BTK cell lines were stimulated by cross-linking the BCR with anti mIgM antibodies for a set length of time (as indicated in the figures). Cells were then lysed and PLCγ1 was immunoprecipitated from 1000 μg of whole cell lysate using a PLCγ1-specific antibody. The immunoprecipitates were then resolved by SDS-PAGE, and the resultant gels were transferred to nitrocellulose filters that were subsequently immunoblotted with a pan-phospho-tyrosine specific antibody (4G10) (Figure 5.3).

As can be seen in Figure 5.3, there appears to be an increase in phosphorylated PLCγ1 following BCR cross-linking in the BCR/BTK, BCR/Syk and BCR/Syk/BTK cell lines. However, this increase is barely detectable in the BCR/BTK cell line (Fig. 5.3c) and appears minimal in the BCR/Syk and BCR/Syk/BTK cell lines (Fig. 5.3b and d). Interestingly, while both Syk and BTK appear independently sufficient to reconstitute BCR-induced PLCγ phosphorylation they do not appear to act synergistically to enhance PLCγ phosphorylation within this system (Fig. 5.3b and c compared to Fig. 5.3d). There are several possible explanations for this observation. First, Syk may phosphorylate the same PLCγ sites as BTK such that a synergistic effect is not apparent. Alternatively, phosphorylation of PLCγ by one kinase may preclude further phosphorylation by the other kinase. However, neither of these explanations seem likely given that loss-of-function studies clearly suggest that Syk and BTK function co-operatively to phosphorylate PLCγ (Takata *et al.*, 1994; Takata and Kurosaki, 1996). Else wise, Syk and BTK may well be acting synergistically to enhance BCR-induced PLCγ phosphorylation but this may not be readily observable within this system due to the fact that BTK-dependent phosphorylation itself is barely detectable (Fig. 5.3c).

The above findings suggest that both Syk and BTK may be independently sufficient to reconstitute BCR-induced PLCγ1 phosphorylation within this system. However, it remains to be determined if such a minute increase in phosphorylation is sufficient to be physiologically relevant. This would seem unlikely given that BCR-induced PLCγ phosphorylation is typically very robust in B cell lines (Carter *et al.*, 1991; Coggeshall *et al.*, 1992; Hempel *et al.*, 1992; Roifman and Wang, 1992; DeBell *et al.*, 1999). Furthermore, this appears unlikely as the observed reconstitution of PLCγ1 phosphorylation within the BCR/Syk, BCR/BTK and BCR/Syk/BTK cell lines does not appear to correlate with reconstitution of BCR-induced PLCγ-dependent Erk phosphorylation within said cell lines (refer to chapter 4).

The above findings are not surprising given the proposed model of BCR-induced PLCγ activation. In fact, BLNK is expected to be necessary to facilitate robust BCR-induced PLCγ phosphorylation. Thus, further studies were performed to determine if co-expression of BLNK could assist in further reconstituting BCR-induced PLCγ phosphorylation within the AtT20 system.

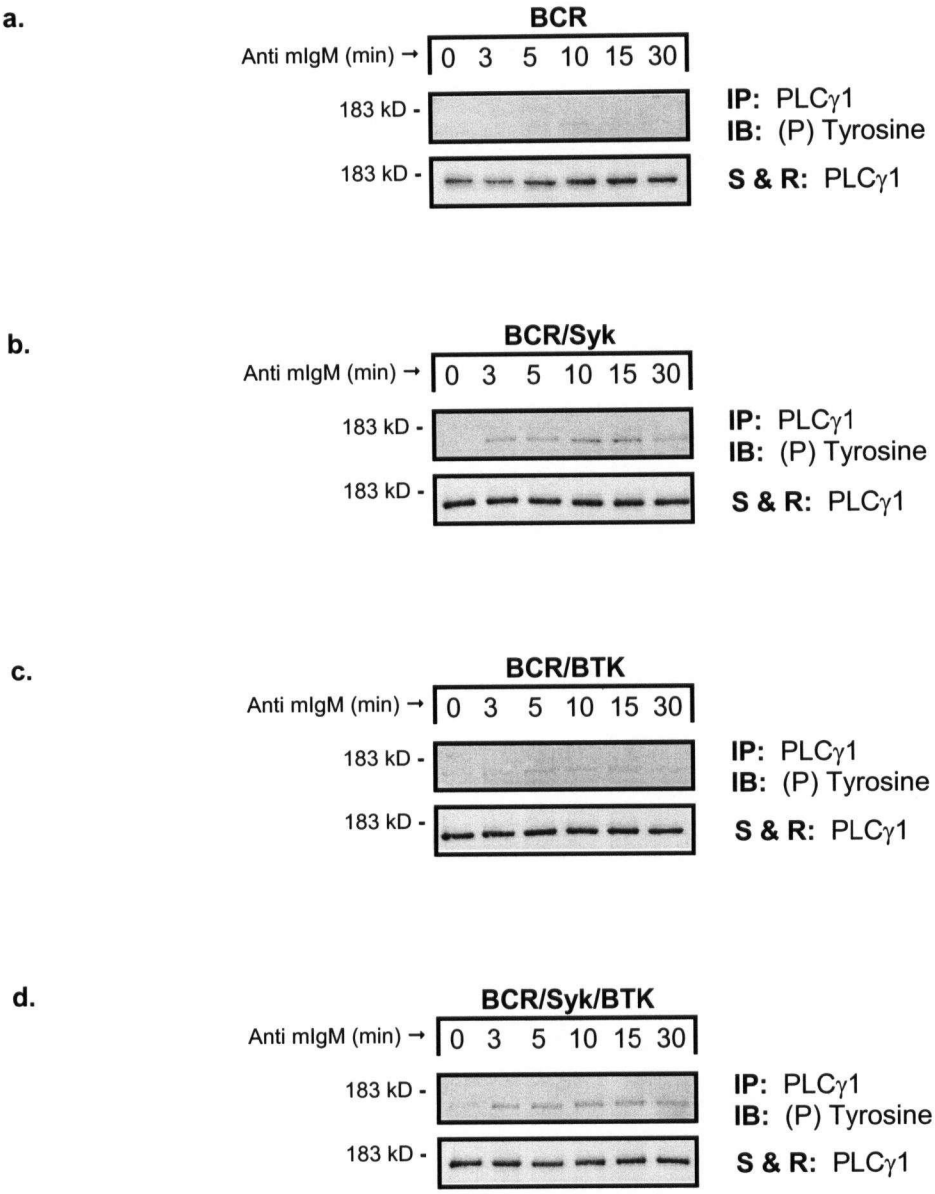

Figure 5.3. Co-Expression of the BCR, along with Syk or BTK, Is Sufficient to Reconstitute BCR-Induced PLCγ1 Phosphorylation in AtT20-Derived Cell Lines. The BCR was cross-linked with anti mIgM antibodies at 37 °C for the indicated length of time. Cells were then lysed and PLCγ1 was immunoprecipitated from 1000 μg of whole cell lysate using Protein A-Sepharose and a PLCγ1 specific antibody. Immunoprecipitates were resolved by SDS-PAGE. Following electrophoresis, gels were transferred to nitrocellulose filters that were subsequently immunoblotted with a pan-phospho-tyrosine specific antibody (4G10 monoclonal antibody). Finally, filters were stripped and reprobed with a PLCγ1 specific antibody. IP indicates the immunoprecipitating antibody, IB indicates the immunoblotting antibody and S&R indicates the antibody that was used to reprobe the filter. Data are representative of three independent experiments.

5.2.3 Co-expression of the BCR and BLNK with Syk and/or BTK Does Not Significantly Enhance BCR-Induced PLCγ Phosphorylation

The BCR/BTK/BLNK, BCR/Syk/BLNK and BCR/Syk/BLNK/BTK cell lines were used to determine if co-expression of BLNK could further assist in reconstituting BCR-induced PLCγ phosphorylation. These cell lines were stimulated by cross-linking the BCR with anti mIgM antibodies for a set length of time (as indicated in the figures). Cells were then lysed and PLCγ1 was immunoprecipitated from 1000 μg of whole cell lysate using a PLCγ1-specific antibody. The immunoprecipitates were then resolved by SDS-PAGE with the resolved gels being transferred to nitrocellulose filters that were subsequently immunoblotted with a pan-phospho-tyrosine specific antibody (4G10) (Figure 5.4).

Comparing the BCR/BTK cell line to the BCR/BTK/BLNK cell line, co-expression of BLNK does not appear to enhance BCR-induced PLCγ1 phosphorylation (Fig. 5.4a). Similarly, comparing the BCR/Syk cell line to the BCR/Syk/BLNK cell line, co-expression of BLNK does not appear to enhance BCR-induced PLCγ1 phosphorylation (Fig. 5.4b). In contrast, comparing the BCR/Syk/BTK cell line to the BCR/Syk/BTK/BLNK cell line, co-expression of BLNK appears to slightly enhance BCR-induced PLCγ1 phosphorylation (Fig. 5.4c). However, this enhanced PLCγ1 phosphorylation still pales in comparison to what is typically observed following BCR cross-linking in B cell lines (Carter *et al.*, 1991; Coggeshall *et al.*, 1992; Hempel *et al.*, 1992; Roifman and Wang, 1992; DeBell *et al.*, 1999) and thus, again calls into question whether or not such as small increase is physiologically relevant.

Recalling Chapter 4, PLCγ activation is reconstituted in the BCR/Syk/BLNK cell line. Thus, a very small amount of PLCγ phosphorylation does appear to be sufficient to reconstitute PLCγ activation, at least in this cell line. This finding is surprising as it was hypothesized that a much more robust level of PLCγ phosphorylation would be required to reconstitute measurable PLCγ activation based on the observation that PLCγ phosphorylation is very robust in activated B cells (Carter *et al.*, 1991; Coggeshall *et al.*, 1992; Hempel *et al.*, 1992; Roifman and Wang, 1992; DeBell *et al.*, 1999). While this finding may suggest that the downstream Erk pathway is sensitive to very subtle changes in PLCγ activation the question arises as to whether or not maximal PLCγ phosphorylation and activation is being achieved in this system, and if not, why.

Interestingly, while a minimal amount of PLCγ phosphorylation appears sufficient to reconstitute PLCγ activity in the BCR/Syk/BLNK cell line a comparable or even slightly greater amount of PLCγ phosphorylation does not appear sufficient to reconstitute PLCγ activation in the BCR/Syk/BLNK/BTK cell line. This suggests that PLCγ activation may not be predicated solely on its phosphorylation status. Indeed, additional factors such as specific protein associations and specific localization within the cell (i.e., compartmentalization) may also influence PLCγ activity. Thus these factors, as they relate to the BCR, Syk, BLNK, BTK and PLCγ were further investigated within the AtT20 system (refer to Chapter 5.2.8 and 5.2.9)

a.

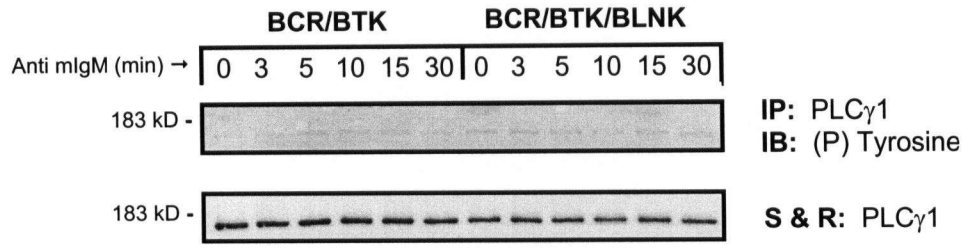

b.

c.

Figure 5.4. Co-Expression of the BCR and Syk Is Sufficient to Reconstitute BCR-Induced PLCγ1 Phosphorylation in AtT20-Derived Cell Lines. The BCR was cross-linked with anti mIgM antibodies at 37 °C for the indicated length of time. Cells were then lysed and PLCγ1 was immunoprecipitated from 1000 μg of whole cell lysate using Protein A-sepharose and a PLCγ1 specific antibody. Immunoprecipitates were resolved by SDS-PAGE. Following electrophoresis, gels were transferred to nitrocellulose filters that were subsequently immunoblotted with a pan-phospho-tyrosine specific antibody (4G10 monoclonal antibody). Finally, filters were stripped and reprobed with a PLCγ1 specific antibody. IP indicates the immunoprecipitating antibody, IB indicates the immunoblotting antibody and S&R indicates the antibody that was used to reprobe the filter. Data are representative of three independent experiments.

5.2.4 BTK Is Constitutively Phosphorylated in AtT20-Derived Cell Lines

As observed in the previous section, BCR-induced PLCγ phosphorylation and/or activation may not be maximally reconstituted within the AtT20 system. Considering the proposed model, attempts to reconstitute this pathway could be limited if any of Syk, BTK or BLNK were to be inappropriately phosphorylated. Thus, the phosphorylation status of these proteins was investigated.

Previous studies have indicated that co-expression of the BCR and Syk is sufficient to reconstitute BCR-induced Syk phosphorylation and activation with the AtT20 system (Richards *et al.*, 1996) and therefore, studies investigating Syk phosphorylation status have been done previously and were not further pursued here. In contrast, BTK's phosphorylation status was assayed in the BCR/BTK, BCR/BTK/BLNK, BCR/Syk/BTK and BCR/Syk/BLNK/BTK cell lines. To do this, the cell lines were stimulated by cross-linking the BCR with anti mIgM antibodies for a set length of time (as indicated in the figures). Cells were then lysed and BTK was immunoprecipitated from 1000 μg of whole cell lysate using a BTK-specific antibody. The immunoprecipitates were then resolved by SDS-PAGE and the gels were transferred to nitrocellulose filters that were subsequently immunoblotted with a phospho-BTK (Tyr223) specific antibody (Figure 5.5). It should be noted that BTK becomes sequentially phosphorylated on tyrosine residues 551 and 223, and that phosphorylation of this latter residue is generally considered to be indicative of active BTK (Rawlings *et al.*, 1996; Park *et al.*, 1996).

As can be seen in Figure 5.5, BTK appears to be constitutively phosphorylated on tyrosine 223 in the BCR/BTK, BCR/BLNK/BTK, BCR/Syk/BTK and BCR/Syk/BLNK/BTK cell lines. Furthermore, BTK's phosphorylation does not appear to increase following BCR cross-linking (Fig. 5.5). The finding that co-expression of the BCR and BTK is sufficient to reconstitute BTK phosphorylation is not unexpected as BTK phosphorylation has been shown to be mediated by Src family members (Afar *et al.*, 1996; Rawlings *et al.*, 1996; detailed in Chapter 1.9.2) and as the AtT20 system endogenously expresses the Src family member, Fyn (Richards *et al.*, 1996). However, the observation that BTK phosphorylation is constitutive as opposed to inducible is somewhat surprising. While it is not unusual to observe constitutive activation in over-expression systems (Kurosaki *et al.*, 1994; Rawlings *et al.*, 1996) one of the advantages of the AtT20 system is that, to date, it has proven to be a system where over-expression does not

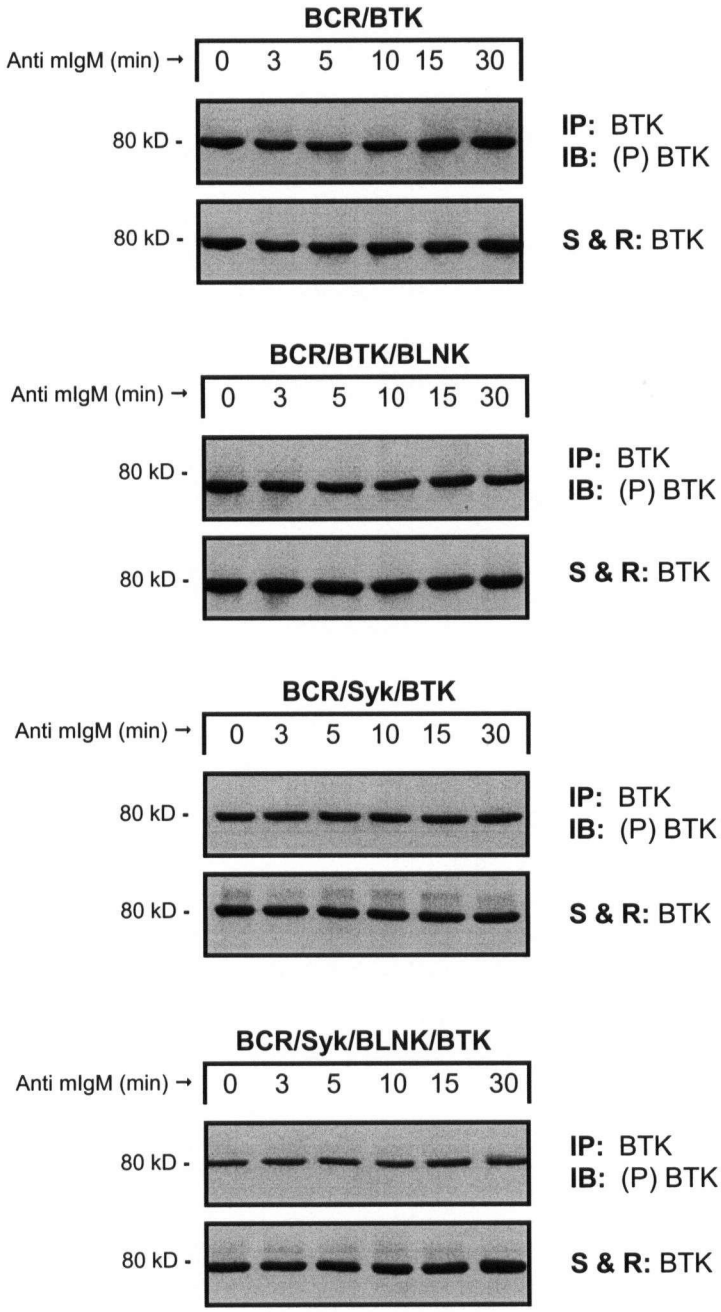

Figure 5.5. Co-Expression of the BCR and BTK is Sufficient to Reconstitute BCR-Induced BTK Phosphorylation in AtT20-Derived Cell Lines. The BCR was cross-linked with anti mIgM antibodies at 37 °C for the indicated length of time. Cells were then lysed and BTK was immunoprecipitated from 1000 μg of whole cell lysate using Protein G-Sepharose and a BTK specific antibody. Immunoprecipitates were resolved by SDS-PAGE. Following electrophoresis, gels were transferred to nitrocellulose filters that were subsequently immunoblotted with a phospho-BTK (Tyr223) specific antibody. Finally, filters were stripped and reprobed with a BTK specific antibody. IP indicates the immunoprecipitating antibody, IB indicates the immunoblotting antibody and S&R indicates the antibody that was used to reprobe the filter. Data are representative of three independent experiments.

necessitate activation and thus it lends itself well to studies that are concerned with investigating inducible pathways (Richards *et al.*, 1996).

Several controls were performed to confirm that the observed BTK phosphorylation was not merely a methodological artifact. First, it was confirmed that the phospho-BTK (Tyr223) specific antibody can indeed distinguish between phosphorylated BTK and non-phosphorylated BTK. To do this the Daudi and Ramos human B cell lines were used as controls. These cell lines, along with the BCR/BLNK/BTK and BCR/Syk/BLNK/BTK cell lines, were left either non-stimulated or were stimulated for 10 minutes by cross-linking the BCR with an anti mIgM specific antibody. Cells were then lysed and 50 μg of whole cell lysate were resolved by SDS-PAGE. The resolved gels were then transferred to nitrocellulose filters that were subsequently immunoblotted with a phospho-BTK (Tyr223) specific antibody (Figure 5.6a).

The Daudi and Ramos B cell lines were used as controls as it has previously been established that there are small amounts of phosphorylated BTK in resting/non-stimulated B cells and that this amount dramatically increases following BCR engagement (Mahajan *et al.*, 1995; Rawlings *et al.*, 1996; Afar *et al.*, 1996; Kurosaki *et al.*, 1997; Baba *et al.*, 2001). Thus, if the phospho-BTK (Tyr223) specific antibody is specific for phosphorylated BTK a small amount of phosphorylated BTK should be observed in the non-stimulated cells while a much greater amount should be observed in stimulated cells. In contrast, if the phospho-BTK (Tyr223) specific antibody is unable to distinguish between phosphorylated and non-phosphorylated BTK the similar amounts of supposedly phosphorylated BTK should be observe in the non-stimulated and stimulated cells as the antibody will likely be detecting the entire pool of BTK (a pool that is not anticipated to change in response to stimulation). As can be seen in Figure 5.6a, a small amount of phosphorylated BTK is observed in the non-stimulated B cell lines and this amount dramatically increases following stimulation. In contrast, there appears to be a relatively large and consistent amount of phosphorylated BTK in both the non-stimulated and stimulated AtT20-derived cell lines. The former observation suggests that the phospho-BTK (Tyr223) specific antibody can indeed distinguish between phosphorylated BTK and non-phosphorylated BTK while the latter observation, coupled with the former, suggests that BTK is indeed constitutively phosphorylated in the AtT20-derived cell lines.

While the above findings are suggestive it is still possible that the phospho-BTK (Tyr223) specific antibody is non-specifically cross-reacting with a protein within the AtT20 system such that it is creating a background band that could be misinterpreted as being representative of phosphorylated BTK. This possibility was addressed using the BCR/Syk/BLNK cell line as a negative control (5.6b). Similar to before, the BCR/Syk/BLNK and the BCR/Syk/BLNK/BTK cell lines were first stimulated by cross-linking the BCR with anti mIgM antibodies for a set length of time (as indicated in the figures). Cells were then lysed and BTK was immunoprecipitated from 1000 μg of whole cell lysate using a BTK-specific antibody. The immunoprecipitates were then resolved by SDS-PAGE and the resolved gels were transferred to nitrocellulose filters that were subsequently immunoblotted with a phospho-BTK (Tyr223) specific antibody (Figure 5.6b). If the phospho-BTK (Tyr223) specific antibody is non-specifically cross-reacting with a protein within the AtT20 system it is expected that the subsequent background band will coincide with the supposed phospho-BTK band and be apparent in both the BCR/Syk/BLNK cell line and the BCR/Syk/BLNK/BTK cell lines. As can be seen in Figure 5.6b, there are not any background bands coinciding with the phospho-BTK band in the BCR/Syk/BLNK cell line as compared to the BCR/Syk/BLNK/BTK cell line. Thus, when considered with the above findings, it appears that the phospho-BTK (Tyr223) specific antibody is indeed specific for phospho-BTK and that BTK is indeed constitutively phosphorylated within the AtT20 system. Having determined that BTK is constitutively phosphorylated within the AtT20 system, the mechanism of this phosphorylation was briefly investigated. In particular, studies were performed to determine if BTK phosphorylation was attributable to Fyn activity.

a.

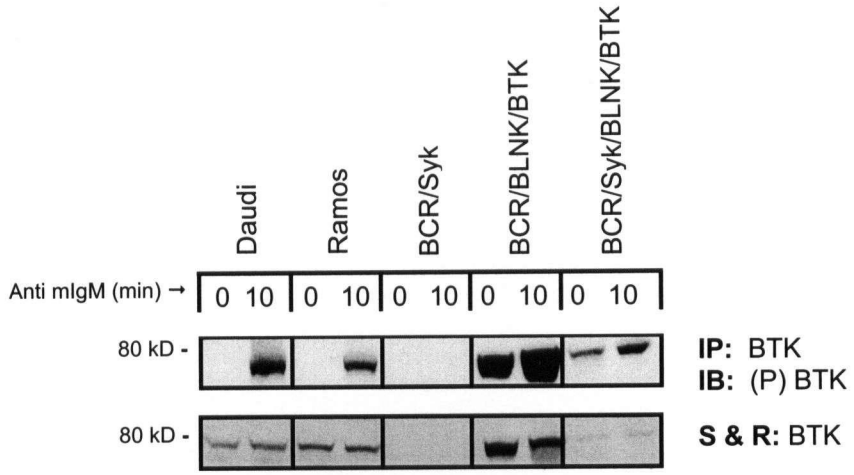

b.

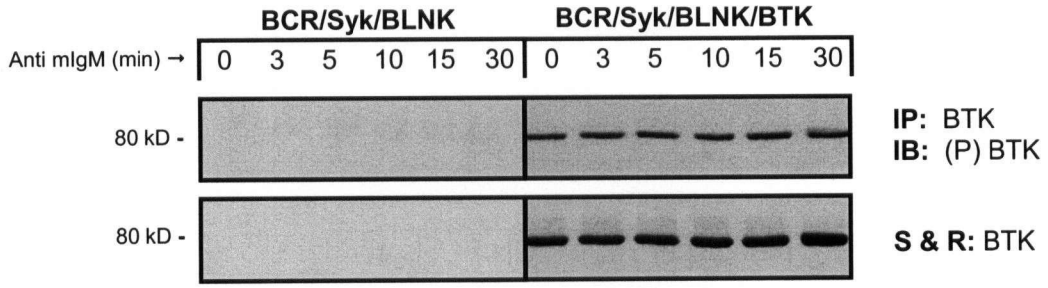

Figure 5.6. The phospho-BTK (Tyr223) specific antibody is specific for phosphorylated BTK. (a) The phospho-BTK (Tyr223) specific antibody does not appear to detect non-phosphorylated BTK. The BCR was cross-linked with anti mIgM antibodies at 37 °C for 10 minutes. Cells were then lysed and 50 μg of whole cell lysate were resolved by SDS-PAGE. Following electrophoresis, gels were transferred to nitrocellulose filters that were subsequently immunoblotted with a phospho-BTK (Tyr223) specific antibody. Finally, filters were stripped and reprobed with a BTK specific antibody. IB indicates the immunoblotting antibody and S&R indicates the antibody that was used to reprobe the filter. The Daudi and Ramos cell lines are human B cell lines that should be observed to express low levels of phosphorylated BTK when not stimulated and high levels of phosphorylated BTK when stimulated. **(b)** The phospho-BTK (Tyr223) specific antibody does not appear to cross-react with any other proteins in the AtT20 system). The BCR was cross-linked with anti mIgM antibodies at 37 °C for the indicated length of time. Cells were then lysed and BTK was immunoprecipitated from 1000 μg of whole cell lysate using Protein G-Sepharose and a BTK specific antibody. Immunoprecipitates were resolved by SDS-PAGE. Following electrophoresis, gels were transferred to nitrocellulose filters that were subsequently immunoblotted with a phospho-BTK (Tyr223) specific antibody. Finally, filters were stripped and reprobed with a BTK specific antibody. IP indicates the immunoprecipitating antibody, IB indicates the immunoblotting antibody and S&R indicates the antibody that was used to reprobe the filter. Data are representative of three independent experiments. The BCR/Syk/BLNK cell line serves as a negative control for the phospho-BTK (Tyr223) specific antibody as it is an AtT20-derived cell line that does not express BTK.

5.2.5 BTK Phosphorylation Is At Least Partially Dependent on Fyn Activity in AtT20-Derived Cell Lines

Previous studies have indicated that the Src kinases are responsible for trans-phosphorylating BTK in B cells (Afar *et al., 1996;* Rawlings *et al.*, 1996). Once so phosphorylated BTK then auto-phosphorylates such that it is believed to have maximal kinase activity (Rawlings *et al.*, 1996; Kurosaki *et al.*, 1997; Wahl *et al.*, 1997). Thus, investigations were performed to determine if the endogenous Fyn (a Src family member) was mediating the observed constitutive phosphorylation of BTK within the AtT20 system. To do this the BCR/BTK, BCR/BTK/BLNK, BCR/Syk/BTK and BCR/Syk/BLNK/BTK cell lines were treated overnight with PP2, a Src family kinase inhibitor (added to a final concentration of 5 μM). The following morning, the cell lines were stimulated by cross-linking the BCR with anti mIgM antibodies for 10 minutes. Cells were then lysed and 50 μg of whole cell lysate were resolved by SDS-PAGE. The gels were transferred to nitrocellulose filters that were subsequently immunoblotted with a phospho-BTK (Tyr223) specific antibody (Fig. 5.7). As can be seen in Figure 5.7, treatment with PP2 appears to decrease the amount of phosphorylated BTK observed in both the non-stimulated and stimulated AtT20-derived cell lines. However, PP2 treatment does not appear to completely inhibit BTK phosphorylation in these cell lines (Fig. 5.7). This may suggest either that PP2 treatment is not sufficient to completely inhibit Fyn activity or that an unidentified PTK is contributing to BTK phosphorylation within this system. However, this second explanation is unlikely given that no other Src family kinase members appear to be expressed within the AtT20-derived system (Richards *et al.*, 1996).

It should be noted that the results for the BCR/Syk/BTK and BCR/Syk/BLNK/BTK cell lines are somewhat unusual as compared to the two cell lines that do not express Syk (Fig. 5.7). Specifically, multiple bands are apparent above the band that is taken to represent phosphorylated BTK (Fig. 5.7). These bands could be background bands that become evident only in the presence of Syk. However, if these bands are attributable to Syk it might be expected that these bands would appear more prevalent in the BCR/Syk/BLNK/BTK cell line as compared to the BCR/Syk/BTK cell line as the former appears to express more Syk than the latter (Fig. 4.2). Yet, the opposite observation is apparent in that the background bands appear more prevalent in the BCR/Syk/BTK cell line as compared to the BCR/Syk/BLNK/BTK cell line (Fig. 5.7). Arguably, the presence of BLNK could somehow be counteracting the effect of Syk

on these proposed background bands. Alternatively, these bands may represent differentially phosphorylated BTK and may only exist within the Syk expressing cell lines due to the differential phosphorylation being mediated by Syk. This explanation could help to account for the difference in intensity of the bands between the two cell lines as the BCR/Syk/BTK/BLNK cell line expresses considerably less BTK than the BCR/Syk/BTK cell line (Fig. 4.2). This theory could be better supported by using cell lines that show similar expression levels of both Syk and BTK. Unfortunately, it was not reasonably possible to obtain a selection of clones that expressed similar levels these proteins and thus, such a comparison can not be made. The proposal that Syk may be contributing BTK phosphorylation is not novel. In fact, Kurosaki and his colleagues have recently shown that Syk may contribute to BTK phosphorylation (Kurosaki and Kurosaki, 1997; Baba *et al.*, 2001)

Thus, the above findings hint at a mechanism for constitutive BTK phosphorylation within the AtT20 system. In particular, it appears that Fyn is at least partially responsible for mediating constitutive BTK phosphorylation. Furthermore, Syk may be able to contribute to BTK phosphorylation. Ideally, further studies could be performed within this system to further define the mechanisms involved in phosphorylating BTK including performing studies with a Syk inhibitor. However, central to this thesis is the ability to reconstitute BTK phosphorylation as a step towards reconstituting BCR-induced PLCγ activation. As this appears to have been achieved, the focus of the study returned to more direct investigations of BCR-induced PLCγ activation including investigating BLNK's phosphorylation status.

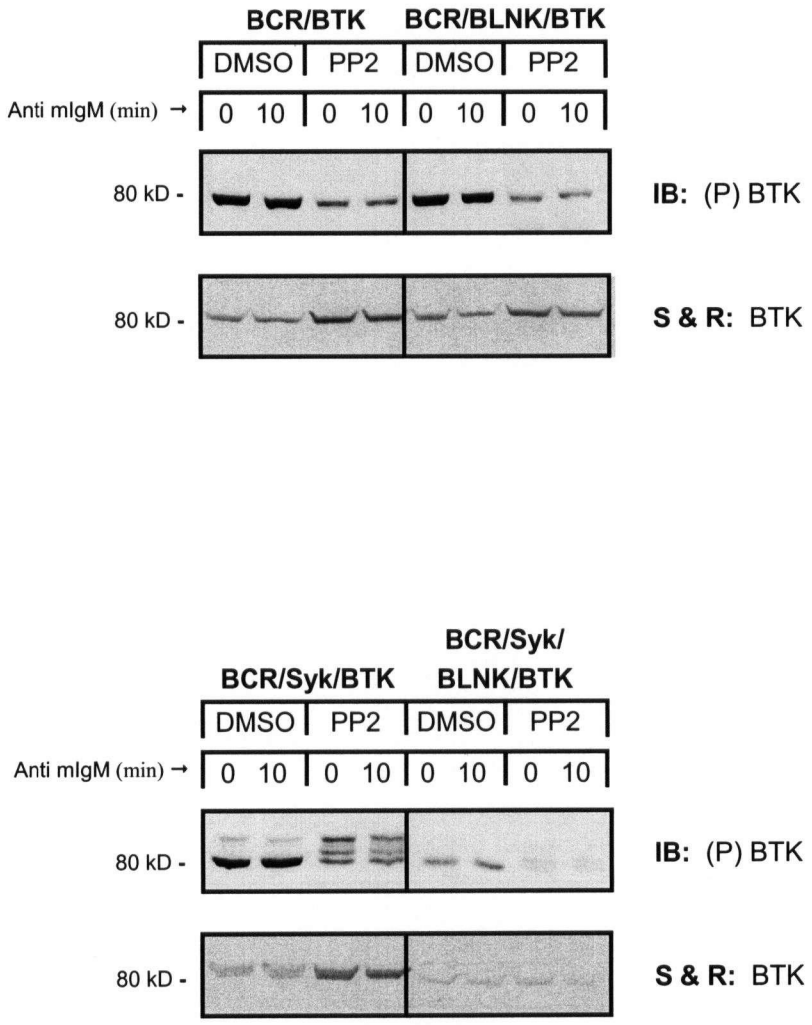

Figure 5.7. Constitutive Phosphorylation of BTK is, At Least, Partly Dependent on Fyn Activity in AtT20-Derived Cell Lines. Cells were treated overnight with either DMSO (negative control) or the Src Family Kinase inhibitor, PP2 (at a final concentration of 5 μM). The BCR was then cross-linked with anti mIgM antibodies at 37 °C for the indicated length of time. Cells were then lysed and 50 μg of whole cell lysate were resolved by SDS-PAGE. Following electrophoresis, gels were transferred to nitrocellulose filters that were subsequently immunoblotted with a phospho-BTK (Tyr223) specific antibody. Finally, filters were stripped and reprobed with a BTK specific antibody. IB indicates the immunoblotting antibody while S&R indicates the antibody used to reprobe the filter. Data are representative of at least three similar independent experiments.

5.2.6 Co-Expression of the BCR, BLNK and BTK Is Not Sufficient to Reconstitute BCR-Induced BLNK Phosphorylation in AtT20-Derived Cell Lines

Previous studies have clearly shown that BTK and PLCγ associate with phosphorylated BLNK via their SH2 domains (Hashimoto *et* al., 1999; Su *et al.*, 1999; and Ishiai *et al.*, 1999; respectively). Thus, if BLNK is to function as an adapter protein within this system it must become appropriately phosphorylated. Failure to do so could contribute to the apparent inability to reconstitute robust BCR-induced PLCγ phosphorylation (refer to Chapter 5.2.1-5.2.3) and PLCγ activation within this system (refer to chapter 4). Given this, studies were performed to investigate whether or not BCR-induced BLNK phosphorylation was reconstituted within the AtT20-derived system.

Prior studies have indicated that Syk is necessary to mediate BCR-induced BLNK phosphorylation (Fu *et al.*, 1998). Nonetheless, endogenous PTKs, such as Fyn, may be able to mediate BCR-induced BLNK phosphorylation in the AtT20-derived system. Alternatively, exogenous BTK may be able to mediate BCR-induced BLNK phosphorylation in this system. To investigate these possibilities BLNK phosphorylation was initially assayed in the BCR/BLNK and BCR/BLNK/BTK cell lines. To do this, the cell lines were first stimulated by cross-linking the BCR with anti mIgM antibodies for a set length of time (as indicated in the figures). Cells were then lysed and myc-tagged BLNK was immunoprecipitated from 1000 μg of whole cell lysate using a myc specific antibody (9E10). The immunoprecipitates were then resolved by SDS-PAGE and the resultant gels were transferred to nitrocellulose filters that were subsequently immunoblotted with a pan-phospho-tyrosine specific antibody (4G10) (Fig. 5.8) before being stripped and reprobed with a BLNK specific antibody (AC). Alternatively, 50 μg of whole cell lysate were resolved by SDS-PAGE. The resolved gels were then transferred to nitrocellulose filters that were subsequently immunoblotted with a phospho-BLNK (Tyr96) specific antibody (Fig. 5.9).

Based on these experiments, BCR engagement does not appear sufficient to induce BLNK phosphorylation in either the BCR/BLNK cell line (Fig. 5.8) or the BCR/BLNK/BTK cell line (Fig. 5.9). The former result suggests that there are not any endogenous PTKs sufficient to reconstitute BCR-induced BLNK phosphorylation within the AtT20-derived system. Similarly,

the latter result suggests that BTK alone is not sufficient to reconstitute BCR-induced BLNK phosphorylation within the AtT20-derived system. Given that the aforementioned model of BCR-induced PLCγ activation envisions BLNK being phosphorylated in a Syk-dependent manner, the above findings are as expected. Thus, studies progressed to investigate whether or not co-expression of the BCR, BLNK and Syk was sufficient to reconstitute BCR-induced BLNK phosphorylation.

a.

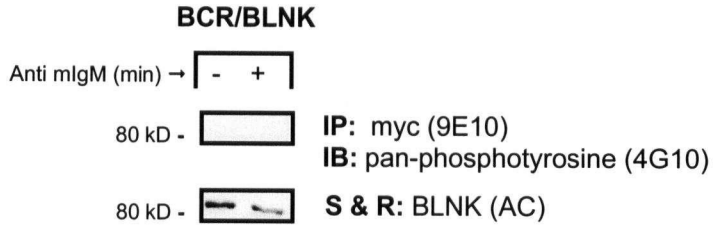

b.

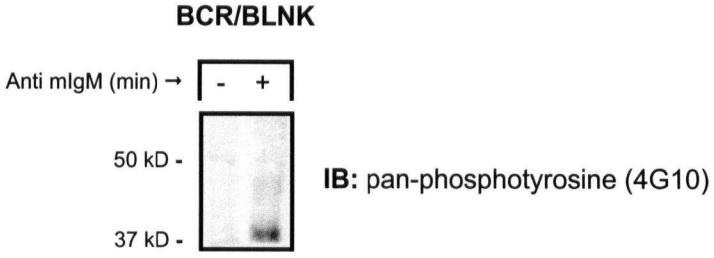

Figure 5.8. Co-Expression of the BCR and BLNK is Not Sufficient to Reconstitute BCR-Induced BLNK Phosphorylation in AtT20-Derived Cell Lines. In Contrast, Co-Expression of the BCR, Syk and BLNK is Sufficient to Reconstitute BCR-Induced BLNK Phosphorylation in AtT20-Derived Cell Lines. (a) The BCR was not cross-linked in the non-stimulated samples (-) and was cross-linked with anti mIgM antibodies at 37 °C for the 5 minutes in the stimulated samples (+). Cells were then lysed and myc-tagged human BLNK was immunoprecipitated from 1000 μg of whole cell lysate using a myc specific antibody (9E10). Immunoprecipitates were resolved by SDS-PAGE. The gels were then transferred to nitrocellulose filters that were subsequently immunoblotted with a pan-phospho-tyrosine specific antibody (4G10). Finally, filters were stripped and reprobed with a BLNK specific antibody (AC). IP indicates the immunoprecipitating antibody, IB indicates the immunoblotting antibody while S&R indicates the antibody that was used to reprobe the filter. Data are representative of three independent experiments. Similar results were obtained with multiple clones expressing the same combination of proteins. **(b)** Control blot demonstrating that cross-linking of the BCR was successful. Ten micrograms of whole cell lysate from the above samples were resolved by SDS-PAGE. The resolved gels were then transferred to nitrocellulose filters that were subsequently immunoblotted with a pan-phospho-tyrosine specific antibody (4G10). Following BCR cross-linking an increase in total tyrosine phosphorylation is evident indicating that BCR cross-linking was successful.

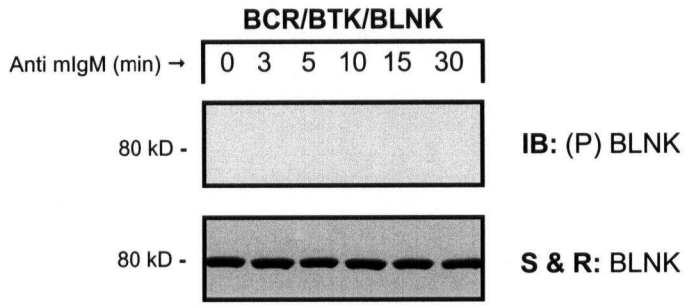

Figure 5.9. Co-Expression of the BCR, BTK and BLNK is Not Sufficient to Reconstitute BCR-Induced BLNK Phosphorylation in AtT20-Derived Cell Lines. The BCR was cross-linked with anti mIgM antibodies at 37 °C for the indicated length of time. Cells were then lysed and 50 μg of whole cell lysate were resolved by SDS-PAGE. Following electrophoresis, gels were transferred to nitrocellulose filters that were subsequently immunoblotted with a phospho-BLNK (Tyr96) specific antibody. Finally, filters were stripped and reprobed with a BLNK specific antibody. IB indicates the immunoblotting antibody while S&R indicates the antibody that was used to reprobe the filter. Data are representative of three independent experiments.

5.2.7 Co-Expression of the BCR, Syk and BLNK is Sufficient to Reconstitute BCR-Induced BLNK Phosphorylation in AtT20-Derived Cell Lines

As observed in the previous section, BCR-induced PLCγ phosphorylation and/or activation may not be maximally reconstituted within the AtT20 system. Considering the proposed model, attempts to reconstitute this pathway could be limited if any of Syk, BTK or BLNK were to be inappropriately phosphorylated. Thus, the phosphorylation status of these proteins was investigated.

To determine if co-expression of the BCR, Syk and BLNK is sufficient to reconstitute BCR-induced BLNK phosphorylation the BCR/Syk/BLNK and BCR/Syk/BLNK/BTK cell lines were first stimulated by cross-linking the BCR with anti mIgM antibodies for a set length of time (as indicated in the figures). Cells were then lysed and 50 μg of whole cell lysate were resolved by SDS-PAGE. The resolved gels were then transferred to nitrocellulose filters that were subsequently immunoblotted with a phospho-BLNK (Tyr96) specific antibody (Fig. 5.10a and 5.11). Alternatively, BLNK was immunoprecipitated from 1000 μg of whole cell lysate using a BLNK-specific antibody (2B11 or H80, as indicated in the figures). The immunoprecipitates were then resolved by SDS-PAGE and the resolved gels were then transferred to nitrocellulose filters that were subsequently immunoblotted with a pan-phospho-tyrosine specific antibody (4G10) (Fig. 5.10b; also refer to Fig. 5.8).

BCR-induced BLNK phosphorylation appears to be reconstituted in both the BCR/Syk/BLNK cell line (Fig. 5.8 and 5.10) and the BCR/Syk/BLNK/BTK cell line (Figure 5.11). Upon initial inspection, it appears that BCR-induced BLNK phosphorylation is enhanced in the BCR/Syk/BLNK/BTK cell line as compared to the BCR/Syk/BLNK cell line (Fig. 5.10b compared to 5.11). From this it may be tempting to conclude that co-expression of BTK, along with Syk, enhances BCR-induced BLNK phosphorylation. However, the apparent enhanced BLNK phosphorylation may merely reflect the fact that more BLNK is expressed in the BCR/Syk/BLNK/BTK cell line as compared to the BCR/Syk/BLNK cell (refer to Fig. 4.2). This fact may not be readily apparent as, according to the strip and reprobe, there appears to be less BLNK in the BCR/Syk/BLNK/BTK cell line as compared to the BCR/Syk/BLNK cell (compare bottom panels of Fig 5.10b and 5.11). However, this is likely an artifact of the strip and reprobe process as it has been a consistent observation within the Matsuuchi lab that the intensity of

reprobed bands appear to be inversely proportional to the intensity of the initial phospho-tyrosine band (for example compare the zero minute time point to the thirty minute time point in Fig. 5.11). Additionally, it should be noted that a basal level of BLNK tyrosine phosphorylation is evident prior to BCR engagement within this system (refer to the zero time points in Figs. 5.10 and 5.11). Such basal phosphorylation may be an artifact of the various exogenous B cell components being over-expressed however; basal phosphorylation of BLNK is also evident in B cell lines (Hashimoto *et al.*, 1999). Regardless, co-expression of the BCR, Syk and BLNK appears sufficient to reconstitute BCR-induced BLNK phosphorylation within the AtT20-derived system (Fig. 5.8, Fig. 5.10 and 5.11). Furthermore, BCR-induced BLNK phosphorylation appears to be Syk-dependent as neither endogenous Fyn (Fig. 5.8) nor exogenous BTK (Fig. 5.9) appear sufficient to reconstitute this event in this system.

Given that BLNK phosphorylation appears to be reconstituted it could be predicted that BLNK should be able to associate with BTK and PLCγ within this system. However, BLNK's ability to associate with various proteins appears dependent upon which of its tyrosine residues become phosphorylated (Chiu *et al.*, 2002). While reconstitution of BCR-induced BLNK phosphorylation is evident within this system, beyond tyrosine 96 (Fig. 5.10b and 5.11), it is not clear which tyrosines are becoming phosphorylated. It may be that all the tyrosine residues are becoming phosphorylated or it may be that only a subset of the residues is becoming phosphorylated. Thus, while BLNK phosphorylation may appear to be reconstituted within this system it does not necessarily follow that BLNK's association with BTK and PLCγ has likewise been reconstituted. Accordingly, investigations were performed to determine if the ability to reconstitute BCR-induced BLNK phosphorylation correlated with an ability to reconstitute BCR-induced BLNK/PLCγ/BTK association.

a.

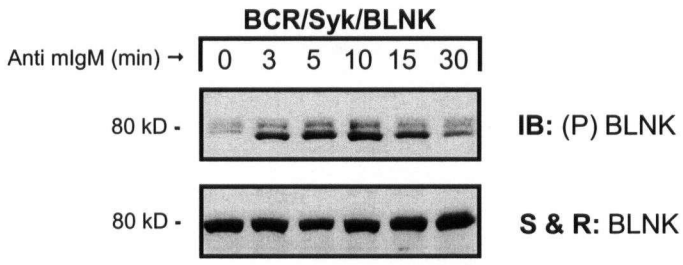

b.

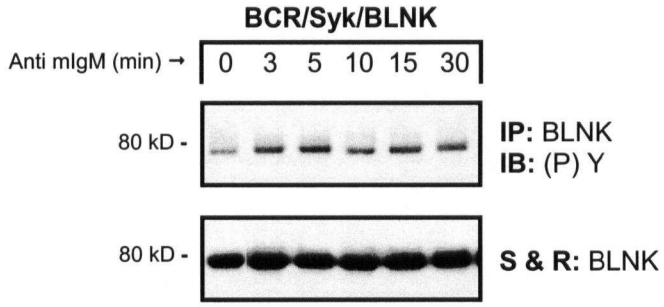

Figure 5.10. Co-Expression of the BCR, Syk and BLNK is Sufficient to Reconstitute BCR-Induced BLNK Phosphorylation in AtT20-Derived Cell Lines. (a) The BCR was cross-linked with anti mIgM antibodies at 37 °C for the indicated length of time. Cells were then lysed and 50 μg of whole cell lysate were resolved by SDS-PAGE. Following electrophoresis, gels were transferred to nitrocellulose filters that were subsequently immunoblotted with a phospho-BLNK (Tyr96) specific antibody. Finally, filters were stripped and reprobed with a BLNK specific antibody. IB indicates the immunoblotting antibody while S&R indicates the antibody that was used to reprobe the filter. Data are representative of three independent experiments. **(b)** The BCR was cross-linked with anti mIgM antibodies at 37 °C for the indicated length of time. Cells were then lysed and BLNK was immunoprecipitated from 1000 μg of whole cell lysate using Protein A-Sepharose and a BLNK specific antibody (H80). Immunoprecipitates were resolved by SDS-PAGE. Following electrophoresis, gels were transferred to nitrocellulose filters that were subsequently immunoblotted with a pan-phospho-tyrosine specific antibody (4G10 monoclonal antibody). Finally, filters were stripped and reprobed with a BLNK specific antibody (H80). IP indicates the immunoprecipitating antibody, IB indicates the immunoblotting antibody and S&R indicates the antibody that was used to reprobe the filter. Data are representative of three independent experiments.

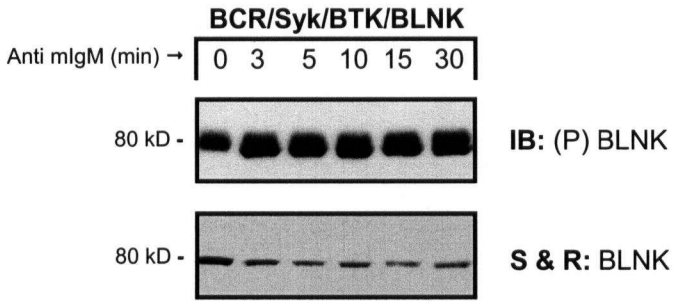

Figure 5.11. Co-Expression of the BCR, Syk, BLNK and BTK is Sufficient to Reconstitute BCR-Induced BLNK Phosphorylation in AtT20-Derived Cell Lines. The BCR was cross-linked with anti mIgM antibodies at 37 °C for the indicated length of time. Cells were then lysed and 50 μg of whole cell lysate were resolved by SDS-PAGE. Following electrophoresis, gels were transferred to nitrocellulose filters that were subsequently immunoblotted with a phospho-BLNK (Tyr96) specific antibody. Finally, filters were stripped and reprobed with a BLNK specific antibody. IB indicates the immunoblotting antibody while S&R indicates the antibody that was used to reprobe the filter. Data are representative of three independent experiments.

5.2.8 Protein Association Studies are Inconclusive in Lymphoid and AtT20-Derived Cell Lines (refer to Appendix II)

As noted above, BCR-induced PLCγ phosphorylation and/or activation may not be maximally reconstituted within the AtT20 system. According to the proposed model, attempts to reconstitute this pathway could be limited if any of the BCR, Syk, BTK, BLNK or PLCγ did not properly associate to form a functional BCR/PLCγ signaling complex. Of particular concern is BLNK's ability to associate with the various proteins as BLNK is proposed to nucleate the BCR/PLCγ signaling complex. Thus, the ability of BLNK to associate with BTK and PLCγ was assayed within this system. To do this, the various cell lines were initially stimulated by cross-linking the BCR with anti mIgM antibodies. Cells were then lysed and BLNK was immunoprecipitated from 1000 μg of whole cell lysate using a BLNK-specific antibody. The immunoprecipitates were then resolved by SDS-PAGE and the resultant gels were transferred to nitrocellulose filters. Subsequently, the filters were immunoblotted with a PLCγ1 specific antibody to determine if PLCγ1 had co-immunoprecipitated with BLNK as this would be indicative of an association. Finally, the filters were striped and re-probed with a BLNK specific antibody to confirm that the immunoprecipitation had been successful. Alternately, the filters were first immunoblotted with a BTK specific antibody to determine if BTK had co-immunoprecipitated with BLNK. Furthermore, reciprocal immunoprecipitation studies were performed with antibodies specific for PLCγ1 and BTK.

Based on the above approach, BLNK, BTK and PLCγ1 do not appear to co-immunoprecipitate either before or following BCR cross-linking in this system (data not shown; summarized in Appendix II). These results may suggest that these proteins do not co-associate within this system. This could suggest either that BLNK is inappropriately/incompletely phosphorylated such that it can not serve its function as an adapter protein and/or that additional lymphoid components may be required to facilitate these associations. Alternatively, BLNK may not be able to associate with the PLCγ1 isoform that is endogenously expressed within the AtT20 system. However, this seems unlikely as previous studies have demonstrated that BLNK can associate with both PLCγ1 and PLCγ2 (Fu and Chan; 1997; Fu *et al*, 1998). Nonetheless, the AtT20 system was transfected with PLCγ2 and further immunoprecipitation assays were performed to address this possibility. Unfortunately, the findings for these assays were as before in that BLNK, BTK and PLCγ2 do not appear to co-immunoprecipitate (data not shown;

summarized to Appendix II). Thus, again these results may suggest that these proteins do not co-associate within this system.

The above results may also suggest that the immunoprecipitation assay is not optimized for detecting protein associations within this system. If the immunoprecipitation assay is functional it should be able to replicate the findings of previous immunoprecipitation studies. Thus, attempts were made to replicate the findings that BLNK and PLCγ co-associate in the human Daudi B cell line following BCR cross-linking (previously demonstrated by Fu *et al.*, 1998). To do this the Daudi B cell line was stimulated by cross-linking the BCR with anti mIgM antibodies for a set length of time (as indicated in the figures). Cells were then lysed and PLCγ1 and PLCγ2 were immunoprecipitated from 1000 μg of whole cell lysate using PLCγ specific antibodies. The immunoprecipitates were then resolved by SDS-PAGE and the resolved gels were transferred to nitrocellulose filters. The filters were then immunoblotted with a BLNK specific antibody to determine if BLNK had co-immunoprecipitated with PLCγ (Fig. 5.12). Subsequently the filters were striped and re-probed with PLCγ specific antibodies to confirm that the immunoprecipitation had been successful (Fig. 5.12). Furthermore, reciprocal immunoprecipitation studies were performed with antibodies specific for BLNK (Fig. 5.13).

As can be seen in figure 5.12a, a very small amount of BLNK can be seen to co-immunoprecipitate with PLCγ1 in the Daudi B cell line. However, this amount is barely detectable and does not appear to significantly increase following BCR cross-linking (Fig. 5.12a). Similarly, only a very small amount of BLNK can be seen to co-immunoprecipitate with PLCγ2 in the Daudi B cell line (Fig. 5.12b). And again, this amount is barely detectable and does not appear to significantly increase following BCR cross-linking (Fig. 5.12b). Furthermore, only a very small amount of PLCγ2, while no PLCγ1, appears to co-immunoprecipitate with BLNK in the reciprocal immunoprecipitation assays (Fig. 15.14 and 5.13, respectively). Thus, BLNK's association with PLCγ1 and PLCγ2 appears to be very difficult to detect with this assay. While these findings appear to be contrary to what is reported in the literature (Fu *et al.*, 1998), personal communications with Dr. T. Kurosaki (a co-author of the original paper reporting BLNK/PLCγ1/PLCγ2 association) has confirmed that this association is indeed very difficult to detect. This is not to suggest that the association does not occur or that it is not significant, but rather that the association is difficult to detect, and as such, the apparently negative co-immunoprecipitation results within the AtT20-system should be interpreted with caution.

a.

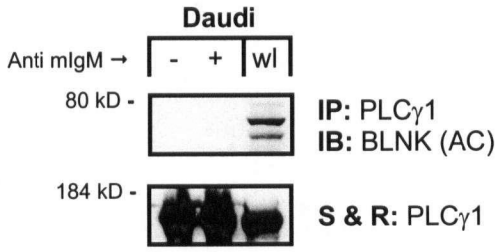

b.

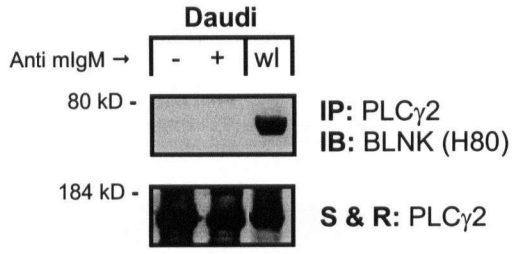

Figure 5.12. BLNK Does Not Appear to Co-Immunoprecipitate with Either PLCγ1 or PLCγ2 in the Daudi B Cell Line. (a) The BCR was not cross-linked in non-stimulated samples (-) and was cross-linked with anti mIgM antibodies at 37 °C for 5 minutes in stimulated samples (+). Cells were then lysed in TX-100 buffer and PLCγ1 was immunoprecipitated from 300 μg of whole cell lysate using Protein A-sepharose and a PLCγ1 specific antibody. Immunoprecipitates were resolved by SDS-PAGE. The resolved gels were transferred to nitrocellulose filters that were subsequently immunoblotted with a BLNK (AC) specific antibody. Finally, filters were stripped and reprobed with a PLCγ1 specific antibody. IP indicates the immunoprecipitating antibody, IB indicates the immunoblotting antibody and S&R indicates the antibody that was used to reprobe the filter. 25 μg of non-immunoprecipitated, whole cell lysate was resolved in the lane labeled "wl". **(b)** Experiments were performed as described for (a) except that a PLCγ2 specific antibody was used to immunoprecipitate PLCγ2 from 3000 μg of whole cell lysate, the BLNK (H80) specific antibody was used for the BLNK immunoblot and 50 μg of non-immunoprecipitated, whole cell lysate was resolved in the lane labeled "wl".

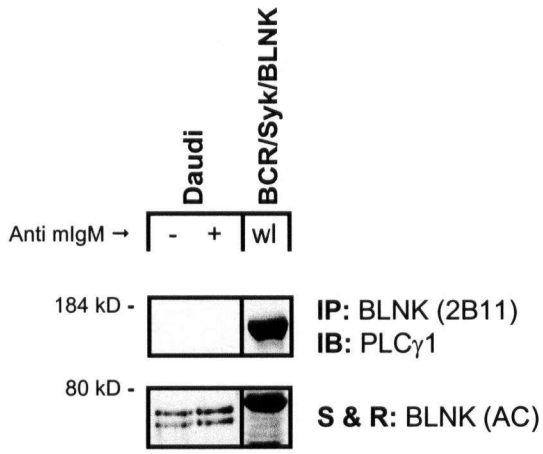

Figure 5.13. PLCγ1 Does Not Appear to Co-Immunoprecipitate with BLNK in the Daudi B Cell Line. The BCR was not cross-linked in non-stimulated samples (-) and was cross-linked with anti mIgM antibodies at 37 °C for 5 minutes in stimulated samples (+). Cells were then lysed in TX-100 buffer and BLNK was immunoprecipitated from 300 μg whole cell lysate using Protein A-sepharose and a mixture of two BLNK specific antibodies (2B11 and H80). Immunoprecipitates were resolved by SDS-PAGE. The resolved gels were transferred to nitrocellulose filters that were subsequently immunoblotted with a PLCγ1 specific antibody. Finally, filters were stripped and reprobed with a mixture of two BLNK antibodies (2B11 and H80). IP indicates the immunoprecipitating antibody, IB indicates the immunoblotting antibody and S&R indicates the antibody that was used to reprobe the filter. 25 μg of non-immunoprecipitated, whole cell lysate from the BCR/Syk/BLNK cell line was resolved in the lane labeled "wl" as a control for the BLNK antibody as this cell line expresses a myc-tagged version of exogenous human BLNK that is slightly heavier than the endogenous BLNK isoforms expressed in the Daudi cell line (68 kD and 70 kD).

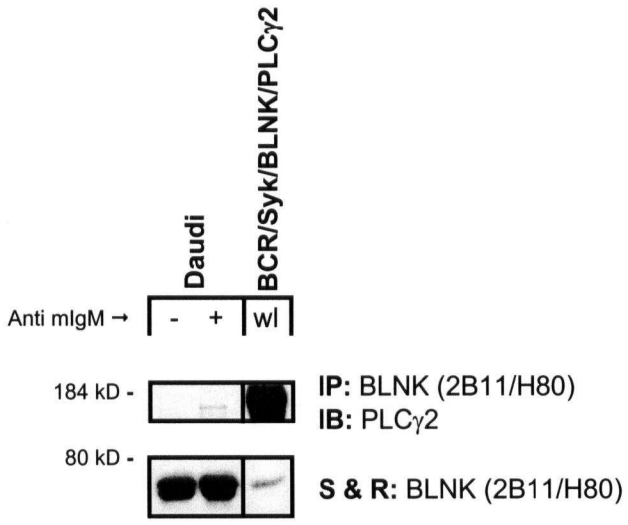

Figure 5.14. PLCγ2 Does Not Appear to Effectively Co-Immunoprecipitate with BLNK in the Daudi B Cell Line. The BCR was not cross-linked in non-stimulated samples (-) and was cross-linked with anti mIgM antibodies at 37 °C for 90 seconds in stimulated samples (+). Cells were then lysed in NP-40 buffer and BLNK was immunoprecipitated from whole cell lysate from $2x10^7$ cells using Protein A-sepharose and a mixture of two BLNK specific antibodies (2B11 and H80). Immunoprecipitates were resolved by SDS-PAGE. The resolved gels were transferred to nitrocellulose filters that were subsequently immunoblotted with a PLCγ1 specific antibody. Finally, filters were stripped and reprobed with a mixture of two BLNK antibodies (2B11 and H80). IP indicates the immunoprecipitating antibody, IB indicates the immunoblotting antibody and S&R indicates the antibody that was used to reprobe the filter. 25 μg of non-immunoprecipitated, whole cell lysate from the BCR/Syk/BLNK/PLCγ2 cell line was resolved in the lane labeled "wl" as a control for the PLCγ2 antibody as this cell line expresses exogenous human PLCγ2.

Given the above results, the immunoprecipitation assay does not appear to be optimized. In particular, this assay may not be able to detect protein associations if the association levels are low, or if the associations were relatively weak such that they can be disturbed by the detergents required by the experiment, or if the associations occur in a manner that occlude the immunoprecipitating antibody from binding to the protein of interest. Thus, the immunoprecipitation protocol was adapted to address these possibilities including using more whole cell lysate per immunoprecipitation, using a variety of detergent conditions and using a variety of antibodies specific for different regions of the proteins of interest (summarized in Appendix II). Regardless of the approach, the majority of these studies were unable to detect a reproducible association between BLNK, BTK and/or PLCγ (summarized in Appendix II) in either the AtT20 system or in B cell lines. Thus, the immunoprecipitation assays were deemed inconclusive and were not pursued further. Rather, investigations were performed to assay the compartmentalization status of BLNK, Syk, BTK and PLCγ within the AtT20 system.

5.2.9 BCR-Induced Membrane Recruitment of Syk, BLNK, BTK and PLCγ Is Not Reconstituted in the AtT20-Derived Cell Lines

Despite their difficulties, the co-immunoprecipitation assays did not completely confound this thesis. Rather, progress was made by investigating the compartmentalization status of the various proteins. In particular, BCR-induced membrane recruitment of Syk, BLNK, BTK and PLCγ was investigated as such recruitment is proposed to be necessary to BCR-induced PLCγ phosphorylation and activation. Indeed, inappropriate compartmentalization could explain the apparently limited BCR-induced PLCγ phosphorylation that was observed within this system. Moreover, because compartmentalization is generally dependent on regulated and specific protein associations, failed compartmentalization could also hint at failed protein associations.

To investigate membrane recruitment, the various cell lines were stimulated by cross-linking the BCR with anti mIgM antibodies for five minutes. The cells were then fractioned into membrane-enriched fractions and cytosolic fractions (refer to Chapter 2.7 for details). The fractions were then resolved by SDS-PAGE and the resolved gels were transferred to nitrocellulose filters that were subsequently immunoblotted with BLNK, BTK, Syk, PLCγ1, Igα or tubulin specific antibodies (Figure 5.15). It should be noted that this approach is limited to distinguishing whether a protein is localized to the cytosol and/or to cellular membranes. This approach can not

distinguish whether a protein is localized to the plasma membrane and/or to other cellular membranes. Nonetheless, this approach can be suggestive as to whether or not a cytosolic protein is being recruited to the membrane-fraction following BCR cross-linking.

As can be seen in Figure 5.15, Syk appears to be associated with both the cytosolic and membrane-enriched fractions in the AtT20-derived cell lines. Similar results are observed for BTK, BLNK and PLCγ (Fig. 5.15). However, while Syk and BTK appear to be equally distributed between the cytosolic and membrane fractions, the vast majority of BLNK and PLCγ1 appear to be distributed in the cytosolic fraction (Fig. 5.15). Moreover, the distribution of the various components does not appear to change following BCR cross-linking (Fig. 5.15). Thus, Syk, BTK, BLNK and PLCγ1 do not appear to be recruited to the membrane-enriched fraction, following BCR cross-linking in this system. This suggests that these components may not be appropriately compartmentalized within this system and this may explain why co-expression of these components does not appear sufficient to reconstitute robust BCR-induced PLCγ1 phosphorylation (refer to Chapter 5.2.1 – 5.2.3).

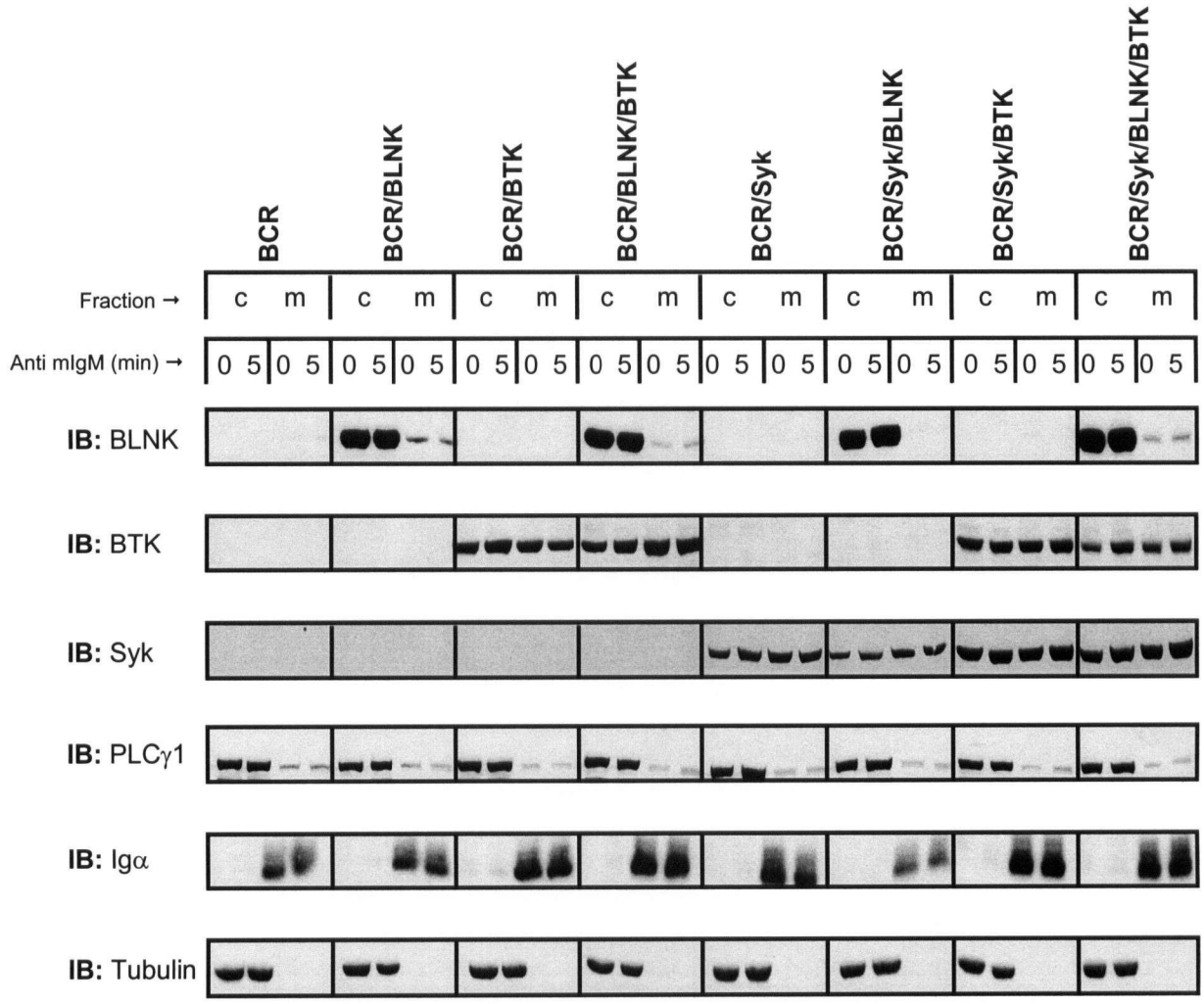

Figure 5.15. BCR-Induced Membrane Recruitment of Syk, BLNK, BTK and/or PLCγ is not Apparent in AtT20 Derived Cell Lines. The BCR was cross-linked with anti mIgM antibodies at 37 °C for 5 minutes. Cells were then fractionated according to the membrane-enrichment protocol (detailed in Chapter 2.7). 50 μg of each fraction was then resolved by SDS-PAGE. The resolved gels were then transferred to nitrocellulose filters that were subsequently immunoblotted with BLNK, BTK, Syk, PLCγ1, Igα or Tubulin specific antibodies. Igα and Tubulin localization was used to confirm that the fractions were not cross-contaminated. Igα is a transmembrane protein and as such is expected to be apparent only in the membrane-enriched fraction whereas Tubulin is a cytosolic protein and as such is expected to be apparent only in the cytosolic fraction. IB indicates the immunoblotting antibody. C indicates the cytosolic fraction and M indicates the membrane-enriched fraction. Data are representative of three independent experiments.

5.3 Discussion

5.3.1 Recalling the Proposed Model of the BCR/PLCγ Pathway

Recall the aforementioned model of the BCR/PLCγ pathway. It is proposed that:

1. BCR cross-linking leads the BCR to translocate into lipid rafts.
2. Lipid raft translocation brings the BCRs into close proximity with active Lyn.
3. Active Lyn then phosphorylates the BCR on the Igα/β ITAMs.
4. The SFKs (including Lyn) are then recruited to the BCR by way of their SH2 domains binding to the phosphorylated Igα/β ITAMs
5. Such recruitment brings the SFK into close proximity with each other enabling them to trans-phosphorylate and activate each other as well as to further phosphorylate the Igα/β ITAMs, creating a positive feedback loop.
6. Syk is also recruited from the cytosol to plasma membrane/BCR by way of its SH2 domain binding to the phosphorylated Igα/β ITAMs.
7. Such recruitment brings Syk into close proximity with the active SFK such that they can phosphorylate and activate Syk.
8. BLNK is also recruited from the cytosol to the plasma membrane/BCR by way of its SH2 domain binding to phosphorylated Igα tyrosines that exist outside of the ITAMs.
9. Such recruitment brings BLNK into close proximity with active Syk such that Syk can phosphorylate BLNK.
10. BTK and PLCγ are then recruited from the cytosol to the plasma membrane/BCR signaling complex by way of their SH2 domains binding to the BCR-associated, phosphorylated BLNK
11. Such recruitment brings PLCγ into close proximity with BTK and Syk such that they can phosphorylate PLCγ.
12. Such recruitment also brings PLCγ into close proximity with its plasma membrane-bound substrate, PIP_2.
13. The combined phosphorylation and membrane-recruitment of PLCγ is proposed to facilitate its activation such that it can then hydrolyze PIP_2 to produce the second messengers, IP_3 and DAG.
14. Ultimately, PLCγ activation leads to increased IP_3 and DAG levels, to increased intracellular calcium levels and to the activation of several downstream signaling

pathways including the MAPK pathway that leads to an increase in phosphorylated Erk levels.

Based on this model it was hypothesized that co-expression of the BCR, Syk, BLNK and BTK would be both necessary and sufficient to maximally reconstitute BCR-induced PLCγ activation in the AtT20 system. Additionally, it was hypothesized that co-expression of the BCR, Syk and BLNK may be sufficient to at least partially reconstitute BCR-induced PLCγ activation with the AtT20 system. This latter hypothesis was based on the observation that genetic ablation of BTK does not completely inhibit PLCγ phosphorylation and/or activation (Takata and Kurosaki, 1996).

Now recall the two key findings in Chapter Four:

1. BCR, Syk and BLNK co-expression *is sufficient* to reconstitute BCR-induced PLCγ activation in the AtT20 system (as determined by monitoring BCR-induced PLC-dependent increases in Erk phosphorylation).
2. BCR, Syk, BLNK and BTK co-expression *is not sufficient* to reconstitute BCR-induced PLCγ activation in the AtT20 system (as determined by monitoring BCR-induced PLC-dependent increases in Erk phosphorylation).

While the former finding is as expected with respect to the initial hypothesis the latter is not. Thus, the AtT20 system was further analyzed in an attempt to determine how or why the results were diverging from the hypothesis, as such an understanding could reveal any shortcomings in the AtT20 system and/or the proposed model of the BCR/PLCγ signaling pathway. In particular, the protein phosphorylation, association and compartmentalization status of Syk, BTK, BLNK and PLCγ were investigated, as "defects" within these processes could explain a divergence from the hypothesis and/or model.

5.3.2 BCR-Induced PLCγ1 Phosphorylation in the AtT20 System

Before discussing the implications of the findings it may be helpful to first recap the key findings regarding PLCγ phosphorylation and activation within this system. This is done below in Table 5.1.

Table 5.1. Summary of Key Findings Regarding BCR-Induced PLCγ1 Phosphorylation and Activation in the AtT20 System. Please note that the colour of the arrow is meant to roughly represent the intensity of the observed phosphorylation where the darker the colour the greater the phosphorylation (e.g. = very weak phosphorylation, ↑ = weak phosphorylation, ↑ = strong phosphorylation, ↑ = very strong phosphorylation).

Cell Line	PLCγ Phosphorylation	PLCγ Activation
BCR	No phosphorylation	**No activation**
BCR/Syk	↑	**No activation**
BCR/BTK		**No activation**
BCR/Syk/BTK	↑	**No activation**
BCR/Syk/BLNK	↑	**Activation**
BCR/BTK/BLNK		**No Activation**
BCR/Syk/BTK/BLNK	↑	**No Activation**

The first finding of note is the observation that co-expression of the BCR with Syk and/or BTK is sufficient to reconstitute BCR-induced PLCγ1 phosphorylation. This finding is quite surprising as, according to the model, BLNK is proposed to be necessary to couple these PTKs to PLCγ. This finding suggests that these PTKs may be able to associate with PLCγ via a BLNK-independent pathway. If this is indeed the case, some residual BCR-induced PLCγ phosphorylation should be evident in BLNK knockout cells. Interestingly, while such a cell line exists the authors only reported on the status of BCR-induced PLCγ activation, which was found to be completely ablated, and not on the status of PLCγ phosphorylation (Ishiai *et al.*, 1999). On the other hand, the observed independence from BLNK could be an artifact of Syk and BTK over-expression within the AtT20 system.

Importantly, co-expression of the BCR with Syk and/or BTK is sufficient to reconstitute *only a minimal amount* of BCR-induced PLCγ phosphorylation *and* it is not sufficient to reconstitute BCR-induced PLCγ activation. This finding has several implications. First, the minimal phosphorylation may suggest that BLNK *is* necessary to efficiently couple these PTKs to PLCγ. Second, the inability to activate PLCγ may suggest either that PLCγ is not being sufficiently phosphorylated to be active or that PLCγ is being activated but not at level sufficient to be detected. Alternatively, the inability to activate PLCγ could suggest that phosphorylation in itself is not sufficient to activate PLCγ. Thus, we go back to considering the role of BLNK in this process.

Interestingly, BCR-induced PLCγ phosphorylation is comparable in the BCR/Syk versus the BCR/Syk/BLNK cell line (Fig. 5.4b) and in the BCR/BTK versus the BCR/BTK/BLNK cell line

(Fig. 5.4a). This suggests that BLNK is not assisting Syk and BTK to phosphorylate PLCγ in this system. This may suggest that BLNK is not appropriately associating with these proteins which in turn may suggest that BLNK is not becoming appropriately phosphorylated in this system or that an additional lymphoid component may be required for BLNK to associate with these proteins. However, while BLNK co-expression does not appear sufficient to enhance BCR-induced PLCγ phosphorylation it does appear sufficient to reconstitute PLCγ activation (Figs. 4.6b and 4.7b). This finding is intriguing as it suggests that BLNK may be involved in a component of PLCγ activation that is independent from its phosphorylation. For example, it could be that BLNK *is* associating with PLCγ and thereby localizing it such that it can act on its substrate. However, if this is the case the question arises as to why BLNK may be associating with PLCγ yet not facilitating its phosphorylation as predicted by the aforementioned model. One possible explanation could be that, contrary to the proposed model, BLNK only facilitates PLCγ's phosphorylation by BTK and not by Syk. Thus, when the BCR, Syk and BLNK are co-expressed you may not see enhanced PLCγ phosphorylation but you may see enhanced PLCγ activation due to a change in the localization of PLCγ due to its association with BLNK. Alternatively, when the BCR, BTK and BLNK are co-expressed you may not see enhanced PLCγ phosphorylation or activation as BTK is not likely to associate with BLNK given that BLNK is not predicted to be phosphorylated in the absence of Syk expression. Initially, this explanation appears to challenge the existing model of the BCR/PLCγ signaling. Indeed, it appears contradictory to publications such as those by Ishiai and colleagues (1999) that report that "BLNK is required for coupling Syk to PLCγ". However, upon further inspection, it is evident that these reports only establish that BLNK is required to couple the BCR to PLCγ activation while they do little to convince the reader that this requirement involves BLNK facilitating Syk's phosphorylation of PLCγ. Indeed, Ishiai (1999) and colleagues themselves point out that PLCγ may well directly associate with phosphorylated Syk via its C-terminal SH2 domain. Thus, BLNK's predominant roles in the BCR/PLCγ pathway may be to appropriately localize PLCγ to the plasma membrane/BCR signaling complex and to couple BTK to PLCγ phosphorylation and thereby, facilitate PLCγ's activation (refer to Chapter 7.4.2 for further discussion).

Two final findings worth noting in this section are:

1. That co-expression of the BCR, Syk, BTK and BLNK appears to slightly enhance PLCγ1 phosphorylation as compared to co-expression of the BCR, Syk and BLNK alone or the BCR, BTK or BLNK alone.
2. That co-expression of the BCR, Syk, BTK and BLNK is no longer sufficient to reconstitute BCR-induced PLCγ activation whereas co-expression of the BCR, Syk and BLNK is sufficient.

These findings have three major implications. First, they support the proposed model in that co-expression of BLNK with Syk and BTK appears to facilitate BCR-induced PLCγ phosphorylation. Second, they suggest that the phosphorylation status of PLCγ is not necessarily indicative of its activation. This finding is not completely unexpected as PLCγ phosphorylation has long been accepted as a required step in PLCγ activation yet rejected as a hallmark of its activation. Rather, it has been suspected that other factors, such as specific protein associations and appropriate localization (i.e., compartmentalization), may also contribute to its activation. Third, they suggest that BTK is inhibiting rather than enhancing PLCγ activation in this system. This is contrary to all expectations and suggests that the proposed model and/or the system is deficient in some manner. As suggested in Chapter Four, BLNK and BTK may be coming together in this system to form a non-functional signaling complex. And while this complex may be able to facilitate the phosphorylation of PLCγ it may not be able to facilitate the correct localization and therefore, activation of PLCγ. To address this possibility the protein association and compartmentalization status of PLCγ was investigated. As well, it was hypothesized that PLCγ activation may not be being maximally reconstituted within this system as BCR-induced PLCγ phosphorylation appears greatly limited as compared to what is observed in B cells. Thus, the phosphorylation, protein association and compartmentalization statuses of BLNK, Syk and BTK were also further investigated to determine if there where any defects in these processes that may be limiting PLCγ phosphorylation and/or activation.

5.3.3 BCR-Induced Syk and BTK Phosphorylation in the AtT20 System

Syk and BTK must be tyrosine phosphorylated and activated if they are to contribute to PLCγ phosphorylation (Kurosaki *et al.*, 1994; Zoller *et al.*, 1997; and Afar *et al.*, 1996; Rawlings *et al.*, 1996; respectively). Thus, an inability to appropriately phosphorylate either Syk or BTK could be a contributing factor to the apparently limited ability to reconstitute BCR-induced PLCγ

phosphorylation and/or activation within the AtT20 system. As such, the phosphorylation status of these components was investigated.

Previous studies have demonstrated that co-expression of the BCR and Syk is sufficient to reconstitute BCR-induced Syk phosphorylation and activation within the AtT20 system (Richards *et al.*, 1996). Likewise, co-expression of the BCR and BTK appears sufficient to reconstitute BTK phosphorylation and activation within the AtT20 system (Fig. 5.5)[1]. Moreover, this phosphorylation appears to be constitutive, at least partly Fyn-dependent (Fig.5.7) and does not appear to be enhanced either by BCR cross-linking or by the co-expression of Syk and/or BLNK (Fig. 5.5). Thus, in terms of their respective kinase activities, Syk and BTK should be able to contribute to PLCγ phosphorylation and activation in this system. However, these components may be unable to contribute to PLCγ phosphorylation and/or activation if they are unable to appropriately associate with the BCR/PLCγ signaling complex. As such, the compartmentalization status of these components was investigated (refer to 5.3.4).

It is important to note that the apparently constitutive phosphorylation of BTK does not appear to be inhibiting its ability to phosphorylate PLCγ within this system following BCR cross-linking. Nonetheless, the constitutive phosphorylation may explain the unusual observation that BTK appears to be negatively influencing the BCR-induced PLC-independent pathway within this system. In particular, this constitutive phosphorylation may be driving an abnormal and negative association between BTK and some component of the PLC-independent pathway. Additionally, the constitutive phosphorylation may be contributing to BTK's apparent negative effect on PLCγ activation. For instance the constitutive phosphorylation of BTK may somehow be "trapping" PLCγ in a non-productive signaling complex with BTK and BLNK such that it can not appropriately compartmentalize with its membrane-bound substrate, PIP_2. Ideally, this hypothesis could be investigated through the combined use of immunoprecipitation assays and compartmentalization assays. And certainly, the compartmentalization assays were performed (refer to below). However, the immunoprecipitation assays were not extensively pursued due to their apparent unreliability (as discussed earlier). Given this limitation, the focus of the study returned to more direct investigations of BCR-induced PLCγ activation including investigating BLNK's phosphorylation status.

[1] Phosphorylation of tyrosine residue 223 (as was observed) is generally accepted to be indicative of BTK kinase activity (Rawlings *et al.*, 1996; Park *et al.*, 1996; Kurosaki *et al.*, 1997). However, BTK activity could be further confirmed with a kinase assay.

5.3.4 BCR-Induced BLNK Phosphorylation in the AtT20 System

BLNK must be tyrosine phosphorylated if it is to associate with BTK and PLCγ and subsequently facilitate PLCγ phosphorylation (Hashimoto *et* al., 1999; Su *et al.*, 1999; Ishiai *et al.*, 1999). Thus, an inability to appropriately phosphorylate BLNK could be a contributing factor in the apparently limited ability to reconstitute BCR-induced PLCγ phosphorylation and/or activation in this system. As such, the phosphorylation status of BLNK was investigated within the AtT20 system.

Based on these investigations, BCR-induced BLNK phosphorylation appears to be reconstituted in a Syk-dependent fashion within the AtT20 system (Fig. 5.10). This is in accordance with the proposed model (Fig. 5.1). This suggests that BLNK should be able to bind to the SH2 domains of BTK and PLCγ and serve its function as an adapter protein. However, it is unclear whether or not BLNK is becoming phosphorylated on all its tyrosine residues or merely a subset of the residues. In fact, only phosphorylation of tyrosine residue 96 (Tyr96) has been confirmed (Fig. 5.10a). This is of concern as phosphorylation of multiple BLNK tyrosine residues has been demonstrated as being necessary to efficiently couple the BCR to PLCγ activation (Fu *et al.*, 1998; Chiu *et al.*, 2002). Thus, even though BLNK appears to be tyrosine phosphorylated, it may yet be unable to perform its adapter function within the AtT20 system. As such, further investigations were performed to determine whether or not BLNK was able to associate with BTK and PLCγ and essentially compartmentalize these components within a functional BCR/PLCγ signaling complex.

5.3.5 BCR-Induced Compartmentalization of Syk, BTK, BLNK and PLCγ in the AtT20 System

The components of the BCR/PLCγ signaling pathway must be compartmentalized within a macromolecular signaling complex for PLCγ to be activated. According to the model (Fig. 5.1), this involves BTK and PLCγ associating with BLNK as well as Syk, BLNK, BTK and PLCγ being recruited to the BCR complex and therefore, to the plasma membrane. Failure of these components either to associate with BLNK or to be recruited to the plasma membrane could be a contributing factor to the apparently limited ability to reconstitute BCR-induced PLCγ

phosphorylation and/or activation within this system. As such, the compartmentalization status of these components was investigated within the AtT20 system.

Initial co-immunoprecipitation studies investigated whether or not BTK and PLCγ were associating with BLNK in the AtT20 system. The results of these investigations (summarized in Appendix II) were predominantly negative, suggesting that this association was not being reconstituted. However, similar studies employing B cell lines as positive controls were also predominantly negative (Figs. 5.12, 5.13 and 5.14 as well as Appendix II) and as such these studies were deemed inconclusive and were not pursued further. Alternatively, membrane-recruitment of the various components was analyzed.

According to the model, the fact that the Syk, BTK and BLNK all appear to be phosphorylated may suggest that these components are being recruited to the BCR signaling complex (and as such to the plasma membrane). However, it is possible that phosphorylation of these components is occurring in the cytosol, without specific compartmentalization, due to over-expression effects. Thus, investigations were performed to determine if these components were indeed being membrane-recruited. To do this the cells lines were fractionated into cytosolic and membrane-enriched fractions prior to and following BCR cross-linking. The subsequent fractions were then analyzed for the presence or absence of the various components. While this approach can not distinguish whether or not a component is being recruited to the plasma membrane or to some other cellular membrane it is able to determine whether a component is being recruited from the cytosol fraction to the membrane-fraction and as such is suggestive. Based on these studies it was determined that none of the components appear to be recruited to the membrane fraction following BCR cross-linking (Fig. 5.15). This may suggest that the components of the pathway are not being appropriately compartmentalized within this system and as such, efficient PLCγ phosphorylation and/or activation may not be occurring. Thus, BLNK and PLCγ were constitutively targeted to the plasma membrane in an attempt to bypass any compartmentalization defects (detailed in Chapter 6).

CHAPTER 6

Co-Expression of the BCR, Syk and Acylated-PLCγ2 Is Sufficient to Reconstitute BCR-Induced PLCγ Activation in AtT20-Derived Cell Lines

6.1 Introduction

According to the prevalent models of BCR signaling, co-expression of Syk, BTK and BLNK should be sufficient to couple the BCR to PLCγ. However, the findings of this thesis suggest that this is not the case, at least in AtT20-Derived Cell Lines (refer to Chapter Four). Upon further investigation it was found that neither Syk, BTK, BLNK nor PLCγ were being recruited to the plasma membrane following BCR cross-linking (refer to Chapter Five). Given this, it was hypothesized that the apparent inability to couple the BCR to PLCγ may be reflective of an inability to appropriately compartmentalize the various components in a functional BCR/PLCγ signaling complex. Thus, to investigate this hypothesis, BLNK and PLCγ were constitutively targeted to the plasma membrane.

Membrane targeting of BLNK and PLCγ was achieved using two different strategies. In the first, mammalian expression vectors were created that encode for the extracellular domain of human CD16 (amino acids 1-208) fused to the transmembrane domain of TCR ζ (amino acids 31-58) fused to the respective sequences of human BLNK and PLCγ2 (refer to Chapter 2.1.3 for details and Fig. 6.1a). In the second, mammalian expression vectors were created that encode for the Lyn (a Src family member) acylation-targeting sequence fused to human BLNK and human PLCγ2 (refer to Chapter 2.1.3 for details and Fig. 6.1b).

The first targeting strategy has been used previously to successfully target rat PLCγ2 to the plasma membrane (Ishiai *et* al., 1999). This strategy targets the fusion proteins to the plasma membrane by way of the extracellular and transmembrane domains. This approach is advantageous as the extracellular domain allows for the detection of cell-surface expression of the fusion protein through surface staining procedures (e.g., surface biotinylation assays and/or FACS analysis). As well the extracellular domain allows the fusion protein to be cross-linked with the BCR. This may be achieved either by the extracellular domain (which is that of human CD16, a known Fc receptor) directly binding to the Fc portion of the BCR cross-linking

antibodies or by treating the cell lines with antibodies specific for the extracellular domain of CD16 and for the BCR and then further cross-linking the proteins with the addition of Streptavidin A. In either case, such cross-linking would bring the BCR and the fusion protein in closer proximity such as would be expected in the formation of a BCR/PLCγ signaling complex. However, this approach has two drawbacks. First, while such cross-linking is theoretically possible in practice it may be more difficult to achieve and substantiate. Second, the sequences encoding for the extracellular domain and the transmembrane domain are quite large (~ 0.7 kB combined) and as such, result in a rather large expression vector when further fused to the sequence of interest. This is of concern as it has been our laboratory's experience that larger expression vectors tend to be less efficiently expressed in AtT20-Derived Cell Lines. Thus, a second targeting strategy was also employed.

The second targeting strategy has been used previously to successfully target human PLCγ to the plasma membrane (DeBell *et al.*, 1999). This strategy targets the fusion protein to the plasma membrane by way of the acylation sequence. In particular, it has been shown that N-terminal myristoylation or palmitoylation is sufficient to target Src family members to the plasma membrane and more specifically to lipid raft microdomains in the plasma membrane (Robbins *et* al., 1995). Thus, in this approach the fusion proteins are anticipated to be localized to lipid rafts in the plasma membrane. This is desirable as it should bring the fusion proteins in close proximity to the BCR which itself is proposed to translocate into lipid rafts upon cross-linking. A drawback of this approach however, is that the fusion proteins can not be directly cross-linked with the BCR. Additionally, it is difficult to confirm that the fusion proteins are indeed being expressed at the plasma membrane as they lack an extracellular domain that could be detected by surface staining. Nonetheless, association of these proteins with the membrane fraction is likely indicative of lipid raft association and moreover, of plasma membrane association as the majority of lipid rafts localize to the plasma membrane.

a.

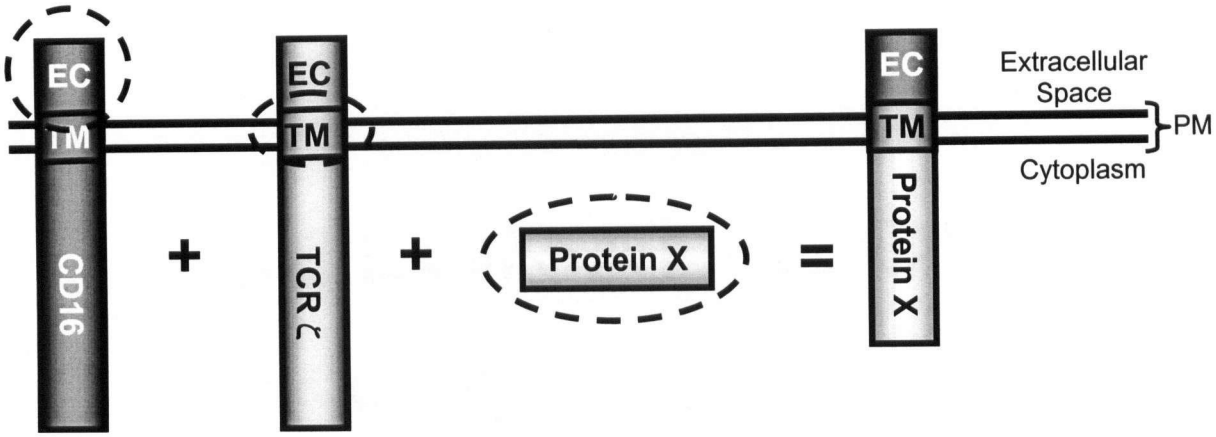

b.

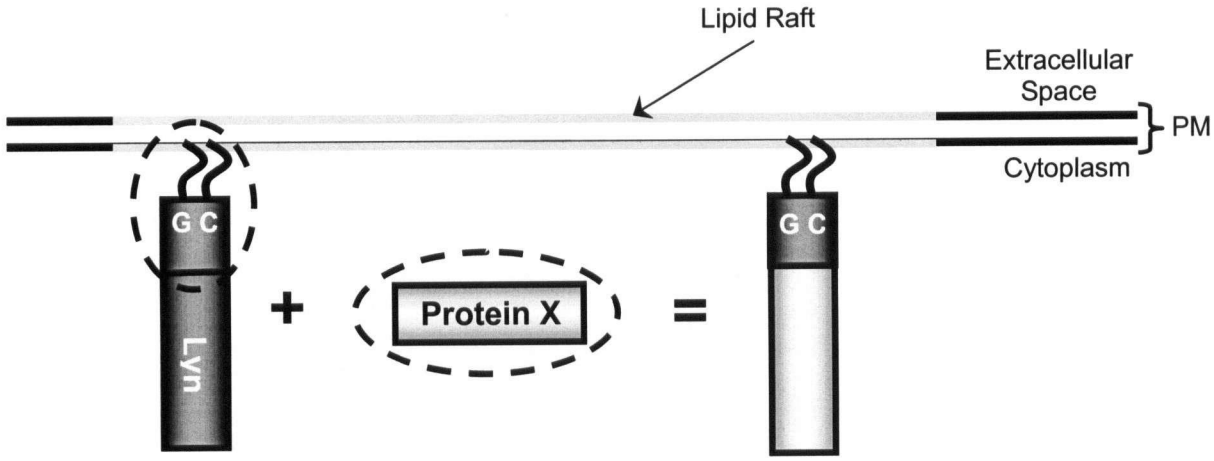

Figure 6.1. Strategies for Constitutively Targeting human BLNK and human PLCγ2 to the Plasma Membrane In AtT20-Derived Cell Lines. (a) Transmembrane Targeted Construct. Human BLNK and human PLCγ2 were targeted to the plasma membrane by fusing their respective sequences (minus the start codon) downstream and in-frame of the sequences encoding for the extracellular domain of CD16 (amino acids 1-112) and the transmembrane domain of the TCR zeta chain (amino acids 30-58) as previously described by Ishiai *et al.* (1999). The resulting fusion proteins are referred to as TmBLNK and TmPLCγ2, respectively. **(b) Acylation Targeted Constructs.** Human BLNK and human PLCγ2 were targeted to lipid rafts in the plasma membrane by fusing their respective sequences (minus the start codon) downstream and in-frame of the acylation sequence of the Src kinase family member, Lyn (amino acids 1-12) in an approach similar to that described by DeBell *et al.* (1999). Protein X can represent any protein of interest, in this case human BLNK or human PLCγ2. PM refers to the plasma membrane, EC refers to the extracellular domain, TM refers to the transmembrane domain and GC refers to the acylation sequence.

6.2 Results

6.2.1 Expression of Membrane-Targeted BLNK (TmBLNK), Acylated BLNK (AcBLNK) and Acylated PLCγ2 (AcPLCγ2) in AtT20-Derived Cell Lines

The various membrane targeting constructs (RSVpLpA-TM-human BLNK, RSVpLpA-TM-human PLCγ2, RSVpLpA-Ac-human BLNK and RSVpLpA-Ac-human PLCγ2) were transfected into the previously established BCR/Syk cell line. Drug resistant clones were then isolated and screened for their ability to express the desired construct. From this process several AtT20-derived cell lines were established including the BCR/Syk/TmBLNK BCR/Syk/AcBLNK, BCR/Syk/AcPLCγ2 and BCR/Syk/AcBLNK/AcPLCγ2 cell lines. The BCR/Syk/TmBLNK cell line was found to express two molecular weight forms of TmBLNK (~114 kD and ~ 105 kD, respectively) (Fig. 6.2). This observation is not unanticipated as similar results were observed when Ishiai *et al.* (1999) used the same transmembrane-targeting construct to target rat PLCγ2 to the plasma membrane. In this case, the two different molecular weight forms of the protein were taken to represent differentially glycosylated forms of the same proteins. However, upon further investigation and reflection this does not appear to be the case for the TmBLNK construct. Rather it seems that the two different molecular weight forms may be due to some other post-translational modification. Alternatively the lower molecular weight form of TmBLNK may represent a splice-variant of the higher molecular weight form. Regardless, as the lower molecular weight form appears to be sequestered away from the cytosol and the plasma membrane (perhaps in the endoplasmic reticulum) it was not predicted to negatively influence subsequent signaling studies. Similarly, the BCR/Syk/AcBLNK and BCR/Syk/AcBLNK/AcPLCγ cell line was found to express two molecular weight forms of AcBLNK (~80 kD and ~70 kD, respectively)(Fig. 5.2). And again, upon further investigation and reflection it appears that the lower molecular weight form of AcBLNK may represent a splice-variant of the higher molecular weight form (discussed in detail in Chapter 6.3.1). However, in this case the lower molecular weight form appears to be expressed in the cytosol (Fig. 6.3) where it could potentially influence signaling and as such subsequent signaling studies need to be interpreted with caution. Unfortunately, TmPLCγ2 expressing cell lines were not successfully established (data not shown; discussed in Chapter 6.3.1). It should also be noted that several clones were obtained for both the BCR/Syk/TmBLNK and the BCR/Syk/AcBLNK cell lines and that initial experiments were performed with multiple clones (data not shown).

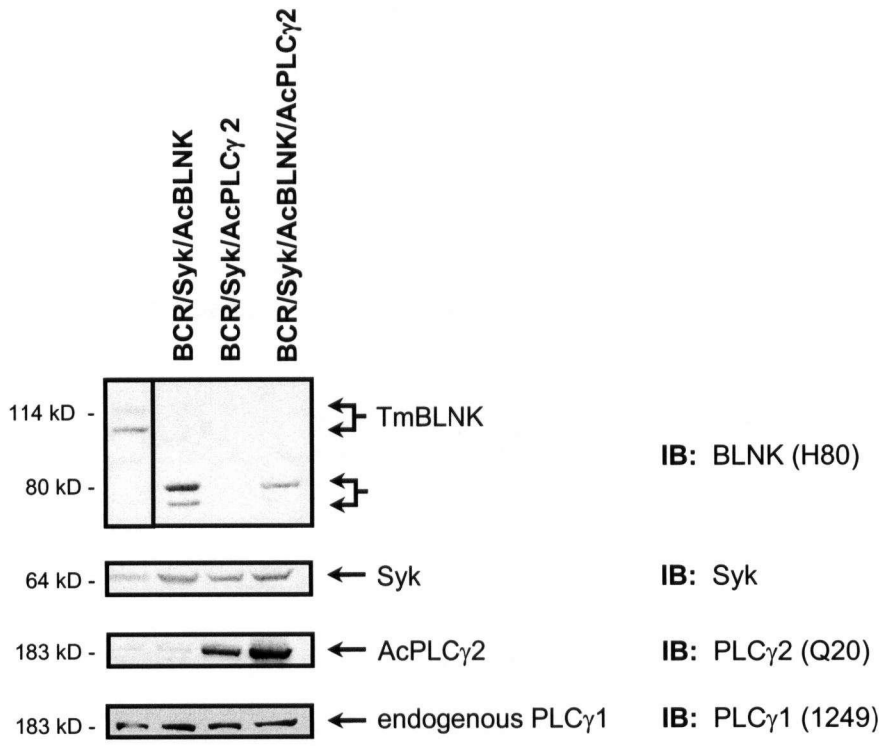

Figure 6.2. Characterization of TmBLNK, AcBLNK, AcPLCγ2 and PLCγ1 Expression in Transfected AtT20 Cell Lines. 35 μg of whole cell lysate were resolved by SDS-PAGE. Following electrophoresis, gels were transferred to nitrocellulose filters that were subsequently immunoblotted with antibodies specific for BLNK, PLCγ2, Syk and PLCγ1. Note that both TmBLNK and AcBLNK appear as doublets. This appears to be indicative of differential glycosylation and/or differential acylation of the proteins. IB indicates the immunoblotting antibody. It should be noted that several clones were obtained for each described cell line and that initial experiments were performed with multiple clones (data not shown). Having established that the various clones gave rise to consistent results further experiments were performed with a single representative clone.

Subsequent experiments were performed with a single representative clone as the various clones gave rise to similar results in the initial investigation (data not shown).

Having established cell lines that express TmBLNK, AcBLNK and AcPLCγ2 it was necessary to confirm that these fusion proteins were indeed being targeted to cellular membranes. To do this the various cell lines were fractioned into membrane-enriched fractions and cytosolic fractions (refer to Chapter 2.7). The fractions were then resolved by SDS-PAGE with the resultant gels being transferred to nitrocellulose filters that were subsequently immunoblotted with BLNK and PLCγ2 specific antibodies (Fig. 6.3). As a control, the filters were also immunoblotted with Igα and tubulin specific antibodies (Fig. 6.3) as Igα is a constitutive membrane protein and tubulin is a constitutive cytosolic protein. The fractionation protocol appears effective as Igα and tubulin were observed only in the membrane and cytosolic fractions, respectively (Fig. 6.3). This suggests that each fraction is not contaminated with the other fraction and as such any proteins observed in the membrane fraction are likely to be truly membrane-associated. Based on this, TmBLNK appears to be efficiently targeted to the membrane as both molecular weight forms appear to constitutively associate with the membrane fraction (Fig. 6.3). The AcBLNK and AcPLCγ2 constructs also appear to associate with the membrane fraction (Fig. 6.3). However, the acylation constructs may not be targeted to the membrane as efficiently as the transmembrane construct. In particular, the lower molecular weight form of AcBLNK does not appear to associate with the membrane fraction suggesting that it is not targeted to the membrane (Fig. 6.3). This situation could arise if the lower molecular weight form of AcBLNK is incompletely or inappropriately acylated. As well, a small portion of both the higher molecular weight form of AcBLNK and of AcPLCγ appears to associate with the cytosolic fraction (Fig. 6.3) suggesting that the acylated constructs may not be solely targeted to the membrane. Regardless, a significant portion of TmBLNK, AcBLNK and AcPLCγ2 appears to be targeted to the cellular membranes (Fig. 6.3) lending promise to further experimentation.

While the above approach suggests that the proteins are targeted to cellular membranes, it alone can not determine whether the proteins are being localized to the plasma membrane or to some other cellular membrane. Thus, surface biotinylation assays were used to determine if TmBLNK is indeed targeted to the plasma membrane. Initially, cells were exposed to biotin such that all proteins with extracellular domains should become biotinylated (refer to Chapter 2.14 for details). Lysates were then prepared from the biotinylated cells and TmBLNK was

immunoprecipitated from the lysates using BLNK specific antibodies. The immunoprecipitates were then resolved by SDS-PAGE and the resultant gels were transferred to nitrocellulose filters. The filters were then blotted with Streptavidin A-HRP which specifically detects biotin-labeled proteins. As controls Syk and the μ heavy chain were also immunoprecipitated from the lysates with the expectation that Syk should remain non-biotinylated as it is a cytosolic protein and that μ heavy chain should be biotinylated as it contains an extracellular domain. Based on this approach, the higher molecular weight form of BLNK (~114 kD) appears to biotinylated (Fig. 6.4) and therefore targeted to the plasma membrane. In contrast, the lower molecular weight form of TmBLNK (~ 105 kD) does not appear to biotinylated and as such does not appear to be targeted to the plasma membrane (Fig. 6.4).

Unfortunately, the surface biotinylation assay could not be used to determine if the acylated constructs were targeted to the plasma membrane as these constructs do not contain extracellular domains. Rather, the acylated constructs are anticipated to be associated with the plasma membrane based on several criteria. First, the acylated constructs can associate with the membrane fraction (Fig. 6.3). Second, the acylated constructs are targeted to the membrane using the Lyn acylation motif, a motif that has been repeatedly demonstrated to target proteins to lipid rafts (DeBell *et al.*, 1999). And third, it is known that the vast majority of lipid rafts are localized to the plasma membrane (DeBell *et al.*, 1999). Thus, the membrane associated acylation constructs are anticipated to be associated with lipid rafts and therefore are likely associated with the plasma membrane.

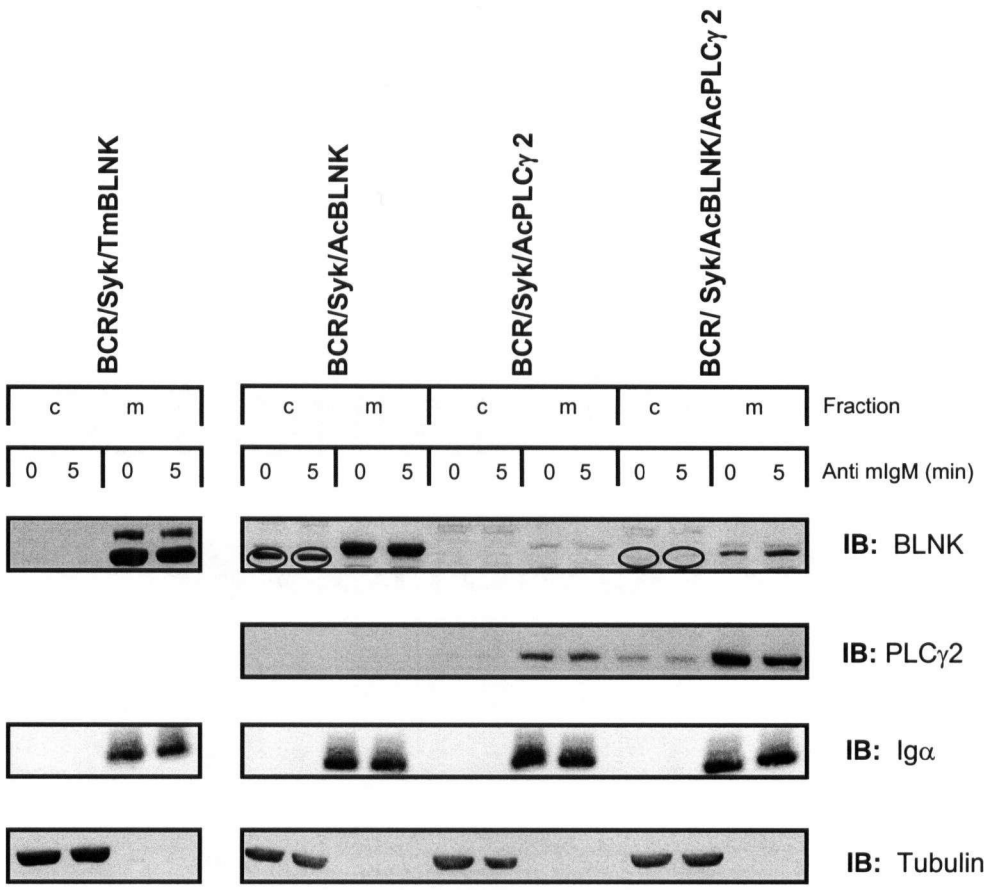

Figure 6.3. Both Molecular Weight Forms of TmBLNK (~114 kD and ~105 kD) Appear To Constitutively Associate with the Membrane Fraction in AtT20-Derived Cell Lines. A Significant Portion of AcBLNK and AcPLCγ2 Appear to Be Constitutively Associated with the Membrane Fraction in AtT20-Derived Cell Lines. The BCR was cross-linked with goat anti mIgM antibodies at 37 °C for 5 minutes. Cells were then fractionated according to the membrane-enrichment protocol (detailed in Chapter 2.7). 50 μg of each fraction was then resolved by SDS-PAGE. The resolved gels were then transferred to nitrocellulose filters that were subsequently immunoblotted with BLNK, PLCγ2, Igα or Tubulin specific antibodies. Igα and Tubulin localization was used to confirm that the fractions were not cross-contaminated with Tubulin serving as a cytosolic fraction marker and Igα serving as a membrane fraction marker. IB indicates the immunoblotting antibody. "c" indicates the cytosolic fraction and "m" indicates the membrane-enriched fraction. Data are representative of three independent experiments. Interestingly, the lower molecular weight form of AcBLNK (circled in the figure) does not appear to associate with the membrane fraction. This lower molecular weight form of AcBLNK is hypothesized to be incompletely acylated and as such it is predicted that it may not associate with the membrane fraction.

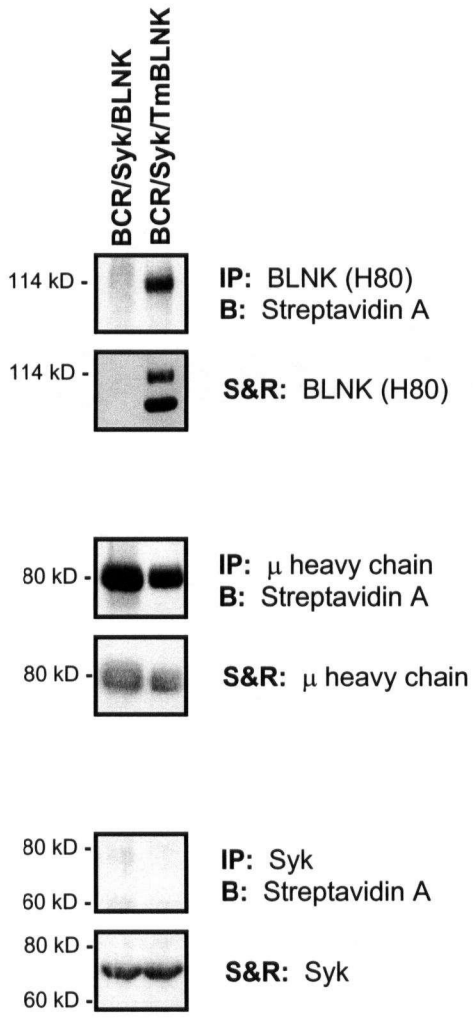

Figure 6.4. The Heavier Form of TmBLNK (~114 kD) Appears to Be Expressed on the Cell Surface in AtT20-Derived Cell Lines. Cell lines were surface biotinylated for 20 minutes. Cells were then lysed and BLNK, μ and Syk were immunoprecipitated from 1000 μg of whole cell lysate using a BLNK, μ and Syk specific antibodies, respectively. Immunoprecipitates were resolved by SDS-PAGE. The resolved gels were then transferred to nitrocellulose filters that were subsequently blotted with a Strepavidin A-HRP which specifically binds to biotin. Finally, filters were stripped and reprobed with BLNK, μ and Syk specific antibodies, respectively. IP indicates the immunoprecipitating antibody, B indicates the blotting reagent while S&R indicates the specificity of the antibody that was used to reprobe the filter. Data are representative of three independent experiments.

6.2.2 Co-Expression of the BCR, Syk and TmBLNK or AcBLNK is Sufficient to Reconstitute BCR-Induced, PLC-Dependent Erk Phosphorylation in AtT20-Derived Cell Lines

Having established that TmBLNK and AcBLNK are successfully targeted to the plasma membrane, the sufficiency of these constructs to reconstitute BCR-induced PLCγ activation was investigated next. As explained previously in Chapter Four, BCR-induced PLCγ activation was assessed by monitoring for BCR-induced, PLC-dependent increases in Erk phosphorylation. To do this the relevant cell lines were stimulated by cross-linking the BCR with anti mIgM antibodies for a set length of time (as indicated in the figures), in the presence or absence of a PLC inhibitor (U73122). Recall, if the Erk phosphorylation is being mediated by a PLC-independent pathway one would predict that addition of the inhibitor should not effect BCR-induced Erk phosphorylation. In contrast, if the Erk phosphorylation is being mediated by a PLC-dependent pathway one would predict that addition of the inhibitor will inhibit Erk phosphorylation. Following stimulation, the cells were lysed and 50 μg of whole cell lysate were resolved by SDS-PAGE. The gels were then transferred to nitrocellulose filters that were subsequently immunoblotted with a phospho-Erk (Thr202/Tyr204) specific antibody. Finally, filters were stripped and reprobed with an Erk specific antibody.

As can be seen in Figure 6.5, an increase in Erk phosphorylation is not apparent following BCR cross-linking in either the BCR/Syk/TmBLNK cell line or the BCR/Syk/AcBLNK cell line as compared to that BCR/Syk cell line. Additionally, a slight decrease in BCR-induced Erk phosphorylation is apparent in the BCR/Syk/TmBLNK cell line following treatment with the PLC inhibitor suggesting that at least some of the observed Erk phosphorylation is due to a PLC-dependent pathway (Fig. 6.6a and b). In contrast, there does not appear to be a significant or consistent decrease in BCR-induced Erk phosphorylation in the BCR/Syk/TmBLNK cell line following treatment with the PLC inhibitor (Fig. 6.6a and c, and data not shown). These findings suggest that co-expression of the BCR, Syk and TmBLNK is sufficient to reconstitute BCR-induced PLCγ activation whereas co-expression of the BCR, Syk and AcBLNK is not. As well, these results suggest that TmBLNK has a slight negative effect on BCR-induced PLC-independent Erk phosphorylation in this system. This based on the observation that the overall BCR-induced Erk phosphorylation does not appear to be enhanced (Fig. 6.5) despite an apparent increase in BCR-induced PLCγ-dependent Erk phosphorylation in these cell lines (Fig. 6.6). For

such an observation to occur the apparent increase in the BCR-induced PLCγ-dependent Erk phosphorylation must be balanced by a concurrent decrease in BCR-induced, PLC-dependent Erk phosphorylation. Thus, TmBLNK may also play a yet to be determined role in the BCR-induced PLC-independent Erk pathway. Overall, the TmBLNK findings are similar to those observed for cytosolic BLNK (Chapter 4.2.4 and top panel of Fig. 6.6) and suggest that membrane targeting of BLNK does not further the reconstitution of BCR-induced PLCγ activation as compared to cytosolic BLNK. And thus, similar to the BCR/Syk/BLNK cell line, the question arises as to whether or not maximal reconstitution of BCR-induced PLCγ activation is being achieved in the BCR/Syk/TmBLNK cell line. As well, the AcBLNK results suggest that targeting BLNK to lipid rafts in the plasma membrane may actually inhibit BLNK ability to reconstitute the BCR/PLCγ pathway in this system. This too raises further questions, especially with regards to why, counter to expectation, such targeting impedes rather than enhances BLNK activity in this system.

Ultimately, the inability to further reconstitute BCR-induced PLCγ activation with membrane BLNK suggests that there may be an additional deficiency, beyond BLNK membrane recruitment, in this system. This deficiency may lie in any of the numerous steps that are proposed to be required to couple the BCR to PLCγ activation. In particular, it may be that membrane BLNK and/or PLCγ are not becoming appropriately phosphorylated and/or associated with each other in this system. Thus, further investigations were performed to address these possibilities.

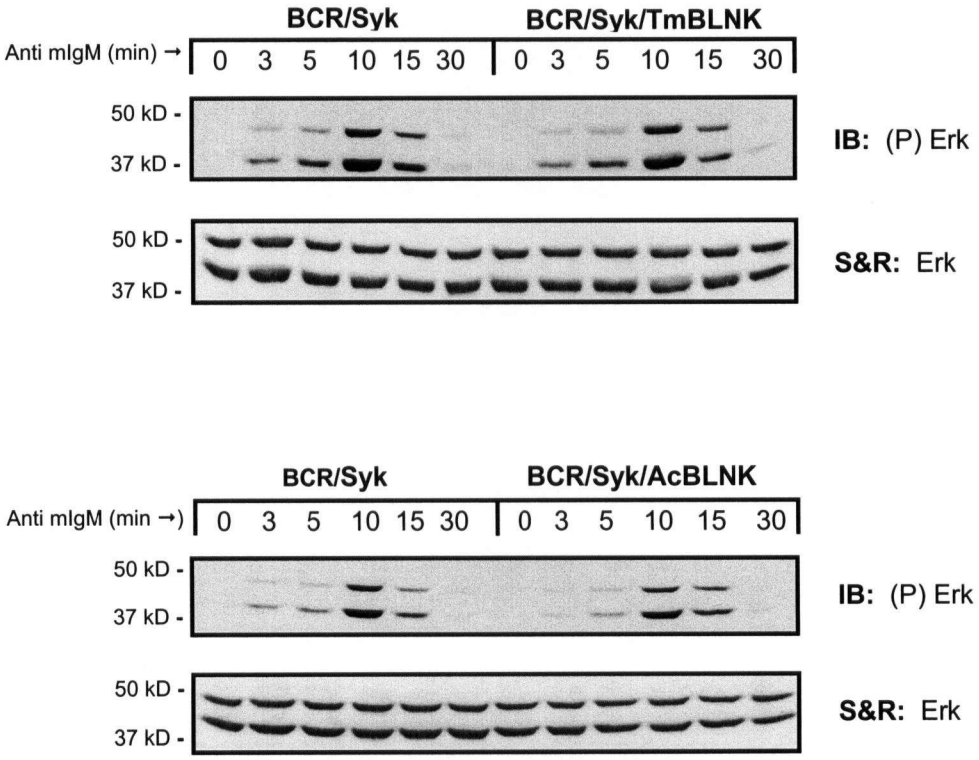

Figure 6.5. Co-Expression of the BCR, Syk and TmBLNK or AcBLNK May Inhibit Rather than Enhance BCR-Induced Erk Phosphorylation in AtT20-Derived Cell Lines. The BCR was cross-linked with anti mIgM antibodies at 37 °C for the indicated length of time. Cells were then lysed and 50 μg of whole cell lysate were resolved by SDS-PAGE. Following electrophoresis, gels were transferred to nitrocellulose filters that were subsequently immunoblotted with a phospho-Erk (Thr202/Tyr204) specific antibody. Finally, filters were stripped and reprobed with an Erk specific antibody. IB indicates the immunoblotting antibody while S&R indicates the antibody used to reprobe the filter. Data are representative of three independent experiments.

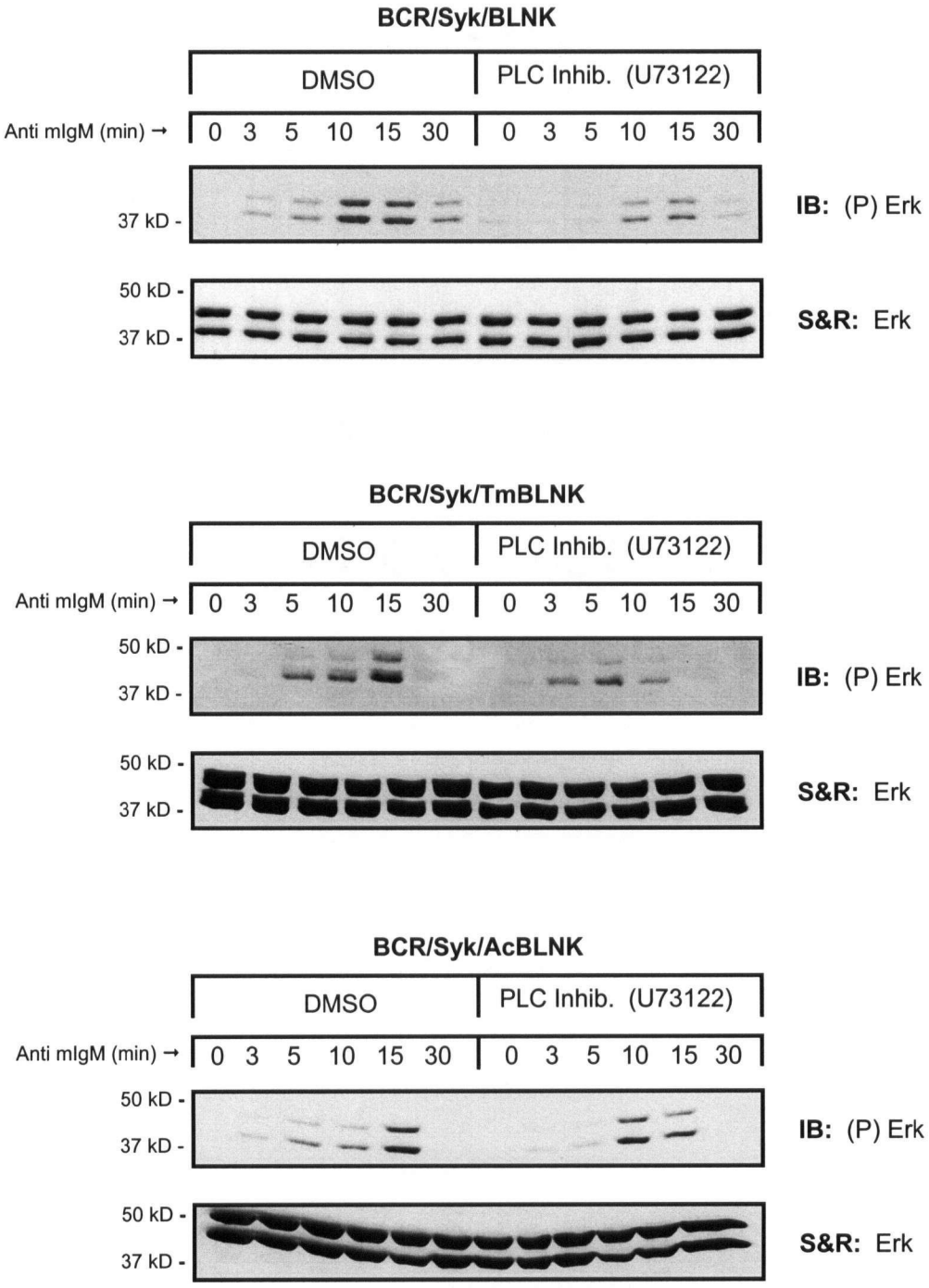

Figure 6.6. (a) Co-Expression of the BCR, Syk and TmBLNK or AcBLNK is Sufficient to Reconstitute BCR-Induced, PLC-Dependent Erk Phosphorylation in AtT20-Derived Cell Lines. Cells were treated either with DMSO (negative control) or the PLC inhibitor, U73122 (at a final concentration of 10 μM) for 1 hour. The BCR was then cross-linked with anti mIgM antibodies at 37 °C for the indicated length of time. Cells were then lysed and 50 μg of whole cell lysate were resolved by SDS-PAGE. Following electrophoresis, gels were transferred to nitrocellulose filters that were subsequently immunoblotted with a phospho-Erk (Thr202/Tyr204) specific antibody. Finally, filters were stripped and reprobed with an Erk specific antibody. IB indicates the immunoblotting antibody while S&R indicates the antibody used to reprobe the filter. Data are representative of three independent experiments.

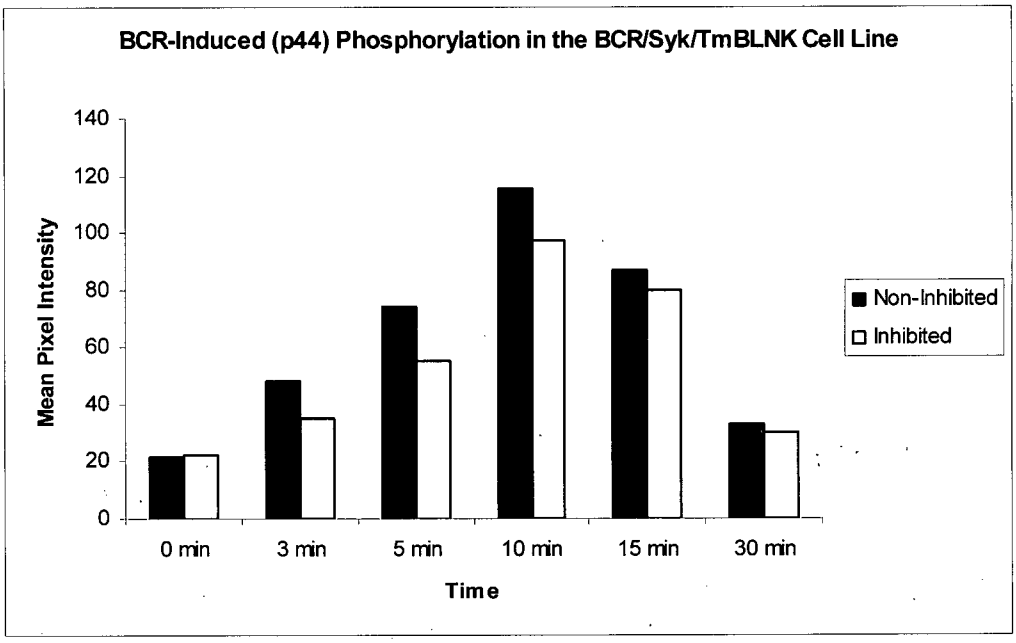

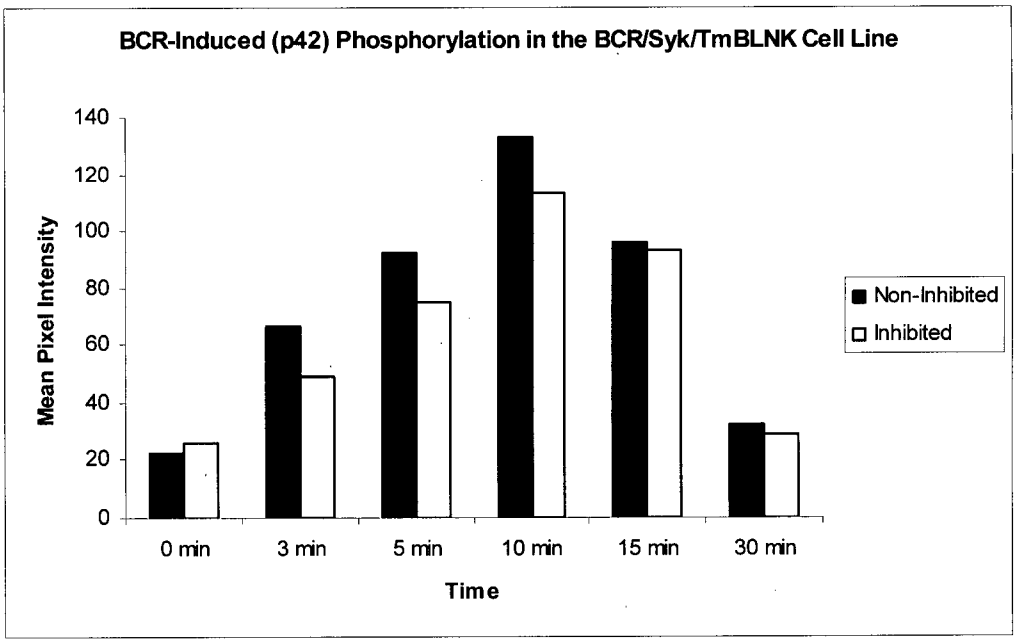

Figure 6.6. (b) Comparison of Mean Pixel Intensity of the Phosphorylated Erk "Bands" in the BCR/Syk/TmBLNK Cell Line in Non-Inhibited and PLC-Inhibited Co-Expression Samples. To calculate the mean pixel intensity of the phosphorylated Erk "band" it was first necessary to define the "band". This was done by visually identifying the largest band in the immunoblot and then manually selecting a square area around that band that captured all the pixels of the band yet minimized the capture of background pixels. An equivalent square area was then selected around the remaining bands again ensuring that all the pixels of the band were captured. The mean pixel intensity of the "bands" was then calculated using Matlab (refer to Chapter 2.15 for further details). By this method the mean pixel intensity should correlate to the band size and intensity such that the larger the mean pixel intensity the larger and more intense the band. The top graph considers the band intensities of the top phosphorylated Erk band (p44) and the bottom graph considers the band intensities of the bottom phosphorylated Erk band (p42).

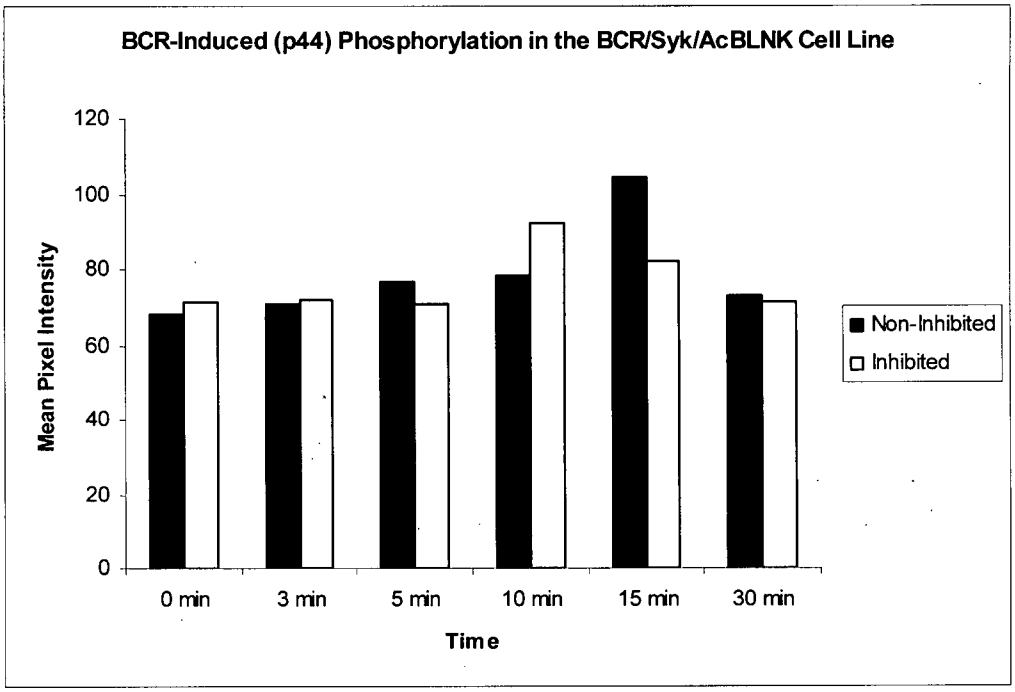

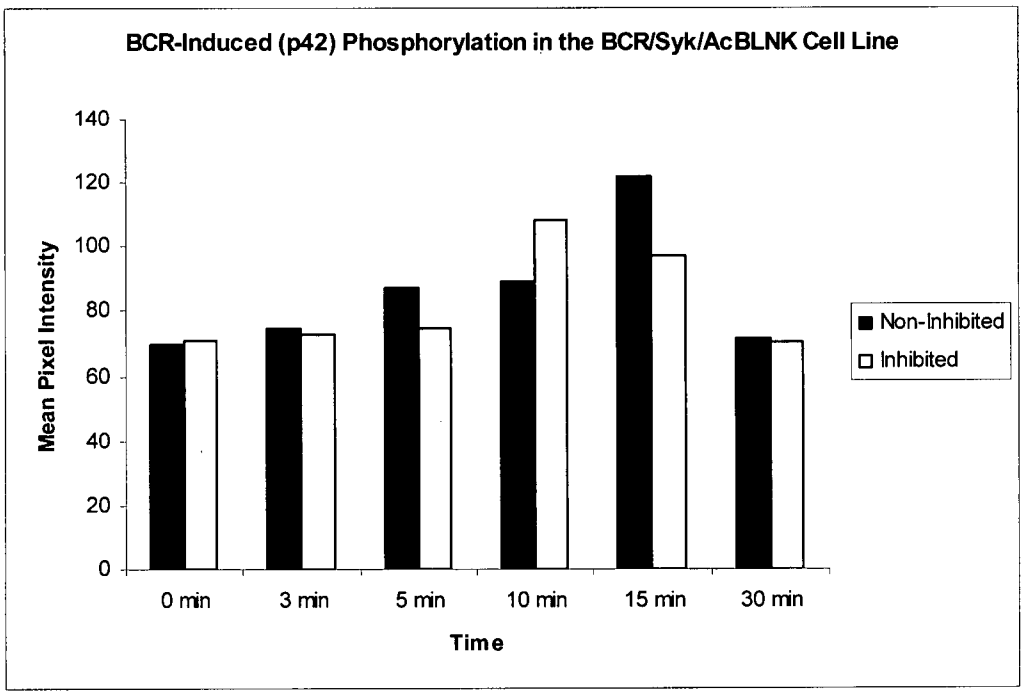

Figure 6.6. (c) Comparison of Mean Pixel Intensity of the Phosphorylated Erk "Bands" in the BCR/Syk/AcBLNK Cell Line in Non-Inhibited and PLC-Inhibited Samples. To calculate the mean pixel intensity of the phosphorylated Erk "band" it was first necessary to define the "band". This was done by visually identifying the largest band in the immunoblot and then manually selecting a square area around that band that captured all the pixels of the band yet minimized the capture of background pixels. An equivalent square area was then selected around the remaining bands again ensuring that all the pixels of the band were captured. The mean pixel intensity of the "bands" was then calculated using Matlab (refer to Chapter 2.15 for further details). By this method the mean pixel intensity should correlate to the band size and intensity such that the larger the mean pixel intensity the larger and more intense the band. The top graph considers the band intensities of the top phosphorylated Erk band (p44) and the bottom graph considers the band intensities of the bottom phosphorylated Erk band (p42).

6.2.3 Co-Expression of the BCR, Syk, and TmBLNK is Sufficient to Reconstitute BCR-Induced Phosphorylation of TmBLNK in AtT20-Derived Cell Lines

According to the aforementioned model BLNK must become tyrosine phosphorylated to facilitate the assembly of a BCR/PLCγ signaling complex. Given this, a failure to appropriately phosphorylate BLNK would be predicted to result in a failure to form the signaling complex and ultimately in a failure to phosphorylate and activate PLCγ. Thus, the phosphorylation status of TmBLNK and AcBLNK was assayed to determine if the apparently limited ability to effectively reconstitute BCR-induced PLCγ activation is reflective of an inability to phosphorylate membrane targeted BLNK. To do this the relevant cell lines were first stimulated by cross-linking the BCR with anti mIgM antibodies for a set length of time (as indicated in the figures). Cells were then lysed and 50 μg of whole cell lysate were resolved by SDS-PAGE. The resolved gels were then transferred to nitrocellulose filters that were subsequently immunoblotted with a phospho-BLNK (Tyr96) specific antibody (Fig. 6.7 and 6.9). Alternatively, BLNK was immunoprecipitated from 1000 μg of whole cell lysate using a BLNK-specific antibody. The immunoprecipitates were then resolved by SDS-PAGE and the resolved gels were then transferred to nitrocellulose filters that were subsequently immunoblotted with a pan-phospho-tyrosine specific antibody (4G10) (Fig. 6.8).

Co-expression of the BCR and Syk appears sufficient to reconstitute BCR-induced phosphorylation of both TmBLNK (Figs. 6.7 and 6.8) and AcBLNK (Fig. 6.9) in AtT20-Derived Cell Lines. Of interest is the observation that only the higher molecular weight form of BLNK, appears to be phosphorylated in the BCR/Syk/TmBLNK cell line (Figs. 6.7 and 6.8). This observation may correlate with the earlier observation that only the higher molecular weight form of BLNK appears to be associated with the plasma membrane (Fig. 6.4) in that failure of the lower molecular weight form to associate with the plasma membrane may preclude it from associating with and being phosphorylated by Syk. Also interesting is the observation that the higher molecular weight form of AcBLNK appears to be phosphorylated to a greater degree than the lower molecular weight form (Fig. 6.9). This may be a reflection of the fact that the higher molecular weight form appears to be more highly expressed than the lower weight form (Fig. 6.2). Alternatively, it may suggest that membrane association of BLNK allows it to be more efficiently phosphorylated as the higher molecular weight form appears to be predominantly

membrane associated while the lower molecular weight form appears to be predominantly cytosolic (Fig. 6.3). Regardless, BCR-induced phosphorylation of TmBLNK and AcBLNK appears to have been successfully reconstituted in this system. Yet, it remains to be determined if all of the necessary tyrosine residues in the constructs are being phosphorylated. It is possible that only a subset of the residues (including tyrosine 96) is becoming phosphorylated such that membrane targeted BLNK is unable to efficiently associate with PLCγ1 in this system. Accordingly, investigations were performed to determine if the ability to reconstitute BCR-induced phosphorylation of membrane targeted BLNK correlated with an ability to reconstitute assembly of a membrane targeted BLNK/PLCγ1 complex. Unfortunately, these studies were inconclusive (data not shown, refer to Appendix III). Alternatively, the phosphorylation status of PLCγ1 was investigated as, according to the initial model, an inability to reconstitute this event may be reflective of an inability to form a functional signaling complex. Furthermore, an inability to effectively reconstitute BCR-induced PLCγ phosphorylation would go towards explaining the apparent inability to reconstitute its activation.

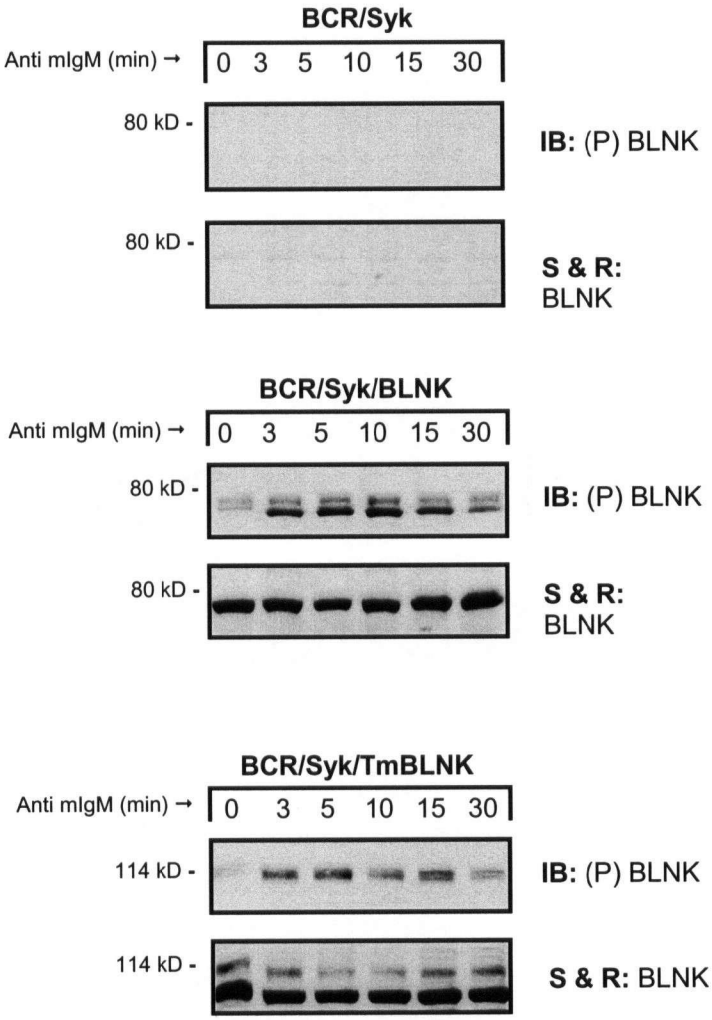

Figure 6.7. Co-Expression of the BCR, Syk and TmBLNK is Sufficient to Reconstitute BCR-Induced TmBLNK Phosphorylation in AtT20-Derived Cell Lines. The BCR was cross-linked with anti mIgM antibodies at 37 °C for the indicated length of time. Cells were then lysed and 50 μg of whole cell lysate were resolved by SDS-PAGE. Following electrophoresis, gels were transferred to nitrocellulose filters that were subsequently immunoblotted with a phospho-BLNK (Tyr96) specific antibody. Finally, filters were stripped and reprobed with a BLNK specific antibody. IB indicates the immunoblotting antibody while S&R indicates the antibody that was used to reprobe the filter. Data are representative of three independent experiments.

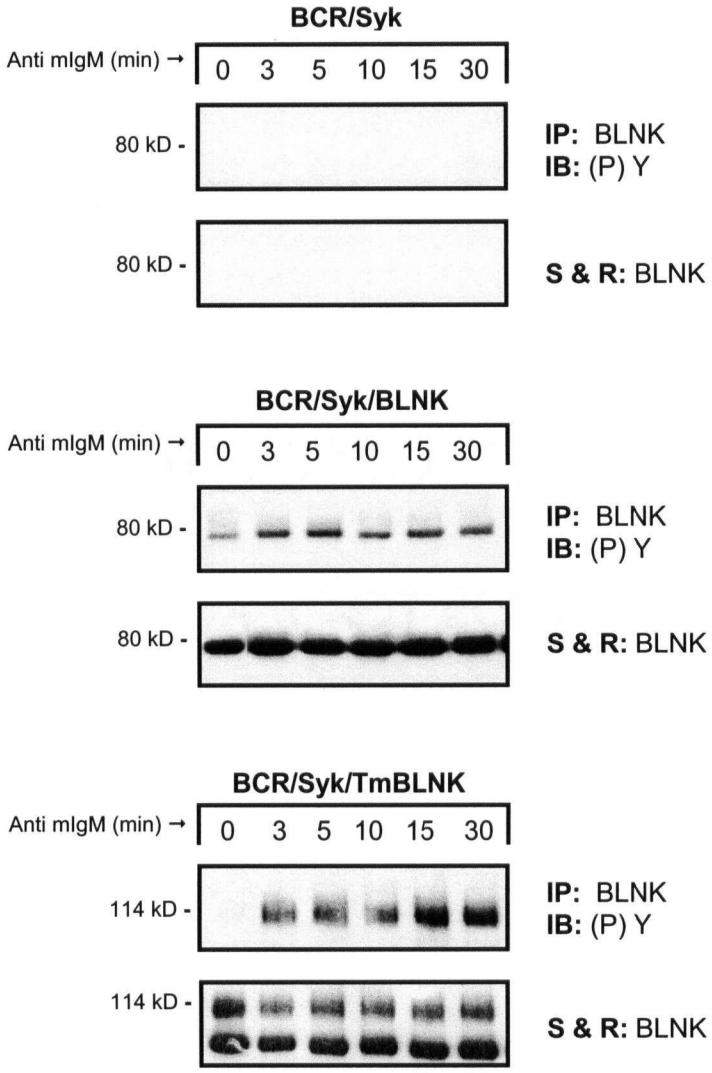

Figure 6.8. Co-Expression of the BCR, Syk and TmBLNK is Sufficient to Reconstitute BCR-Induced TmBLNK Phosphorylation in AtT20-Derived Cell Lines. The BCR was cross-linked with anti mIgM antibodies at 37 °C for the indicated length of time. Cells were then lysed and BLNK was immunoprecipitated from 1000 μg of whole cell lysate using Protein A-Sepharose and a BLNK specific antibody (H80). Immunoprecipitates were resolved by SDS-PAGE. Following electrophoresis, gels were transferred to nitrocellulose filters that were subsequently immunoblotted with a pan-phospho-tyrosine specific antibody (4G10 monoclonal antibody). Finally, filters were stripped and reprobed with a BLNK specific antibody (H80). IP indicates the immunoprecipitating antibody, IB indicates the immunoblotting antibody and S&R indicates the antibody that was used to reprobe the filter. Data are representative of three independent experiments.

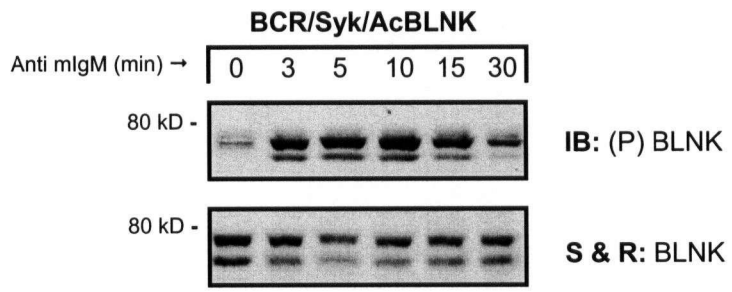

Figure 6.9. Co-Expression of the BCR, Syk and AcBLNK is Sufficient to Reconstitute BCR-Induced AcBLNK Phosphorylation in AtT20-Derived Cell Lines. The BCR was cross-linked with anti mIgM antibodies at 37 °C for the indicated length of time. Cells were then lysed and 50 μg of whole cell lysate were resolved by SDS-PAGE. Following electrophoresis, gels were transferred to nitrocellulose filters that were subsequently immunoblotted with a phospho-BLNK (Tyr96) specific antibody. Finally, filters were stripped and reprobed with a BLNK specific antibody. IB indicates the immunoblotting antibody while S&R indicates the antibody that was used to reprobe the filter. Data are representative of three independent experiments.

6.2.4 Co-Expression of the BCR, Syk and TmBLNK Appears to Enhance BCR-Induced PLCγ1 Phosphorylation in AtT20-Derived Cell Lines

As mentioned previously, PLCγ activation is dependent, in part, on it being phosphorylated (Carter *et al.*, 1991; Coggeshall *et al.*, 1992; Hempel *et al.*, 1992; reviewed in Rhee, 2001). Given this, the apparent inability to effectively reconstitute BCR-induced PLCγ activation may reflect an inability to appropriately phosphorylate PLCγ. Thus, investigations were performed to assay PLCγ's phosphorylation status in this system. To do this, the relevant cell lines were first stimulated by cross-linking the BCR with anti mIgM antibodies for a set length of time (as indicated in the figures). Cells were then lysed and PLCγ1 was immunoprecipitated from 1000 μg of whole cell lysate using a PLCγ1-specific antibody. The immunoprecipitates were then resolved by SDS-PAGE. The resultant gels were then transferred to nitrocellulose filters that were subsequently immunoblotted with a pan-phospho-tyrosine specific antibody (4G10) (Figs. 6.10, 6.11 and 6.12).

As can be seen in Figures 6.10 and 6.11, BCR-induced PLCγ1 phosphorylation appears to be enhanced in the BCR/Syk/TmBLNK cell line as compared to either the BCR/Syk or the BCR/Syk/BLNK cell line. This enhancement does not appear to be an artefact of expression levels as the BCR/Syk/TmBLNK cell line does not appear to express greater levels of BLNK as compared to the BCR/Syk/BLNK cell line (compare Fig. 4.2 to Figure 6.2 and data not shown). However, it should be noted that it is difficult to accurately compare expression levels of BLNK versus TmBLNK as the BLNK specific antibody may not recognize the two proteins with the same affinity. Barring the possibility of expression level effects, the enhancement of BCR-induced PLCγ1 phosphorylation in the BCR/Syk/TmBLNK cell line suggests that plasma membrane-targeting of BLNK may enhance its ability to form a functional BCR/PLCγ signaling complex in this system. In contrast, AcBLNK expression does not appear to significantly enhance BCR-induced PLCγ1 phosphorylation (Fig. 6.12). This suggests that all forms of plasma membrane targeting may not be equivalent (refer to Chapter 6.3.2 for further discussion). Regardless, while membrane targeting of BLNK may enhance BCR-induced PLCγ1 phosphorylation it does not appear to significantly enhance BCR-induced PLCγ1 activation as compared to cytosolic BLNK. Thus, the apparent inability to maximally reconstitute BCR-induced PLCγ1 activation is not merely a reflection of an inability to recruit BLNK to the plasma membrane in this system. Given this, further experiments were performed to investigate why

this pathway may still be failing to maximally reconstitute. In particular, PLCγ may be unable to appropriately associate with the various BLNK constructs and therefore, be unable to be recruited to the plasma membrane-associated BCR signaling complex. Thus, investigations were performed to determine where PLCγ1 is localized in this system.

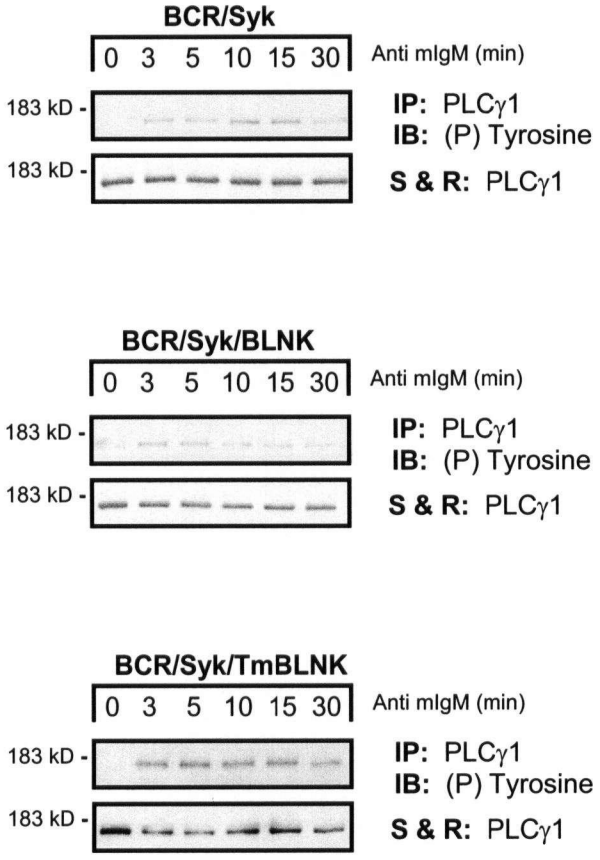

Figure 6.10. Co-Expression of the BCR, Syk and TmBLNK Appears to Enhance BCR-Induced PLCγ1 Phosphorylation in AtT20-Derived Cell Lines. The BCR was cross-linked with anti mIgM antibodies at 37 °C for the indicated length of time. Cells were then lysed and PLCγ1 was immunoprecipitated from 1000 μg of whole cell lysate using Protein A-Sepharose and a PLCγ1 specific antibody. Immunoprecipitates were resolved by SDS-PAGE. Following electrophoresis, gels were transferred to nitrocellulose filters that were subsequently immunoblotted with a pan-phospho-tyrosine specific antibody (4G10 monoclonal antibody). Finally, filters were stripped and reprobed with a PLCγ1 specific antibody. IP indicates the immunoprecipitating antibody, IB indicates the immunoblotting antibody and S&R indicates the antibody that was used to reprobe the filter. Data are representative of two independent experiments.

Figure 6.11. Co-Expression of the BCR, Syk and TmBLNK Appears to Enhance BCR-Induced PLCγ1 Phosphorylation in AtT20-Derived Cell Lines. The BCR was cross-linked with anti mIgM antibodies at 37 °C for the indicated length of time. Cells were then lysed and PLCγ1 was immunoprecipitated from 1000 μg of whole cell lysate using Protein A-Sepharose and a PLCγ1 specific antibody. Immunoprecipitates were resolved by SDS-PAGE. Following electrophoresis, gels were transferred to nitrocellulose filters that were subsequently immunoblotted with a pan-phospho-tyrosine specific antibody (4G10 monoclonal antibody). Finally, filters were stripped and reprobed with a PLCγ1 specific antibody. IP indicates the immunoprecipitating antibody, IB indicates the immunoblotting antibody and S&R indicates the antibody that was used to reprobe the filter. Data are representative of three independent experiments. As well, similar results were observed with two additional clones.

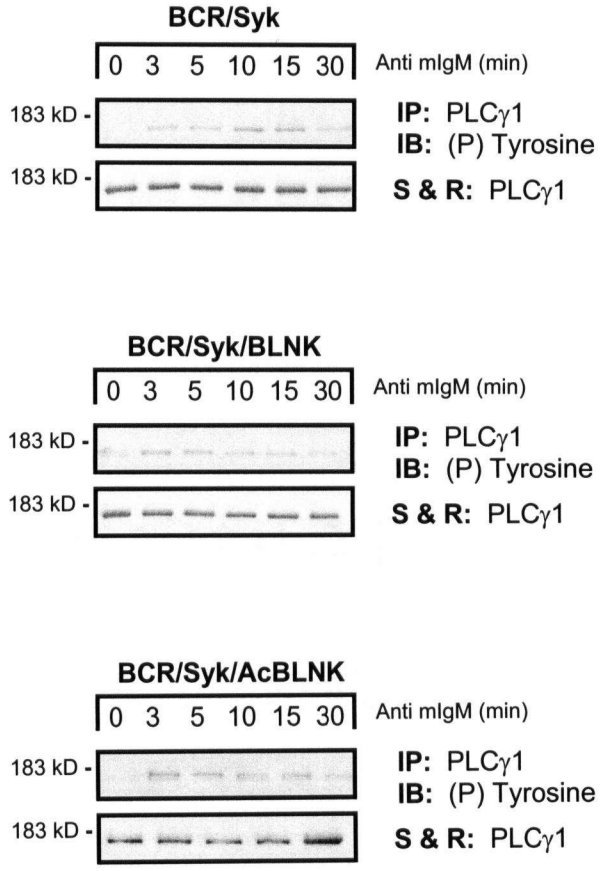

Figure 6.12. Co-Expression of AcBLNK along with the BCR and Syk Does Not Appear to Significantly Enhance BCR-Induced PLCγ1 Phosphorylation in AtT20-Derived Cell Lines. The BCR was cross-linked with anti mIgM antibodies at 37 °C for the indicated length of time. Cells were then lysed and PLCγ1 was immunoprecipitated from 1000 μg of whole cell lysate using Protein A-Sepharose and a PLCγ1 specific antibody. Immunoprecipitates were resolved by SDS-PAGE. Following electrophoresis, gels were transferred to nitrocellulose filters that were subsequently immunoblotted with a pan-phospho-tyrosine specific antibody (4G10 monoclonal antibody). Finally, filters were stripped and reprobed with a PLCγ1 specific antibody. IP indicates the immunoprecipitating antibody, IB indicates the immunoblotting antibody and S&R indicates the antibody that was used to reprobe the filter. Data are representative of three independent experiments.

6.2.5 Co-Expression of the BCR, Syk and TmBLNK or AcBLNK Is Not Sufficient to Reconstitute Inducible Membrane Recruitment of PLCγ1 in AtT20-Derived Cell Lines

Initial attempts to reconstitute the BCR/PLCγ signaling pathway in AtT20-derived cell lines proved unsuccessful (refer to Chapter 4). This lack of success may be due to an inability to effectively recruit BLNK and PLCγ1 to the plasma membrane to form a functional BCR/PLCγ signaling complex (as evidenced in Chapter 5.2.6). Thus, BLNK was constitutively targeted to the plasma membrane in anticipation that once so targeted it could become appropriately phosphorylated and subsequently associate with and recruit PLCγ1 into a functional signaling complex. Unfortunately, such targeting does not appear sufficient to reconstitute BCR-induced PLCγ1 activation in this system (Chapter 6.2.2 and 6.2.4). A possible explanation for this finding may be that membrane targeted BLNK, despite being phosphorylated, is still unable to associate with and recruit PLCγ1. Thus, the localization status of PLCγ1 was investigated. To do this the relevant cell lines were stimulated by cross-linking the BCR with anti mIgM antibodies for five minutes. The cells were then fractioned into membrane-enriched fractions and cytosolic fractions (refer to Chapter 2.7 for details). The fractions were resolved by SDS-PAGE and the resolved gels were transferred to nitrocellulose filters that were subsequently immunoblotted with BLNK, PLCγ1, Igα or tubulin specific antibodies (Figure 6.13). As mentioned previously, this approach is limited to distinguishing whether a protein is localized to the cytosol and/or to cellular membranes. This approach can not distinguish whether a protein is localized to the plasma membrane and/or to other cellular membranes. Nonetheless, this approach can be suggestive as to whether or not a cytosolic protein is being recruited to the membrane-fraction following BCR cross-linking.

As can be seen in Figure 6.13, PLCγ1 appears associate with both the cytosolic and membrane-enriched fractions in the AtT20-derived cell lines. However, the vast majority of PLCγ1 appears to be in the cytosolic fraction (Fig. 6.13). Moreover, the distribution of the PLCγ1 does not appear to change following BCR cross-linking in either the cell line expressing cytosolic BLNK or the cell lines expression membrane targeted BLNK (Fig. 6.13). Thus, membrane-targeting of BLNK does not appear sufficient to reconstitute BCR-induced PLCγ1 plasma membrane recruitment. Given this, the apparent inability to reconstitute BCR-induced PLCγ1 activation may reflect an inability to form a functional plasma membrane-associated BCR/PLCγ1 signaling

complex in this system. To address this possibility PLCγ was constitutively targeted to the plasma membrane.

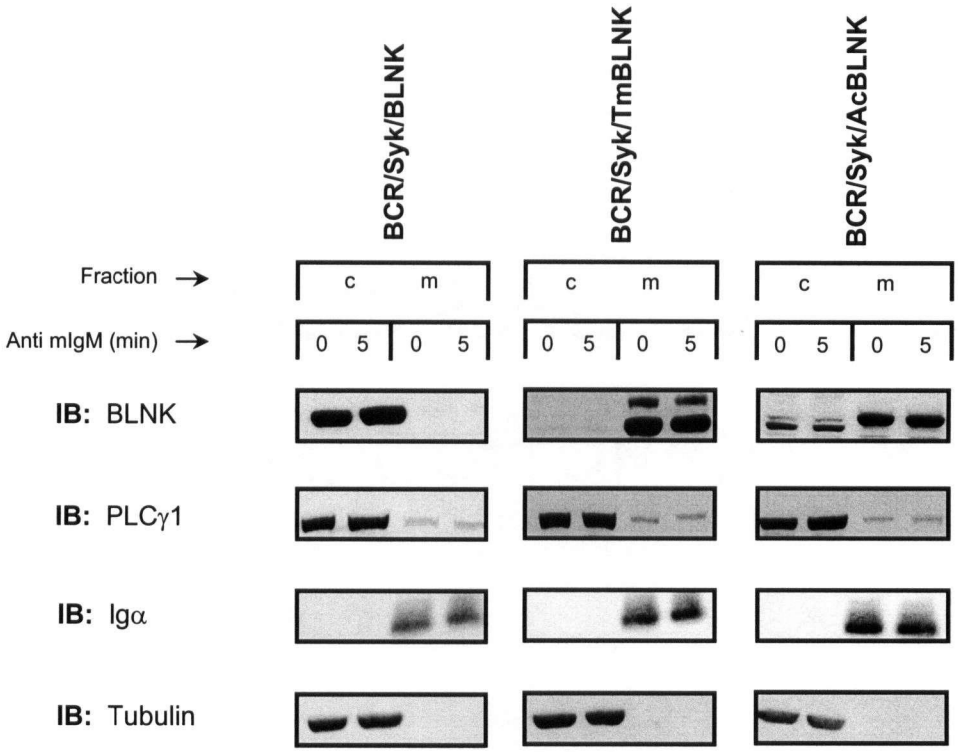

Figure 6.13. Co-expression of TmBLNK or AcBLNK, Along with the BCR and Syk, Does not Appear Sufficient to Reconstitute Inducible Membrane Recruitment of PLCγ1 in AtT20-Derived Cell Lines. The BCR was cross-linked with anti mIgM antibodies at 37 °C for 5 minutes. Cells were then fractionated according to the membrane-enrichment protocol (detailed in Chapter 2.7). 50 μg of each fraction was resolved by SDS-PAGE. The resolved gels were then transferred to nitrocellulose filters that were subsequently immunoblotted with BLNK, PLCγ1, Igα or Tubulin specific antibodies. Igα and Tubulin localization was used to confirm that the fractions were not cross-contaminated. Igα is a transmembrane protein and as such is expected to be apparent only in the membrane-enriched fraction whereas Tubulin is a cytosolic protein and as such is expected to be apparent only in the cytosolic fraction. IB indicates the immunoblotting antibody. "c" indicates the cytosolic fraction and "m" indicates the membrane-enriched fraction. Data are representative of three independent experiments.

6.2.6 Co-Expression of the BCR, Syk and AcPLCγ2 Appears to Enhance BCR-Induced, PLC-Dependent Erk Phosphorylation in AtT20-Derived Cell Lines

The BCR/Syk/AcPLCγ2 and BCR/Syk/AcBLNK/AcPLCγ2 cell lines were established as described in Chapter 6.2.1. The PLCγ2 isoform was targeted to the plasma membrane as opposed to the PLCγ1 isoform simply because the plasmid encoding for human PLCγ2 was readily available. As both PLCγ1 and PLCγ2 have been shown to be activated in the BCR signaling pathway (Carter *et al.*, 1991, Coggeshall *et al.*, 1992, Hemple *et al.*, 1992, Roifman and Wang, 1992) and to interact with BLNK (Fu *et al.*, 1998), use of the PLCγ2 isoform was not anticipated to be detrimental to these investigations. However, control experiments were performed with the cytoplasmic form of PLCγ2 to ensure that any results observed were attributable to the membrane targeting of PLCγ2 as opposed to being attributable to either isoform specific effects or over-expression effects (refer to Chapter 6.2.8). Having established that AcPLCγ2 is successfully targeted to the plasma membrane (Chapter 6.2.1), the sufficiency of this construct to reconstitute BCR-induced PLCγ activation (as evidenced by BCR-induced, PLC-dependent increases in Erk phosphorylation) was assayed. To do this the relevant cell lines were stimulated by cross-linking the BCR with anti mIgM antibodies for a set length of time (as indicated in the figures), in the presence or absence of a PLC inhibitor (U73122). Cells were then lysed and 50 μg of whole cell lysate were resolved by SDS-PAGE. Following electrophoresis, gels were transferred to nitrocellulose filters that were subsequently immunoblotted with a phospho-Erk (Thr202/Tyr204) specific antibody. Finally, filters were stripped and reprobed with an Erk specific antibody.

As can be seen in Figure 6.14, Erk phosphorylation is significantly enhanced following BCR cross-linking in both the BCR/Syk/AcPLCγ2 cell line and the BCR/Syk/AcBLNK/AcPLCγ2 cell line as compared to the BCR/Syk cell line. This increase appears to be PLC-dependent as it is inhibited when the cell lines are treated with the PLC inhibitor, U73122 (Fig. 6.15a, b and c). Interestingly, BCR-induced, PLC-dependent Erk phosphorylation appears to be more significantly enhanced in the BCR/Syk/AcBLNK/AcPLCγ2 cell line as compared to the BCR/Syk/AcPLCγ2 cell line (Figs. 6.14 and 6.15). While this may suggest that co-expression of AcBLNK and AcPLCγ2 has a synergistic effect on BCR-induced AcPLCγ2 activation this observation may also be due to differences in the expression levels of the AcPLCγ2 construct. In particular, the BCR/Syk/AcPLCγ cell line appears to express significantly more AcPLCγ2 than

the BCR/Syk/AcBLNK/AcPLCγ2 cell line (Fig. 6.2). Ideally, expression level effects could be ruled out by comparing clones that express similar levels of these clones. Unfortunately, this was unable to be achieved as attempts to isolate multiple BCR/Syk/AcBLNK/AcPLCγ2 clones were unsuccessful. Regardless, these data suggest that co-expression of the BCR, Syk and acylated PLCγ2 is sufficient to reconstitute BCR-induced, PLC-dependent Erk phosphorylation. Thus, it may well be that previous attempts to reconstitute BCR-induced PLCγ activation in this system were unsuccessful due to an inability to appropriately compartmentalize PLCγ to the plasma membrane. However, the observed reconstitution of BCR-induced PLCγ activation may also be due to either isoform effects (i.e., PLCγ2 as opposed to PLCγ1) or due to over-expression effects. To rule out these latter possibilities, control experiments were performed in AtT20-derived cell lines that express exogenous, cytosolic human PLCγ2.

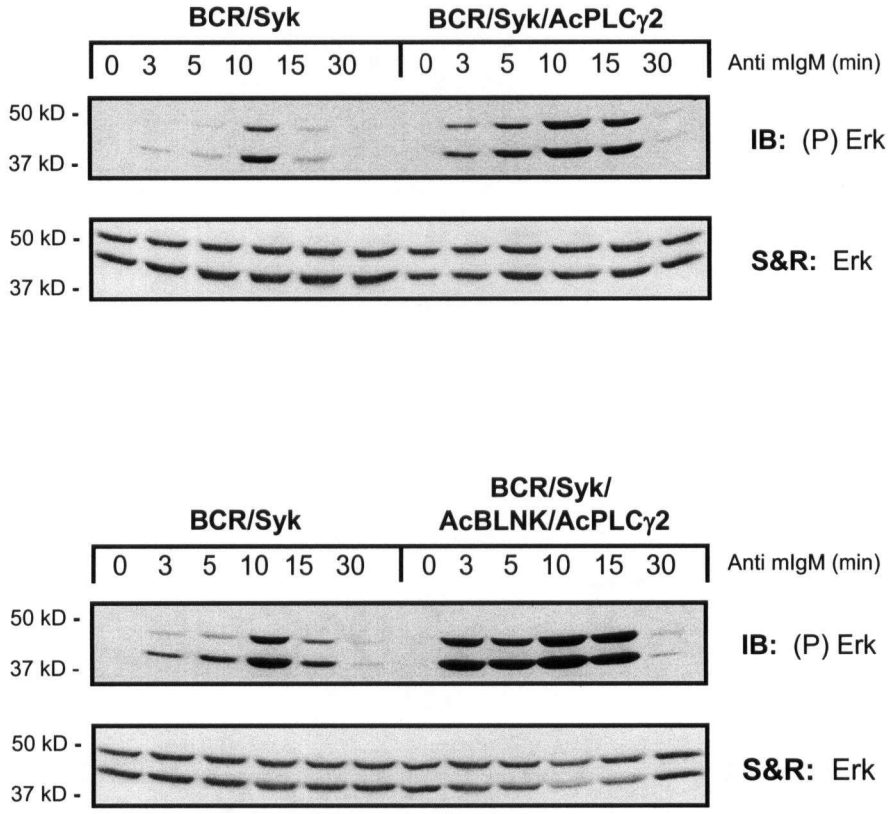

Figure 6.14. Co-Expression of the BCR, Syk, and AcPLCγ2 Significantly Enhances BCR-Induced Erk Phosphorylation in AtT20-Derived Cell Lines. The BCR was cross-linked with anti mIgM antibodies at 37 °C for the indicated length of time. Cells were then lysed and 50 μg of whole cell lysate were resolved by SDS-PAGE. Following electrophoresis, gels were transferred to nitrocellulose filters that were subsequently immunoblotted with a phospho-Erk (Thr202/Tyr204) specific antibody. Finally, filters were stripped and reprobed with an Erk specific antibody. IB indicates the immunoblotting antibody while S&R indicates the antibody used to reprobe the filter. Data are representative of three independent experiments.

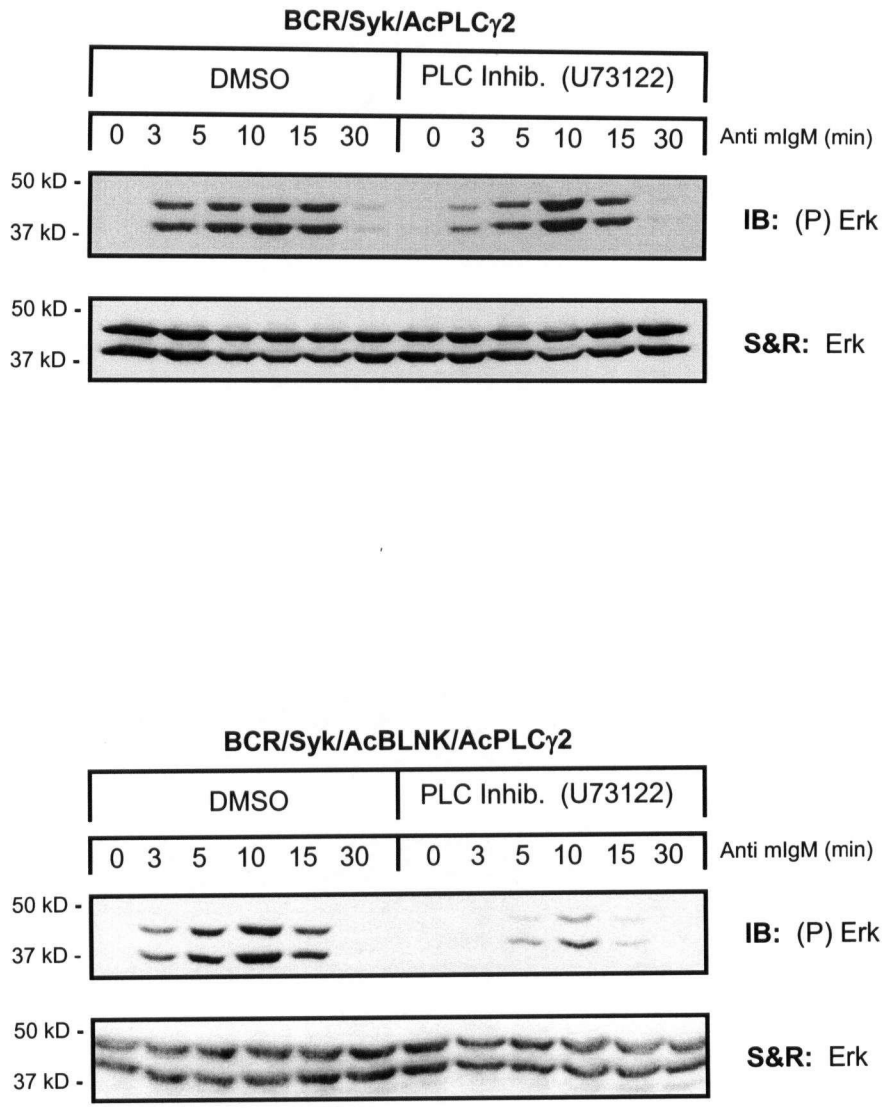

Figure 6.15. (a) Co-Expression of the BCR, Syk and AcPLCγ2 is Sufficient to Reconstitute BCR-Induced, PLC-Dependent Erk Phosphorylation in AtT20-Derived Cell Lines. Cells were treated either with DMSO (negative control) or the PLC inhibitor, U73122 (at a final concentration of 10 μM) for 1 hour. The BCR was then cross-linked with anti mIgM antibodies at 37 °C for the indicated length of time. Cells were then lysed and 50 μg of whole cell lysate were resolved by SDS-PAGE. Following electrophoresis, gels were transferred to nitrocellulose filters that were subsequently immunoblotted with a phospho-Erk (Thr202/Tyr204) specific antibody. Finally, filters were stripped and reprobed with an Erk specific antibody. IB indicates the immunoblotting antibody while S&R indicates the antibody used to reprobe the filter. Data are representative of three independent experiments.

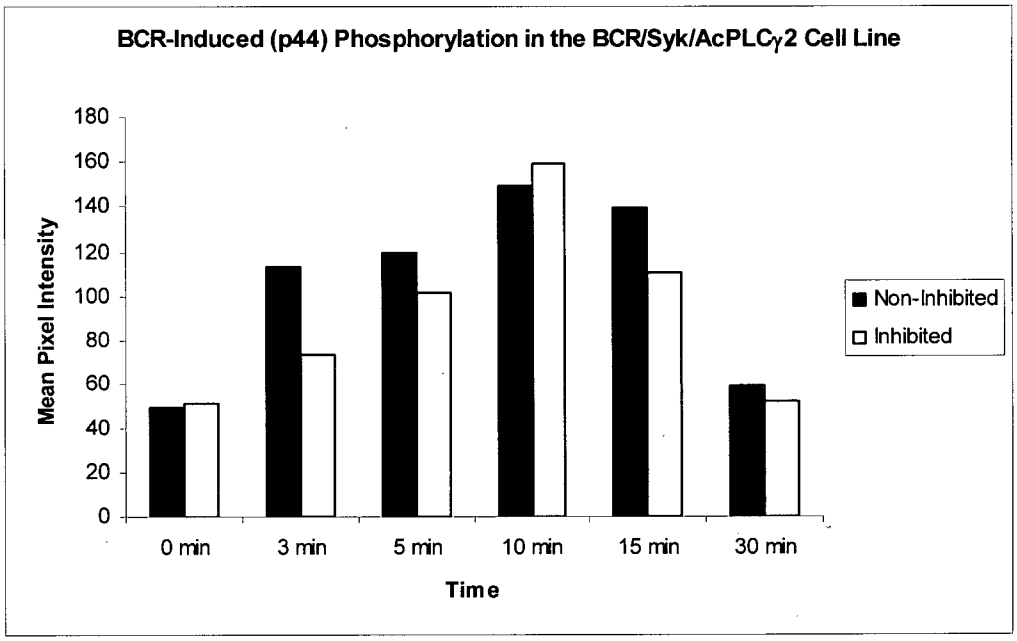

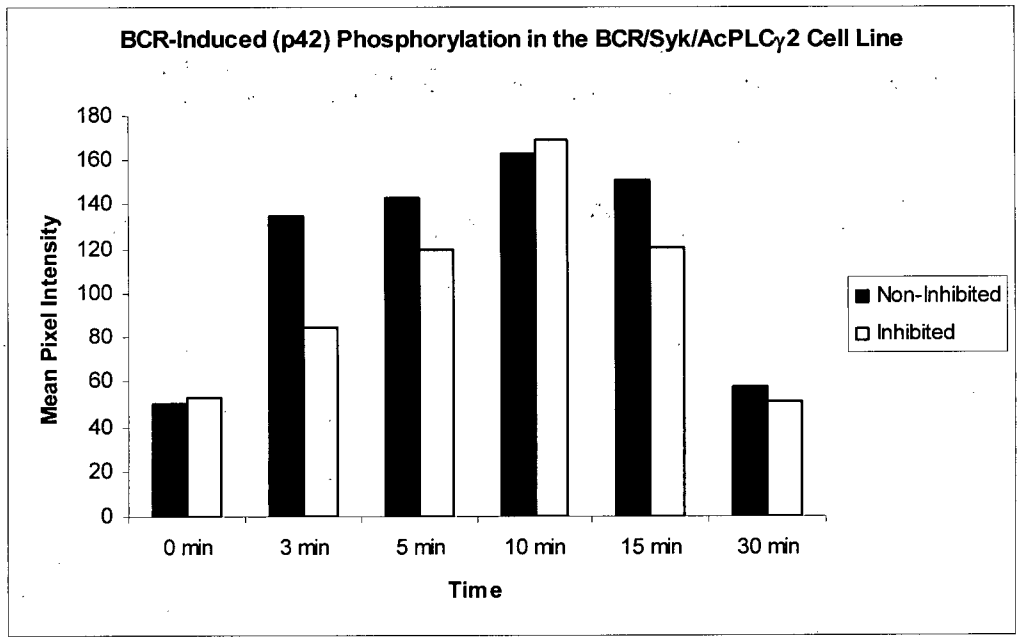

Figure 6.15. (b) Comparison of Mean Pixel Intensity of the Phosphorylated Erk "Bands" in the BCR/Syk/AcPLCγ2 Cell Line in Non-Inhibited and PLC-Inhibited Co-Expression Samples. To calculate the mean pixel intensity of the phosphorylated Erk "band" it was first necessary to define the "band". This was done by visually identifying the largest band in the immunoblot and then manually selecting a square area around that band that captured all the pixels of the band yet minimized the capture of background pixels. An equivalent square area was then selected around the remaining bands again ensuring that all the pixels of the band were captured. The mean pixel intensity of the "bands" was then calculated using Matlab (refer to Chapter 2.15 for further details). By this method the mean pixel intensity should correlate to the band size and intensity such that the larger the mean pixel intensity the larger and more intense the band. The top graph considers the band intensities of the top phosphorylated Erk band (p44) and the bottom graph considers the band intensities of the bottom phosphorylated Erk band (p42).

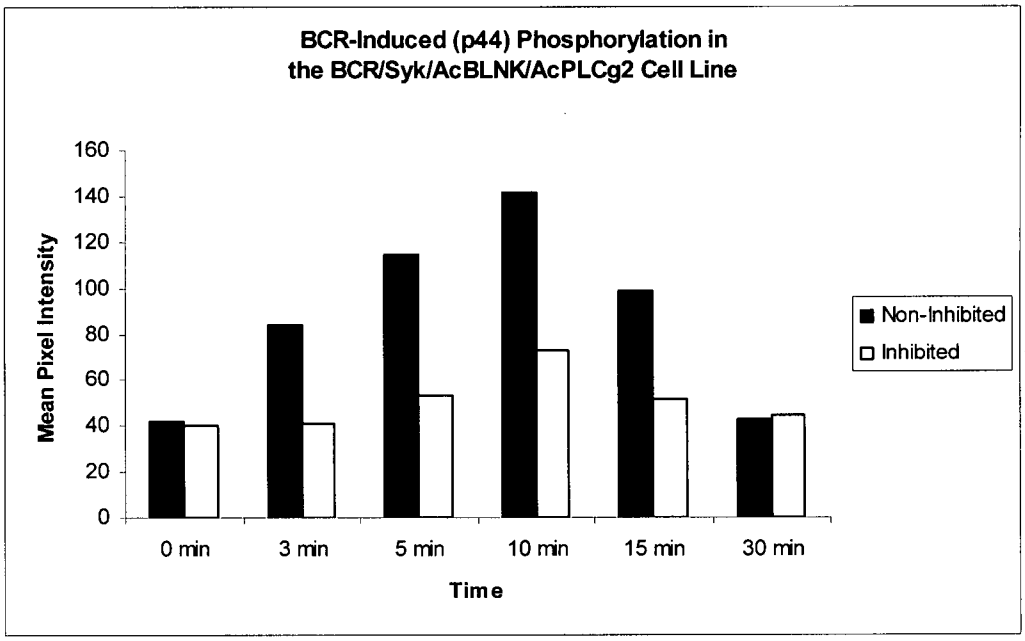

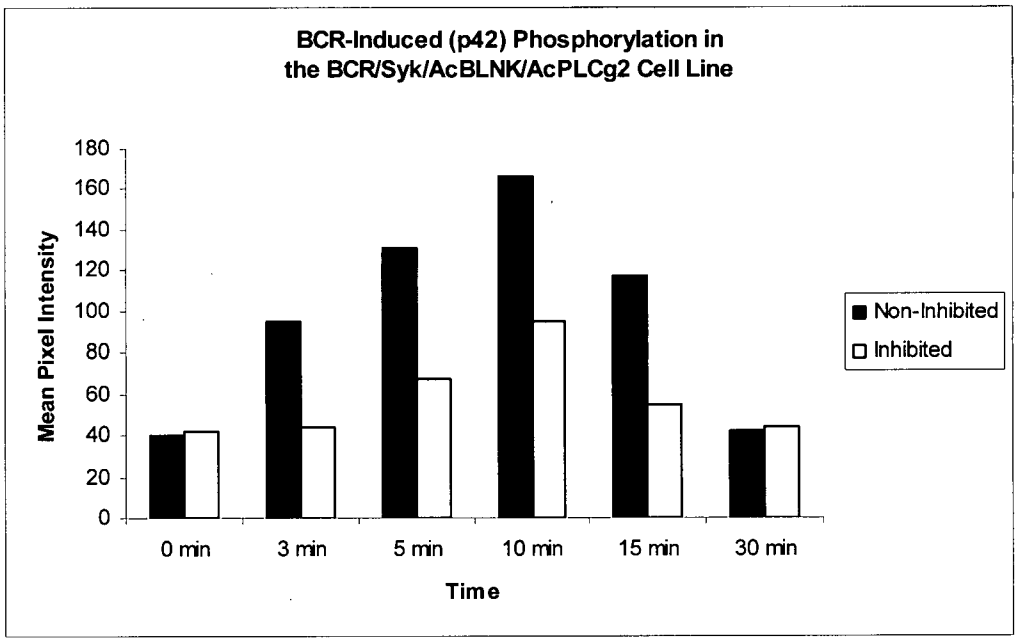

Figure 6.15. (c) Comparison of Mean Pixel Intensity of the Phosphorylated Erk "Bands" in the BCR/Syk/AcBLNK/AcPLCγ2 Cell Line in Non-Inhibited and PLC-Inhibited Co-Expression Samples. To calculate the mean pixel intensity of the phosphorylated Erk "band" it was first necessary to define the "band". This was done by visually identifying the largest band in the immunoblot and then manually selecting a square area around that band that captured all the pixels of the band yet minimized the capture of background pixels. An equivalent square area was then selected around the remaining bands again ensuring that all the pixels of the band were captured. The mean pixel intensity of the "bands" was then calculated using Matlab (refer to Chapter 2.15 for further details). By this method the mean pixel intensity should correlate to the band size and intensity such that the larger the mean pixel intensity the larger and more intense the band. The top graph considers the band intensities of the top phosphorylated Erk band (p44) and the bottom graph considers the band intensities of the bottom phosphorylated Erk band (p42).

6.2.7 Co-Expression of the BCR, Syk and AcPLCγ2 Is Sufficient to Reconstitute BCR-Induced AcPLCγ2 Phosphorylation in AtT20-Derived Cell Lines.

Before, looking at possible isoform and expression level effects, it was of interest to determine if enhanced PLCγ activation correlates with enhanced PLCγ phosphorylation. To do this, the AcPLCγ expressing cell lines and the BCR/Syk/BLNK cell line were stimulated by cross-linking the BCR with anti mIgM antibodies for a set length of time (as indicated in the figures). Cells were then lysed and PLCγ1 or PLCγ2 was immunoprecipitated from 1000 μg of whole cell lysate using a PLCγ1 or PLCγ2 specific antibody. The immunoprecipitates were then resolved by SDS-PAGE. The resolved gels were then transferred to nitrocellulose filters that were subsequently immunoblotted with a pan-phospho-tyrosine specific antibody (4G10) (Figs. 6.16) such that the phosphorylation levels of endogenous PLCγ1 and exogenous AcPLCγ2 could be compared. From this it is apparent that BCR-induced AcPLCγ2 phosphorylation is not significantly enhanced relative to what is observed for endogenous PLCγ1 in a comparable cell line (top panel versus bottom two panels of Fig. 6.16). This finding is significant in that it first suggests that a minimal increase in PLCγ phosphorylation can be sufficient for significant activation (as is seen with AcPLCγ2, Fig, 6.15) and second, that such phosphorylation does not necessarily equate with significant activation (as is seen with endogenous PLCγ1, Fig. 4.6). And, while it is possible that this differential activation status is actually reflective of PLCγ1 and AcPLCγ2 being differentially phosphorylated (i.e., phosphorylated to a similar extent yet on different sites) it seems more likely that this is indicative of a further requirement, beyond tyrosine phosphorylation, for PLCγ activation. This requirement could include the compartmentalization of PLCγ in lipid rafts and as such explain the success of AcPLCγ2 in reconstituting BCR-induced PLCγ activation in this system.

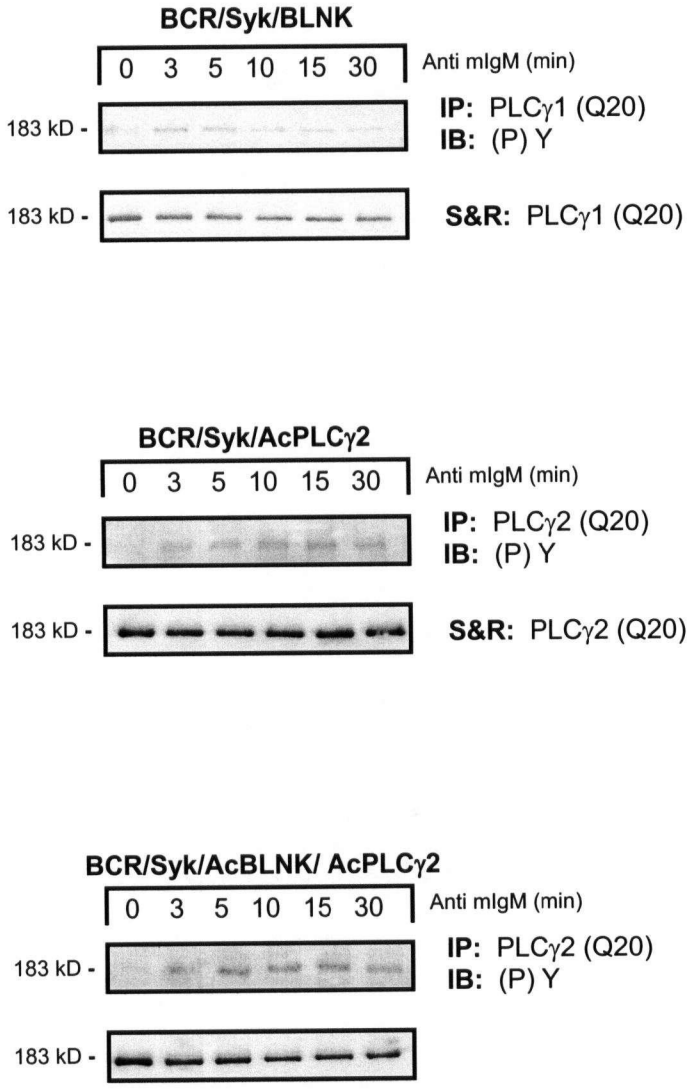

Figure 6.16. Co-Expression of the AcPLCγ2, Along with the BCR and Syk, Appears to Sufficient to Reconstitute BCR-Induced AcPLCγ2 Phosphorylation in AtT20-Derived Cell Lines. The BCR was cross-linked with anti mIgM antibodies at 37 °C for the indicated length of time. Cells were then lysed and PLCγ1 or PLCγ2 was immunoprecipitated from 1000 μg of whole cell lysate using Protein A-Sepharose and a PLCγ1 or PLCγ2 specific antibody (as indicated). Immunoprecipitates were resolved by SDS-PAGE. Following electrophoresis, gels were transferred to nitrocellulose filters that were subsequently immunoblotted with a pan-phospho-tyrosine specific antibody (4G10 monoclonal antibody). Finally, filters were stripped and reprobed with a PLCγ1 or PLCγ2 specific antibody (as indicated). IP indicates the immunoprecipitating antibody, IB indicates the immunoblotting antibody and S&R indicates the antibody that was used to reprobe the filter. Data are representative of two independent experiments.

6.2.8 Co-Expression of PLCγ2, Along with the BCR, BLNK and Syk, Does Not Appear to Enhance BCR-Induced Erk Phosphorylation in AtT20-Derived Cell Lines

AtT20 cell lines were established that express exogenous human PLCγ2. These cell lines serve as a control to ensure that the observed enhanced BCR-induced PLCγ activation was due to targeting PLCγ2 to the plasma membrane as opposed to being due to either isoform effects or over-expression effects. To do this the previously established BCR/Syk/BLNK cell line was further transfected with a plasmid encoding for a drug resistant marker and a plasmid encoding for human PLCγ2 (detailed in Chapter 2.1.3). Following transfection drug-resistant clones were isolated and screened for the ability to express human PLCγ2. From this, several clones were established, each of which expresses a different amount of cytosolic human PLCγ2 (data not shown and Fig. 6.17). As can be seen in Figure 6.17, BCR/Syk/BLNK/PLCγ2 clone 1 and clone 2 both appear to express high levels of cytosolic PLCγ2. Furthermore, these expression levels appear to be greater than that observed for AcPLCγ2 in the BCR/Syk/AcBLNK/AcPLCγ2 cell line (Fig. 6.17). This is a desirable situation as the former two cell lines are to be used to confirm that the observed enhancement of PLCγ2 activation in the BCR/Syk/AcBLNK/AcPLCγ2 cell line is not merely a consequence of over-expressing PLCγ2. However, it should be noted that it is difficult to directly compare PLCγ2 versus AcPLCγ2 expression levels as the PLCγ2 specific antibody may not recognize the two proteins with the same affinity. Regardless, BCR-induced Erk phosphorylation does not appear to be enhanced in the BCR/Syk/PLCγ2 cell lines as compared to the BCR/Syk cell line (Fig. 6.18). This is in stark contrast to what is observed for the BCR/Syk/AcPLCγ2 and BCR/Syk/AcBLNK/AcPLCγ2 cell lines (Fig. 6.15). Given this, it appears that enhancement of BCR-induced PLCγ activation in the latter two cell lines is likely a consequence of compartmentalizing PLCγ2 to the plasma membrane as opposed to being a consequence of either an isoform-specific or an over-expression effect. Ultimately, these findings concur with those of Chapter 5 that suggest that PLCγ phosphorylation itself may not predicate PLCγ activation. Rather, it seems that phosphorylation must also be accompanied by appropriate membrane compartmentalization, putatively in lipid rafts, for PLCγ to be effectively/maximally activated.

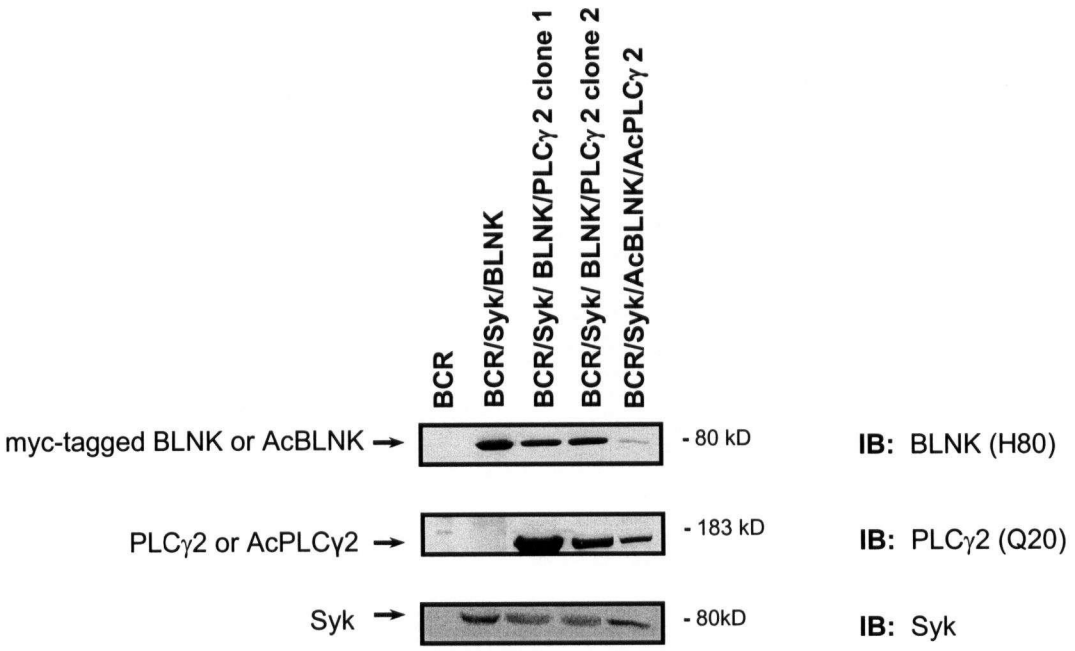

Figure 6.17. Characterization of Syk, BLNK, and PLCγ2 Expression in Transfected AtT20 Cell Lines. Thirty five micrograms of whole cell lysate were resolved by SDS-PAGE. Following electrophoresis, gels were transferred to nitrocellulose filters that were subsequently immunoblotted with antibodies specific for BLNK, Syk and PLCγ2. IB indicates the immunoblotting antibody.

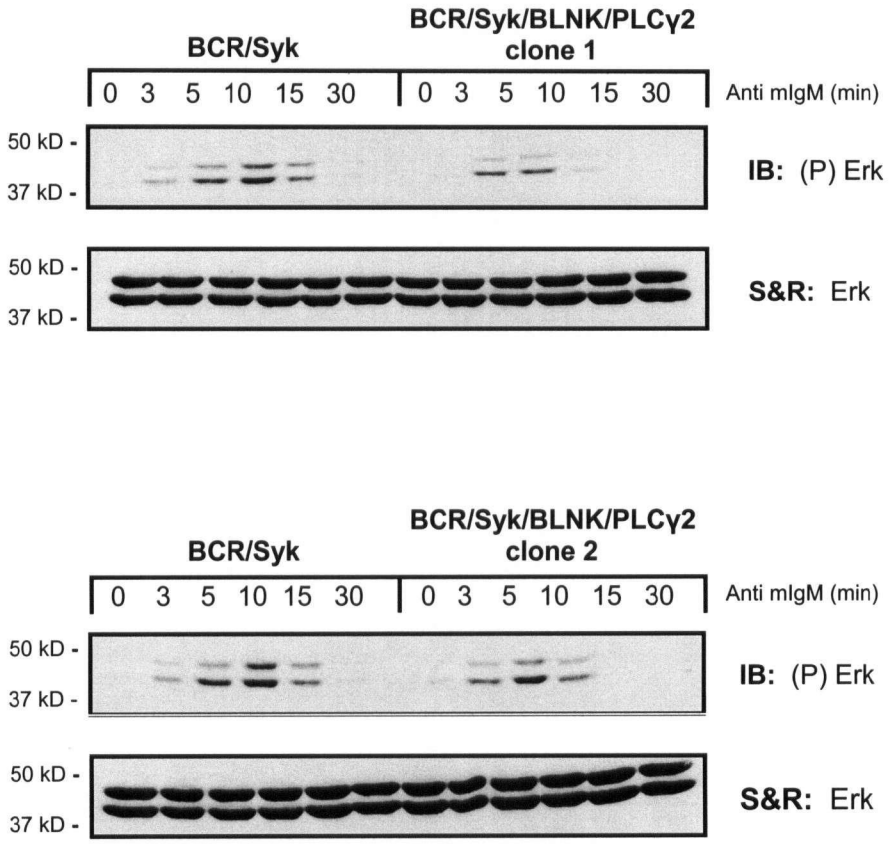

Figure 6.18. Co-Expression of AcPLCγ2, Along with the BCR and Syk, Does Not Appear to Enhance BCR-Induced Erk Phosphorylation in AtT20-Derived Cell Lines. The BCR was cross-linked with anti mIgM antibodies at 37 °C for the indicated length of time. Cells were then lysed and 50 μg of whole cell lysate were resolved by SDS-PAGE. Following electrophoresis, gels were transferred to nitrocellulose filters that were subsequently immunoblotted with a phospho-Erk (Thr202/Tyr204) specific antibody. Finally, filters were stripped and reprobed with an Erk specific antibody. IB indicates the immunoblotting antibody while S&R indicates the antibody used to reprobe the filter. Data are representative of three independent experiments.

6.3 Discussion

6.3.1 Targeting Human BLNK and Human PLCγ2 to the Plasma Membrane in AtT20 Derived Cell Lines

Signaling pathways are regulated, in part, by controlled compartmentalization of their various signaling components in various cellular compartments and/or complexes. In the case of the BCR/PLCγ signaling pathway, both BLNK and PLCγ are compartmentalized to the cytosol in resting B cells. These components are then recruited to the plasma membrane where they purportedly form a BCR/PLCγ signaling complex upon BCR cross-linking (reviewed in Kurosaki and Tsukada, 2000; Gold, 2002). Moreover, recent studies have suggested that this complex forms in specialized plasma membrane microdomains termed lipid rafts (Su *et al.*, 2002; Stoddart *et al.*, 2002; Cheng *et al.*, 2001; Aman and Ravichandran, 2000; Guo *et al.*, 2000; Petrie *et al.*, 2000; Wientraub *et al.*, 2000; Cheng *et al.*, 1999). Thus, compartmentalization of BLNK and PLCγ to the plasma membrane, and perhaps more specifically to lipid rafts in the plasma membrane, is thought to be required to couple the BCR to PLCγ activation.

In this thesis, initial attempts to reconstitute the BCR/PLCγ pathway were met with limited success. Upon further investigation it was found that BLNK and PLCγ were not being recruited to lipid rafts (data not shown) nor even more generally to the plasma membrane (Chapter 5.2.6) in AtT20-Derived Cell Lines. As such, it was hypothesized that the limited ability to reconstitute this pathway was a consequence of an inability to appropriately compartmentalize BLNK and PLCγ following BCR cross-linking. Thus, to test this hypothesis, BLNK and PLCγ were constitutively targeted to the plasma membrane in this system.

As discussed in the introduction to this chapter, TmBLNK and TmPLCγ constructs were created to constitutively target these proteins to the plasma membrane (Fig. 6.1a). Additionally, AcBLNK and AcPLCγ constructs were created to constitutively target these proteins to lipid rafts in the plasma membrane (Fig. 6.1b). These constructs were then expressed in AtT20-derived cell lines where their membrane localization was confirmed and their ability to reconstitute the BCR/PLCγ pathway was assessed.

Following numerous attempted transfections it was concluded that the TmPLCγ2 construct was inexpressible in AtT20-Derived Cell Lines. The inability to express this vector may be due to an undetected mutation in the sequence that may have arisen during the various PCR manipulations that were required to engineer the construct. Unfortunately, this could not be confirmed as attempts to sequence this rather large construct did not yield a reliable, complete sequence. Alternatively, the inability to express this vector may be attributable to its rather large size (the expression vector is ~ 9.2 kB). In fact, previous attempts to express a similar vector (a TmPLCγ2 construct containing rat PLCγ2 as opposed to human PLCγ2) also proved unsuccessful in this system. Another possibility could be that this construct is expressible in AtT20-derived cell lines but that it has a lethal effect such that clones can not be successfully isolated. Regardless of the reason for its inexpressibility, studies with this construct were necessarily abandoned. This is unfortunate as it precluded an opportunity to investigate whether or not general compartmentalization to the plasma membrane affected signaling differently than specific compartmentalization to lipid rafts.

In contrast, the TmBLNK construct was found to be expressible in AtT20-derived cell lines (Fig. 6.2). Moreover, this construct was found to be membrane associated (Fig. 6.3) and confirmed to be expressed on the cell surface (i.e., at the plasma membrane) (Fig. 6.4). Interestingly, two different molecular weight isoforms of TmBLNK were observed to be expressed in this system (Fig. 6.2). Similar results were observed by Ishiai *et al.* (1999) when they used essentially the same CD16/TCR ζ construct to target rat PLCγ to the plasma membrane. Interestingly, Ishiai and colleagues (1999) concluded that the two isoforms represented differentially glycosylated forms of the same protein. Likewise, in this system the two TmBLNK isoforms may represent differentially glycosylated forms of the same protein such that the lower molecular weight form (~105 kD) is incompletely glycosylated as compared to the higher molecular weight form (~ 114 kD). If this were to be the case, it would be predicted that treatment of these proteins with Endogycosidase H and/or PNGase F to remove all carbohydrate side chains would reduce these proteins to a single, stripped molecular weight form. However, such treatment did not reduce these proteins to a single molecular weight form but rather reduced the molecular weight of both forms by an approximately equivalent amount (data not shown). This suggests that the forms may actually represent two different forms of the protein that are equivalently glycosylated (i.e., the lower molecular weight form may represent a splice variant). Alternatively, the two different molecular weight forms may result from differences in other post-translational modifications

(e.g., phosphorylation, ubiquitination, sumoylation, acylation, nitrosylation or sulfation) or due to alternative splicing. Nonetheless, the lower molecular weight form is not expressed at the cell surface (Fig. 6.4) and appears to be membrane associated as opposed to being localized to the cytoplasm (Fig. 6.3), and as such is likely sequestered in the endoplasmic reticulum where it is unlikely to influence and/or interfere with signaling processes that occur at the cell surface and in the cytosol. This supposition is supported in part by the finding that, unlike the higher molecular weight form, the lower molecular weight form of TmBLNK does not appear to become tyrosine phosphorylated following BCR cross-linking in this system (Figs. 6.7 and 6.8). Given all of this, signaling studies proceeded with AtT20-derived cell lines that expressed the TmBLNK construct.

Additionally, the AcBLNK and AcPLCγ constructs were found to be expressible in AtT20-Derived Cell Lines (Fig. 6.2). In this case, one molecular weight form of AcPLCγ2 and two molecular weight forms of AcBLNK (~70 kD and ~80 kD) were observed (Fig. 6.2). Thus, it appears that, similar to TmBLNK, the AcBLNK construct exists as two different splice-variants. And while it could be argued that the two forms could represent the same protein in different stages of glycosylation/acylation it seems unlikely given that similar results are not observed for the AcPLCγ2 construct. It is of some concern that the lower molecular weight form is expressed in the cytosol where it may be able to influence signaling. Thus, any signaling studies performed in AtT20-derived cell lines expressing the AcBLNK construct are viewed with some caution.

6.3.2 Co-Expression of the BCR, Syk and Membrane Targeted BLNK Is Sufficient to Reconstitute BCR-Induced PLCγ Activation in AtT20-Derived Cell Lines

General membrane targeting of BLNK appears sufficient to reconstitute BCR-induced, PLC-dependent Erk phosphorylation in the presence of Syk in AtT20-derived cell lines (Fig. 6.6). However, PLC-dependent Erk phosphorylation does not appear to be significantly enhanced as compared to what was observed for the cell line co-expressing the BCR, Syk and cytosolic BLNK (Fig. 6.6). This suggests that constitutively compartmentalizing BLNK to the plasma membrane (e.g., with TmBLNK) in itself is not sufficient to more effectively couple the BCR to PLCγ in this system. One possible explanation for this finding could be that TmBLNK is no more able to associate with PLCγ than cytosolic BLNK. Additionally, specifically targeting BLNK to lipid rafts in the plasma membrane is not sufficient to reconstitute BCR-induced, PLC-

dependent Erk phosphorylation in the AtT20 system. This suggests that such targeting actually inhibits BLNK function as cytosolic BLNK was able to reconstitute the BCR/PLCγ pathway in the system. Similar to above, one possible explanation for this finding could be that AcBLNK is not able to efficiently associate with PLCγ. Unfortunately, due to the inconclusive nature of the protein association studies (refer to Appendix III) this possibility had to be indirectly investigated by assaying the phosphorylation status of BLNK as well as the phosphorylation and localization status of PLCγ.

According to the proposed model, BLNK (whether cytosolic or membrane targeted) must become phosphorylated on specific tyrosine residues to associate with PLCγ. Failure of such phosphorylation to occur should result in a failure to form a functional BCR/PLCγ signaling complex. Thus, the phosphorylation status of membrane targeted BLNK was assayed. From this it was determined that both TmBLNK and AcBLNK become tyrosine phosphorylated following BCR cross-linking in AtT20-derived cell lines that co-express Syk (Figs. 6.8 and 6.9, respectively). This suggests that membrane targeted BLNK should be able to associate with PLCγ to facilitate the formation of a functional BCR/PLCγ signaling complex. However, as with cytosolic BLNK, the possibility remains that not all of the tyrosine residues are being phosphorylated such that membrane-targeted BLNK is unable to effectively associate with PLCγ. Hence, further investigations were performed to assay the phosphorylation and localization status of PLCγ1.

Upon investigation, BCR-induced PLCγ1 phosphorylation appears to be enhanced in the cell line expressing TmBLNK as compared to the cell line expressing cytosolic BLNK (Figs. 6.11 and 6.12). This may suggest that plasma membrane targeting of BLNK promotes the formation of a BCR/PLCγ signaling complex, given that such a complex is thought necessary to facilitate PLCγ1 phosphorylation. However, if such a complex is being formed it should be reflected in the finding that PLCγ1 is being recruited to the BCR in the plasma membrane. Unfortunately, such recruitment is not evident in the BCR/Syk/TmBLNK cell line (Fig. 6.13). It may seem difficult to reconcile these two observations but upon further inspection it is evident that there is a small pool of PLCγ1 constitutively associated with the plasma membrane (Fig. 6.13) and it is possible that it is this pool, as opposed to the cytoplasmic pool, that is associating with TmBLNK and becoming tyrosine phosphorylated. There is also the possibility that rather than facilitating the formation of a BCR/PLCγ signaling complex, TmBLNK actually influences kinase activity

such that PLCγ1 can be more efficiently phosphorylated. However, this seems less likely as there is little in the existing literature to suggest such a role for BLNK. Regardless, the enhanced PLCγ1 phosphorylation does not appear sufficient to reconstitute PLCγ1 activity as judged by the phosphorylation status of its downstream target, Erk (Fig. 6.2 and 6.3). This could indicate either that PLCγ1 is incompletely phosphorylated or that the level of phosphorylated PLCγ1 is insufficient to initiate downstream signaling. Alternatively, it could be that PLCγ1 is becoming appropriately phosphorylated but that it is yet to be appropriately compartmentalized such that it can act on its substrate.

In contrast, to TmBLNK, AcBLNK does not appear to enhance BCR-induced PLCγ1 phosphorylation beyond what was observed with cytosolic BLNK (Fig. 6.11). This apparently suggests that formation of a BCR/PLCγ1 signaling complex is not promoted by constitutively targeting BLNK to lipid rafts in the plasma membrane. This is contrary to expectation, especially when considered along with the TmBLNK findings. Nonetheless, the possible explanations for this finding are numerous. First, these different findings could reflect differences in expression levels of the various constructs such that a greater expression level of TmBLNK as compared to AcBLNK could contribute to the appearance of enhanced PLCγ1 phosphorylation. Yet this appears unlikely as, if anything, AcBLNK appears to be both expressed and phosphorylated to a greater degree than TmBLNK (~ 114 kD form) (Fig. 6.3 and Fig. 6.8 versus Fig. 6.9, respectively). Nonetheless, the possibility remains that TmBLNK is indeed expressed and phosphorylated at a higher level but that this is not evident due to the antibodies having a lower affinity for this construct as compared to AcBLNK. Second, these results could be explained if PLCγ phosphorylation and activation were to occur in a step-wise process where PLCγ1 would first be recruited via BLNK to the BCR signaling complex at the plasma membrane and become phosphorylated and then subsequently translocate into lipid rafts such that it can act on its substrate. If this is so then constitutively targeting BLNK to the lipid rafts may interfere with efficient PLCγ1 phosphorylation. This hypothesis could be tested in wild-type cells by disrupting lipid rafts with cholesterol sequestering agents and determining whether or not PLCγ1 is still able to be phosphorylated and/or activated. If the model proposed here were accurate it would be predicted that lipid raft disruption would still allow for phosphorylation of PLCγ1 yet would disrupt its activation and therefore, its downstream signaling pathways. Third, the lower molecular weight, cytosolic form of AcBLNK (~70 kD) may be having a negative effect on the higher molecular weight, membrane associated form's

(~80 kD) ability to facilitate that formation of a BCR/PLCγ signaling complex. And fourth, similar to what was proposed for TmBLNK; it could be that AcBLNK is only associating with PLCγ1 from the constitutively membrane-associated pool of PLCγ1. Furthermore, it may be that only a fraction of this pool is actually associated with lipid rafts. As such AcBLNK may appear to be associating with and facilitating the phosphorylation of a smaller amount of PLCγ1 as compared to TmBLNK not because the actual association is less efficient but because there is a smaller pool of PLCγ1 available for it to associate with. Regardless, it is evident that AcBLNK is not sufficient to significantly enhance BCR-induced PLCγ1 phosphorylation and or activation as compared to cytosolic BLNK. Moreover, it is evident that membrane targeting of BLNK (either in the form of TmBLNK or AcBLNK) is not sufficient to reconstitute a highly functional BCR/PLCγ signaling complex in this system. Thus, PLCγ was constitutively targeted to the plasma membrane to determine if such compartmentalization could reconstitute maximal BCR-induced PLCγ activation in AtT20-derived cell lines.

6.3.3 Co-Expression of the BCR, Syk and AcPLCγ2 Appears Sufficient to Reconstitute BCR-Induced PLCγ Activation in AtT20-Derived Cell Lines

BCR-induced, PLC-dependent Erk phosphorylation is significantly enhanced in the BCR/Syk/AcBLNK/AcPLCγ2 cell line as compared to the BCR/Syk/AcPLCγ2 cell line (Fig. 6.15). As mentioned above, this may suggest that co-expression of AcBLNK and AcPLCγ2 has a synergistic effect on BCR-induced AcPLCg2 activation. However, this enhancement may also be due to the fact that AcPLCγ2 is expressed to a greater degree in the BCR/Syk/AcBLNK/AcPLCγ2 cell line as compared to the BCR/Syk/AcPLCγ2 cell line. More importantly, these data suggest that plasma membrane compartmentalization of PLCγ2 is sufficient to couple the BCR to PLCγ activation in this system. Furthermore, when considered in conjunction with the membrane-recruitment studies performed on the various cell lines, it furthers the notion that such compartmentalization is not only sufficient but also necessary for BCR-induced PLCγ activation. Thus, it ultimately appears that limited ability to reconstitute BCR-induced PLCγ activation is reflective of an inability to appropriately compartmentalize PLCγ in this system. Consequentially, these findings both highlight the importance of compartmentalization to BCR signaling and, along with the findings of the previous chapters, challenge the initial hypothesis of this thesis where co-expression of Syk, BTK and BLNK was envisioned to be sufficient to couple the BCR to PLCγ activation (discussed in Chapter 7).

Chapter 7

Discussion

7.1 Introduction

The BCR/PLCγ signaling pathway has come to the attention of various researchers because defects in this pathway lead to defects in B cell function. This in turn compromises immune system function and ultimately compromises the life of the affected individual. Thus, studies have focused on elucidating this pathway with the hope that the resulting knowledge could be used to help those who suffer from defects in this pathway.

In the past decade a model of the BCR/PLCγ pathway emerged (summarized below). This model has been predominantly built upon the findings of loss-of-function studies that have identified numerous proteins that are *necessary* to connect the cross-linked BCR to PLCγ activation. While these studies are invaluable, they have certain drawbacks. Indeed, they can reveal that a certain combination of proteins is *necessary* for a process and/or pathway yet they can not confirm that that same set of proteins is *sufficient* for that pathway. In fact, loss-of-function studies may fail to identify all the proteins that may be involved and/or required for a certain pathway. As well, loss-of-function studies may overlook or underestimate the role of certain proteins in the pathway due to the compensatory effects of functionally redundant proteins in the loss-of-function system. Thus, while loss-of-function studies have identified that Syk, BTK and BLNK are all required to couple the cross-linked BCR to maximal PLCγ activation the question remains, "Are these proteins alone sufficient to reconstitute this pathway?" This thesis employed a non-lymphoid AtT20 reconstitution system to address this question and to further investigate and elucidate the BCR/PLCγ pathway.

7.2 Review of Proposed Model and Initial Hypotheses

At the onset of this thesis the BCR/PLCγ pathway was proposed to include the following steps:

1. BCR cross-linking leads the BCR to translocate into lipid rafts.
2. Lipid raft translocation brings the BCRs into close proximity with active Lyn.
3. Active Lyn then phosphorylates the BCR on the Igα/β ITAMs.

4. The SFKs (including Lyn) are then recruited to the BCR by way of their SH2 domains binding to the phosphorylated Igα/β ITAMs
5. Such recruitment brings the SFKs into close proximity with each other enabling them to trans-phosphorylate and activate each other as well as to further phosphorylate the Igα/β ITAMs, creating a positive feedback loop.
6. Syk is also recruited from the cytosol to plasma membrane/BCR by way of its SH2 domain binding to the phosphorylated Igα/β ITAMs.
7. Such recruitment brings Syk into close proximity with the active SFKs such that they can phosphorylate and activate Syk.
8. BLNK is also recruited from the cytosol to the plasma membrane/BCR by way of its SH2 domain binding to phosphorylated Igα tyrosines that exist outside of the ITAMs.
9. Such recruitment brings BLNK into close proximity with active Syk such that Syk can phosphorylate BLNK.
10. BTK and PLCγ are then recruited from the cytosol to the plasma membrane/BCR signaling complex by way of their SH2 domains binding to the BCR-associated, phosphorylated BLNK
11. Such recruitment brings PLCγ into close proximity with BTK and Syk such that they can phosphorylate PLCγ.
12. Such recruitment also brings PLCγ into close proximity with its plasma membrane-bound substrate, PIP_2.
13. The combined phosphorylation and membrane-recruitment of PLCγ is proposed to facilitate its activation such that it can then hydrolyze PIP_2 to produce the second messengers, IP_3 and DAG.
14. Ultimately, PLCγ activation leads to increased IP_3 and DAG levels, to increased intracellular calcium levels and to the activation of several downstream signaling pathways including the MAPK pathway that leads to an increase in phosphorylated Erk levels.

Based on this model it was hypothesized that co-expression of the BCR, Syk, BLNK and BTK would be both necessary and sufficient to maximally reconstitute BCR-induced PLCγ activation in the AtT20 system. Additionally, it was hypothesized that co-expression of the BCR, Syk and BLNK may be sufficient to at least partially reconstitute BCR-induced PLCγ activation in the AtT20 system. This latter hypothesis was based on the observation that genetic ablation of BTK,

unlike that of Syk, does not completely inhibit PLCγ phosphorylation and/or activation (Takata and Kurosaki, 1996).

7.3 Review of Key Findings

In hopes of providing the reader with some clarity, the key findings of this thesis are summarized below in Table 7.1.1.

7.4 Discussion of Findings and Future Considerations

7.4.1 Findings Regarding the BCR-induced PLC-Independent Erk Pathway

As mentioned previously, increased Erk phosphorylation is a downstream consequence of BCR-induced PLCγ activation. Thus, by monitoring BCR-induced Erk phosphorylation we are able to determine whether or not BCR-induced PLCγ activation has been successfully reconstituted in this system. However, this assay is complicated by the fact that the BCR can also induce Erk phosphorylation by a PLC-independent pathway (Chapter 1.5.4). Consequently, a PLC inhibitor was used to distinguish PLC-dependent from PLC-independent increases in Erk phosphorylation in this system. Through this process several unexpected observations were made regarding the PLC-independent pathway. While the PLC-independent pathway was not a focus of this thesis, these findings are noted here as they will be considered further when interpreting the observations regarding the PLC-dependent pathway.

The first unexpected finding was that co-expression of the BCR, Syk and BLNK appears to enhance BCR-induced PLC-dependent Erk phosphorylation while concomitantly inhibiting BCR-induced PLC-independent Erk phosphorylation as compared to the BCR/Syk cell line. This finding is unexpected as there is little in the literature to suggest that BLNK would have a negative effect on the BCR/PLC-independent Erk pathway. While BLNK has been reported to associate with the Grb2 protein of the PLC-independent pathway, this association has been hypothesized to be of a positive nature with respect to Erk phosphorylation (Fu *et al.*, 1998). Thus, the observed inhibitory effect of BLNK may be indicative of some inadequacy or anomaly in the AtT20 system. Indeed, it may be that BLNK is inappropriately associating with a component of the PLC-independent pathway such that the pathway is inhibited in the AtT20

Table 7.1. Summary of the Key Findings of This Thesis. Note that arrow indicates that BCR-induced phosphorylation was detected. The colour of the arrow is intended to roughly indicate the intensity of the observed phosphorylation relative to the other cell lines. BCR-induced PLC-dependent Erk phosphorylation is distinguished from BCR-induced PLC-independent with the aid of the PLC inhibitor, U73122. The intensity of the PLC-independent phosphorylation is inferred by comparing the overall Erk phosphorylation to the PLC-dependent Erk phosphorylation. BCR-induced PLCγ activation is inferred to occur if BCR-induced PLC-dependent Erk phosphorylation is observed. It was initially inferred that the observed BCR-induced PLCγ activation may be limited ("limited?") based on the observation that PLCγ phosphorylation, a requirement of PLCγ activation, appeared extremely limited compared to what is generally observed in wild-type B cell. However, when the findings of the thesis are considered in the totality, it becomes apparent that the amount of PLCγ phosphorylation does not necessarily correlate with the amount of PLCγ activation.

AtT20-Derived Cell Line	Overall Erk (P) (observed)	PLC-dependent Erk (P) (observed)	PLC-independent Erk (P) (inferred)	PLCγ (P) (observed)	PLCγ Activation (inferred)
BCR	none	none	none	none	none
BCR/Syk	⇧	none	⇧	⇧	none
BCR/BTK	none	none	none		none
BCR/BLNK	none	none	none	none	none
BCR/Syk/BTK	⇧	none	⇧	⇧	none
BCR/Syk/BLNK	⇧	⇧	⇧	⇧	yes, limited?
BCR/BTK/BLNK	none	none	none		none
BCR/Syk/BLNK/BTK	⇧	none	⇧	⇧	none
BCR/Syk/TmBLNK	⇧	⇧	⇧	⇧	yes, limited?
BCR/Syk/AcBLNK	⇧	⇧	⇧	⇧	yes, limited?
BCR/Syk/AcPLCγ2	⇧	⇧	⇧	⇧	yes, limited?
BCR/Syk/AcBLNK/AcPLCγ2	⇧	⇧	⇧	⇧	yes

system.

Such an association may be non-functional in the AtT20 system due to the system lacking some required lymphoid-specific component(s). This theory could be explored with a series of investigations. First, the role of BLNK in the PLC-independent Erk pathway could be better delineated by investigating BCR-induced Erk phosphorylation in a PLCγ knockout cell line versus a PLCγ/BLNK knockout cell line. If BLNK positively influences the BCR-induced PLC-independent Erk pathway then, BCR-induced Erk phosphorylation should be further reduced in the PLCγ/BLNK knockout as compared to the PLCγ knockout alone. Conversely, if BLNK negatively influences the pathway then, BCR-induced Erk phosphorylation should be enhanced in the PLCγ/BLNK knockout as compared to the PLCγ knockout. Second, the hypothesis that BLNK associates with a component of the PLC-independent pathway in the AtT20 system could be investigated by performing co-immunoprecipitation assays (assuming a functional co-immunoprecipitation assay could be achieved). In particular, these co-immunoprecipitation studies may begin by looking at BLNK's association with Grb2. And third, the hypothesis that BLNK is forming a non-functional complex in the AtT20 system due to the absence of a required lymphoid-specific component could be investigated with further reconstitution experiments (as directed by current loss-of-function models). However, these investigations have yet to be performed, primarily because the focus of this thesis was to elucidate the BCR/PLCγ pathway as opposed to the BCR/PLC-independent Erk pathway.

The second unexpected finding was that co-expression of the BCR, BTK and BLNK appears to inhibit BCR-induced PLC-independent Erk phosphorylation as compared to the BCR/Syk cell line. This finding is unexpected as there is little in the literature to suggest that BTK would have a negative effect on the BCR/PLC-independent Erk pathway. However, similar to what was discussed above for BLNK, it may be that BTK is inappropriately associating with a component of the PLC-independent pathway such that the pathway is inhibited in the AtT20 system. This theory could be explored with a series of investigations. First, the role of BTK in the PLC-independent Erk pathway could be better delineated by investigating BCR-induced Erk phosphorylation in a PLCγ knockout cell line versus a PLCγ/BTK knockout cell line. If BTK positively influences the BCR-induced PLC-independent Erk pathway, then BCR-induced Erk phosphorylation should be further reduced in the PLCγ/BTK knockout as compared to the PLCγ knockout alone. Conversely, if BTK negatively influences the pathway then, BCR-induced Erk

phosphorylation should be enhanced in the PLCγ/BTK knockout as compared to the PLCγ knockout. And second, the hypothesis that BTK associates with a component of the PLC-independent pathway in the AtT20 system could be investigated by performing co-immunoprecipitation assays (assuming a functional co-immunoprecipitation assay could be achieved). However, these investigations were put aside in favour of those that were seen to be more directly focused on the BCR/PLCγ pathway.

The third unexpected finding was that co-expression of the BCR, Syk, BLNK *and* BTK appears to release the inhibition of the BCR-induced PLC-independent pathway observed in the BCR/Syk/BLNK and BCR/BTK/BLNK cell lines. At first, these three findings may appear difficult to reconcile. However, as mentioned in Chapter Four, one possible explanation could be that BLNK and BTK preferentially associate with each other when co-expressed in the AtT20 system. In forming such a preferential association they may no longer interact with components of the PLC-independent pathway and as such, may no longer inhibit the pathway. The difficulty with this explanation is that it is based on the untested hypothesis that BTK and BLNK are negatively influencing the PLC-independent Erk pathway by forming inhibitory associations with the components of this pathway. Nonetheless, this hypothesis can be tested through a series of co-immunoprecipitation studies. First, BLNK can be immunoprecipitated from the BCR/Syk/BLNK cell line and the BCR/Syk/BLNK/BTK cell line. If the hypothesis is correct, then, BLNK should co-immunoprecipitate with protein "X" from the PLC-independent pathway in the former cell line and with BTK, as opposed to X, in the latter cell line. Similarly, BTK can be immunoprecipitated from the BCR/BTK/BLNK cell line and the BCR/Syk/BLNK/BTK cell line. If the hypothesis is correct, then BTK should co-immunoprecipitate with protein "Y" from the PLC-independent Erk pathway in the former cell line and with BLNK, as opposed to Y, in the latter cell line. However, given the limited success of the co-immunoprecipitation studies in this thesis, this line of investigation was not pursued. Rather, the focus of this thesis returned to investigations that were seen to be more directly related to the BCR/PLCγ pathway.

7.4.2 Initial Findings Regarding the BCR/PLCγ Pathway

The initial finding of this thesis was that co-expression of the BCR, Syk and BLNK is sufficient to reconstitute BCR-induced PLCγ1 activation in the AtT20 system. Considered alone, this finding appears to support the proposed model. However, co-expression of the BCR, Syk,

BLNK *and* BTK *is not sufficient* to reconstitute BCR-induced PLCγ1 activation in the AtT20 system. This suggests that BTK has a negative effect on the BCR/PLCγ pathway in the AtT20 system. This is completely unexpected as BTK is hypothesized to have a positive effect on the pathway. Ultimately, this finding suggests that there is a deficit in the AtT20 system and/or the proposed model. Thus, the BCR/PLCγ pathway was further dissected in the AtT20 system in an effort to determine where and why the pathway may be diverging from the proposed B cell model. In particular, the phosphorylation, association and compartmentalization statuses of the various components of the pathway were investigated.

BLNK phosphorylation was investigated as the model proposes that BLNK must become tyrosine phosphorylated to associate with BTK and PLCγ. Moreover, the model proposes that such an association is required to facilitate PLCγ phosphorylation and activation. Thus, reconstitution of BCR-induced BLNK phosphorylation can be seen as a requisite step to reconstituting BCR-induced PLCγ activation. These investigations demonstrated that co-expression of the BCR, Syk and BLNK was sufficient to reconstitute robust BCR-induced BLNK phosphorylation in this system. This finding is as expected as the model proposes that Syk is responsible for phosphorylating BLNK. Furthermore, this finding suggests that BLNK should be able to associate with BTK and PLCγ in this system to facilitate the phosphorylation and activation of PLCγ. However, one limitation of this finding is that it does not confirm that BLNK is becoming phosphorylated on all of its tyrosine residues. Rather, phosphorylation is only confirmed for tyrosine residue 96 (Chapter 5). In fact, if BLNK were to be phosphorylated on only a subset of its tyrosines it may not be able to associate with BTK and PLCγ. In particular, BLNK must become phosphorylated on tyrosines 103, 194 and 205 to associate with PLCγ and on tyrosine 115 to associate with BTK (Chiu *et al.*, 2002). Thus, further investigations are necessary to confirm whether or not tyrosine residues 103, 115, 194 and 205 are phosphorylated in this system. To do this, one could analyze BLNK phosphorylation by immunoblotting with antibodies specific for particular phospho-tyrosine residues in BLNK. However, to date, commercial phospho-specific antibodies are only available for tyrosine residues 84 and 96 of BLNK. Alternatively, co-immunoprecipitation studies could be performed to indirectly infer whether or not BLNK was becoming appropriately phosphorylated such that it could associate with PLCγ1. Indeed, these studies were pursued but unfortunately, they proved to be inconclusive (Chapter 5 and Appendix II). Finally, phospho-peptide mapping could be performed to analyze BLNK phosphorylation in this system. Yet, without further evidence,

BLNK phosphorylation can not be eliminated as confounding factor in the attempt to reconstitute BCR-induced PLCγ activation in the AtT20 system.

Phosphorylation of BTK was investigated as phosphorylation of tyrosine residue 223 is generally accepted to be indicative of BTK kinase activity (Rawlings *et al.*, 1996; Park *et al.*, 1996; Kurosaki *et al.*, 1997). Furthermore, the model proposes that BCR cross-linking induces BTK phosphorylation such that BTK can then further phosphorylate and activate PLCγ. Thus, reconstitution of BCR-induced BTK phosphorylation and activation can be seen as a requisite step to reconstituting BCR-induced PLCγ activation. These investigations demonstrated that BTK is constitutively phosphorylated and presumably active in the AtT20 system. This finding is unexpected as one of the advantages of the AtT20 system is that it has proven to be a system where over-expression does not necessitate activation (Richards *et al.*, 1996). While it remains unclear as to why BTK is constitutively phosphorylated in this system it does appear that this phosphorylation is at least partly dependent on endogenous Fyn activity (Chapter 5.2.5). Ideally, further studies could be performed to determine how and why BTK is constitutively phosphorylated in this system. However, such studies were not pursued herein as it was *initially* held that as long as BTK was phosphorylated it should not represent a limiting factor in the activation of the BCR/PLCγ pathway. And thus, the focus of the thesis returned to investigations of the phosphorylation, association and compartmentalization statuses of the other components of the BCR/PLCγ pathway.

Syk phosphorylation and activation was also considered as the model proposes that Syk directly contributes to PLCγ phosphorylation and activation and indirectly contributes to both by phosphorylating BLNK. Thus, reconstitution of BCR-induced Syk phosphorylation and activation can be seen as a requisite step to reconstituting BCR-induced PLCγ activation. However, previous studies clearly established that co-expression of the BCR and Syk is sufficient to reconstitute BCR-induced Syk phosphorylation and activation with the AtT20 system (Richards *et al.*, 1996). Thus, these studies were not repeated herein. Given the previous findings, Syk phosphorylation and activation can be eliminated as confounding factor in the attempt to reconstitute BCR-induced PLCγ activation in the AtT20 system.

Not having found any overt defects in Syk, BTK[1] or BLNK phosphorylation that could readily account for the inability to effectively reconstitute the BCR/PLCγ pathway in the AtT20 system it is necessary to consider PLCγ phosphorylation itself. Indeed, PLCγ phosphorylation is requisite to its activation and thus, any inability to effectively reconstitute BCR-induced PLCγ phosphorylation should translate to an inability to effectively reconstitute BCR-induced PLCγ activation. As a consequence of investigating PLCγ phosphorylation in the AtT20 system many interesting and revealing observations were made (summarized in Chapter 5 and below).

The first interesting observation was that co-expression of the BCR and Syk is sufficient to reconstitute a limited amount of BCR-induced PLCγ1 phosphorylation in the AtT20 system. When considering the model, this finding is surprising as BLNK is proposed to be necessary to couple Syk to PLCγ. However, upon further inspection of the literature it is noted that PLCγ1 can associate with phosphorylated Syk via its SH2 domain (Stillman and Monroe, 1995; Law *et al.*, 1996). Thus, it could be that Syk is able to associate with PLCγ1 and facilitate its phosphorylation in the AtT20 system. However, it is unlikely that a similar such mechanism would exist in B cells as B cells predominantly express PLCγ2 (Hempel and DeFranco, 1991; Hempel *et al.*, 1992; Coggeshall *et al.*, 1992) and PLCγ2 does not appear to likewise associate with Syk (reviewed in Kurosaki *et al.*, 2000) Additionally, given the limited amount of phosphorylation, this mechanism does not appear very efficient even in the AtT20 system. Moreover, the observed phosphorylation of PLCγ in the BCR/Syk cell line does not correlate with any observable PLCγ1 activation (Chapter 4), further suggesting that BLNK may indeed be required to effectively couple Syk to PLCγ1.

The second interesting observation was that co-expression of the BCR and BTK is sufficient to reconstitute a very limited amount of PLCγ phosphorylation. Given the minimal amount of phosphorylation detected it may be worth considering whether this finding is an artefact. However, this does not appear to be the case as this minimal amount of phosphorylation is consistently detected across all replicates. Nonetheless, it should be noted that this finding may be a consequence of the fact that BTK is constitutively phosphorylated and presumably active in

[1] Arguably, constitutive phosphorylation of BTK could be considered an overt defect. However, it is not considered as such here because phosphorylation should not directly limit BTK's activity and therefore, should not directly limit any attempt to reconstitute the BCR/PLCγ pathway in the AtT20 system.

the AtT20 system (Chapter 5.2.4 and discussed above). Indeed, this may explain why PLCγ1 phosphorylation is detected even prior to BCR cross-linking in BTK expressing cell lines (Fig. 5.3). Thus, while this finding suggests that BTK may be able to couple to PLCγ1 in the absence of BLNK in the AtT20 system, such coupling may be an anomaly of the system rather than a reflection of the physiological reality. Regardless, the observed phosphorylation of PLCγ1 in the BCR/BTK cell line does not correlate with any observable PLCγ1 activation (Chapter 4), further suggesting that BLNK may be required to effectively couple BTK to PLCγ1.

The third interesting observation was that BCR-induced PLCγ1 phosphorylation is not enhanced in the BCR/Syk/BLNK cell line as compared the BCR/Syk cell line. When considering the model, this finding is surprising as BLNK is proposed to couple Syk to PLCγ and thereby facilitate PLCγ's phosphorylation. This finding could be quite easily explained if BLNK phosphorylation was deficient such that BLNK could not associate with PLCγ1 in this system. Yet this seems unlikely given the fact that BLNK becomes robustly phosphorylated in the BCR/Syk/BLNK cell line following BCR cross-linking. Nonetheless, as explained above, it is possible that BLNK is only being phosphorylated on a subset of tyrosine residues and as such, is not able to associate PLCγ to facilitate its phosphorylation. Thus, further investigations are necessary to confirm whether or not BLNK phosphorylation is being fully reconstituted in this system. Without such investigations it is not possible to eliminate BLNK phosphorylation as a confounding factor in the attempts to reconstitute the BCR/PLCγ pathway in this system.

The fourth interesting observation was that BCR-induced PLCγ activation is reconstituted in the BCR/Syk/BLNK cell line whereas it is not in the BCR/Syk cell line. Thus, while BLNK expression does not appear to overtly alter PLCγ phosphorylation it does appear to dramatically alter PLCγ activity in this system. This finding has many implications. First, it suggests that PLCγ phosphorylation does not necessarily translate to PLCγ activation as the two cell lines show comparable levels of PLCγ phosphorylation yet disparate levels of PLCγ activation. This in turn suggests that there are additional factors that predicate PLCγ activation. And what is more, BLNK expression appears to be one of these additional factors. Yet the question immediately arises, "How does BLNK facilitate PLCγ activation if not through facilitating its phosphorylation?" At least two possible answers come to mind. First, it could be that BLNK associates with PLCγ, causing a conformational change in PLCγ that renders it active. Alternatively, it could be that BLNK associates with PLCγ and in doing so, appropriately

compartmentalizes PLCγ such that it can act on its substrate. In either case, the assumption is made that BLNK is in some way associating with PLCγ. Thus, the question arises, "If BLNK is able to associate with PLCγ, why is not able to facilitate PLCγ's phosphorylation in this system?" As suggested in Chapter Five, one possible explanation could be that, contrary to the proposed model, BLNK only facilitates PLCγ's phosphorylation by BTK and not by Syk. This explanation challenges the existing model of the BCR/PLCγ signaling proposed by Ishiai and colleagues (1999) whereby BLNK is envisioned to recruit PLCγ to the plasma membrane such that it can be phosphorylated by BTK *and* Syk. Thus, further investigations are required to determine whether BLNK facilitates PLCγ phosphorylation by BTK alone or by BTK and Syk. This could be done by comparing BCR-induced PLCγ phosphorylation levels in BTK deficient cell lines to those in BLNK deficient cell lines. If BLNK only facilitates BTK-mediated PLCγ phosphorylation, then the PLCγ phosphorylation levels should be comparable in both cell lines. However, if BLNK facilitates both BTK-mediated and Syk-mediated PLCγ phosphorylation, then the PLCγ phosphorylation levels should be greater in the BTK deficient cell line as compared to the BLNK deficient cell line. Interestingly, there does not appear to be a publication reporting such a comparison despite the fact that both such cell lines exist. Furthermore, Ishiai *et al.* (1999) do not report any data regarding PLCγ phosphorylation in their BLNK deficient cell line despite investigating PLCγ activation. Thus, revealed is a key question regarding the current model of the BCR/PLCγ pathway and BLNK's role in it. Namely, "Does BLNK truly couple Syk to PLCγ such that the former can phosphorylate the latter, or is it that Syk couples BLNK to BTK and PLCγ by phosphorylating BLNK to enable its association with BTK and PLCγ?" Given this question, further studies are clearly in order (as suggested above). Nonetheless, one caveat to this finding is that it may only apply to PLCγ1, the predominant isoform expressed in the AtT20 system and not to PLCγ2, the predominant isoform expressed in B cells. This is based on the observation that PLCγ1 can directly associate with Syk (Law *et al.*, 1996) and perhaps thereby circumvent the need for BLNK whereas PLCγ2 does not appear able to form such a direct association with Syk.

The fifth interesting observation was that BCR-induced PLCγ phosphorylation is enhanced in the BCR/Syk/BLNK/BTK cell line as compared to either the BCR/Syk/BLNK cell line or the BCR/BTK/BLNK cell line. When considering the proposed model of the BCR/PLCγ pathway this finding is as expected. However, PLCγ activation is not reconstituted in the BCR/Syk/BLNK/BTK cell line. Coupled with the finding that PLCγ activation is reconstituted

in the BCR/Syk/BLNK, this finding suggests that BTK expression actually inhibits PLCγ activation in the AtT20 system. This finding is quite unexpected as the model proposes that BTK expression should enhance both PLCγ phosphorylation and PLCγ activation. Given the discrepancy between the expectations and the findings, there appears to be some deficiency in the proposed model and/or the AtT20 system.

One possible explanation for the apparent inhibitory effect of BTK could be that BLNK and BTK are forming a malfunctioning signaling complex in the AtT20 system. Indeed, the findings regarding the PLC-independent pathway also alluded to the likelihood that BTK and BLNK were forming a complex in this cell line (refer to Chapter 7.4.1). Such a complex could be sufficient to reconstitute PLCγ phosphorylation yet insufficient to reconstitute PLCγ activation. While it is unclear why the BLNK/BTK complex may malfunction it may be related to the fact that BTK is constitutively phosphorylated in this system (discussed above). In particular, BTK may be inappropriately compartmentalized to the membrane in this system such that it is constitutively phosphorylated. Certainly, membrane-enrichment studies indicate that a majority of BTK is constitutively associated with the membrane fraction in this system, counter to expectation (Fig. 5.15). Such inappropriate localization could result in the entire BCR/PLCγ signaling complex being misplaced and therefore nonfunctional. For example, rather than BCR-associated phosphorylated BLNK recruiting BTK and PLCγ to a functional BCR signaling complex, perhaps misplaced BTK is recruiting phosphorylated BLNK and PLCγ to a nonfunctional complex. Unfortunately, this hypothesis can not be directly tested in the AtT20 system without determining first why and how BTK is being constitutively phosphorylated. These experiments are impending and will involve membrane fractionation studies that will further define BTK's compartmentalization in this system. Similar studies will also be performed to define BLNK and PLCγ's compartmentalization in BTK expressing and BTK deficient cell lines. Additionally, it is imperative to develop functional co-immunoprecipitation assays in this system so that it can be determined whether BLNK is preferentially associating with the BCR or BTK. Nonetheless, this hypothesis could be investigated in a B cell line that has been transfected with a constitutively membrane targeted BTK construct. If such a construct proves to be constitutively phosphorylated and if the hypothesis is correct, expression of the construct should not impair PLCγ phosphorylation but it should impair PLCγ activation.

Finally, considering the above findings it was concluded that:

1. Co-expression of the BCR, Syk, BLNK and BTK is not sufficient to reconstitute the BCR/PLCγ pathway in the AtT20 system. And, that
2. PLCγ phosphorylation does not predicate PLCγ activation.

Furthermore, it was hypothesized that:

1. Appropriate compartmentalization is likely a key component to PLCγ activation.
2. Appropriate compartmentalization is likely not being achieved in the AtT20 system.

Thus, the focus of the thesis shifted from concentrating on determining whether or not co-expression of the BCR, Syk, BLNK and BTK is sufficient to reconstitute PLCγ activation in this system to concentrating on the compartmentalization of these components in the system. Indeed, membrane-enrichment studies were performed to determine whether or not BCR-induced membrane recruitment of these various components was being successfully reconstituted in the AtT20 system. From these studies, it became apparent that co-expression of the BCR, Syk, BLNK or BTK, in any combination, is not sufficient to reconstitute BCR-induced membrane recruitment of BLNK or PLCγ (Fig. 5.15). Consequently, BLNK and PLCγ were constitutively targeted to the plasma membrane in an attempt to bypass any compartmentalization defects that could be confounding the attempts to reconstitute the BCR/PLCγ pathway in the AtT20 system. If membrane-targeting of PLCγ proved able to enhance PLCγ activation it would further support the idea that there was a PLCγ compartmentalization defect in the system and subsequent studies could focus on determining why this defect existed. Similarly, if membrane-targeting of BLNK proved able to enhance PLCγ activation it would further support the idea that there was a BLNK compartmentalization defect in this system and subsequent studies could focus on determining why this defect existed.

7.4.3 Subsequent Findings Regarding the BCR/PLCγ Pathway

The results of constitutively targeting BLNK and PLCγ to the plasma membrane in the AtT20 system are presented and discussed Chapter 6 and thus, will not be reviewed at length here. Rather, this discussion will focus only on the most salient findings of these investigations. First, it was found that targeting BLNK to the plasma membrane (TmBLNK) or to lipid rafts in the plasma membrane (AcBLNK) is not sufficient to enhance BCR-induced PLCγ activation as

compared to cytoplasmic BLNK (BLNK). Furthermore, it was found that constitutively targeting BLNK to the plasma membrane is not sufficient to reconstitute BCR-induced PLCγ membrane recruitment. These findings suggest that, regardless of form, BLNK may not be able to associate with and appropriately localize PLCγ in the AtT20 system. Alternatively, it may be that maximal PLCγ activation has been achieved in the BCR/Syk/BLNK cell line and thus, no gain is to be had by targeting BLNK to the plasma membrane. To address these possibilities PLCγ was constitutively targeted to the plasma membrane with the expectation that an increase in PLCγ activity will be observed if there truly is a PLCγ compartmentalization defect in the AtT20 system.

As expected, BCR-induced PLCγ activity was found to be enhanced in cell lines expressing AcPLCγ2 (i.e., lipid raft targeted PLCγ) as compared to those that expressed endogenous PLCγ1. And after ruling out possible isoform and over-expression effects (Chapter 6.2.8) it was concluded that this increased activity was indeed a consequence of targeting PLCγ to lipid rafts in the plasma membrane. Furthermore, it is tempting to infer that this finding demonstrates that maximal PLCγ activation had not been achieved in the previous cell lines and that it has not been achieved due to mis-compartmentalization of PLCγ. However, it could be argued the high level of PLCγ activity observed is not an indication of a deficit in the previously cell lines but rather merely an artefact of "over-localizing" PLCγ to the plasma membrane. Without further evidence, it would be difficult to distinguish between these possibilities. Nevertheless, when this finding is considered along with the membrane-enrichment studies it appears fair to conclude that BLNK and PLCγ are mis-compartmentalized in the AtT20 system and that this mis-compartmentalization is impairing the attempts to reconstitute the BCR/PLCγ pathway. Given this, the question naturally arises as to why these components are being mis-compartmentalized in the AtT20 system. However, before considering this question I would like to take a moment to consider some related work conducted by my contemporaries in the field of BCR/PLCγ signaling.

Shortly after I had begun the membrane-targeted BLNK and PLCγ studies a paper was published by Rodriguez *et al.*, (2003) entitled "Requirements for distinct steps of phospholipase Cγ2 regulation, membrane-raft targeting and subsequent enzyme activation in B-cell signaling". In this paper the authors dissect the BCR/PLCγ pathway using a series of mutant and/or chimeric PLCγ constructs that they then introduce into chicken DT40 B cells that are deficient in PLCγ2,

BLNK, BTK or Syk. From this approach they determined that targeting PLCγ to lipid rafts is sufficient to reconstitute BCR-induced PLCγ activation in BLNK deficient cell lines. However, they found that a more general targeting of PLCγ to the plasma membrane is not sufficient to reconstitute PLCγ activation in BLNK deficient cell lines. This finding is significant as it highlights that not all membrane-targeting is equal (similar to what was observed in this thesis for TmBLNK and AcBLNK and their effects on PLCγ phosphorylation) and that precise compartmentalization is a key requirement for PLCγ activation. Furthermore, this finding suggests that targeting PLCγ to the plasma membrane is sufficient to overcome the requirement for BLNK in the BCR/PLCγ pathway. Similarly, co-expression of the BCR, Syk and AcPLCγ was found sufficient to reconstitute BCR-induced PLCγ activation in the AtT20 system despite the absence of BLNK. At this point one may question, "If these studies have been previously performed and reported, why they were repeated in this thesis?" To answer this it is important to consider that the focus of this study was on sufficiency while the focus of the other study was on necessity. Granted, this other study coupled a loss-of-function and gain-of-function approach to effectively dissect the BCR/PLCγ pathway but their experiments were performed in B cells and thus, could not fully address the concept of sufficiency. In contrast, the focus of this study was to determine whether or not the BCR, Syk, BLNK and BTK are sufficient to reconstitute the BCR/PLCγ pathway in the AtT20 system and in doing so, hopefully determine whether or not the present model of the BCR/PLCγ pathway is complete. When, in the course of this study, it was found that these components were not sufficient to reconstitute the BCR/PLCγ pathway, investigations turned to determining why this pathway may be defective in the AtT20 system. From these investigations it was determined that BCR-induced BLNK and PLCγ membrane recruitment may not be reconstituted in this system. Thus, BLNK and PLCγ were constitutively targeted to the plasma membrane in an attempt to overcome this apparent defect. From these studies it was determined that: (1) that membrane-targeting of PLCγ is sufficient to reconstitute its activation in the AtT20 system even in the absence of BLNK and (2) that membrane-targeting of BLNK is not sufficient to reconstitute PLCγ membrane recruitment or activation in the AtT20 system. Ultimately these studies suggest that there is a defect in the BCR/PLCγ pathway beyond the mere mis-compartmentalization of BLNK. And thus, we return to considering why BLNK and PLCγ may be mis-compartmentalized in this system.

7.5 Outstanding Questions, Possible Explanations and Future Work

7.5.1 Mis-Compartmentalization of BLNK in the AtT20 System.

Co-expression of the BCR, Syk, and BLNK is sufficient to reconstitute BCR-induced PLCγ activation. However, it is hypothesized that this reconstitution is only partial. Indeed, BCR-induced membrane-recruitment of BLNK and PLCγ is not apparent in the AtT20 system, in stark contrast to what is observed in B cells. Thus, BLNK and PLCγ do not appear to be appropriately compartmentalizing in the AtT20 system. Given this, the question is asked as to why? To answer this it is best to recall the initial steps of the proposed model of the BCR/PLCγ pathway.

At the onset of this thesis the BCR/PLCγ pathway was proposed to include the following steps:

1. BCR cross-linking leads the BCR to translocate into lipid rafts.
2. Lipid raft translocation brings the BCRs into close proximity with active Lyn.
3. Active Lyn then phosphorylates the BCR on the Igα/β ITAMs.
4. The SFKs (including Lyn) are then recruited to the BCR by way of their SH2 domains binding to the phosphorylated Igα/β ITAMs
5. Such recruitment brings the SFKs into close proximity with each other enabling them to trans-phosphorylate and activate each other as well as to further phosphorylate the Igα/β ITAMs, creating a positive feedback loop.
6. Syk is also recruited from the cytosol to plasma membrane/BCR by way of its SH2 domain binding to the phosphorylated Igα/β ITAMs.
7. Such recruitment brings Syk into close proximity with the active SFKs such that they can phosphorylate and activate Syk.
8. BLNK is also recruited from the cytosol to the plasma membrane/BCR by way of its SH2 domain binding to phosphorylated Igα tyrosines that exist outside of the ITAMs.
9. Such recruitment brings BLNK into close proximity with active Syk such that Syk can phosphorylate BLNK.
10. BTK and PLCγ are then recruited from the cytosol to the plasma membrane/BCR signaling complex by way of their SH2 domains binding to the BCR-associated, phosphorylated BLNK.
11. Such recruitment brings PLCγ into close proximity with BTK and Syk such that they can phosphorylate PLCγ.

Based on this model it was hypothesized that co-expression of the BCR, Syk and BLNK should be sufficient to reconstitute BCR-induced BLNK membrane recruitment and phosphorylation and subsequently PLCγ membrane-recruitment in the AtT20 system. Furthermore, it was hypothesized that these components should be sufficient to reconstitute at least partial BCR-induced PLCγ phosphorylation and activation via Syk (only partial due to the absence of BTK). Importantly, it was hypothesized that co-expressions of the SFKs would not be necessary as the AtT20 system endogenously expresses the Src family kinase, Fyn. Furthermore, expression of the BCR alone has been shown to be sufficient to reconstitute BCR-induced Igα/Igβ phosphorylation in the AtT20 system (Richards *et al.*, 1996). However, as discussed above, these components do not appear sufficient to reconstitute BCR-induced BLNK membrane-recruitment. Given this, it is necessary to reconsider both the system and the model.

One possible explanation for the apparent mis-compartmentalization of BLNK could be that Igα is failing to recruit BLNK in the AtT20 system. According to the model, Igα must become phosphorylated on a non-ITAM tyrosines to associate with BLNK (Y204, murine) (Engles *et al.*, 2001; Kabak *et al.*, 2002). However, it has yet to be confirmed that Igα is being phosphorylated on this residue in the AtT20 system. It may be that Igα is only phosphorylated on the ITAM tyrosines (Y182 and Y193, murine) and as such, is unable to associate with BLNK. Indeed, co-immunoprecipitation studies were attempted to determine whether or not BLNK is able to associate with Igα in this system. Unfortunately, these studies proved inconclusive. Still, this theory could be further investigated by using either residue-specific phospho-tyrosine antibodies or phospho-peptide mapping techniques to clearly define which Igα tyrosine residues are becoming phosphorylated in this system. Furthermore, if Igα was found to be phosphorylated only on its ITAM residues, studies should focus on attempting to fully reconstitute Igα phosphorylation. In particular, reconstitution studies with the entire gamut of lymphoid-specific SFKs may be in order.

Another possible explanation for the apparent mis-compartmentalization of BLNK is that phosphorylated Igα alone is not sufficient to recruit BLNK to the plasma membrane. Rather, there may be additional lymphoid components required for this process. Initially, this theory appears at odds with the literature which suggests that BLNK can directly bind to phosphorylated Igα (Engles *et al.*, 2001; Kabak *et al.*, 2002). However, upon closer inspections of Engles *et al.*'s (2001) work it is found that while they clearly demonstrate that phospho-tyrosine 204 is required

for BLNK's membrane recruitment they do not show that the association is direct. Rather, association studies are performed using whole lysates from B cells leaving the possibility that there is an intermediary lymphoid-specific component involved in linking BLNK to the phosphorylated Igα. Similarly, Kabak and colleagues (2002) do not entirely rule out the possibility of the requirement for an intermediary lymphoid-specific component in their studies. True, they do show that a PDGFRβ/Igα chimera can bind directly to a GST-BLNK-SH2 domain construct in a far Western, but considering the use of chimeras and partial proteins in this experiment the question arises as to whether or not this finding can be extrapolated to a physiological association. Thus, if it is found that Igα phosphorylation is fully reconstituted in the AtT20 system subsequent studies may do well to focus on whether or not an additional lymphoid-specific component is required to facilitate BLNK's membrane recruitment.

Indeed, many studies have focused on identifying the components involved in recruiting BLNK to the plasma membrane. From its first identification BLNK was recognized to be related to the T cell adapter protein, Slp-76 (hence Slp-65 as an alternate name for BLNK) that is required to couple the TCR to PLCγ in T cells (reviewed in Jordan *et al.*, 2003). In T cells, Slp-76 is proposed to facilitate membrane-recruitment and phosphorylation of PLCγ1 via a multi-protein complex. In particular, Slp-76 is proposed to constitutively associate with PLCγ1 and another adapter protein, Gads to form a Gads/Slp-76/PLCγ1 complex. Upon TCR cross-linking the TCR translocates into lipid rafts where it induces the activation of a PTK cascade that in turn phosphorylates a lipid raft-localized, transmembrane adapter protein termed LAT. LAT then recruits the Gads/Slp-76/PLCγ1 complex to the TCR signaling complex via Gads' SH2 domain. Once so recruited, Slp-76 becomes tyrosine phosphorylated and able to associate with the Tec kinase, IKT. IKT, in turn, phosphorylates the co-localized PLCγ1 and thereby contributing to its activation. And thus, by analogy it has been proposed that BLNK would likewise be recruited to the plasma membrane via a transmembrane protein and/or a multi-adapter complex. Consequently, numerous studies have attempted to identify the "missing linker" in the BCR/PLCγ pathway.

Aside from identifying Igα as the potential "missing linker" studies have also identified the Linker of Activated B Cells (LAB, also known as Non-T cell Activation Linker [NTAL]) as a potential candidate (Bridcka *et al.*, 2002; Janssen *et al.*, 2003; reviewed in Wu and Koretzky, 2003). In brief, LAB is a transmembrane protein that contains 9 tyrosines in its cytoplasmic

domain that become tyrosine phosphorylated upon BCR cross-linking (Bridcka *et al.*, 2002; Janssen *et al.*, 2003, reviewed in Wu and Koretzky, 2003). The adapter protein Grb2 is then recruited to these phosphorylated tyrosines via its SH2 domain. Concurrently Grb2's SH3 domain is thought to associate with BLNK's proline rich domain such that BLNK is also recruited to the plasma membrane where it may further interact with the components of the BCR/PLCγ pathway (Bridcka *et al.*, 2002; Janssen *et al.*, 2003, reviewed in Wu and Koretzky, 2003). However, a caveat of this model is the fact that it has been difficult to establish an association between BLNK and LAB *in vivo*. Nonetheless, loss-of-function studies indicate that LAB is required for maximal BCR-induced calcium flux and Erk activation in B cells (Janssen *et al.*, 2003; reviewed in Wu and Koretzky, 2003).

Alternatively, BLNK could be recruited to the plasma membrane by way of BTK. In the aforementioned model it has been proposed that BTK is recruited to the plasma membrane/BCR signaling complex by way of its interaction with membrane-localized, tyrosine phosphorylated BLNK. However, BTK can also be recruited to the plasma membrane by way of its PH domain binding to PIP_3 (Li *et al.*, 1997; Vernai *et al.*, 1999). In turn, BTK's SH2 domain may associate with phosphorylated BLNK, thereby recruiting it to the membrane. However, the difficulty with this model is that BTK can only associate with phosphorylated BLNK and BLNK phosphorylation is thought to require BLNK's membrane recruitment. Thus, BLNK would already need to be recruited to the membrane before it could associate with BTK, which of course brings us back to the question of how BLNK would first be recruited to the membrane. Nonetheless, the possibility that phosphorylated BLNK could be associated with membrane-associated BTK is recalled here as it may have implications in the AtT20 system where a large portion of BTK appears to be constitutively membrane-associated. As mentioned previously, it may be that BLNK is being mis-compartmentalized in this system, in part, by associating with this membrane-associated BTK. Indeed, this possibility must be addressed before future reconstitution studies can truly assess the role of BTK in the BCR/PLCγ pathway in the AtT20 system.

And finally, studies have suggested that a novel adapter, the B Lymphocyte Adaptor Molecule of 32 kD (Bam32), may recruit PLCγ to the BCR signaling complex independent of BLNK (Marshall *et al.*, 2000; Niiro *et al.*, 2003). Bam32 is a cytosolic adapter protein that contains a C-terminal PH domain that binds to PIP_3 at the plasma membrane and an N-terminal SH2

domain that binds to PLCγ2 (Marshall *et al.*, 2000; Niiro *et al.*, 2003). Thus, Bam32 is hypothesized to facilitate PLCγ2 membrane recruitment (Marshall *et al.*, 2000; Niiro *et al.*, 2003). This hypothesis is supported by loss-of-function studies that indicate that Bam32 is required for maximal BCR-induced calcium flux, Erk activation and PLCγ phosphorylation (Niiro *et al.*, 2002). However, Bam32 may not be involved in the initial BCR-induced activation of PLCγ2 as its membrane recruitment is dependent on PI3K activation. And, perhaps more strikingly, its association with PLCγ2 is dependent on PLCγ2 phosphorylation which is an event that putatively requires previous membrane recruitment of PLCγ. Regardless, it can be seen that numerous lymphoid-specific components, beyond those investigated in this thesis, exist that may be involved in the BCR/PLCγ pathway. And thus, future investigators may do well to consider these components in any further attempts to reconstitute the BCR/PLCγ pathway in the AtT20 system.

7.5.2 Mis-Compartmentalization of PLCγ in the AtT20 System.

It was initially hypothesized that PLCγ was mis-compartmentalized as a consequence of BLNK being mis-compartmentalized in the AtT20 system. However, constitutively targeting BLNK to the plasma membrane (TmBLNK) or to lipid rafts in the plasma membrane (AcBLNK) is not sufficient to reconstitute BCR-induced PLCγ membrane-recruitment in this system. This suggests that there may be some other factor that is limiting PLCγ's compartmentalization. For example, it may be that BLNK is not being sufficiently tyrosine phosphorylated and thus, is unable to associate with and facilitate PLCγ's phosphorylation, localization and activation. To directly test this theory it is necessary to develop effective co-immunoprecipitation strategies for this system. In the meantime, phospho-peptide mapping should be performed to definitively determine which tyrosines in BLNK are becoming phosphorylated. Depending on the results of this mapping, several courses of investigation could follow. If BLNK is found to be phosphorylated on only a subset of its tyrosines then further experiments might focus on attempting to fully reconstitute BLNK phosphorylation in this system. Again, reconstitution studies with the entire gamut of lymphoid-specific SFKs may be in order. Alternatively, if BLNK is found to be fully phosphorylated then further experiments might focus on determining whether or not an additional lymphoid-specific component is required to facilitate the BLNK/PLCγ association.

7.6 Compartmentalization of the BCR to Lipid Rafts

During the tenure of this thesis the importance of lipid rafts in BCR signaling was increasingly revealed. Yet the mechanisms involved in regulating the inducible translocation of the BCR into lipid rafts remained undefined. Fortunately, the Matsuuchi lab possessed some unique cell lines that could be used to further investigate and define these mechanisms. Thus, in conjunction with my colleagues, Lorna Santos and May Dang-Lawson, I became involved in such studies. The findings of these studies have been presented and discussed in Chapter Three of this thesis and have been published in an article entitled "Localization in membrane microdomains of the Igα/β component of the BCR expressed by a B lymphoma variant" (Jackson *et al.*, 2005).

Through this work it was established that the intact BCR can translocate into lipid rafts in the immature B cell line, WEHI 231 (Jackson *et al.*, 2005). This finding is important as it challenges previous reports that claim that such translocation does not occur in immature B cells (Cheng *et al.*, 2001; Sproul *et al.*, 2000). While the reason for these reported differences remain unclear their mere existence highlights some of the difficulties that face investigators in the field of lipid raft research. Furthermore, it suggests the need for further investigation into the role of lipid rafts in BCR signaling in immature B cells.

Regardless, having established that the wild-type BCR translocates into lipid rafts in the WEHI 231 cell line we proceeded to investigate solo Igα/β lipid raft translocation in the mIgM-deficient WEHI mutant, WEHI 303.1.5. From this it was found that the solo Igα/β can associate with and translocate into lipid rafts in the WEHI 303.1.5 cell line (Jackson *et al.*, 2005). This finding suggests that the Igα/β contains structural information that is sufficient to mediate its association with lipid rafts. When this finding is considered along with the finding that solo mIgM contains similar information (Cheng *et al.*, 2001) it suggests that mIgM and Igα/β may contain a common lipid raft affinity domain (LRAD). Given this, future studies aimed at identifying LRADs may do well to focus on analyzing the structural features that are common to both mIgM and Igα/β, such as their transmembrane domains and their membrane proximal domains.

Additionally, it was found that solo Igα/β can translocate into lipid rafts and induce BCR-like signaling in the WEHI 303.1.5. This finding is important as it may have physiological relevance. Indeed, previous studies have indicated that the putative pro-B cell receptor is expressed on the

surface of pro-B cells as a solo Igα/β in association with calnexin (Nagata *et al.*, 1997). Furthermore, this receptor has been proposed to be involved in development-dependent signaling (Nagata *et al.*, 1997). Yet it has been unclear whether such signaling could occur in the absence of an antigen-binding subunit. The findings here suggest that such signaling could indeed occur, and may occur from within lipid rafts, providing that there is a physiological ligand capable of cross-linking the solo Igα/β. To further test this hypothesis lipid raft loss-of-function studies may be performed in pro-B cells. In particular, lipid rafts could be disrupted with cholesterol sequestering agents to determine whether or not lipid rafts are necessary to pro-B cell signaling and development. And finally, it would be necessary to identify a physiological ligand that it is able to bind and cross-link the putative pro-B cell receptor and initiate its activation.

7.7 Final Words

The work of this thesis has established that co-expression of the BCR, Syk, BLNK and BTK is not sufficient to reconstitute the BCR/PLCγ pathway in the AtT20 system. This finding may be attributable to a deficiency in the AtT20 system as BTK appears to be constitutively membrane associated, phosphorylated and presumably active and as such may be inappropriately interacting with the BCR/PLCγ pathway. However, the fact that BTK is constitutively membrane-associated and activated may also be a reflection of a deficiency in the proposed model as a missing lymphoid-specific component may be required to regulate BTK's membrane-localization and activation in the AtT20 system. Thus, future studies will need to address this issue.

Additionally, it was established that co-expression of the BCR, Syk and BLNK is not sufficient to reconstitute BCR-induced BLNK and PLCγ membrane recruitment in this system. This finding may be a reflection of a requirement for additional lymphoid-specific components to reconstitute BCR-induced BLNK and PLCγ membrane compartmentalization, and accordingly PLCγ activation, in this system. Thus, future studies will also need to address this issue.

As well, it was established that co-expression of the BCR, Syk and membrane-targeted BLNK is not sufficient to reconstitute BCR-induced PLCγ membrane-recruitment or activation. This finding suggests that BLNK and PLCγ are unable to appropriately associate in this system. This could be attributable either to insufficient BLNK phosphorylation or to the requirement for an

intermediary lymphoid-specific component in this system. Thus, future studies will also need to address this issue.

And finally, it was established that co-expression of the BCR, Syk and membrane-targeted PLCγ is sufficient reconstitute BCR-induced PLCγ activation. This finding demonstrates that the BCR/PLCγ pathway can be successfully reconstituted in the AtT20 system as long as PLCγ is appropriately compartmentalized. Additionally, it demonstrates that membrane-targeting of PLCγ can overcome the requirement for BLNK in the BCR/PLCγ pathway. And thus, this finding highlights the importance of compartmentalization in the BCR/PLCγ pathway and moreover the importance of BLNK in facilitating PLCγ's compartmentalization.

In conclusion, the findings of this thesis do not support the original hypothesis. However, neither do they necessitate that our current map of the BCR/PLCγ pathway be completely re-configured. Rather, the findings herein suggest, as originally anticipated, that the details of the map still need to be refined. In particular, this thesis has raised the possibility that the SFKs may be more prominent in the topography of the BCR/PLCγ pathway than initially hypothesized. Indeed, these SFKs may be required to reconstitute the full phosphorylation of Igα and BLNK such that a functional BCR/PLCγ signaling complex can be achieved in the AtT20 system. As well, this thesis has raised that possibility that we may have yet to identify all the lymphoid-specific components required for the BCR/PLCγ pathway. Indeed, key landmarks may yet be missing from our map. And thus, I finish this thesis knowing that the map remains incomplete yet also knowing that I have helped to provide those who would continue this work with a direction and a compass with which to proceed.

References

Abram CL, and Courtneidge SA. 2000. Src family tyrosine kinases and growth factor signaling. *Experimental Cell Research* 254:1-13.

Afar DEH, Park H, Howell BW, Rawlings DJ, Cooper J, and Witte ON. 1996. Regulation of Btk by Src family tyrosine kinases. *Molecular and Cellular Biology* 16:3465-3471.

Alessi DR, Deak M, Casamayor A, Caudwell FB, Morrice N, Norman DG, Gaffney PRJ, Reese CB, MacDougall CN, Harbison D, Ashworth A, and Bownes M. 1997b. 3-Phosphoinositde-dependent protein kinase-1 (PDK1): structural and functional homology with *Drosophila* DSTPK61 kinase. *Current Biology* 7:776-779.

Alessi DR, James SR, Downes CP, Holmes AB, Gaffney PRJ, Resse CB, and Cohen P. 1997a. Characterization of a 3-phosphinositide-dependent protein kinase which phosphorylates and activates protein kinase Ba. *Current Biology* 7:261-269.

Alland L, Peseckis SM, Atherton RE, Berthiaume LG, and Resh MD. 1994. Dual myristylation and palmitylation of Src family member p59fyn affects subcellular localization. *Journal of Biological Chemistry* 269:16701-16705.

Aman MJ, and Ravichandran KS. 2000. A requirement for lipid rafts in B cell receptor induced Ca^{2+} flux. *Current Biology* 10:396.

Anderson D, Koch CA, E. C. Grey L, Moran MF, and Pawson T. 1990. Binding of SH2 domains of phospholipase C gamma 1, GAP, and Src to activated growth factor receptors. *Science* 250:979-982.

Anderson KE, Coadwell J, Stephens LR, and Hawkins PT. 1998. Translocation of PDK-1 to the plasma membrane is important in allowing PDK-1 to activate protein kinase B. *Current Biology* 8:684.

Aoki Y, Isselbacher KJ, and Pillai S. 1994. Bruton tyrosine kinase is tyrosine phosphorylated and activated in pre-B lymphocytes and receptor-ligated B cells. *Proceedings of the National Academy of Sciences* 91:10606-10609.

Astoul E, Watton S, and Cantrell D. 1999. The dynamics of protein kinase B regulation during B cell antigen receptor engagement. *Journal of Cell Biology* 145:1511-1520.

Baba Y, Hashimoto S, Matsushita M, Watanabe D, Kishimoto T, Kurosaki T, and Tsukada S. 2001. BLNK mediates Syk-dependent Btk activation. *Proceedings of the National Academy of Sciences USA* 98:2582-2586.

Barbazuk SM, and Gold MR. 1999. Protein kinase C-delta is a target of B-cell antigen receptor signaling. *Immunology Letters* 69:259-267.

Barthwal MK, Sathyanarayana P, Kundu CN, Rana B, Pradeep A, Sharma C, Woodgett JR, and Rana A. 2003. Negative regulation of mixed lineage kinase 3 by protein kinase B/Akt leads to cell survival. *Journal of Biological Chemistry* 278.

Bernard, A. Coitot, S. Bremont, A. Bernard, Ghislaine. 2005. T and B Cell Cooperation: A Dance of Life and Death. *Transplantation* 79(3) Supplement:S8-S11.

Benschop RJ, and Cambier JC. 1999. B cell development: signal transduction by antigen receptors and their surrogates. *Current Opinion in Immunology* 11:143-151.

Bijsterbosch MK, Meade CJ, Turner GA, and Klaus GGB. 1985. B lymphocyte receptors and phosphoinositide degradation. *Cell* 41:999-1006.

Broome MA, and Hunter T. 1996. Requirement for c-Src Catalytic Activity and the SH3 Domain in Platelet-derived Growth Factor BB and Epidermal Growth Factor Mitogenic Signaling. *Journal of Biological Chemistry* 271:16798 - 16806.

Brown DA, and London E. 1998. Functions of Lipid Rafts in Biological Membranes. *Annual Review of Cell and Developmental Biology* 14:111-136.

Brown DA, and London E. 2000. Structure and Function of Sphingolipid- and Cholesterol-rich Membrane Rafts. *Journal of Biological Chemistry* 275:17221-17224.

Brown DA, and Rose JK. 1992. Sorting of GPI-anchored proteins to glycolipid-enriched membrane subdomains during transport to the apical cell surface. *Cell* 68:533–544.

Burg DL, Furlong MT, Harrison ML, and Geahlen. 1994. Interactions of Lyn with the antigen receptor during B cell activation. *Journal of Biological Chemistry* 269:28136-28142.

Campbell KS, Hager EJ, Friedrich RJ, and Cambier JC. 1991. IgM antigen receptor complex contains phosphoprotein products of B29 and *mb-1* genes. *Proceedings of the National Academy of Sciences USA* 88.

Campbell M, and Sefton BM. 1990. Protein tyrosine phosphorylation is induced in murine B lymphocytes in response to stimulation with anti-immunoglobulin. *EMBO Journal* 9:2125-2131.

Campbell M, and Sefton BM. 1992. Association between B-lymphocyte membrane immunoglobulin and multiple members of the Src family of protein tyrosine kinases. *Molecular and Cellular Biology* 12:2315-2321.

Cardone MH, Roy N, Stennicke HR, Salvesen GS, Franke TFS, Frisch S, and Reed JC. 1998. Regulation of cell death protease caspase-9 by phosphorylation. *Science* 282:1318-1321.

Carpenter G, and Ji Q. 1999. Phospholipase C as a signal-transducing element. *Experimental Cell Research* 253:15-24.

Carter RH, Park DJ, Rhee SG, and Fearon DT. 1991. Tyrosine phosphorylation of phospholipase C induced by membrane immunoglobulin cross-linking in B lymphocytes. *Proceedings of the National Academy of Sciences USA* 88:2745-2749.

Casillas A, H. C., Williams K, Katz R, Nel AE. 1991. Stimulation of B-cells via the membrane immunoglobulin receptor or with phorbol myristate 13-acetate induces tyrosine phosphorylation and activation of a 42-kDa microtubule-associated protein-2 kinase. *Journal of Biological Chemistry* 266:19088-19094.

Castagnoli L, Constantini A, Dall'Armi C, Gonfloni S, Montecchi-Palazzi L, Panni S, Paoluzi S, Santonico E, and Cesareni G. 2004. Selectivity and promiscuity in the interaction network mediated by protein recognition molecules. *FEBS Letters* 567:74-79.

Cheng PC, Brown BK, Song W, and Pierce SK. 2001. Translocation of the B Cell Antigen Receptor into Lipid Rafts Reveals a Novel Step in Signaling. *The Journal of Immunology* 166:3693-3701.

Cheng PC, Dykstra M, Mitchell RN, and Pierce SK. 1999. A Role for Lipid Rafts in B Cell Antigen Receptor Singaling and Antigen Targeting. *Journal of Experimental Medicine* 190:1549-1560.

Cherukuri A, Dykstra M, and Pierce SK. 2001. Floating the Raft Hypothesis: Lipid Rafts Play a Role in Immune Cell Activation. *Immunity* 14:657-660.

Chiu CW, Dalton M, Ishiai M, Kurosaki T, and Chan AC. 2002. BLNK: molecular scaffolding through '*cis*'-mediated organization of signaling proteins. *EMBO Journal* 21:6461-6472.

Church, J. Baxter KA. McLarnon JG. 1998. pH modulation of Ca^{2+} responses and a Ca^{2+}-dependent K^+ channel in cultured rat hippocampal neurones. *Journal of Physiology* 511(1):119-132.

Clark MR, Johnson SA, and Cambier JC. 1994. Analysis of Ig-α-tyrosine kinase interaction reveals two levels of binding specificity and tyrosine phosphorylated Ig-α stimulation of Fyn activity. *EMBO Journal* 13:1911-1919.

Clayton E, Bardi G, Bell SE, Chantry D, Downes CP, Gray A, Humphries LA, Rawlings DJ, Reynolds H, Vigorito E, and Turner M. 2002. A crucial role for the p110d subunit of phosphatidylinositol 3-kinase in B cell development and activation. *Journal of Experimental Medicine* 196:753-763.

Coggeshall KM, and Cambier JC. 1984. Membrane Immunoglobulins Transduce Signals via Activation of Phosphatidylinositol Hydrolysis. *Journal of Immunology* 133:3382-3386.

Coggeshall KM, McHugh JC, and Altman A. 1992. Predominant expression and activation-induced tyrosine phosphorylation of phospholipase C-g2 in B lymphocytes. *Proceedings of the National Academy of Sciences USA* 89:5660-5664.

Condon C, Hourihane SL, Dang-Lawson M, Escribano J, and Matsuuchi L. 2000. Aberrant Trafficking of the B Cell Receptor Ig-ab Subunit in a B Lymphoma Cell Line. *The Journal of Immunology* 165:1427-1437.

Cook SJ, and McCormick F. 1993. Inhibition by cAMP of Ras-dependent activation of Raf. *Science* 262:1069-1072.

Craxton A, Jiang A, Kurosaki T, and Clark EA. 1999. Syk and Bruton's tyrosine kinase are required for B cell antigen receptor-mediated activation of the kinase Akt. *Journal of Biological Chemistry* 274:30644-30650.

Crespo P, Schuebel KE, Ostrom AA, Gutkind JS, and Bustelo XR. 1997. Phosphorylation-dependent activation of Rac-1 GDP/GTP exchange by the *vav* proto-oncogene product. *Nature* 385:169-172.

Cross DAE, Alessi DR, Cohen P, Andjelkovic M, and Hemmings BA. 1995. Inhibition of glycogen synthase kinase-3 by insulin mediated protein kinase B. *Nature* 378:785-789.

Danielsen EM. 1995a. A Transferrin-Like GPI-Linked Iron Binding Protein in Detergent-Insoluble Non-Caveolar Microdomains at the Apical Surface of Fetal Intestinal Epithelial Cells. *Biochemistry* 34:1596-1605.

Danielsen EM. 1995b. Involvement of detergent-insoluble complexes in the intracellular transport of intestinal brush border enzymes. *Biochemistry* 34:1596–1605.

Davis RJ. 2000. Signal transduction by the JNK group of MAP kinases. *Cell* 103:239-252.

de Weers M, Mensink RG, Kraakman ME, and Schuurman RK. 1994. Mutation analysis of the Bruton's tyrosine kinase gene in X-linkedagammaglobulinemia: identification of a mutation which affects the same codonas is altered in immunodeficient xid mice. *Human Molecular Genetics* 3:161-166.

Deans JP, Robbins SM, Polyak MJ, and Savage JA. 1998. Rapid redistribution of CD20 to a low density detergent-insoluble membrane compartment. *Journal of Biological Chemistry* 273:344-348.

DeBell KE, Stoica BA, Veri MC, Di Baldassarre A, Miscia S, Graham LJ, Rellahann SLP, Ishiai M, Kurosaki T, and Bonvini E. 1999. Functional independence and interdependence of the Src homology domains of phospholipase Cγ1 in B-cell receptor signal transduction. *Molecular and Cellular Biology* 19:7388-7398.

DiDonato JA, Hayakawa M, Rothwarf DM, Zandi E, and Karin M. 1997. A cytokine-responsive IB kinase that activates the transcription factor NF-B. *Nature* 388:548-554.

Dillon SR, Mancini M, Rosen A, and Schlissel MS. 2000
Annexin V binds to viable B cells and co-localizes with a marker of lipid rafts upon B cell receptor activation *Journal of Immunology* 164:1322-1332.

Dolmetsch RE, Lewis RS, Goodnow CC, and Healy JI. 1997. Differential activation of transcription factors induced by Ca2+ response amplitude and duration. *Nature* 386:855-858.

Dykstra M, Cherukuri A, and Pierce SK. 2001. Rafts and synapses in the spatial organization of immune cell signaling receptors. *Journal of Leukocyte Biology* 70:699-707.

Dykstra M, Cherukuri A, Sohn HW, Shiang-Jong T, and Pierce SK. 2003. Location is Everything: Lipid Rafts and Immune Cell Signalling. *Annual Review Immunology* 21:457-481.

Engels N, Wollscheid B, and Wienands J. 2000. Association of SLP-65/BLNK with the B cell antigen receptor through a non-ITAM tyrosine of Ig-a. *European Journal of Immunology* 31:2126-2134.

Fahey KA, and DeFranco AL. 1987. Cross-linking membrane IgM induces production of inositol trisphosphate and inositol tetrakisphosphate in WHI-231 B lymphoma cells. *Journal of Immunology* 138:3935-3942.

Falasca M, Logan SK, Lehto VP, Baccante G, Lemmon MA, and Schlessinger J. 1998. Activation of phospholipase C gamma by PI 3-kinase-induced PH domain-mediated membrane targeting. *EMBO Journal* 17:414-422.

Fillipa N, Sable CL, Hemmings BA, and van Obberghen E. 2000. Effect of phosphoinositide-dependent kinase 1 on protein kinase B translocation and its subsequent activation. *Molecular and Cellular Biology* 20:5712-5721.

Fluckiger AC, Li Z, Kato RM, Wahl MI, Ochs HD, Longnecker R, Kinet JP, Witte ON, Shcarenberg AM, and Rawlings DJ. 1998. Btk/Tec kinases regulate sustained increases in intracellular Ca^{2+} following B-cell receptor activation. *EMBO Journal* 17:1973-1985.

Fra AM, Williamson E, Simons K, and Parton RG. 1994. Detergent-insoluble glycolipid microdomains in lymphocytes in the absence of caveolae. *Journal of Biological Chemistry* 269:30745-30748.

Fruman DA, Rameh LE, and Cantley LC. 1999. Phosphoinositide binding domains: embracing 3-phosphate. *Cell* 97:817-820.

Fu C, and Chan AC. 1997. Identification of two tyrosine phosphoproteins, pp70 and pp68, that interact with PLC, Grb2, and Vav following B cell antigen receptor activation. *Journal of Biological Chemistry* 272:27362–27368.

Fu C, Turck CW, Kurosaki T, and Chan AC. 1998. BLNK: A central linker protein in B cell activation. *Immunity* 9:93-103.

Goitsuka R, Fujimara Y, Mamada H, Umeda A, Morimura T, Uetsuka K, Doi K, Tsuji S, and Kitamura D. 1998. Cutting Edge: BASH, a novel signaling molecule preferentially expressed in B cells of the bursa of fabricius. *Journal of Immunology* 161:5804-5808.

Gold MR. 2000. Intermediary signaling effectors coupling the B cell receptor to the nucleus. *Current Topics in Microbiology and Immunology* 245:78-134.

Gold MR. 2002. To make antibodies or not: signaling by the B-cell antigen receptor. *TRENDS in Pharmacological Sciences* 23:316-324.

Gold MR, and Aebersold RA. 1994. Both phosphatidylinositol 3-kinase and phosphatidylinositol 4-kinase products are increased by antigen receptor signaling in B lymphocytes. *Journal of Immunology* 152:42-50.

Gold MR, Ingham RJ, McLeod SJ, Christian SL, Scheid MP, Duronio V, Santos L, and Matsuuchi L. 2000. Targets of B-cell antigen receptor signaling: the phosphatidylinositol 3-kinase/Akt/glycogen synthase kinase-3 signaling pathway and the Rap1 GTPase. *Immunological Reviews* 176:47-68.

Gold MR, Law DA, and D. Al. 1990. Stimulation of protein tyrosine phosphorylation by the B-lymphocyte recptor. *Nature* 345:810-813.

Gold MR, Matsuuchi L, Kelly RB, and Defranco AL. 1991. Tyrosine phosphorylation of components of the B-cell antigen recpetors following receptor crosslinking. *Proceedings of the National Academy of Sciences USA* 88:3436-3440.

Gold MR, Sanghera JS, Stewart J, and Pelech SL. 1992. Selective activation of p42 mitogen-activated protein (MAP) kinase in murine B lymphoma cell lines by membrane immunoglobulin cross-linking. Evidence for protein kinase C-independent and -dependent mechanisms of activation. *Biochemical Journal* 287:269-276.

Gold MR, Scheid MP, Santos L, Dang-Lawson M, Roth RA, Matsuuchi L, Duronio V, and Krebs DL. 1999. The B cell antigen receptor activates the Akt (protein kinase B)/glycogen synthase kinase-3 signaling pathway via phosphatidylinositol 3-kinase. *Journal of Immunology* 163 (4):1894-1905.

Gomez-Mouton C, Abad JL, Mira E, Lacalle RA, Gallardo E, Jimenez-Baranda S, Illa I, Bernard A, Manes S, and Martinez-A C. 2001. Segragation of leading-edge and uropod components into specific lipid rafts during T cell polarization. *Proceedings of the National Academy of Sciences USA* 98:9642-9647.

Gong S, and Nussenzweig MC. 1996. Regulation of an Early Developmental Checkpoint in the B Cell Pathway by Igβ. *Science* 272:411-414.

Gruenberg J. 2001. The endocytic pathway: a mosaic of domains *Nature Reviews Molecular Cell Biology* 2:721-730.

Gu H, Pratt JC, Burakoff SJ, and Neel BG. 1998. Cloning of p97/Gab2, the major SHP-2 binding protein in hematopoietic cells reveals a novel pathway for cytokine induced gene activation. *Molecular Cell* 2:729-740.

Guo B, Kato RM, Garcia-Lloret M, Wahl MI, and Rawlings DJ. 2000. Engagement of the Human Pre-B Cell Receptor Generates a Lipid Raft-Dependent Calcium Singaling Complex. *Immunity* 13:243-253.

Hajduch E, Alessi DR, Hemmings BA, and Hundal HS. 1998. Constitutive activation of protein kinase Ba by membrane targeting promotes glucose and system A amino acid transport, protein synthesis, and inactivation of glycogen synthase kinase 3 in L6 muscle cells. *Diabetes* 47:1006-1013.

Harwood AE, and Cambier JC. 1993. B cell antigen receptor cross-linking triggers rapid PKC independent activation of P21 Ras. *Journal of Immunology* 151:4513-4522.

Hashimoto A, Takeda K, Inaba M, Sekimata M, Kaisho T, Ikehara S, Homma Y, Akira S, and Kurosaki T. 2000. Cutting Edge: Essential role of phospholipase Cγ2 in B cell development and function. *Journal of Immunology* 165.

Hashimoto R, Nakamura Y, Goto H, Wada Y, Sakoda S, Kaibuchi K, Inagaki M, and Takeda M. 1998. Domain- and site-specific phosphorylation of bovine NFκB by Rho-associated kinase. *Biochemical and Biophysical Research Communications* 245:407-411.

Hashimoto S, Iwamatsu A, Ishiai M, Okawa K, Yamadori T, Matsushita M, Baba Y, Kishimoto T, Kurosaki T, and Tsukada S. 1999. Identification of the SH2 domain binding protein of Bruton's tyrosine kinase as BLNK--Functional significance of Btk-SH2 domain in B-cell antigen receptor-coupled calcium signaling. *Blood* 94:2357-2364.

Hayashi K, Nittono R, Okamoto N, Tsuji S, Hara Y, Goitsuka R, and Kitamura D. 2000. The B cell-restricted adaptor BASH is required for normal development and antigen receptor-mediated activation of B cells. *Proceedings of the National Academy of Sciences USA* 97:2755-2760.

Hayashi K, Nojima T, Goitsuka R, Kitamura D, and J. I. 5980-8. 2004. Impaired receptor editing in the primary B cell repertoire of BASH-deficient mice. *Journal of Immunology* 173.

Hempel WM, and DeFranco AL. 1991. Expression of Phospholipase C Isozymes by Murine B Lymphocytes. *Journal of Immunology* 146:3713-3720.

Hempel WM, Schatzman RC, and DeFranco AL. 1992. Tyrosine phosphorylation of phospholipase Cγ2 upon cross-linking of membrane Ig on murine B lymphocytes. *Journal of Immunology* 148:3021-3027.

Hermanson G, Eisenberg D, Kincade P, and Wall R. 1988. B29: A membrane of the immunoglobulin gene superfamily exclusively expressed on B-lineage cells. *Proceedings of the National Academy of Sciences* 85:6890-6894.

Hombach J, Leclerq L, Radbruch A, Rajewsky K, and Reth M. 1988. A novel 34-kd protein co-isolated with the IgM molecule in surface IgM-expressing cells. *EMBO Journal* 7:3451-3456.

Horejsi V, Drbal K, Cebecauer M, Cerny J, and Brdicka T. 1999. GPI-Linked Microdomains: A Role in Signaling Via Immune Receptors. *Immunology Today* 20:356-361.

Hutchcroft JE, Harrison ML, and Geahlen RL. 1991. B lymphocyte activation is accompanied by phosphorylation of a 72-kDa protein-tyrosine kinase. *Journal of Biological Chemistry* 266:14846-14849.

Hutchcroft JE, Harrison ML, and Geahlen RL. 1992. Association of the 72 kDa protein-tyrosine kinase PTK72 with the B cell antigen receptor. *Journal of Biological Chemistry* 267.

Ingham RJ, Holgado-Madruga M, Siu C, Wong AJ, and Gold. MR. 1998. The Gab1 protein is a docking site for multiple proteins involved in signaling by the B cell antigen receptor. *Journal of Biological Chemistry* 273:30630-30637.

Iritani BM, Forbush KA, Farrar MA, and Perlmutter RM. 1997. Control of B cell development by Ras-mediated activation of Raf. *EMBO Journal* 16:7019-7031.

Ishiai M, Kurosaki M, Pappu R, Okawa K, Ronko I, Fu C, Shibata M, Iwamatsu A, Chan AC, and Kurosaki T. 1999. BLNK required for coupling Syk to PLCγ2 and Rac1-JNK in B cells. *Immunity* 10:117-125.

Ishiai M, Sugawara H, Kurosaki M, and Kurosaki T. 1999. Cutting Edge: Association of Phospholipase C-γ2 Src Homology 2 Domains with BLNK is Critical for B Cell Antigen Receptor Signaling. *Journal of Immunology* 163:1746-1749.

Jackson T, Santos L, Dang-Lawson M, Matsuuchi L. 2005. Localization in Membrane Microdomains of the Igα/β Component of the BCR Expressed by a B Lymphoma Variant. *Immunology Letters* 99:69-79

Janeway Jr. CA, and Medzhitov R. 2002. Innate Immune Recognition. *Annual Review Immunology* 20:197-216.

Janssen E, Zhu M, Zhang W, Koonpaew S, and Zhang W. 2003. LAB: A new membrane-associated adaptor molecule in B cell activation. *Nature Immunology* 4:117-123.

Ji QS, Winnier GE, Niswender KD, Horstman D, Wisdom R, Magnuson MA, and Carpenter G. 1997. Essential role of the tyrosine kinase substrate phospholipase C-γ1 in mammalian growth and development. *Proceedings of the National Academy of Sciences* 94.

Jiang A, Craxton A, Kurosaki T, and Clark EA. 1998. Different protein tyrosine kinases are required for B cell antigen receptor-mediated activation of extracellular signal-regulated kinase, c-Jun NH_2-terminal kinase 1, and p38 mitogen-activated protein kinase. *Journal of Experimental Medicine* 188:1297-1306.

Johnson SA, Pleiman CM, Poa L, Schnerigner J, Hippen K, and Cambier JC. 1995. Phosphorylated immunoreceptor signaling motifs (ITAMS) exhibit unique abilities to bind and activate Lyn and Syk tyrosine kinase of the second-messenger subfamily. *Proceedings of the National Academy of Sciences USA* 88:4171-4175.

Jordan MS, Singer AL, and K. GA. 2003. Adaptors as central mediators of signal transduction in immune cells. *Nature Reviews Immunology* 4:110-116.

Jumaa H, Wollscheid B, Mitterer M, Wienands J, Reth M, and Nielsen PJ. 1999. Abnormal development and function of B lymphocytes in mice deficient for the signaling adaptor protein SLP-65. *Immunity* 11:547-554.

Kabak S, Skaggs BJ, Gold MR, Affolter M, West KL, Foster ML, Siemasko K, Chan AC, Aebersold R, and Clark MR. 2002. The direct recruitment of BLNK to immunoglobulin a couples the B-cell antigen receptor to distal signaling pathways. *Molecular and Cellular Biology* 22:2524-2535.

Kane LP, Shapiro VS, Stokoe D, and Weiss A. 1999. Induction of NF-κB by the Akt/PKB kinase. *Current Biology* 9:601-604.

Karasuyama H, Rolink A, and Melchers F. 1993. A complex of glycoproteins is associated with *VpreB/lambda 5* surrogate light chain on the surface of mu heavy chain-negative early precursor B cell lines. *Journal of Experimental Medicine* 178:469-478.

Kashishian A, and Cooper JA. 1993. Phosphorylation sites at the C-terminus of the platelet-derived growth factor receptor bind phospholipase C gamma 1. *Molecular and Cellular Biology* 4:49-57.

Katan M. 1998. Families of phosphoinositide-specific phospholipase C: structure and function. *Biochimica et Biophysica Acta* 1436:5-17.

Kelly ME, and Chan AC. 2000. Regulation of B cell function by linker proteins. *Current Opinion in Immunology* 12:267-275.

Kim AH, Khurisigara G, Sun X, Franke TF, and Chao MV. 2001. Akt phosphorylates and negatively regulates apoptis signal-regulating kinase 1. *Molecular and Cellular Biology* 21(3): 893-901.

Klaus GGB, Bijsterbosch MK, and Parkhouse ME. 1984. A comparison of the effects of intact (IgG) and $F(ab')_2$ anti-m or anti-d antibodies. *Immunology* 54:677-683.

Koegl M, Zlatkine P, Ley SC, Courtneidge SA, and Magee AI. 1994. Palmitoylation of multiple Src-family kinases at a homologous N-terminal motif. *Biochemical Journal* 303:749-753.

Kojima T, Fukuda M, Watanabe Y, Hamazato F, and Mikoshiba K. 1997. Characterization of the pleckstrin homology domain of Btk as an inositol polyphosphate and phosphoinositide binding domain. *Biochemical and Biophysical Research Communications* 236:333–339.

Kong GH, Bu JY, Kurosaki T, Shaw AS, and Chan AC. 1995. Reconstitution of syk function by the ZAP-70 protein tyrosine kinase. *Immunity* 2:485-492.

Kosugi A, Hayashi F, Liddicoat DR, Yasada K, Saitoh SI, and Hamaoka T. 2001. A pivotal role of cysteine 3 of Lck tyrosine kinase for localization to glycolipid-enriched microdomains and T cell activation. *Immunology Letters* 76:133-138.

Koyama M, Ishihara K, Karasuyama H, Cordell JL, Iwamoto A, and Nakamura T. 1997. CD79alpha/CD79beta heterodimers are expressed on pro-B-cell surfaces without associated mu heavy chain. *International Immunology* 9:1767-1772.

Kudo A, and Melchers F. 1987. A second gene, *VpreB* in the 15 locus of the mouse, which appears to be selectively in Pre-B lymphomas. *EMBO Journal* 6:2267-2272.

Kurosaki T. 1999. Genetic analysis of B-cell antigen receptor signaling. *Annual Review Immunology* 17:555-592.

Kurosaki T. 2000. Functional dissection of BCR signaling pathways. *Current Opinion in Immunology* 12:276-281.

Kurosaki T, and Kurosaki M. 1997. Transphosphorylation of Bruton's tyrosine kinase on tyrosine 551 is critical for B cell antigen receptor function. *Journal of Biological Chemistry* 272:15595–15598.

Kurosaki T, Maeda A, Ishiai M, Hashimoto A, Inabe K, and Takata M. 2000. Regulation of the phospholipase C-g2 pathway in B cells. *Immunological Reviews* 176:19-29.

Kurosaki T, Takata M, Yamanshi Y, Taniguchi T, Yamamoto T, and Y. H. 1994. Syk activation by the Src-family tyrosine kinase in the B cell receptor signaling. *Journal of Experimental Medicine* 179:1725-1729.

Kurosaki T, and Tsukada S. 2000. BLNK: connecting Syk and Btk to calcium signals. *Immunity* 12:1-5.

Lam KP, Kuhn R, and Rajewsky K. 1997. In vivo ablation of surface immunoglobulin on mature B cells by inducible gene targeting results in rapid cell death *Cell* 90:1073–1083.

Langlet C, Bernard AM, Drevot P, and He HT. 2000. Membrane rafts and signaling by the multichain immune recognition receptors. *Current Opinion in Immunology* 12:250-255.

Law CL, Chandran KA, Svetlana P, Sidorenko P, and Clark EA. 1996. Phospholipase Cγ1 Interacts with Conserved Phosphotyrosyl Residues in the Linker Region of Syk and is a Substrate for Syk. *Molecular and Cellular Biology* 14:1305-1315.

Law CL, Sidiorenko SP, Chandran KA, Draves KE, Chan AC, Weiss A, Edelhoff S, and Disteche CM. 1994. Molecular cloning of human Syk. *Journal of Biological Chemistry* 269:12310-12319.

Law DA, Chan VWF, Datta SK, and DeFranco AL. 1993. B-cell antigen receptor motifs have redundant signaling capabilities and bind the tyrosine kinases PTK72, Lyn and Fyn. *Current Biology* 3:645-657.

Law DA, Gold MR, and Defranco AL. 1992. Examination of B lymphoid cell lines for membrane immunoglobulin-stimulated tyrosine phosphorylation and Src-family tyrosine kinase mRNA expression. *Molecular Immunology* 29:917-926.

Lazarus AH, Kawauchi K, Rapaport MJ, and Delovitch TJ. 1993. Antigen-induced B lymphocyte activation involves the p21Ras and RasGAP signaling pathway. *Journal of Experimental Medicine* 178:1765-1769.

Lemaitre B, Nicolas E, Michaut L, Reichhart J.M, and Hoffmann J.A. 1996. The Dorsoventral regulatory gene cassette spätzle/Toll/cactus controls the potent antifungal response in Drosophila adults. *Cell* 86:973-983

Lenardo MJ, and Baltimore D. 1989. NF-kappa B: a pleiotropic mediator of inducible and tissue-specific gene control *Cell* 58:227-229.

Leo A, and Schraven B. 2001. Adapters in lymphocyte signaling. *Current Opinion in Immunology* 13:307-316.

Lewis MC, C. B., Czar MJ, and Schwartzberg PL. 2001. Tec kinases: modulators of lymphocyte signalling and development. *Current Opinion in Immunology* 13:317-325.

Lin J, and Justement LB. 1992. The mb-1/B29 heterodimer couples the B cell antigen receptor to multiple Src family protein tyrosine kinases. *Journal of Immunology* 149:1548-1555.

MacCarthy-Morrogh L, Cory GOC, Hinshelwood S, and Kinnon C. 1999. The SH3 domain of Btk displays altered ligand binding properties when phosphorylated at the Btk autophosphorylation site Y223. *European Journal of Immunology* 29:2269-2279.

Mahajan S, Fargnoli J, Burkhardt AL, Kut SA, Saouaf SA, and Bolen JB. 1995. Src family protein tyrosine kinases induce autoactivation of Bruton's tyrosine kinase. *Molecular and Cellular Biology* 15:5304-5311.

Manes S, Mira E, Gomez-Mouton C, del Real G, Mira E, and Martinez-A C. 2001. Membrane raft microdomains in chemokines receptor function. *Seminars in Immunology* 13:147-157.

Manes S, Mira E, Gomez-Mouton C, Lacalle RA, Keller P, Labrador JP, and Martinez-A C. 1999. Membrane raft microdomains mediate front-rear polarity in mitigating cells. *EMBO Journal* 18:6211-6220.

Margolis B, Li N, Koch A, Mohammadi M, Hurwitz DR, Zilberstein A, Ullrich A, Pawson T, and Schlessinger J. 1990. The tyrosine phosphorylated carboxy terminus of the EGF receptor is a binding site for GAP and PLC-gamma. *EMBO Journal* 13:4375-4380.

Marshall AJ, Niiro H, Yun TJ, and Clark EA. 2000. Regulation of B-cell activation and differentiation by the phosphatidylinositol 3-kinase and phospholipase Cγ pathways. *Immunological Reviews* 176:30-46.

Martensson I, and Ceredig R. 2000. Role of the surrogate light chain and the pre-B-cell receptor in mouse B-cell development. *Immunology* 101:435-441.

Matsuo T, Kimoto M, and Sakaguchi N. 1991. Direct identification of the putative surface IgM receptor-associated molecule encoded by murine B cell-specific *mb-1* gene. *Journal of Immunology* 146:1584-1590.

Matsuuchi L, and Gold MR. 2001. New views of BCR structure and organization. *Current Opinion in Immunology* 13:270-277.

Matsuuchi L, Gold MR, Travis A, Grosschedl R, DeFranco AL, and Kelly RB. 1992. The membrane IgM-associated MB-1 and Igβ are sufficient to promote surface expression of a partially functional B-cell antigen receptor in a non-lymphoid cell line. *Proceedings of the National Academy of Sciences USA* 89:3404-3408.

Maxfield FR. 2002. Plasma membrane microdomains. *Current Opinion in Immunology* 14:483-487.

McCabe JB, and Berthiaume LG. 1999. Functional roles for fatty acylated amino-terminal domains in subcellular localization. *Molecular Biology of the Cell* 10:3771-3786.

McCabe JB, and Berthiaume LG. 2001. N-terminal protein acylation confers localization to cholesterol, sphingolipid-enriched membranes but not lipid rafts/caveolae. *Molecular Biology of the Cell* 12:3601-3617.

Medzhitov R. 2001. Toll-like receptors and innate immunity. *Nature Reviews* 1:135-145.

Minegishi Y, Hendershot LM, and C. ME. 1999a. Novel mechanisms control the folding and assembley of l_5/14.1 and V_{preB} to produce an intact surrogate light chain. *Proceedings of the National Academy of Sciences USA* 96:3041-3046.

Minegishi Y, Rohrer J, Cousin-Smith E, Lederman HM, Pappu R, Campana D, Chan AC, and Conley ME. 1999b. An essential role for BLNK in human B cell development. *Science* 286:1954-1957.

Misener V, Downey G, and Jongstra J. 1991. The immunoglobulin light chain related protein *lambda 5* is expressed on the surface of mouse pre-B cell lines and can function as a signal transducing molecule. *International Immunology* 3:1129-1136.

Miyakawa H, Woo SK, Dahl SC, Handler JS, and Kwon HM. 1999. Tonicity-responsive enhancer binding protein, a rel-like protein that stimulates transcription in response to hypertonicity. *Proceedings of the National Academy of Sciences* 96:2538-2542.

Miyazaki T, Kato I, Takeshita S, Karasuyama H, and Kudo A. 1999. λ_5 is required for rearrangement of the Ig k light chain gene in pro-B cell lines. *International Immunology* 11:1195-1202.

Monick MM, Carter AB, Robeff PK, Flaherty DM, Peterson MW, and Hunninghake GW. 2001. Lipopolysaccharide activates Akt in human alveolar macrophages resulting in nuclear accumulation and transcriptional activity of b-catenin. *Journal of Immunology* 66:4713-4720.

Moore HPH, Walker MD, Lee F, and Kelly RB. 1983. Expressing a human proinsulin cDNA in a mouse ACTH-secreting cell. Intracellular storage, proteolytic processing, and secretion on stimulation. *Cell* 35:531-538.

Nagata K, Nakamura T, Kitamura F, Kuramochi S, Taki S, Campbell KS, and Karasuyama H. 1997. The Ig-a/Ig-b heterodimer on mu-negative proB cell is competent for transducing signals to induce early B cell differentiation. *Immunity* 7:559-570.

Nel AE, L. G., Goldschmidt-Clermont PJ, Tung HE, Galbraith RM. 1984. Enhanced tyrosine phosphorylation in B lymphocytes upon complexing of membrane immunoglobulin. *Biochimica and Biophysica Research Communications* 125:859-866.

Niiro H, and Clark EA. 2002. Regulation of B-cell fate by antigen-receptor signals. *Nature Reviews Immunology* 2:945-956.

Noh DY, Shin SH, and Rhee SG. 1995. Phosphoinositide-specific phospholipase C and mitogenic signaling. *Biochimica et Biophysica Acta* 1242:99-114.

Oh-hora M, Johmura S, Hashimoto A, Hikida M, and Kurosaki T. 2003. Requirement for Ras Guanine Nucleotide Releasing Protein 3 in Coupling Phospholipase Cγ2 to Ras in B Cell Receptor Signaling *Journal of Experimental Medicine* 198:1841-1851.

Okada T, Maeda A, Iawmatsu A, Gotoh K, and Kurosaki T. 2000. BCAP: The tyrosine kinase substrate that connects B cell receptor to phosphoinositide 3-kinase activation. *Immunity* 13:817-827.

Okkenhaug K, and Vanhaesebroeck B. 2003. PI3K in lymphocyte development, differentiation and activation. *Nature Reviews Immunology* 3:317-330.

Ozes ON, Mayo LD, Gustin JA, Pfeffer SR, Pfeffer LM, and Donner DB. 1999. NF-κB activation by tumour necrosis requires the Akt serine-threonine kinase. *Nature* 401:82-85.

Pande G. 2000. The role of membrane lipids in regulation of integrin functions. *Current Opinion in Cell Biology* 12:569-574.

Pap M, and Cooper GM. 1998. Role of glycogen synthase kinase-3 in the phosphatidylinositol 3-kinase/Akt cell survival pathway. *Journal of Biological Chemistry* 273:19929-19932.

Pappu R, Cheng AM, Li B, Gong Q, Chiu C, Griffin N, White M, Sleckman BP, and Chan AC. 1999. Requirement for B cell linker protein (BLNK) in B cell development. *Science* 286:1949-1954.

Pawson T, and Nash P. 2000. Protein-protein interactions define specificity in signal transduction. *Genes and Development* 14:1027-1047.

Petrie RJ, Schnetkamp PPM, Patel KD, Awasthi-Kalia M, and Deans JP. 2000. Transient Translocation of the B Cell Receptor and Src Homology 2 Domain-Containing Inositol Phosphatase to Lipid Rafts: Evidence Toward a Role in Calcium Regulation. *The Journal of Immunology* 165:1220-1227.

Pierce SK. 2002. Lipid Rafts and B-Cell Activation. *Nature Reviews* 2:96-105.

Pleiman CM, Abrams C, Gauen LT, Bedzyk W, Jongstra J, Shaw AS, and Cambier JC. 1994a. Distinct p53/p56Lyn and p59Fyn domains associate with non-phosphorylated and phosphorylated Ig-a. *Proceedings of the National Academy of Sciences USA* 91:4268-4272.

Pleiman CM, Hertz WM, and Cambier JC. 1994b. Activation of phosphatidylinositol-3-kinase by Src-family SH3 binding to the p85 subunit. *Science* 263:1609-1612.

Prasad KVS, Janssen O, Kapeller R, Raab M, Cantley LC, and Rudd CE. 1993. Src-homology 3 domain of protein kinase p59fyn mediates binding to phosphatidylinositol 3-kinase in T cells. *Proceedings of the National Academy of Sciences* 90:7366-7370.

Rawlings DJ. 1999. Bruton's tyrosine kinase controls a sustained calcium signal essential for B lineage development and function. *Clinical Immunology* 91:243-253.

Rawlings DJ, Scharenberg AM, Park H, Wahl MI, Lin S, Kato RM, Fluckinger AC, Witte O, and Kinet JP. 1996. Activation of BTK by a phosphorylation mechanism initiated by SRC family kinases. *Science* 271:822-825.

Resh MD. 1999. Fatty acylation of proteins: new insights into membrane targeting of myristoylated and palmitoylated proteins. *Biochimica et Biophysica Acta* 1451:1-16.

Reth M. 1989. Antigen receptor tail clue. *Nature* 338:383-384.

Reth M, Wienands J, and Schamel WW. 2000. An unsolved problem of the clonal selection theory and the model of an oligomeric B-cell antigen receptor. *Immunological Reviews* 176:10-18.

Rhee SG. 2001. Regulation of Phosphoinositide-specific Phospholipase C. *Annual Review of Biochemistry* 70:281-312.

Rhee SG, and Bae YS. 1997. Regulation of Phosphoinositide-specific Phospholipase C Isozymes. *Journal of Biological Chemistry* 1997:15045-15048.

Rhee SG, Suh PG, Ryu SH, and Lee SY. 1989. Studies of inositol phospholipid specific phospholipase C. *Science* 244:546-550.

Richards JD, Dave SH, Chou CH, Mamchak AA, and DeFranco AL. 2001. Inhibition of the MEK/ERK signaling pathway blocks a subset of B cell responses to antigen. *Journal of Immunology* 166:3855-3864.

Richards JD, Gold MR, Hourihane SL, DeFranco AL, and Matsuuchi L. 1996. Reconstitution of B cell antigen receptor-induced signaling events in a non-lymphoid cell line expressing the Syk protein-tyrosine kinase. *Journal of Biological Chemistry* 271:6458-6466.

Rodgers W, and Rose JK. 1996. Exclusion of CD45 inhibits activity of p56lck associated with glycolipid-enriched membrane domains. *Journal of Cell Biology* 135:1515-1523.

Rodriquez-Viciana P, Warne PH, Dhand R, Vanhaesebroeck B, Gout I, Fry MJ, Waterfield MD, and Downward J. 1994. Phosphatidylinositol-3-OH kinase direct target of Ras. *Nature* 370:527-532.

Roifman CM, and Wang G. 1992. Phospholipase C-g1 and phospholipaseγ2 are substrates of the B cell antigen receptor associated protein tyrosine kinase. *Biochemical and Biophysical Research Communications* 183:411-416.

Rolink AG, Schaniel C, Andersson J, and Melchers F. 2001. Selection events operating at various stages of B cell development. *Current Opinion in Immunology* 12:202-207.

Romashkova JA, and Makarov SS. 1999. NF-kB is a target of Akt in anti-apoptotic PDGF signaling *Nature* 401:86-89.

Rowley RB, Burkhardt AL, Chao H, Matsueda GR, and Bolen JB. 1995. Syk protein-tyrosine kinase is regulated by tyrosine-phosphorylated Ig-alpha/Ig-beta immunoreceptor tyrosine activation motif binding and autophosphorylation. *Journal of Biological Chemistry* 270:11590-11594.

Rubinfeld BI, Albert I, Porfiri E, Fiol C, Munemitsu S, and Polakis P. 1996. Binding of GSK3b to the APC-b-catenin complex and regulation of complex assembly. *Science* 272:1023-1026.

Sakaguchi N, Kashiwamura SI, Kimoto M, Thalmann P, and Melchers F. 1998. B lymphocyte lineage restricted expression of mb-1, a gene with CD3-like structural properties. *EMBO Journal* 7:3457-3464.

Salim KO, Bottomley MJ, Querfurth E, Zvelibil MJ, Gout I, Scaife R, Margolis RL, Gigg R, Smith CI, Driscoll PC, Waterfield MD, and Panayotou G. 1996. Distinct specificity in the recognition of phosphoinositides by the pleckstrin homology domains of dynamin and Bruton's tyrosine kinase. *EMBO Journal* 15:6241-6250.

Saouaf SA, Mahajan S, Rowley RB, Kut SA, Fargnoli J, Burkhardt AL, Tsukada S, Witte ON, and Bolden JB. 1994. Temporal differences in the activation of three classes of non-transmembrane protein kinases following B-cell antigen receptor surface engagement. *Proceedings of the National Academy of Sciences USA* 91:9524-9528.

Saxton TM, van Oostveen I, Bowtell D, Aebersold R, and Gold MR. 1994. B cell antigen receptor cross-linking induces phosphorylation of the $p21^{ras}$ oncoprotein activators SHC and mSOS1 as well as assembley of complexes containing SHC, GRB-2, mSOS1, and a 145-kDa tyrosine-phosphorylated protein. *Journal of Immunology* 153:623-636.

Schaeffer HJ, and Weber MG. 1999. Mitogen-activated protein kinases: specific messages from ubiquitous messengers. *Molecular and Cellular Biology* 19:2435-2444.

Schamel WWA, and Reth M. 2000. Monomeric and oligomeric complexes of the B cell antigen receptor. *Immunity* 13:5-14.

Schebesta M, Heavey B, and Busslinger M. 2002. The mononuclear phagocyte system revisited. Transcriptional control of B-cell development. *Current Opinion in Immunology* 14:216-223.

Scott PH, Brunn GJ, Kohn AD, Roth AD, and Lawrence Jr. JC. 1998. Evidence of insulin-stimulated phosphorylation and activation of the mammalian target of rapamycin mediated by a protein kinase B signaling pathway. *Proceedings of the National Academy of Sciences USA* 95:7772-7777.

Sekiya F, Bae YS, and Rhee SG. 1999. Regulation of phospholipase C isozymes: activation of phospholipase C-g in the absence of tyrosine-phosphorylation. *Chemistry and Physics of Lipids* 98:3-11.

Shinjo F, Hardy R, and Jongstra J. 1994. Monoclonal anti-*lambda 5* antibody FS1 identifies a 130 kDa protein associated with *lambda 5* and Vpre-B on the surface of early pre-B cell lines. *International Immunology* 6:393-399.

Sidorenko SP, Law CI, Chandran KA, and Clark EA. 1995. Human spleen tyrosine kinase p72Syk associates with the Src-family kinase p53/p56Lyn and a 120-kDa phosphoprotein. *Proceedings of the National Academy of Sciences USA* 92:359-363.

Sidorenko SP, Law CL, Klaus SJ, Chandran KA, Takata M, Kurosaki T, and Clark EA. 1996. Protein kinase C- (PKC) associates with the B-cell antigen receptor complex and regulates lymphocyte signaling. *Immunity* 5:353–363.

Sieling PA, and Modlin RL. 2002. Toll-like receptors: mammalian 'taste receptors' for a smorgasbord of microbial invaders. *Current Opinion in Microbiology* 5:70-75.

Sigal CT, Zhou W, Buser CA, McLaughlin S, and Resh MD. 1994. Amino-terminal basic residues of Src mediate membrane binding through electrostatic interaction with acidic phospholipids. *Proceedings of the National Academy of Sciences* 91:12253–12257.

Sillman AL, and Monroe JG. 1995. Association of p72syk with the src homology-2 (SH2) domains of PLC-γ1 in B lymphocytes. *Journal of Biological Chemistry* 270:11806-11811.

Simons K, and Ikonen E. 1997. Functional rafts in cell membranes. *Nature* 387:569-572.

Simons K, and Toomre D. 2000. Lipid rafts and signal transduction. *Nature Reviews Molecular Cell Biology* 1:31-39.

Sproul TW, Malapati S, Kim J, and Pierce SK. 2000. Cutting Edge: B Cell Antigen Receptor Signaling Occurs Outside Lipid Rafts in Immature B Cells. *The Journal of Immunology* 165:6020-6023.

Stoddart A, Dykstra M, Brown BK, Song W, Pierce SK, and Brodsky FM. 2002. Lipid Rafts Unite Signaling Cascades with Clathrin to Regulate BCR Internalization. *Immunity* 17:451-462.

Su B, and Karin M. 1996. Mitogen-activated protein kinase cascades and regulation of gene expression. *Current Opinion in Immunology* 8:402-411.

Su TT, Guo B, Kawakami Y, Sommer K, Chae K, Humphries LA, Kato RM, Kang S, Patrone L, Wall R, Teitell M, Leitges M, Toshiaki K, and Rawlings DJ. 2002. PKC-b controls IκB kinase lipid raft recruitment and activation in response to BCR signaling. *Nature Immunology* 3:781-786.

Su YW, Zhang Y, Schweikert J, Koretzky GA, Reth M, and Wienands J. 1999. Interactions of SLP adaptors with the SH2 domain of Tec family kinases. *European Journal of Immunology* 29:3702-3711.

Sugawara H, Kurosaki M, Takata M, and Kurosaki T. 1997. Genetic evidence for involvement of type 1, type 2, and type 3 inositol 1,4,5-triphosphate receptors in signal transduction through the B cell antigen receptor. *EMBO Journal* 16:3078-3088.

Suhara T, Kim H-S, Kirshenbaum LA, and Walsh K. 2002. Suppression of Akt signaling induces Fas ligand expression: Involvement of caspase and Jun kinase activation in Akt-mediated Fas ligand regulation. *Molecular and Cellular Biology* 22:680-691.

Sutherland CL, Heath AW, Pelech SL, Young PR, and Gold MR. 1996. Differential activation of the ERK, JNK, and p38 mitogen-activated protein kinases by CD40 and the B cell antigen receptor. *Journal of Immunology* 157:3381-3390.

Suzuki H, Terauchi Y, Fujiwara M, Aizawa S, Yazaki Y, Kadowaki Y, and Koyasu S. 1999. *Xid*-like immunodeficiency in mice with disruption of the p85α subunit of phosphoinositide-3-kinase. *Science* 283:390-392.

Taguchi T, Kiyokawa N, Takenouch H, Matsui J, Tang WR, Nakajima H, Suzuki K, Shiozawa Y, Saito M, Katagiri YU, Takahashi T, Karasuyama H, Matsuo Y, Okita H, and Fujimoto J. 2004. Deficiency of BLNK hampers PLCγ2 phosphorylation and Ca^{2+} influx induced by the pre-B-cell receptor in human pre-B cells. *Immunology* 112:575-582.

Takata M, Homma Y, and Kurosaki T. 1995. Requirement of Phospholipase Cγ2 Activation in Surface Immunoglobulin M-induced B Cell Apoptosis. *Journal of Experimental Medicine* 182:907-914.

Takata M, and Kurosaki T. 1995. The catalytic activity of Src-family tyrosine kinase is required for B cell antigen receptor signaling. *FEBS Letters* 374:407-411.

Takata M, and Kurosaki T. 1996. A role for Bruton's tyrosine kinase in B cell antigen receptor-mediated activation of phospholipase C-g2. *Journal of Experimental Medicine* 184:31-40.

Takata M, Sabe H, Hata A, Inazu T, Homma Y, Nukada T, Yamamura H, and Kurosaki T. 1994. Tyrosine kinases Lyn and Syk regulate B cell receptor-coupled Ca^{2+} mobilization through distinct pathways. *EMBO Journal* 13:1341-1349.

Takeda K, and Akira S. 2001. Roles of Toll-like receptors in innate immune responses. *Genes to Cells* 6:733-742.

Tan JE, Wong SC, Gan SK, Xu S, and Lam KP. 2001. The adaptor protein BLNK is required for b cell antigen receptor-induced activation of nuclear factor-kappa B and cell cycle entry and survival of B lymphocytes. *Journal of Biological Chemistry* 276:20055-20063.

Taniguchi T, Kobayashi T, Kondo J, Takahashi K, Nakamura H, Suzuki J, Nagai K, Yamada T, Nakamura S, and Y. H. 1991. Molecular cloning of a porcine gene *Syk* that encodes a 72-kDa protein-tyrosine kinase showing high susceptibility to proteolysis. *Journal of Biological Chemistry* 266:15790-15796.

Timmerman LA, Clipstone NA, Ho SN, Northrop JP, and Crabtree GR. 1996. Rapid shuttling of NF-AT in discrimination of Ca2+ signals and immunosuppression. *Nature* 383:837-840.

Tognon CE, Kirk HE, Passmore LA, Whitehead IP, Der CJ, and Kay RJ. 1998. Regulation of RasGRP via a phorbol ester-responsive C1 domain. *Molecular and Cellular Biology* 18:6995-7008.

Tomlinson MG, Lin J, and Weiss A. 2000. Lymphocytes with a complex: adapter proteins in antigen receptor signaling. *Immunology Today* 21:584–591.

Tordai A, Franklin RF, Patol H, Gardner AM, Johnson GL, and Gelfand EW. 1994. Cross-linking of surface IgM stimulates the Ras/Raf-1/MEK/MAPK cascade in human B lymphocytes. *Journal of Biological Chemistry* 269:7538-7543.

Torres RM, Flaswinkel H, Reth M, and Rajewsky K. 1996. Aberrant B cell development and immune response in mice with a compromised BCR complex. *Science* 272:1804-1808.

Trujillo MA, Jiang S, Tarara JE, and E. NL. 2003. Clustering of the B Cell Receptor Is Not Required for the Apoptotic Response. *DNA and Cell Biology* 22:513-523.

Tsubata T, and Reth M. 1990. The products of pre-B cell-specific genes (λ5 and V_{preB}) and the immunoglobulin m chain form a complex that is transported onto the cell surface. *Journal of Experimental Medicine* 172:973-976.

Tuveson DA, Carter RH, Soltoff SP, and Faeron DT. 1993. CD19 of B cells as a surrogate kinase insert region to bind phosphatidylinositol 3-kinase. *Science* 260:986-989.

Valius M, and Bazenet C. 1993. Tyrosines 1021 and 1009 are phosphorylation sites in the carboxy terminus of the platelet-derived growth factor receptor subunit and are required for binding of phospholipase C and a 64-kilodalton protein, respectively. *Molecular and Cellular Biology* 13:133-143.

van Weeren PC, de Bruyn KM, de Vries-Smits AM, van Lint J, and Burgering BMT. 1998. Essential role for protein kinase B (PKB) in insulin-induced glycogen synthase kinase 3 inactivation: Characterization of dominant-negative mutant of PKB. *Journal of Biological Chemistry* 273:13150-13156.

van't Hof W, and Resh MD. 1997. Rapid plasma membrane anchoring of newly synthesized p59(fyn): selective requirement for NH2-terminal myristoylation and palmitoylation at cysteine-3. *Journal of Cell Biology* 136:1023-1035.

Varnai P, Rother KI, and Balla T. 1999. Phosphatidylinositol 3-kinase-dependent membrane association of the Bruton's tyrosine kinase pleckstrin homology domain visualized in single living cells. *Journal of Biological Chemistry* 274:10983-10989.

Wang D, Feng J, Wen R, Marine JC, Sangster MY, Parganas E, Hoffmeyer A, Jackson CW, Cleveland JL, Murray PJ, and Ihle JN. 2000. Phospholipase Cγ2 is essential in the functions of B cell and several Fc receptors. *Immunity* 13:25-35.

Weintraub BC, Jun JE, Bishop AC, Shokat KM, Thomas ML, and Goodnow CC. 2000. Entry of B cell receptor into signaling domains is inhibited in tolerant B cells. *Journal of Experimental Medicine* 191:1443-1448.

Wick MG, Dong LQ, Riojas RA, Ramos FJ, and Liu F. 2000. Mechanism of phosphorylation of protein kinase B/Akt by a constitutively active 3-phosphoinositide-dependent protein kinase-1. *Journal of Biological Chemistry* 275:40400-40406.

Wienands J, Schweikert J, Wollscheid B, Jumaa H, Nielsen PJ, and Reth M. 1998. SLP-65: A new signaling component in B lymphocytes which requires expression of the antigen receptor for phosphorylation. *Journal of Experimental Medicine* 188:791-795.

Xu S, and Lam KP. 2002. Delayed cellular maturation and decreased immunoglobulin kappa light chain production in immature B lymphocytes lacking B cell linker protein. *Journal of Experimental Medicine* 196:197-206.

Xu S, Tan JEL, Wong EPY, Manickam A, Ponniah S, and Lam KP. 2000. B cell development and activation defects resulting in *xid*-like immunodeficiency in BLNK/SLP-65-deficient mice. *International Immunology* 12:397-404.

Yamanishi Y, Kakiuchi T, Mizuguchi J, Yamamoto T, and Toyoshima K. 1991. Association of B cell antigen receptor with protein tyrosine kinase Lyn. *Science* 251:192-194.

Yasuda T, Maeda A, Kurosaki M, Tezuka T, Hironaka K, and Yamamoto T. 2000. Cbl suppresses B cell receptor-mediated phospholipase C (PLC)-2 activation by regulating B cell linker protein-PLCγ2 binding. *Journal of Experimental Medicine* 191:641-650.

Zhu G, Decker SJ, and Saltiel AR. 1992. Direct analysis of the binding of Src-homology 2 domains of phospholipase C to the activated epidermal growth factor receptor. *Proceedings of the National Academy of Sciences* 89:9559-9563.

Zioncheck TF, Harrison ML, and Gaehlen RL. 1986. Purification and characterization of a protein-tyrosine kinase from bovine thymus. *Journal of Biological Chemistry* 261:15637-15643.

Zioncheck TF, Harrison ML, Isaacson CC, and Gaehlen RL. 1988. Generation of an active protein-tyrosine kinase from lymphocytes by proteolysis. *Journal of Biological Chemistry* 263:19195-19202.

Appendix I: Summary of Cell Lines

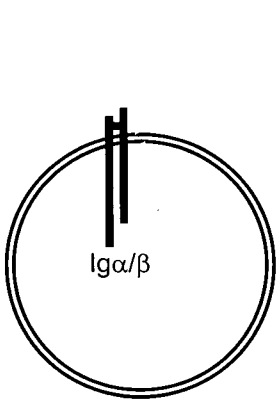

K40B-1
(pro B cell line that expresses Igα/β on its cell surface in the absence of mIgM)

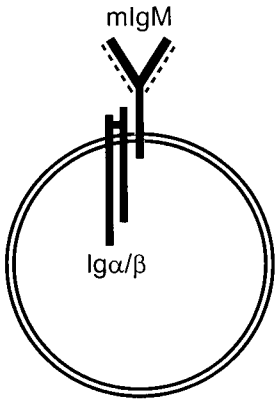

K40B-2
(pre B cell line that expresses the pre-BCR, including Igα/β and mIgM, on its cell surface)

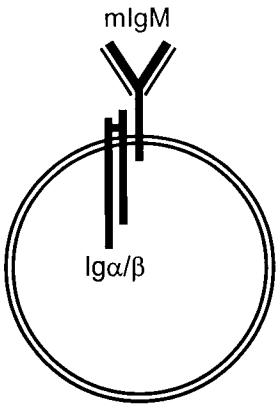

WEHI 231
(immature B cell line that expresses the BCR, including Igα/β and mIgM, on its cell surface)

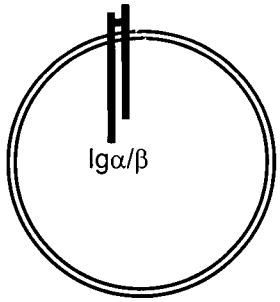

WEHI 303.1.5
(a mutant variant of WEHI 231, WEHI 303.1.5 is an immature B cell line that expresses Igα/β on its cell surface despite the absence of mIgM expression)

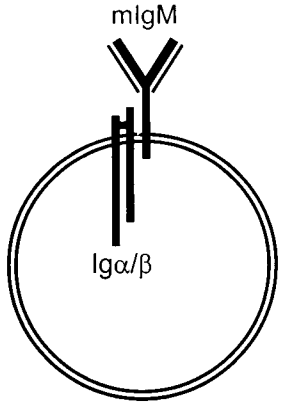

CH31
(immature B cell line that expresses the BCR, including Igα/β and mIgM, on its cell surface)

Figure A1.1. Summary Diagram of Lymphoid Cell Lines Utilized in This Thesis. The K40B-1 cell line is a pro B cell line that expresses Igα/β on its surface in the absence of mIgM (Shapiro *et al.*, 1993 and Matsuuchi, unpublished). The K40B-2 cell line is a pre B cell line that expresses Igα/β on its cell surface in conjunction with a surrogate light chain-containing mIgM (light chain indicated as dashed line in the figure) (Shapiro *et al.*, 1993). The WEHI 231 is an immature B cell line that expresses Igα/β on its cell surface in conjunction with mIgM (Condon *et al.*, 2000). The WEHI 303.1.5 cell line is a mutant variant of the WEHI 231 cell line that expresses mIgM on its cell surface despite the absence of mIgM expression (Condon *et al.*, 2000). The CH31 cell line is another immature B cell line that expresses Igα/β on its cell surface in conjunction with mIgM. The K40B-1 and WEHI 3-3.1.5 cell lines (lacking mIgM expression) serve as the experimental cell lines while the K40B-2, WEHI 231 and CH31 (expressing mIgM) serve as control cell lines for this thesis

Figure A1.2. Summary Diagram of Key AtT20-Derived Cell Lines Utilized in This Thesis (see following page). The AtT20 cell line is an adherent, murine, non-lymphoid, endocrine cell line that has proven amenable to transfection (Matsuuchi *et. al.*, 1992 and Richards *et al.*, 1996). This cell line endogenously expresses several key signaling enzymes including Fyn, PLCγ1 (both indicated in the diagram), Ras and PI3K (Matsuuchi *et. al.*, 1992 and Richards *et al.*, 1996). While these enzymes typically serve a non-lymphoid function within the AtT20 cell line they have also been identified as key components in BCR signaling in B cells. Together, these characteristics make the AtT20 cell line an ideal reconstitution system for studying the molecular requirements and mechanisms of BCR signaling. In particular, various lymphoid-specific components can be transfected into the system to determine whether or not they are sufficient to couple the BCR to the aforementioned signaling enzymes. To this end, the AtT20 cell line was initially transfected with the four chains of the BCR to establish the "BCR" cell line which expresses exogenous BCR on its cell surface (Matsuuchi *et al.*, 1992). The BCR cell line was then further transfected with the PTK, Syk, to establish the "BCR/Syk" cell line (Richards *et al.*, 1996). These two cell lines served as the "parental" cell lines for this thesis and were further transfected with various combinations of BLNK, BTK, TmBLNK, AcBLNK and/or AcPLCγ2 (as indicated in the diagram). TmBLNK refers to the BLNK fusion protein that is constitutively targeted to the plasma membrane via the CD16 extracellular domain/TCR ζ transmembrane domain. AcBLNK and AcPLCγ2 refer to the BLNK and PLCγ2 fusion proteins that are constitutively targeted to the plasma membrane via the Lyn acylation sequence. Previously established cell lines are shaded grey. Cell lines that were created for this thesis are shaded white. Arrows indicate transfection. The name of the resulting cell line is given below the cell and indicates the exogenous components that it expresses.

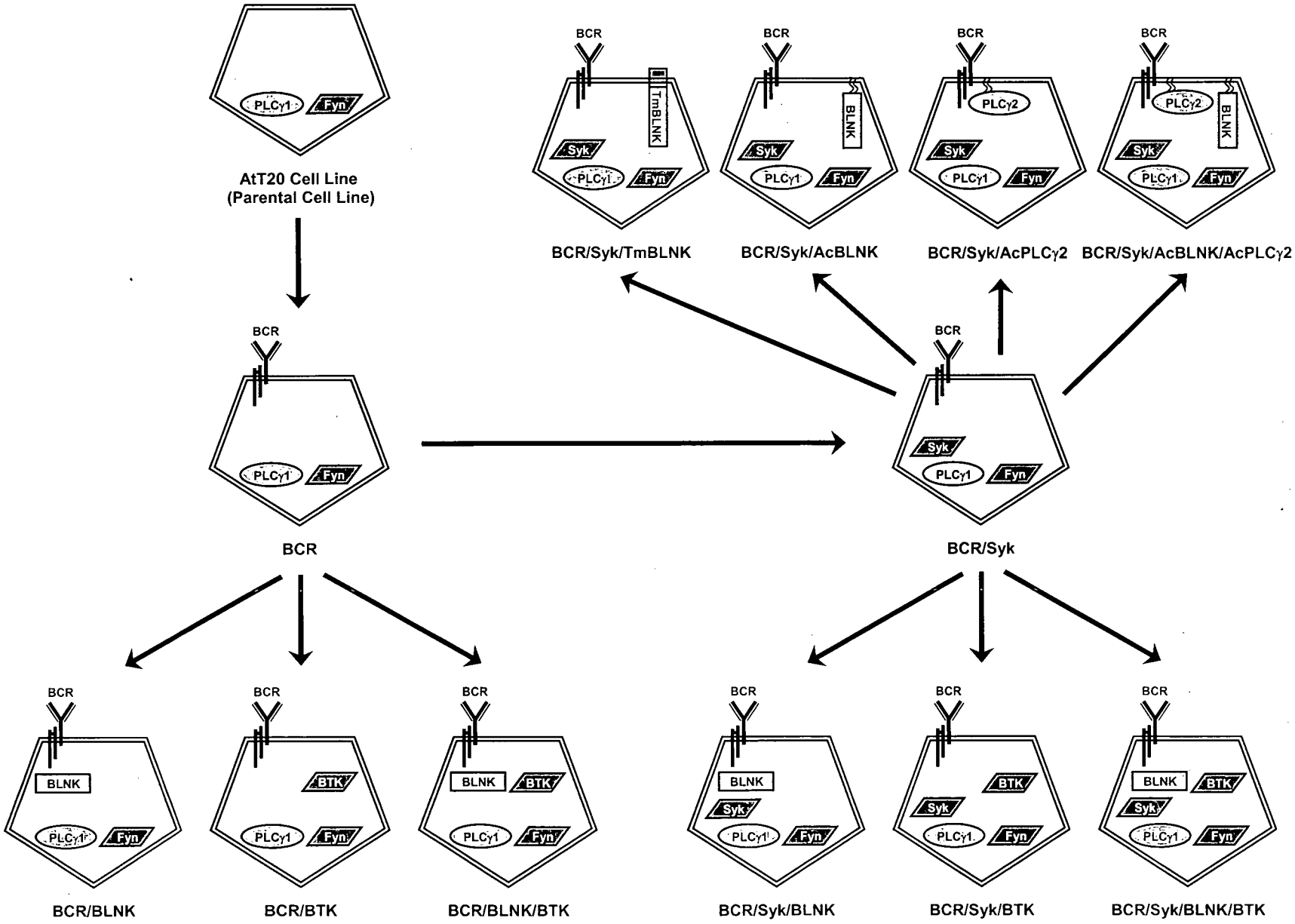
AtT20 Cell Line
(Parental Cell Line)
BCR
PLCγ1
Fyn
BCR/Syk/TmBLNK
BCR/Syk/AcBLNK
BCR/Syk/AcPLCγ2
BCR/Syk/AcBLNK/AcPLCγ2
TmBLNK
BLNK
Syk
PLCγ2
BCR
BCR/Syk
BCR/BLNK
BCR/BTK
BCR/BLNK/BTK
BCR/Syk/BLNK
BCR/Syk/BTK
BCR/Syk/BLNK/BTK
BTK

Table A1.1. Summary of Protein Expression in AtT20-Derived Cell Lines. Endogenous proteins are shaded light grey. "+" indicates that the protein is expressed. Cytosolic indicates that the protein is expressed in the cytosol whereas membrane indicates that the protein is expressed on or at the plasma membrane.

Name of Cell Line	Fyn cytosolic	PLCγ1 cytosolic	BCR membrane	Syk cytosolic	BLNK myc-tagged, cytosolic	BTK cytosolic	TmBLNK membrane	AcBLNK membrane	AcPLCγ2 membrane	PLCγ2 cytosolic
BCR	+	+	+							
BCR/BLNK	+	+	+		+					
BCR/BTK	+	+	+			+				
BCR/BLNK/BTK	+	+	+		+	+				
BCR/Syk	+	+	+	+						
BCR/Syk/BLNK	+	+	+	+	+					
BCR/Syk/BTK	+	+	+	+		+				
BCR/Syk/BLNK/BTK	+	+	+	+	+	+				
BCR/Syk/TmBLNK	+	+	+	+			+			
BCR/Syk/AcBLNK	+	+	+	+				+		
BCR/Syk/AcPLCγ2	+	+	+	+					+	
BCR/Syk/AcBLNK/AcPLCγ2	+	+	+	+				+	+	
BCR/Syk/PLCγ2 Clone 1	+	+	+	+						+
BCR/Syk/PLCγ2 Clone 2	+	+	+	+						+

Appendix II: Confirmation of Specificity of the Various Antibodies Utilized

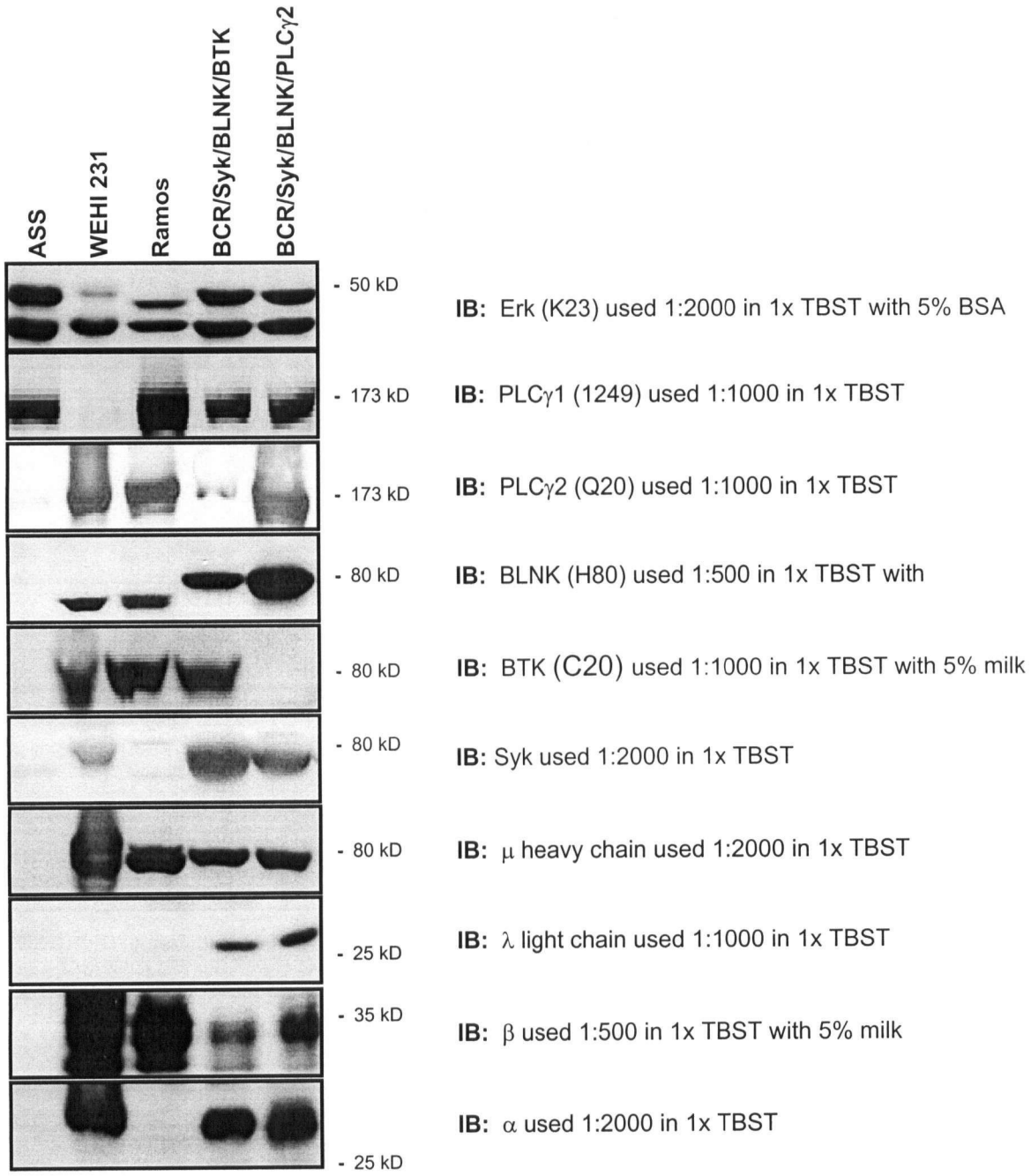

Figure A2.1. Confirmation of Specificity of the Erk, PLCγ1, PLCγ2, BLNK, BTK, Syk, μ heavy chain, λ light chain, β and α antibodies. 35 μg of whole cell lysate were resolved by SDS-PAGE. Following electrophoresis, gels were transferred to nitrocellulose filters that were subsequently immunoblotted with antibodies specific for Erk, PLCγ1, PLCγ2, BLNK, BTK, Syk, μ heavy chain, λ light chain, β and α antibodies (as indicated). The AtT20 cell line (ASS) does not express PLCγ2, BLNK, BTK, Syk, μ heavy chain, λ light chain, β or α and as such serves as a negative control for antibodies specific to these proteins. WEHI 213 is a murine immature B cell line that expresses Erk, PLCγ2, BLNK, BTK, Syk, μ heavy chain, λ light chain, β and α and as such serves as positive control for antibodies specific to these proteins. Ramos is a mature human B cell line that expresses Erk, PLCγ1, PLCγ2, BLNK, BTK, Syk, μ heavy chain, λ light chain, β and α and as such serves as a positive control for antibodies specific to these proteins (note however that the α, λ and Syk antibodies recognize only the murine and not the human isoform of these proteins). The BCR/Syk/BLNK/BTK and BCR/Syk/BLNK/PLCγ2 cell lines are AtT20-derived cell lines that express endogenous Erk and PLCγ1 as well as exogenous BCR (μ heavy chain, λ light chain, α and β), Syk, BLNK,BTK and PLCγ2 (as indicated by their respective names).

Appendix III: Summary of Immunoprecipitation Studies

Table A3.1. Summary of BLNK/PLCγ1 Immunoprecipitation Studies in AtT20-derived Cell Lines.

Cells were lysed in Triton X-100 Lysis Buffer (TXLB). 500-1500 μg of whole cell lysate was pre-cleared for ½ hour at 4 °C with 20 μl of 50% Protein A-Sepharose4B beads. Pre-cleared lysates were then immunoprecipitated for 1 hour at 4 °C with 2 μg of the immunoprecipitating antibody (IP Ab) and 40 μl of 50% Protein A-Sepharose 4B beads. Immunoprecipitated proteins were then collected by centrifugation and washed twice with TXLB. The immunoprecipitated proteins were eluted from the beads by adding 35 μl of 1x SDS-PAGE reducing sample buffer and boiling the sample for 5 minutes. 30 μl of the immunoprecipitated sample was then resolved by SDS-PAGE and transferred to nitrocellulose. Co-immunoprecipitation (i.e., co-association) of various proteins with the immunoprecipitated protein was then investigated by immunoblotting with the indicated antibody (IB Ab). Negative control cell lines are shaded grey.

IP Ab	Cell Line	Replicates	Lysis Buffer	IB Ab	Observations
PLCγ1	BCR	1	TXLB	Myc (9E10)	(-) control, band corresponding to BLNK not apparent (as expected)
	BCR/Syk	2	TXLB	Myc (9E10)	(-) control, band corresponding to BLNK not apparent (as expected)
	BCR/BLNK	1	TXLB	Myc (9E10)	Band corresponding to BLNK not apparent
	BCR/Syk/BLNK	2	TXLB	Myc (9E10)	Band corresponding to BLNK not apparent
PLCγ1	BCR	1	TXLB	BLNK (2B11)	(-) control, band corresponding to BLNK not apparent (as expected)
	BCR/PLCγ2	1	TXLB	BLNK (2B11)	(-) control, band corresponding to BLNK not apparent (as expected)
	BCR/Syk	3	TXLB	BLNK (2B11)	(-) control, band corresponding to BLNK not apparent (as expected)
	BCR/Syk/PLCγ2	1	TXLB	BLNK (2B11)	(-) control, band corresponding to BLNK not apparent (as expected)
	BCR/BLNK	1	TXLB	BLNK (2B11)	Band corresponding to BLNK not apparent
	BCR/Syk/BLNK	1	TXLB	BLNK (2B11)	Band corresponding to BLNK not apparent
	BCR/Syk/BLNK/BTK	1	TXLB	BLNK (2B11)	Band corresponding to BLNK not apparent
	BCR/Syk/BLNK/PLCγ2	3 (2 clones)	TXLB	BLNK (2B11)	Band corresponding to BLNK not apparent
	BCR/Syk/BLNK/BTK/PLCγ2	3 (2 clones)	TXLB	BLNK (2B11)	Band corresponding to BLNK not apparent
PLCγ1	BCR	1	TXLB	BLNK (H80)	(-) control, band corresponding to BLNK not apparent (as expected)
	BCR/BTK	1	TXLB	BLNK (H80)	(-) control, band corresponding to BLNK not apparent (as expected)
	BCR/Syk	1	TXLB	BLNK (H80)	(-) control, band corresponding to BLNK not apparent (as expected)
	BCR/Syk/BTK	1	TXLB	BLNK (H80)	(-) control, band corresponding to BLNK not apparent (as expected)
	BCR/BLNK	1	TXLB	BLNK (H80)	Band corresponding to BLNK not apparent
	BCR/BLNK/BTK	1	TXLB	BLNK (H80)	Band corresponding to BLNK not apparent
	BCR/Syk/BLNK	1	TXLB	BLNK (H80)	Band corresponding to BLNK not apparent
	BCR/Syk/BLNK/BTK	1	TXLB	BLNK (H80)	Band corresponding to BLNK not apparent

Table 1 Continued. Summary of BLNK/PLCγ1 Immunoprecipitation Studies in AtT20-derived Cell Lines.

IP Ab	Cell Line	Replicates	Lysis Buffer	IB Ab	Observations
Myc (9E10)	BCR	2	TXLB	PLCγ1	(-) control, band corresponding to PLCγ1 apparent, suggests 9E10 Ab may non-specifically IP PLCγ1
	BCR/Syk	2	TXLB	PLCγ1	(-) control, band corresponding to PLCγ1 apparent, suggests 9E10 Ab may non-specifically IP PLCγ1
	BCR/BLNK	2	TXLB	PLCγ1	Inconclusive as band corresponding to PLCγ1 also apparent in (-) control
	BCR/Syk/BLNK	2	TXLB	PLCγ1	Inconclusive as band corresponding to PLCγ1 also apparent in (-) control
BLNK (2B11)	BCR/PLCγ2	1	TXLB	PLCγ1	(-) control, band corresponding to PLCγ1 not apparent (as expected)
	BCR/Syk	1	TXLB	PLCγ1	(-) control, band corresponding to PLCγ1 not apparent (as expected)
	BCR/Syk/PLCγ2	1	TXLB	PLCγ1	(-) control, band corresponding to PLCγ1 not apparent (as expected)
	BCR/Syk/BLNK/PLCγ2	1	TXLB	PLCγ1	Band corresponding to PLCγ1 not apparent
	BCR/Syk/BLNK/BTK/PLCγ2	1	TXLB	PLCγ1	Band corresponding to PLCγ1 not apparent

Table A3.2. Summary of BLNK/PLCγ2 Immunoprecipitation Studies in AtT20-derived Cell Lines. Cells were lysed in Triton X-100 Lysis Buffer (TXLB). 500-1500 μg of whole cell lysate was pre-cleared for ½ hour at 4 °C with 20 μl of 50% Protein A-Sepharose4B beads. Pre-cleared lysates were then immunoprecipitated for 1 hour at 4 °C with 2 μg of the immunoprecipitating antibody (IP Ab) and 40 μl of 50% Protein A-Sepharose 4B beads. Immunoprecipitated proteins were then collected by centrifugation and washed twice with TXLB. The immunoprecipitated proteins were eluted from the beads by adding 35 μl of 1x SDS-PAGE reducing sample buffer and boiling the sample for 5 minutes. 30 μl of the immunoprecipitated sample was then resolved by SDS-PAGE and transferred to nitrocellulose. Co-immunoprecipitation (i.e., co-association) of various proteins with the immunoprecipitated protein was then investigated by immunoblotting with the indicated antibody (IB Ab). Negative control cell lines are shaded grey.

IP Ab	Cell Line	Replicates	Lysis Buffer	IB Ab	Observations
PLCγ2	BCR	1	TXLB	Myc (9E10)	(-) control, band corresponding to BLNK not apparent (as expected)
	BCR/Syk/BLNK/PLCγ2	1	TXLB	Myc (9E10)	Band corresponding to BLNK not apparent
	BCR/Syk/BLNK/BTK/PLCγ2	1	TXLB	Myc (9E10)	Band corresponding to BLNK not apparent
PLCγ2	BCR/PLCγ2	1	TXLB	BLNK (2B11)	(-) control, band corresponding to BLNK not apparent (as expected)
	BCR/Syk	2	TXLB	BLNK (2B11)	(-) control, band corresponding to BLNK not apparent (as expected)
	BCR/Syk/PLCγ2	1	TXLB	BLNK (2B11)	(-) control, band corresponding to BLNK not apparent (as expected)
	BCR/Syk/BLNK/PLCγ2	3 (2 clones)	TXLB	BLNK (2B11)	Band corresponding to BLNK not apparent
	BCR/Syk/BLNK/BTK/PLCγ2	3 (2 clones)	TXLB	BLNK (2B11)	Band corresponding to BLNK not apparent
PLCγ2	BCR/PLCγ2	1	TXLB	BLNK (TJ1TB2)	(-) control, band corresponding to BLNK not apparent (as expected)
	BCR/Syk	1	TXLB	BLNK (TJ1TB2)	(-) control, band corresponding to BLNK not apparent (as expected)
	BCR/Syk/PLCγ2	1	TXLB	BLNK (TJ1TB2)	(-) control, background band corresponding to BLNK is apparent (not expected)
	BCR/Syk/BLNK/PLCγ2	1	TXLB	BLNK (TJ1TB2)	Inconclusive as band corresponding to BLNK is also apparent in (-) control (high background)
BLNK (2B11)	BCR	3	TXLB	PLCγ2	(-) control, band corresponding to PLCγ2 not apparent (as expected)
	BCR/PLCγ2	2	TXLB	PLCγ2	(-) control, background band corresponding to PLCγ2 apparent, suggests 2B11 Ab may non-specifically IP PLCγ2
	BCR/Syk	2	TXLB	PLCγ2	(-) control, band corresponding to PLCγ2 not apparent (as expected)
	BCR/Syk/PLCγ2	2	TXLB	PLCγ2	(-) control, background band corresponding to PLCγ2 apparent, suggests 2B11 Ab may non-specifically IP PLCγ2
	BCR/Syk/BLNK/PLCγ2	7 (2 clones)	TXLB	PLCγ2	Inconclusive as band corresponding to PLCγ2 also apparent in (-) control
	BCR/Syk/BLNK/BTK/PLCγ2	8 (2 clones)	TXLB	PLCγ2	Inconclusive as band corresponding to PLCγ2 also apparent in (-) control
BLNK (TJ1TB2)	BCR/PLCγ2	1	TXLB	PLCγ2	(-) control, background band corresponding to PLCγ2 apparent (not expected), high background
	BCR/Syk	1	TXLB	PLCγ2	(-) control, background bands corresponding to PLCγ2 apparent (not expected), high background
	BCR/Syk/PLCγ2	1	TXLB	PLCγ2	(-) control, background bands corresponding to PLCγ2 apparent (not expected), high background
	BCR/Syk/BLNK/PLCγ2	1	TXLB	PLCγ2	Inconclusive as background band corresponding to PLCγ2 also apparent in (-) control

Table A3.3. Summary of Membrane-Targeted BLNK/PLCγ1 Co-Association Studies in AtT20-derived Cell Lines. Cells were lysed in Triton X-100 Lysis Buffer (TXLB). 3000 μg of whole cell lysate was pre-cleared for ½ hour at 4 °C with 20 μl of 50% Protein A-Sepharose4B beads. Pre-cleared lysates were then immunoprecipitated for 1 hour at 4 °C with 2 μg of the immunoprecipitating antibody (IP Ab) and 40 μl of 50% Protein A-Sepharose 4B beads. Immunoprecipitated proteins were then collected by centrifugation and washed twice with TXLB. The immunoprecipitated proteins were eluted from the beads by adding 35 μl of 1x SDS-PAGE reducing sample buffer and boiling the sample for 5 minutes. 30 μl of the immunoprecipitated sample was then resolved by SDS-PAGE and transferred to nitrocellulose. Co-immunoprecipitation (i.e., co-association) of various proteins with the immunoprecipitated protein was then investigated by immunoblotting with the indicated antibody (IB Ab). Negative control cell lines are shaded grey.

IP Ab	Cell Line	Replicates	Lysis Buffer	IB Ab	Observations
PLCγ1	BCR/Syk	1	TXLB	BLNK (H80)	(-) control, band corresponding to BLNK not apparent (as expected)
	BCR/Syk/BLNK	1	TXLB	BLNK (H80)	Faint band corresponding to BLNK apparent, association appears constitutive
	BCR/Syk/TmBLNK	1	TXLB	BLNK (H80)	Faint bands corresponding to TmBLNK apparent, association appears to increase following BCR cross-linking
CD16 (GRM1)	BCR/Syk	1	TXLB	PLCγ1	(-) control, band corresponding to PLCγ1 not apparent (as expected)
	BCR/Syk/BLNK	1	TXLB	PLCγ1	Band corresponding to PLCγ1 not apparent
	BCR/Syk/TmBLNK	1	TXLB	PLCγ1	Band corresponding to PLCγ1 not apparent
BLNK (H80)	BCR/Syk	1	TXLB	PLCγ1	(-) control, band corresponding to PLCγ1 not apparent (as expected)
	BCR/Syk/BLNK	1	TXLB	PLCγ1	Band corresponding to PLCγ1 not apparent
	BCR/Syk/TmBLNK	1	TXLB	PLCγ1	Band corresponding to PLCγ1 not apparent

Table A3.4. Summary of BTK/BLNK Co-Association Studies in AtT20-derived Cell Lines. Cells were lysed in Triton X-100 Lysis Buffer (TXLB). 500-1500 μg of whole cell lysate was pre-cleared for ½ hour at 4 °C with 20 μl of 50% Protein A-Sepharose4B beads. Pre-cleared lysates were then immunoprecipitated for 1 hour at 4 °C with 2 μg of the immunoprecipitating antibody (IP Ab) and 40 μl of 50% Protein A-Sepharose 4B beads. Immunoprecipitated proteins were then collected by centrifugation and washed twice with TXLB. The immunoprecipitated proteins were eluted from the beads by adding 35 μl of 1x SDS-PAGE reducing sample buffer and boiling the sample for 5 minutes. 30 μl of the immunoprecipitated sample was then resolved by SDS-PAGE and transferred to nitrocellulose. Co-immunoprecipitation (i.e., co-association) of various proteins with the immunoprecipitated protein was then investigated by immunoblotting with the indicated antibody (IB Ab). Negative control cell lines are shaded grey.

IP Ab	Cell Line	Replicates	Lysis Buffer	IB Ab	Observations
BTK (C20)	BCR/BTK	3	TXLB	BLNK (H80)	(-) control, band corresponding to BLNK not apparent (as expected)
	BCR/Syk/BTK	3	TXLB	BLNK (H80)	(-) control, band corresponding to BLNK not apparent (as expected)
	BCR/BLNK/BTK	3	TXLB	BLNK (H80)	Band corresponding to BLNK not apparent
	BCR/Syk/BLNK	3	TXLB	BLNK (H80)	Band corresponding to BLNK not apparent
	BCR/Syk/BLNK/BTK	3	TXLB	BLNK (H80)	Band corresponding to BLNK not apparent
BLNK (2B11)	BCR/Syk	2	TXLB	BTK (C20)	(-) control, band corresponding to BTK not apparent (as expected)
	BCR/Syk/BTK	1	TXLB	BTK (C20)	(-) control, band corresponding to BTK not apparent (as expected)
	BCR/Syk/BLNK/BTK/PLCγ2	2 (2 clones)	TXLB	BTK (C20)	Band corresponding to BTK not apparent

Table A3.5. Summary of BLNK/Ig-α Co-Association Studies in AtT20-derived and Lymphoid Cell Lines. Cells were lysed in n-Dodecyl-β-d-Maltoside lysis buffer (DMLB) or Triton X-100 Lysis Buffer (TXLB). 500-1500 μg of whole cell lysate was pre-cleared for ½ hour at 4 °C with 20 μl of 50% Protein A-Sepharose4B beads. Pre-cleared lysates were then immunoprecipitated for 1 hour at 4 °C with 2 μg of the immunoprecipitating antibody (IP Ab) and 40 μl of 50% Protein A-Sepharose 4B beads. Immunoprecipitated proteins were then collected by centrifugation and washed twice with TXLB. The immunoprecipitated proteins were eluted from the beads by adding 35 μl of 1x SDS-PAGE reducing sample buffer and boiling the sample for 5 minutes. 30 μl of the immunoprecipitated sample was then resolved by SDS-PAGE and transferred to nitrocellulose. Co-immunoprecipitation (i.e., co-association) of various proteins with the immunoprecipitated protein was then investigated by immunoblotting with the indicated antibody (IB Ab). Negative control cell lines are shaded grey.

IP Ab	Cell Line	Replicates	Lysis Buffer	IB Ab	Observations
BLNK (2B11)	BCR/Syk	1	DMLB	Alpha	(-) control, band corresponding to alpha not apparent (as expectance)
	BCR/Syk/BLNK	1	DMLB	Alpha	Band corresponding to alpha not apparent
	BCR/Syk/BLNK/BTK	1	DMLB	Alpha	Band corresponding to alpha not apparent
BLNK (2B11)	Daudi	1	TXLB	Alpha	Band corresponding to alpha not apparent

Table A3.6. Summary of BLNK/PLCγ Co-Association Studies in Lymphoid Cell lines. Cells were lysed in n-Dodecyl-β-d-Maltoside lysis buffer (DMLB) or Triton X-100 Lysis Buffer (TXLB) or Nonidet P40 lysis buffer (NPLB). 500-1500 μg of whole cell lysate was pre-cleared for ½ hour at 4 °C with 20 μl of 50% Protein A-Sepharose4B beads. Pre-cleared lysates were then immunoprecipitated for 1 hour at 4 °C with 2 μg of the immunoprecipitating antibody (IP Ab) and 40 μl of 50% Protein A-Sepharose 4B beads. Immunoprecipitated proteins were then collected by centrifugation and washed twice with TXLB. The immunoprecipitated proteins were eluted from the beads by adding 35 μl of 1x SDS-PAGE reducing sample buffer and boiling the sample for 5 minutes. 30 μl of the immunoprecipitated sample was then resolved by SDS-PAGE and transferred to nitrocellulose. Co-immunoprecipitation (i.e., co-association) of various proteins with the immunoprecipitated protein was then investigated by immunoblotting with the indicated antibody (IB Ab).

IP Ab	Cell Line	Replicates	Lysis Buffer	IB Ab	Observations
PLCγ1	Daudi	3	TXLB	BLNK (AC)	Faint doublet corresponding to BLNK apparent (may be slightly enhanced following BCR x-linking)
BLNK (2B11)	Daudi	1	TXLB	PLCγ1	Band corresponding to PLCγ1 not apparent
BLNK (2B11)	Daudi	1	DMLB	PLCγ1	Band corresponding to PLCγ1 not apparent
BLNK (H80 & 2B11)	Daudi	1	NPLB	PLCγ2	Band corresponding to PLCγ2 not apparent
	A20	1	NPLB	PLCγ2	Band corresponding to PLCγ2 not apparent

Appendix IV: Summary of Inositol Phosphate Studies

Once activated, PLCγ hydrolyzes PIP_2 to produce the second messengers, DAG and IP_3. Given this, it was initially proposed that BCR-induced PLCγ activation would be assayed for by monitoring IP_3 production in the AtT20-derived cell lines. This was deemed a tenable approach as such assays had previously been performed in the AtT20 system with some success (Matsuuchi *et al.*, 1992). However, the results of the IP_3 assays proved inconclusive despite numerous attempts to optimize the assay (summarized below). Thus, the IP_3 Assays were abandoned in favour of Calcium Flux Assays.

Summary of Attempts to Optimize the IP_3 Assay.

Note: Each variable was addressed and adjusted independently.

1. Plating of Cells.

   An increase in IP_3 production was observed in the positive control cell lines following stimulation in the initial IP_3 assays (data not shown). However, the total counts per minute (cpm) for ^{3}H-IP_3 were significantly lower than what was previously reported for AtT20-derived cell lines (e.g., 2824 cpm for SR1 following serotonin addition was observed here as compared to 10, 111 cpm in Matsuuchi *et al.*, 1992). While this could be a reflection of numerous deficiencies within the protocol the method of cell plating was addressed first.

   It was observed that the cells were poorly adhered to the well at the point of ^{3}H-inositol addition (seven hours post plating). This in turn could affect the efficiency of the IP_3 assay. Thus, cells were allowed to adhere to the wells for ~24, 48, 96 or 144 hours prior to ^{3}H-inositol addition to determine if changing this variable could improve the efficiency of the assay. From this it was determined that ^{3}H-IP_3 counts were maximized when cells were permitted to adhere to the wells for 96 hours prior to ^{3}H-inositol labeling (data not shown). Thus, this change was made to the optimized protocol.

2. Stimulating PLCγ Activity with FCS

Dialyzed FCS was used to stimulate PLCγ activity (via a BCR-independent pathway) in the AtT20 system as a positive control. Unfortunately, the response to dialyzed FCS was inconsistent as well as lower than anticipated. These inconsistent effects may reflect inconsistencies in the dialysis procedure (e.g., within the timing of dialysis or within the dialysis tubing used). Thus, cells were stimulated with non-dialyzed FCS to determine if this would produce more consistent results. From this it was determined that stimulation with non-dialyzed FCS did indeed produce more consistent results (data not shown). Nonetheless, the response to FCS stimulation still appeared lower than expected. As the cells are being maintained in complete DMEM containing 10 % FCS it was hypothesized that this apparently poor response may reflect that the cells have already largely responded to the FCS within the media such that further FCS stimulation only provides a minimal increase in PLCγ activation and/or IP_3 production. To address this possibility cells were maintained overnight in low serum DMEM (containing only 0.2 % FCS) during the ^{3}H-inositol labeling stage. From this it was observed that the ^{3}H-IP_3 counts were lower in the non-stimulated cell lines and that the ^{3}H-IP_3 counts were increased in the FCS stimulated cell lines that were maintained in low serum DMEM as compared to those that were maintained in complete DMEM (data not shown). Given these findings, cells were maintained in low serum DMEM for approximately 24 hours prior to stimulation and then were stimulated with non-dialyzed FCS in the optimized protocol.

3. Labeling Cells with ^{3}H-Inositol

Despite the above changes ^{3}H-IP_3 counts remained lower than expected for the positive controls. It was further hypothesized that this may reflect inefficient labeling with ^{3}H-inositol and that such labeling could be poor due to competition with cold inositol that existed within the DMEM. Thus, cells were labeled overnight with ^{3}H-inositol in inositol-free, low serum DMEM. However, this was not found to enhance the ^{3}H-IP_3 counts in the positive controls and therefore, was not adopted in the optimized protocol (data not shown).

4. Scintillation Fluid Used to Count ^{3}H-IP$_3$

Next, it was hypothesized that apparently low ^{3}H-IP$_3$ counts may reflect signal quenching that can occur if the scintillation fluid to sample ratio (sf:sample ratio) is not optimized. Thus, the counting efficiencies of various sf:sample ratios were tested. To do this a known amount of ^{3}H-inositol (from Amersham) was diluted in 5 mL of elution buffer and then mixed with either 5mL, 10 mL, 15 mL, 20 mL or 25 mL of ReadyGel. From this it was determined that a 5:1 sf:sample ratio produced the highest counting efficiency (where counting efficiency = output cpm/input cpm *100 %; data not shown) and therefore, the 5:1 ratio was adopted for the optimized protocol.

Even with the optimized sf:sample ratio, the counting efficiency was only between 50-60 % with an input of 25 000 cpm of ^{3}H-inositol. Given this, various scintillation fluids were tested to determine if they could improve the counting efficiency. To do this a known amount of ^{3}H-inositol was diluted in 5 mL of elution buffer and then mixed with either ReadyGel (25 mL) or with ReadySafe, Scintiverse I or Scintiverse II scintillation fluid (using a 10:1, 4:1 and 4:1 sf:sample ratio, respectively; as recommended by the manufacturer). From this ReadyGel was determined to have the best counting efficiency (data not shown) and as such was maintained as the scintillation fluid for the optimized protocol.

5. Column Matrix Used to Extract ^{3}H-IP$_3$

Next, it was hypothesized that the apparently low ^{3}H-IP$_3$ counts may reflect inefficient recovery of ^{3}H-IP$_3$ from the supernatant due to a faulty column and/or an ineffective elution protocol. This was tested by passing a known amount of ^{3}H-IP$_3$ over the column and collecting and determining the ^{3}H-IP$_3$ counts from the various washes and elutions. From this it was determined that the column and elution protocol were functioning efficiently (data not shown) and as such, both were maintained in the optimized protocol.

6. Integrity of the Positive Control

Despite the various attempts to optimize the protocol it was still found the ^{3}H-IP_3 counts of the SR1 positive control appeared low compared to what was observed in Matsuuchi *et al.* (1992). Thus, it was hypothesized that the SR1 cell line may have become less sensitive to serotonin and/or less able to activate PLCβ and to affect an increase in IP_3 production in the intervening years between these assays. If this were the case, the SR1 cell line could be compromised as a positive control. Thus, the Daudi human B cell line and the WEHI 231 murine B cell line were also used as positive controls. However, they too produced lower than expected ^{3}H-IP_3 counts (data not shown). This suggests that the IP_3 assay is still not optimized, raising the concern that even if the BCR/PLCγ pathway were to be partially reconstituted in the AtT20-derived cell lines, the assay may not be sensitive enough to detect this. Thus, the IP_3 assay was abandoned in favour of calcium flux assays (refer to Chapter 2.11 and 2.12 and Appendices 5 and 6).

Summary of Initial IP_3 Assay Protocol as Adapted From Matsuuchi *et al.* (1992).

Note: Cell lines assayed include: WEHI 231, an immature B cell line that activates PLCγ and increases IP_3 production upon BCR cross-linking (positive control) (ref); SR1, an AtT20-derived cell line that expresses the exogenous SR1 receptor on its surface that should activate PLCγ and increase IP_3 production upon binding its agonist, serotonin (positive control) (ref); And the BCR, BCR/Syk, BCR/BLNK, BCR/Syk/BLNK, BCR/Syk/BLNK/BTK AtT20-derived cell lines (the experimental cell lines).

a. Resuspend cells at 2 x 10^5 cell/mL in complete DMEM.
b. Plate in 6 well plates adding 1.5ml of cell suspension/well.
c. Return cells to 37 °C, 10 % CO_2 incubator and allow to adhere for 7 hours.
d. Add 10 μCi of ^{3}H-inositol/well and return cells to 37 °C, 10 % CO_2 incubator for approximately 14 hours (overnight).
e. Stimulate cells for 5 minutes with 150 μl of dialyzed fetal calf serum (FCS)/well (to activate PLCγ via serum factors; positive control) or with 15 μl of 100 μM

serotonin/ well (to activate PLCγ via the SR1 receptor; positive control) or with 30 μg anti mIgM/well (to activate PLCγ via the BCR).

f. Stop stimulation and prepare supernatant (containing soluble IP_3) and insoluble pellet (containing insoluble PIP_2) as detailed in Chapter 2.10.

g. Run supernatant over an AG 1-X8 resin formate column to extract any IP_3 as detailed in Chapter 2.10 .

h. Elute IP_3 from column as detailed in Chapter 2.10.

i. Mix 5 mL of eluant with 10 mL of Beckman ReadyGel liquid scintillation gel and count for ^{3}H-inositol (contained in the IP_3) using a Beckman LS 5000TA scintillation counter. Multiple counts by 4 to give total ^{3}H-IP_3 count as only ¼ of the total supernatant was used for counting.

j. Resuspend insoluble pellet in 1 ml of methanol and mix with 5 mL of Beckman ReadyGel liquid scintillation gel and count for ^{3}H-inositol (contained in the PIP_2) using a Beckman LS 5000TA scintillation counter.

k. Calculate % inositol phosphate production

$$= \frac{\text{[cpm of inositol phosphates]}}{\text{[cpm of inositol phosphates + cpm of inositol phospholipids]} * 100\ \%}$$

or

$$= \frac{\text{[cpm of eluant]}}{\text{[cpm of eluant + cpm of pellet]} * 100\ \%}$$

Summary of Optimized IP_3 Assay Protocol as Adapted From Matsuuchi *et al.* (1992).

Note: Changes made from the initial IP_3 Assay's protocol are in bold. Note that each variable was adjusted and tested independently.

a. Resuspend cells at 2 x 10^5 cell/mL in complete DMEM.

b. Plate in 6 well plates adding 1.5ml of cell suspension/well.

c. Return cells to 37 °C, 10 % CO_2 incubator and allow to adhere **for 4 days**.

d. **On the fourth night, remove complete DMEM by aspiration and replace with 1.5 mL of inositol-free DMEM containing 0.2 % FCS**, add 10 μCi of ^{3}H-

inositol/well and return cells to 37 °C, 10 % CO_2 incubator for approximately 14 hours (overnight).

e. Stimulate cells for **10 minutes** with 150 µl of **FCS**/well (to activate PLCγ via serum factors; positive control) or with 15 µl of 100 µM serotonin/ well (to activate PLCγ via the SR1 receptor; positive control) or **with 60 µg** anti mIgM/well (to activate PLCγ via the BCR).

f. Stop stimulation and prepare supernatant (containing soluble IP_3) and insoluble pellet (containing insoluble PIP_2) as detailed in Chapter 2.10.

g. Run supernatant over an AG 1-X8 resin formate column to extract any IP_3 as detailed in Chapter 2.10 .

h. Elute IP_3 from column as detailed in Chapter 2.10.

i. **Mix 1 mL of eluant with 5 mL of Beckman ReadyGel liquid scintillation gel** and count for ^{3}H-inositol (contained in the IP_3) using a Beckman LS 5000TA scintillation counter. Multiple counts by 4 to give total ^{3}H-IP_3 count as only ¼ of the total supernatant was used for counting.

j. Resuspend insoluble pellet in 1 ml of methanol and mix with 5 mL of Beckman ReadyGel liquid scintillation gel and count for ^{3}H-inositol (contained in the PIP_2) using a Beckman LS 5000TA scintillation counter.

k. Calculate % inositol phosphate production

$$= \frac{\text{[cpm of inositol phosphates]}}{\text{[cpm of inositol phosphates + cpm of inositol phospholipids]} * 100\ \%}$$

or

$$= \frac{\text{[cpm of eluant]}}{\text{[cpm of eluant + cpm of pellet]} * 100\ \%}$$

Appendix V: Summary of Population-Based Calcium Flux Assays

Once activated, PLCγ hydrolyzes PIP_2 to produce the second messengers, DAG and IP_3. Subsequently, IP_3 binds to IP_3 receptors on the endoplasmic reticulum to induce the release of intracellular calcium into the cytosol. Thus, it was proposed that BCR-induced PLCγ activation would be assayed for by monitoring BCR-induced calcium fluxes within the AtT20 system. However, the results of the calcium flux assays proved inconclusive despite numerous attempts to optimize the assay (summarized below and in Appendix 6). Thus, the calcium flux assays were cast aside in favour of Erk phosphorylation assays.

Population-Based Calcium Flux Assays with Cells in Suspension

Population-based calcium flux assays with cells in suspension were performed essentially as described in Chapter 2.11. First, it was confirmed that the typically adherent AtT20-derived cell lines could be successfully stimulated while in suspension (data not shown). Having established this, cells were placed in suspension and then loaded with Fura-2 (3.0 μM final concentration) for 40 minutes at 37 °C. The SR1 cell line was used as a positive control as stimulation with serotonin should induce a calcium flux. Calcium flux was monitored for by measuring the 340 nm/380 nm emission ratio with the expectation that increases in intracellular calcium would be indicated by an increase in the ratio. Using this approach it was determined that the SR1 cell line did flux calcium in response to serotonin treatment (1.0 μM final concentration) with the 340 nm/380 nm emission ratio increasing from a baseline of ~1.2 to ~1.5. However, given the limited nature of the increase it was hypothesized that the assay was not optimized and thus several parameters (summarized below) were adjusted to improve the assay.

Summary of Initial Population Based Calcium Flux Protocol with Cells in Suspension

a. Plate $20x10^6$ cells out on a non-adherent 10 cm plate in 10 ml of complete DMEM.

b. Return cells to 37 °C, 10 % CO_2 incubator for approximately 14 hours (overnight).

c. The next day, resuspend the cells in 10 ml of serum free DMEM.

d. Use 6 X 10^6 cells/sample (i.e., 0.3 ml of the cell suspension). Place each sample in a 15 ml Falcon tube.

e. Load with Fura-2 (at a final concentration of 3.0 μM) at 37 °C for 40 minutes.

f. Place entire sample in cuvette and then place cuvette into the Perkin Elmer LS50B Luminescence Spectrometer and allow sample to warm to 37 °C for 5 minutes.

g. Read the 340 nm/380 nm emission ratio for 2 minutes to collect a baseline ratio.

h. Stimulate with either:

- serotonin to a final concentration of 1.0 μM (for SR1 control)
- 30 μg of anti mIgM antibodies (for AtT20-derived experimental cell lines)

i. Continue reading the 340 nm/380 nm emission ratio for 2 minutes.

j. Lyse cells with digitonin (to a final concentration of 0.1 mM) to release all calcium (positive control to ensure Fura-2 loading was successful). Continue reading the 340 nm/380 nm emission ratio for 2 minutes.

k. Chelate calcium with tris and EDTA (to a final concentration of 70 μM and 10 μM, respectively). Continue reading the 340 nm/380 nm emission ratio for 2 minutes.

Summary of Optimized Population Based Calcium Flux Protocol with Cells in Suspension

Note: Changes made from the initial Calcium Assay's protocol are in bold. Each variable was adjusted and tested independently. As well, the effectiveness of Indo-1 versus Fura-2 was compared and it was determined that Fura-2 was the most effective indicator (data not shown).

a. Plate $20x10^6$ cells out on an **adherent** 10 cm plate in 10 ml of complete DMEM.

b. Return cells to 37 °C, 10 % CO_2 incubator for ~14 hours (overnight).

c. Load with Fura-2 while cells still adhered to plate. Remove media and replace with 1.0 ml of serum free DMEM containing Fura-2 at a final concentration of 10.0 μM. Return cells to 37 °C, 10 % CO_2 incubator for 40 minutes.

d. Collect cells using the flow of a pipette aid to resuspend the cells at 20 x 10^6 cell/ml in the loading media.

e. Use 6 x 10^6 cells/sample (i.e., 0.3 ml of the cell suspension). Place each sample in a 15 ml Falcon tube.

f. Place sample in cuvette and then place cuvette into the Perkin Elmer LS50B Luminescence Spectrometer and allow sample to warm to 37 °C for 5 minutes.

g. Read the 340 nm/380 nm emission ratio for 2 minutes to collect a baseline ratio.

h. Stimulate with either:

   i. serotonin to a final concentration of **6.0 μM** (for SR1 control)

   ii. **50 μg** of anti mIgM antibodies (for AtT20-derived experimental cell lines)

i. Continue reading the 340 nm/380 nm emission ratio for 2 minutes.

j. Add ionomycin to a final concentration of 2.0 μM (a positive control as ionomycin is an ionophore that causes the release of intracellular calcium). Continue reading the 340 nm/380 nm emission ratio for 2 minutes.

k. Lyse cells with digitonin (to a final concentration of 0.1 mM) to release all calcium (positive control to ensure Fura-2 loading was successful). Continue reading the 340 nm/380 nm emission ratio for 2 minutes.

l. Chelate calcium with tris and EDTA (to a final concentration of 70 μM and 10 μM, respectively). Continue reading the 340 nm/380 nm emission ratio for 2 minutes.

Following the optimized protocol the SR1 cell line was observed to flux calcium in response to serotonin treatment (1.0 μM final concentration) with the 340 nm/380 nm emission ratio increasing from a baseline of ~1 to ~2 (Fig. A5.1). As well, as a positive control, the Daudi human B cell line was observed to flux calcium in response to BCR cross-linking with the 340 nm/380 nm emission ratio increasing from a baseline of ~1.2 to ~2 (Fig. A5.1). This suggests that the optimized population-base calcium protocol is a viable approach to monitoring reconstitution of BCR-induced PLCγ activation within the AtT20-derived cell lines. However, several concerns remained. First, at best, the increase in the 340 nm/380 nm emission ratio in response to agonist was only two-fold. Thus, it was questioned whether the assay would be sensitive enough to detect small calcium fluxes which may occur if the BCR/PLCγ pathway is only partially reconstituted. Second, the results of these assays were quite variable. This may be a result of the assay being performed between two buildings and three labs as such a set-up resulted in the samples being left in suspension and on ice for variable amounts of time. As well, differences in cell health and/or cell passage number may also contribute to this variance. Also of concern was the fact that the assay was being performed on adherent cells that were forced into suspension as such an event could negatively influence the cells ability to respond to the agonist and/or to flux calcium. Thus, it was desirable to develop a calcium flux protocol where these concerns could be addressed (refer to Appendix 6).

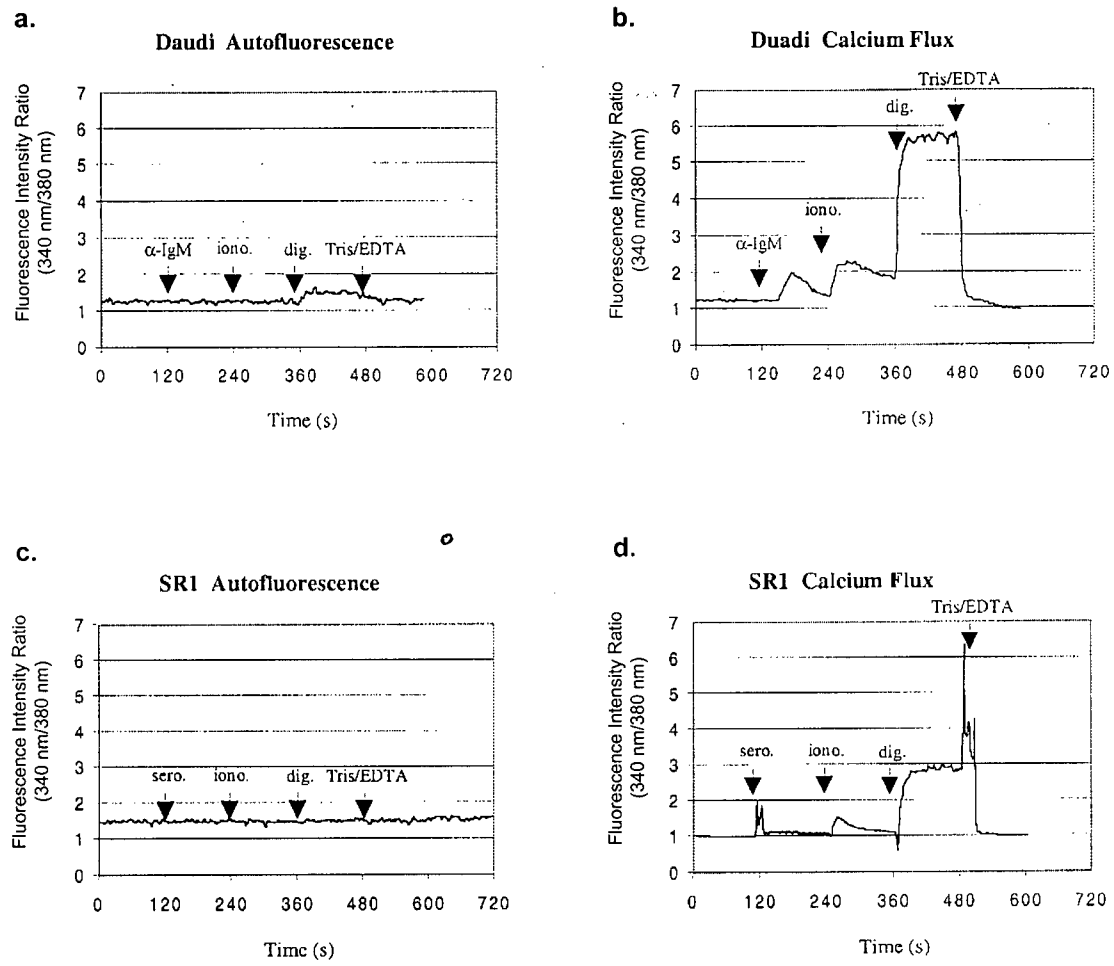

Figure A5.1. Calcium Flux in the Daudi and SR1 Cell Line As Determined by Fura-2 Based Flourometric Ratio Analysis. a) Autoflourescence of the Daudi Human B Cell Line (negative control). **b)** BCR-Induced Calcium Flux in the Daudi Human B Cell Line (positive control). **c)** Autoflourescence of the AtT20-derived SR1 Cell Line (negative control) as determined by Fura-2 based flourometric ratio analysis. **d)** Serotonin Receptor-Induced Calcium Flux in the AtT20-derived SR1 Cell Line (positive control). sero. = serotonin, iono. = ionomycin, dig. = digitonin, Tris/EDTA is as indicated. Arrows indicate time of addition of the various components. Results were obtained using the optimized calcium flux protocol for the SR1 cell line (detailed above) and a slightly modified protocol for the non-adherent Daudi human B cell line.

Appendix VI: Summary of Single-Cell Calcium Flux Assays

Many of the concerns raised regarding the population-based calcium flux assay were best addressed by switching to a single-cell calcium flux assay. One of the key benefits of this approach is that it allows the cells to be labeled, stimulated and monitored while they remain adhered to a poly-D-lysine coated coverslip as compared to the population-based assay where the cells must be disrupted to be placed into suspension. As well, this approach allowed calcium flux to be monitored in individually selected cells.

Single-cell calcium flux assays were performed as detailed in Chapter 2.12 in collaboration with Dr. John Church (University of British Columbia; Vancouver, British Columbia). Intracellular calcium fluxes were monitored using an Atto Instruments fluorescence ratio-imaging system (as described in Sheldon and Church, 2002 and Chapter 2.12). Fura-2 AM loaded cells were excited with 334 nm and 380 nm wavelengths with the respective fluorescence emission intensities being measured at 510 nm. Ratio pairs were acquired approximately every 2.4 seconds from randomly selected individual cells using an intensified charge-coupled device camera (Atto Instruments). A baseline 334 nm/380 nm ratio was established for each cell for approximately 2 minutes prior to exposure to agonists. These baseline readings were used to calculate an average baseline ratio (R_b). The maximum 334 nm/380 nm ratio following agonist exposure was then observed (R_a). These two values were then used to calculate the percent increase in the 334 nm/380 nm ratio (R_i) according to the equation:

$$R_i = 100(R_a - R_b)/R_b$$

Individual cells were then classified as non-responders (NR), minimal responders (min), moderate responders (mod) or maximal responders (max) according to Table A6.1 (below). The data from the first 10 cells classified as "max" responders was then averaged to create a representative trace of the 334 nm/380 nm ratio.

Table A6.1. Classification Criteria For an Individual Cell Based on Its Calcium Flux Response to an Agonist.

Classification	Range of R_i
Non-responder (NR)	R_i <5.0 %
Minimal responder (min)	5.0 % < $R_i \leq$15.0 %
Moderate responder (mod)	15.0 % < $R_i \leq$ 25.0 %
Maximal responder (max)	R_i > 25.0 %

Using this approach, SR1 cells were observed to immediately flux calcium in response to serotonin exposure (Fig. A6.1). Furthermore, the BCR negative SR1 cells did not flux calcium in response to subsequent treatment with the BCR cross-linking antibody (note the ability of the calcium stores to recharge between successive agonist treatments was confirmed; data not shown). Nor did serotonin receptor negative AtT20-derived cells flux calcium in response to serotonin (data not shown). Interestingly, individual SR1 cells were observed to respond differently to serotonin treatment (ergo the reporting of cells as different classes of responders). This is significant as it could help to explain some of the variability observed in the population based assays. While the reasons for these varied responses are unclear they may be attributed to variances within the supposed clonal population including variances in the serotonin receptor expression levels, in intracellular calcium stores, in general cell health and/or in stage of cell cycle. Regrettably, despite numerous procedural changes, the variability persisted. Regardless, this data suggests that the response to serotonin is specific and indicates that AtT20-derived cell lines are capable of releasing intracellular calcium stores in response to stimulation of an exogenous cell-surface receptor. Hence, studies progressed to investigate whether or not BCR-induced calcium flux (and by extrapolation, BCR-induced PLCγ activation) was reconstituted in the various AtT20-derived cell lines.

Alas, a BCR-induced calcium flux was not apparent in the BCR/Syk, BCR/Syk/BLNK, BCR/Syk/TmBLNK nor the BCR/Syk/AcBLNK/AcPLCγ2 cell lines. This may say suggest that these components are not sufficient to reconstitute BCR-induced calcium flux within this system. Alternatively, it could be that the BCR is not being sufficiently cross-linked to induce a calcium flux. This possibility was addressed by varying the amount of cross-linking antibody used from 25 μg to 150 μg (25 μg to eliminate the possibility that the BCR was being saturated as opposed

to cross-linked and 150 μg to eliminate the possibility that not enough antibody was present to sufficiently cross-linked the BCR). As well, attempts were made to co-cross-link the BCR with TmBLNK. Regardless of approach, none of the aforementioned cell lines appeared to flux calcium in response to BCR cross-linking (data not shown). Thus, it may well be that these components are not sufficient to reconstitute BCR-induced calcium flux and, by extrapolation, may not be sufficient to reconstitute BCR-induced PLCγ activation within this system. Nonetheless, the possibility of false negatives could not be ruled out. In particular, concern remains that that the assay may not be sensitive enough to detect BCR-induced calcium fluxes (as there is no guarantee that serotonin and BCR-induced calcium fluxes are comparable) or that BCR-induced PLCγ activation is not appropriately linked to calcium fluxes within this system. And thus, being unable to sufficiently address these concerns, the results of these assays must be interpreted with caution. Moreover, these concerns necessitate a further assay to determine if BCR-induced PLCγ activation was reconstituted within this system and thus, the Erk phosphorylation assay was adopted (refer to Chapter 3).

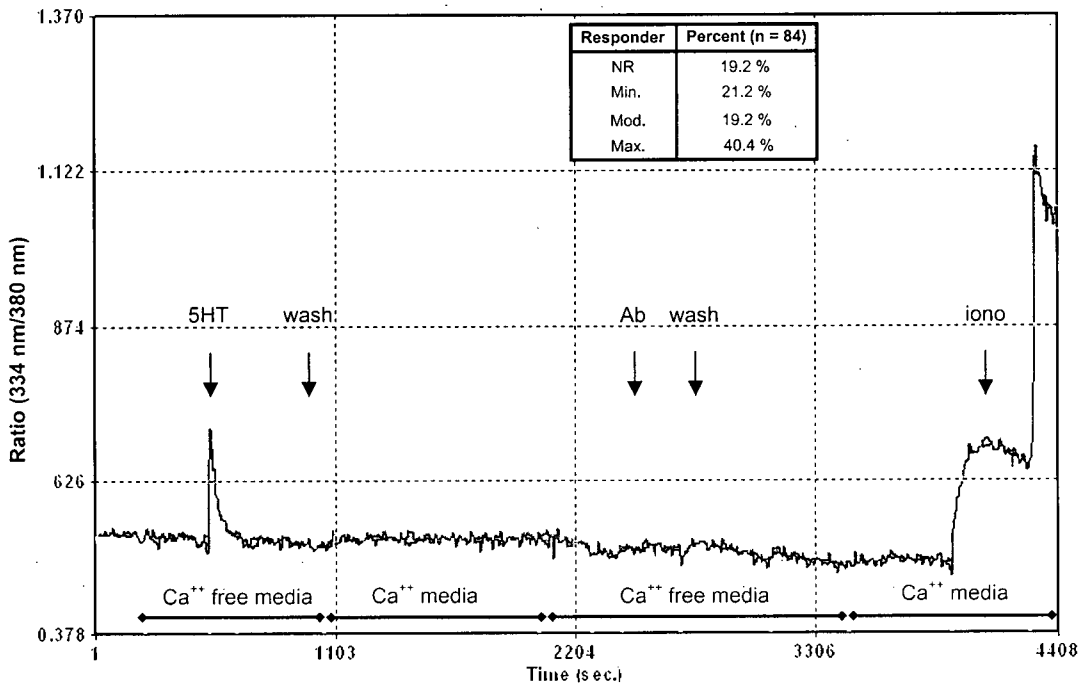

Figure A6.1. Serotonin-Induced Calcium Flux in SR1 Cells. SR1 cells are AtT20-derived cells that express an exogenous serotonin receptor. These cells do not express the BCR. Cells were plated on poly-d-lysine coated, 15 mm coverslips for 72 hours. Cells were then incubated at 35° C in 7.5 mm Fura-2-AM for 1 hour. The coverslip was then mounted on an Atto Instruments fluorescence ratio-imaging system where calcium flux was monitored as the ratio of the fluorescence emission intensities measured at 510 nm following excitation at 334 nm and 380 nm (334 nm/ 380 nm). 5HT indicates where serotonin was added to a final concentration of 6.0 mm. Wash indicates where agonists were removed from the cells and the cells were bathed with fresh media. Ab indicates where the BCR cross-linking antibody was added. The BCR cross-linking antibody was added as a control to confirm that AtT20-derived cells do not non-specifically respond to the antibody. Iono indicates where ionomycin was added to a final concentration of 10 mm. The curve represents the average of 10 responding cells from a single coverslip. This figure is representative of two replicates. Inset table is a summary of the serotonin-induced calcium flux response of individual SR1 cells within this replicate. NR = non –responder, Min. = minimal responder, Mod. = moderate responder, Max. = maximal responder as indicated in Table A6.1. Similar results were observed in at least three similar experiments.